Cyclometalation and Bicyclometalation Reactions of Trimethylphosphine Supported Iron, Cobalt and Nickel Compounds via C-H Activation with Imine and Carbonyl Anchoring Groups

Vom Fachbereich Chemie
der
Technischen Universität Darmstadt

zur

Erlangung des akademischen Grades eines
Doctor rerum naturalium (Dr.rer.nat)

genehmigte Dissertation

vorgelegt von
M.Sc. Şebnem Camadanlı
aus İnegöl

Berichterstatter:	Prof. Dr. H.-F. Klein
Mitberichterstatter:	Prof. Dr. W.-D. Fessner
Tag der Einreichung:	06.06.2005
Tag der mündlichen Prüfung:	18.07.2005

Darmstadt 2005
D 17

To my parents

and

all the good souls around me

whose inspiration, support and love

sustained me during my PhD

Die vorliegende Arbeit wurde im Fachbereich Chemie der Technischen Universität Darmstadt, Fachgebiet Anorganische Chemie I, unter der Anleitung von Prof. Dr. H.–F. Klein in der Zeit von Juli 2000 bis Februar 2005 angefertigt.

Teile dieser Arbeit sind bereits veröffentlicht worden:

Cyclometalation of Substrates Containing Imine and Pyridyl Anchoring Groups by Iron and Cobalt Complexes; Cyclometallierung von Substraten mit Imin- und Pyridyl-Ankergruppen an Eisen- und Cobalt-Komplexzentren
H.-F. Klein, S. Camadanli, R. Beck, D. Leukel, U. Flörke
Angew. Chem. Int. Ed. **2005**, *44*, 975 – 977; *Angew. Chem.* **2005**, *117*, 997 – 999

Meridional Bicyclometalation with Iron: A Novel Way of Forming Dianionic [C,N,C]-Ligands
H.-F. Klein, S. Camadanli, R. Beck, U. Flörke
Chem. Commun. **2005**, 381 – 382.

Ich danke allen Mitgliedern der Arbeitsgruppe Anorganische Chemie I und besonders Herrn Prof. Dr. H.-F. Klein für die wertvollen Anregungen und hilfreichen Diskussionen, die zum Gelingen dieser Arbeit beigetragen haben.

TABLE OF CONTENTS

List of Abbreviations

Ar	Aryl
Bu	Butyl
br	Broad
Cy	Cyclohexyl
d	Doublet
dd	Doublet of doublet
ddd	Doublet of doublet of doublet
δ	Chemical shift (NMR)
dmpe	Doublet of triplet
dt	$Me_2PCH_2CH_2PMe_2$
eq	Equation
h	Hour
η	Shows hapticity in π-bonding
IR	Infrared
^{i}Pr	Isopropyl
J	Coupling constant
κ	Hapticity in σ-bonding ligands
L	Generalized ligand
μ	Descriptor for bridging
m	Medium (IR); multiplet (NMR)
M_W	Molecular weight
Me	Methyl
mer	Meridional
m.p.	Melting Point
NMR	Nuclear magnetic resonance
Np	Neopentyl
ν	Frequency
Ph	Phenyl
q	Quartet

sept	Septet
t	Triplet
t'	Virtual triplet
td	Triplet of doublet
tt	Triplet of triplets
tert	Tertiary
TFA	Trifluoroacetic acid
THF	Tetrahydrofuran
vs	Very strong
vw	Very weak
w	Weak
X	Halogen
Z	Number of molecules per unit cell

1 INTRODUCTION

Transition metal organometallic chemistry lies at the interface between classical organic and inorganic chemistry because it looks at the interaction between inorganic metal ions and organic molecules. The field has provided some powerful new synthetic methods in organic chemistry and is beginning to make links with biochemistry with the discovery of several metalloenzymes that involve organometallic intermediates.[1-4] Organometallic ideas have been useful in interpreting the chemistry of metal surfaces and of metal colloids. The controlled pyrolysis of organometallic species has proved to be a useful way of preparing solid-state materials with unusual properties.[5-6]

Public concern for the environment has led to the rise of "green chemistry", the purpose of which is to minimize the production of chemical waste in industry and commerce. One way to do this is to use catalysts rather than stoichiometric reagents to bring about reactions. Many commercially important processes that rely on transition metal organometallic complexes as catalysts have been developed, and such applications are likely to gain more importance in the future.[7]

1.1 C-H Activation

The carbon-hydrogen bond of alkanes cannot usually be regarded as functional group. Its unique position in organic chemistry is well illustrated by the standard representation of organic molecules: the presence of C-H bonds is indicated simply by the absence of any other bond. This "invisibility" of C-H bonds reflects both their ubiquitous nature and their lack of reactivity. With these characteristics in mind it is clear that if the ability to selectively functionalize C-H bonds were well developed, it could potentially constitute the most broadly applicable and powerful class of transformations in organic synthesis. Realization of such potential could revolutionize the synthesis of organic molecules ranging in complexity from methanol to the most elaborate natural or unnatural products. The activation of C-

H bonds by "organometallic routes" (i.e., those involving the formation of a bond between carbon and a metal center) is a very large, diverse and highly active field.[8-14] The first reported example of "C-H activation" by a transition metal complex is often attributed to *Chatt*.[15] Ru(0)(dmpe)$_2$ was generated, leading to activation of a C-H bond of a ligand phosphinomethyl group or of a C-H bond of naphthalene [Eq. 1.1].

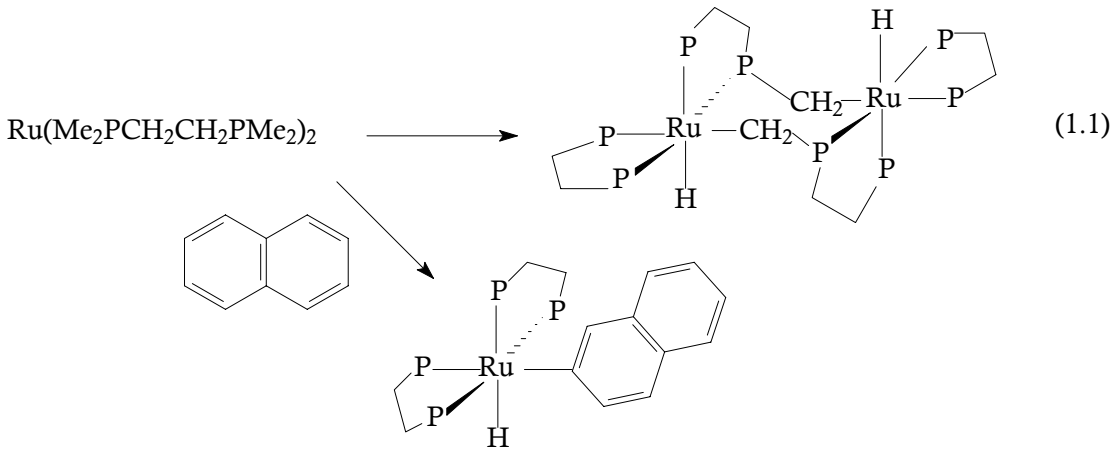

(1.1)

C-H bond activations are often classified as proceeding via either *nucleophilic* (oxidative addition) or *electrophilic* modes. However, these two classes of C-H activation have much in common, perhaps even more so than the corresponding modes of H_2 activation. Both reactions appear to proceed through a σ-bond intermediate.[16-18] Even more striking, putatively electrophilic activations, in most cases, proceed via complete oxidative addition (followed by deprotonation of the resulting metal hydride).[19]

1.1.1 Electrophilic Activation

Certain reactions that lead directly to functionalized alkanes, rather than observable organometallic species (although their participitation as intermediates is strongly indicated), have been classified as electrophilic activation reactions. This type of

reaction is illustrated in equation 1.2 where [M^{x+2}] is a late- or post-transition metal (Pd^{+2}, Pt^{+2} and/or Pt^{4+}, Hg^{2+}, Tl^{3+}), usually in a strongly polar medium such as water or an anhydrous strong acid. [20]

$$LnM^{x+2}X_2 + R\text{-}H \longrightarrow [LnM^{x}] + R\text{-}X + H\text{-}X \qquad (1.2)$$

In 1972, *Shilov* published a dramatic advance on his earlier repot of C-H activation with Pt(II).[21] The addition of Pt(IV) to the aqueous reaction of $PtCl_4^{2-}$ with methane lead to the production of the selectively oxidized species methanol and methyl chloride. Despite the impractical use of platinum as a stoichiometric oxidant, this thirty year old "Shilov System" remains to date one of relatively few catalytic systems that actually accomplishes selective alkane functionalization under mild conditions [Figure 1.1].

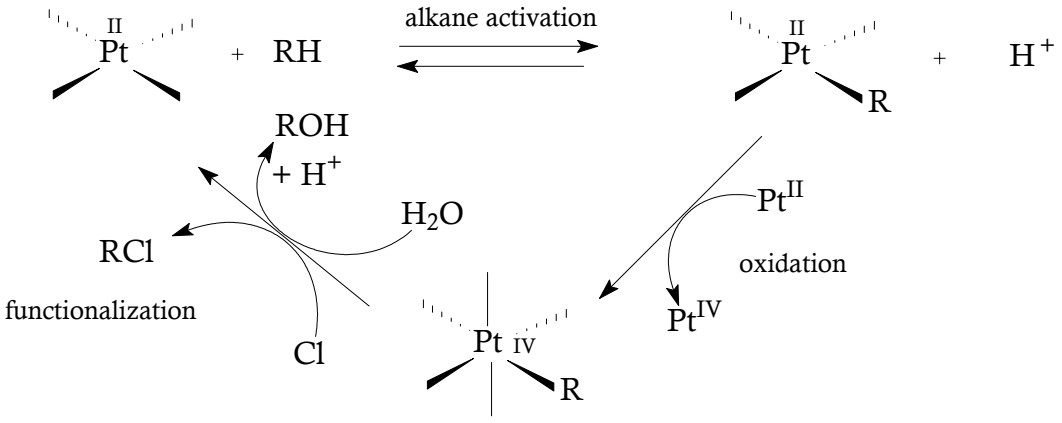

Figure 1.1 Proposed mechanism for Shilov's platinum catalyzed alkane oxidation.

Other metals capable of electrophilic substitution of C-H bonds are salts of palladium and, environmentally unattractive, mercury. Methane conversion to methanol esters has been achieved with metals.[22] Palladium salts will attack C-H

bonds in functionalized aromatics such as acetoaniline to form palladium-carbon bonds that subsequently undergo insertion of alkenes.[23] β-Hydride elimination gave styryl derivatives and palladium hydride, which requires re-oxidation of palladium by benzoquinone. An example of electrophilic C-H activation by palladium (II) is shown in equation 1.3.

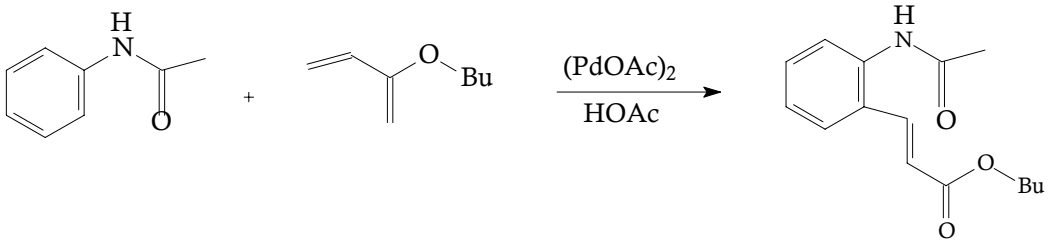

(1.3)

The reaction can be regarded as a combined *Murai* reaction (C-H activation, if electrophilic) and a *Heck* reaction (arylalkene formation), notably without the production of salts as the cross-coupling reactions imply.

1.1.2 Oxidative Addition

Oxidative addition reactions are typical for electron-rich, low-valent complexes of the 'late' transition metals found towards the right side of the periodic table Re, Fe, Ru, Os, Rh, Ir, Pt. In this type of reaction, illustrated in equation 1.4, the reactive species $[L_nM^x]$ is coordinatively unsaturated and hence in general unstable; it is therefore generated in situ by thermal or photochemical decomposition of a suitable precursor.

(1.4)

A typical precursor is $(\eta^5\text{-}C_5Me_5)\text{-}(PMe_3)Ir^{III}H_2$ [Eq. 1.5], which loses H_2 under photoirradiation to give, as reactive species $[LnM^x]$, the unobserved intermediate $[(\eta^5\text{-}C_5Me_5)\text{-}(PMe_3)Ir^I]$.[24]

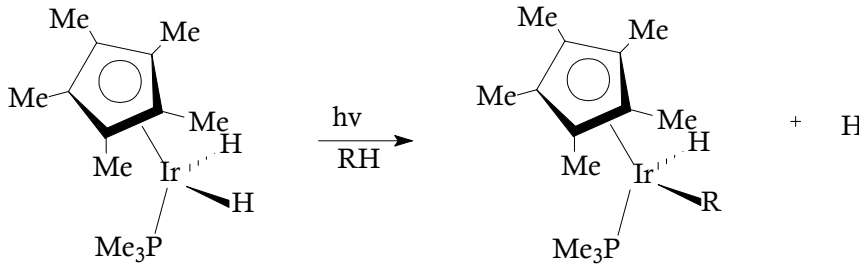

(1.5)

R = Cy, Ph, Np

Whitesides reported that an aliphatic, remote (γ) C-H bond underwent addition [Eq. 1.6].[25]

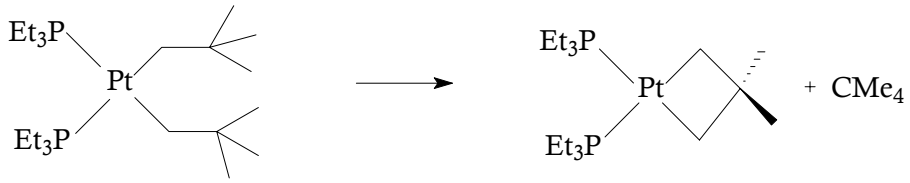

(1.6)

1.1.3 Cyclometalation Reactions

These are intramolecular C-H oxidative additions in which C-H bond breaking and M-C bond formation occurs for alkyl or aryl groups attached to a donor atom (Figure 1.2).

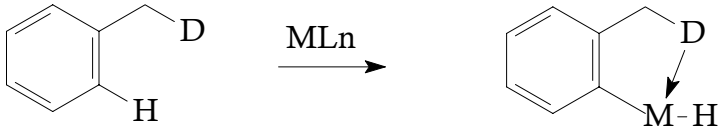

Figure 1.2 Cyclometalation.(D: donor atom).

The result is the formation of a heterocyclic ring. The hydrogen from C-H may in some cases remain bound to the metal, but more commonly an elimination reaction occurs in which H combines with H, Cl, or CH_3 etc. bound to the metal to generate H_2, HCl, CH_4 etc.

Probabaly the most common intramolecular C-H oxidative addition is the so-called *ortho*-metalation reaction of aryl groups. This is of great importance in complexes of trialkylphosphine, but many substrates such as azobenzene, aromatic ketones and thioketones, or imine compounds can react similarly.

Cyclometalation of ligand aryl groups was discovered early and ultimately found to be quite common [Eq. 1.7].[26]

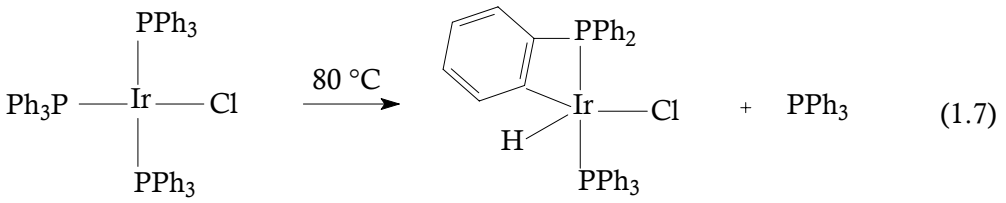

(1.7)

The very favourable intramolecular activation of aryl C-H bonds was exploited by *Shaw* to design remarkably stable carbon ligands via cyclometalation [Eq. 1.8].[27]

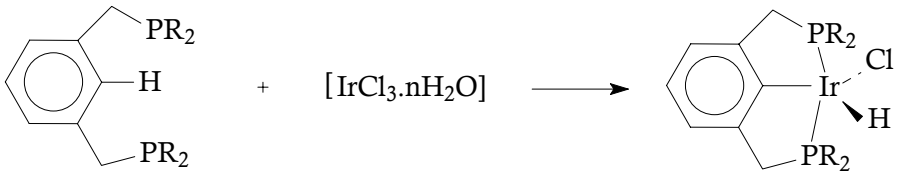

(1.8)

(^{R}PCP)IrHCl

The propensity of the bisphosphine (shown in equation 1.8) to undergo cyclometalation yielding the corresponding "^{R}PCP" tridentate ligand complexes was immediately demonstrated with a wide range of simple metal halide salts including Rh, Ir, Ni, Pd, Pt.[28-29]

1.1.4 Cyclometalation Reactions of Imines with Transition Metal Complexes

Benzylic imines (PhCH=NR) are the most studied ligands in the cyclometalation of transition metals. The first examples of cyclometalated compounds of transition metals are benzylideneaniline (*N*-phenylbenzylideneimine) reactions of Pd, Mn and Re (Figure 1.3).[30-31]

Figure 1.3 Cyclometalation reactions of Pd, Mn and Re.

Thirty years ago *Bruce* et al. studied the main part of cyclomanganation chemistry involving *N*-donor substrates and it is one of the standard procedure for activating C-H bonds ever since. Cyclometalated complexes arise from the reaction of $CH_3Mn(CO)_5$ with benzylideneaniline in light petroleum by refluxing.[32-34] It was suggested that the manganese species was behaving in a nucleophilic fashion, whereas a subsequent report from Sales and coworkers suggested that the mechanism was one whereby the manganese species behaved as an electrophile. [35-36] Manganese was the only first-row metal which has an ability to form cyclometalated complexes with imines until this work on iron and cobalt form cyclometalated compounds with imines which will be discussed in the results part.

Another metal which has been studied very often in reactions with imines is ruthenium.[37-40] Ruthenium complex-catalyzed C-H/olefin coupling and related reactions have been widely recognized as useful synthetic processes for carbon-carbon bond formation.[41] Hiraki observed an unusual formation of cyclometalated C,H-*trans*–hydridoruthenium(II) complex and its isomerization into C,H-*cis*-type [Eq. 1.9].[42]

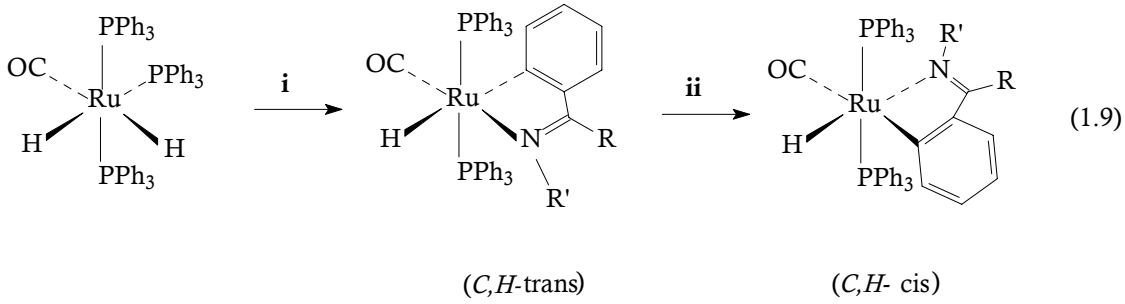

(1.9)

(*C,H*-trans) (*C,H*- cis)

i: triethoxysilane and *N*-Benzylideneaniline at 70 °C

ii: at 110°C

There are many intramolecular C-H activation examples of rhodium with N-donor ligands and C-X (X: halogen) activation with imines.[43-45] The first report of *ortho*-metalation of imines at rhodium via C-H activation recently by *James* has appeared only.[46] Simple imines of the type RN=C(H)R" or RN=C(R')-R", where R, R' and R" are solely alkyl or aryl substituents , react in a 1:1 stoichiometry with cationic Rh(I)-$(PPh_3)_2$ species to form via C-H activation *ortho*-metalated complexes containing a five-membered ring, when a suitable phenyl substituent is available at the imine-C atom [Eq. 1.10]. Their reaction with H_2 generates amines in a stoichiometric reaction which is relevant in the Rh-catalyzed hydrogenation of imines.

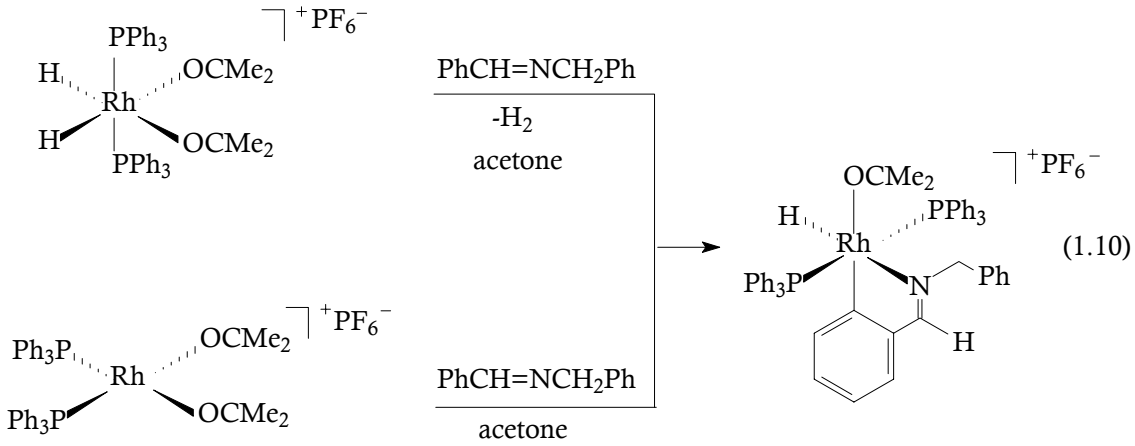

(1.10)

Cyclopalladated compounds are valuable intermediates for regio- and stereoselective organic synthesis. Carbonylation, vinylation, and halogenation of organic compounds have been reported. [47] Sales reported the cyclometalation of benzylideneamines 2,4,6-$(CH_3)C_6H_2CH=N(CH_2)nC_6H_5$ where, for the first time, the metalation of an aliphatic carbon forming a six-membered ring takes place in preference to metalation of an aromatic carbon that would give a five-membered metalacycle [Eq. 1.11].[48]

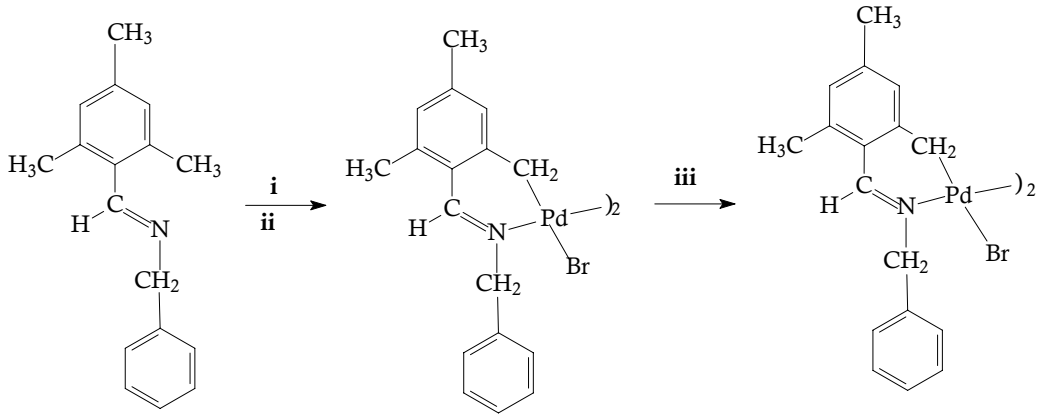

(1.11)

i:$Pd(AcO)_2$, $MeCO_2H$, reflux, 90 min; **i i**: LiBr, EtOH, reflux, 30 min; **iii**: PPh_3, $(Me)_2CO$, reflux, 45 min.

Despite of the high kinetic stability of compounds $CpOsL_3$, the derivative $Os(\eta^5\text{-}C_5H_5)Cl(PiPr_3)_2$ reacts with benzophenoneimine to give metalated hydrido complexes, which is the result of a selective C-H activation of one phenyl group [Eq. 1.12].[49-50]

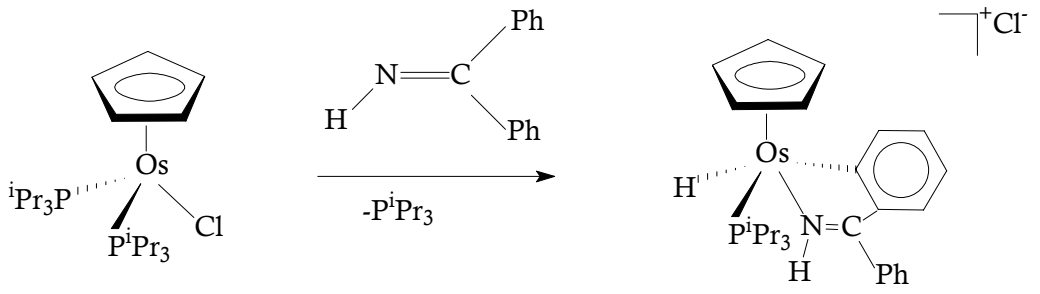

(1.12)

Due to their photechemical, photophysical and electrochemical properties of cyclometalated platinum(II) and platinum(IV) compounds have been studied extensively with *N*-benzylidenebenzylamines and especially with their halogen derivatives mainly by *Crespo* [Eq. 1.13].[51-57]

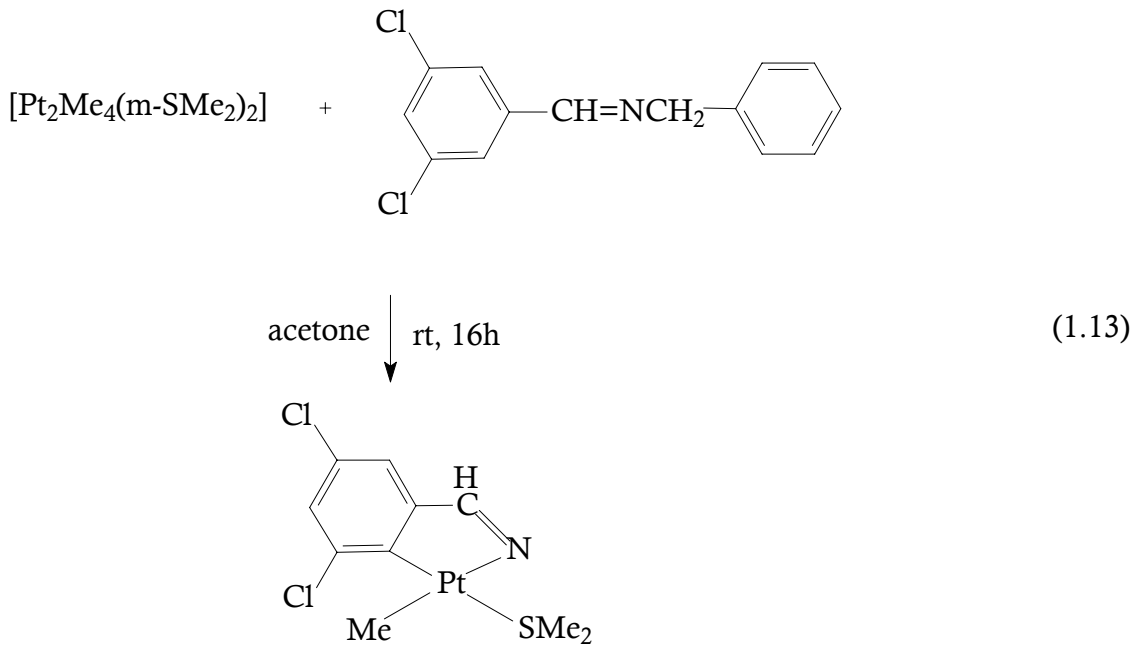

(1.13)

1.2 Catalytic Functinalization Involving Oxidative Addition of C-H Bonds

The catalysis of organic reactions is one of the most important applications of organometallic chemistry and has been a significant factor in the rapid development of the whole field.[58] Organometallic catalysts have long been used in industrial processes but are now being routinely applied in organic synthesis as well. The application of organometallic reagents and catalysts to synthetic problems is one of the fastest growing areas.[59] Continuing rise in environmental concerns and green chemistry led to increasing interest in catalytic reactions, where the metal catalysts is present in minimal quantitiy and the selectivity of the reaction is much enhanced.

1.2.1 Murai Reaction

Cyclometalation has been applied to synthesis in *Murai* reactions.[41,60] This is the most significant breakthrough in the field of insertion of unsaturated C-C bonds into C-H bonds. In this reaction, the C-H bond of aromatic ketones at the *ortho* position selectively adds to the double bond of olefins with $Ru(H)_2(CO)(PPh_3)_3$ catalyst under reflux conditions in toluene solution, giving CH/olefin coupling products [Eq. 1.14].

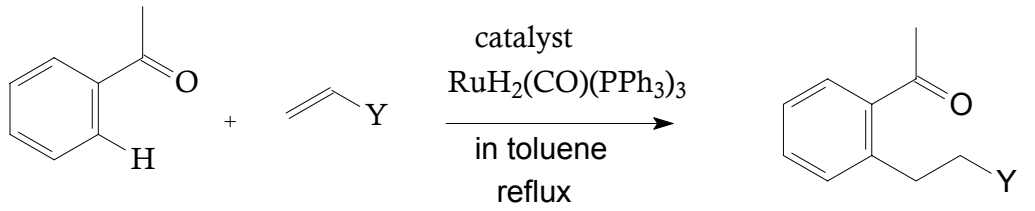

(1.14)

Y= H, $Si(OR)_3$, alkyl

The scope of the system in equation 1.14 has been extended. The cleavage and addition of *ortho* C-H bonds in various aromatic compounds such as ketones, esters, imines, imidates, nitriles, and aldehydes to olefins and acetylenes can be achieved catalytically with the aid of ruthenium catalysts. The reaction is generally highly efficient and useful in synthetic methods.[61-80]

The Ru-catalyzed insertions are very much favored by "directing" groups that are conjugated with the π-system of the C-H bond undergoing reaction (e.g. carbonyl or imine). It appears almost certain that this group plays a role more complex than simply bringing the C-H bond into the proximity of the metal center (i.e. minimizing the entropic cost of C-H addition). Two possible roles were indicated by DFT calculations of *Morokuma,* one of them is to facilitate C-H addition via a transition state as indicated in equation 1.15.[81] The stable metalacycle intermediate **B** is believed to play an important role in the high *ortho* selectivity.

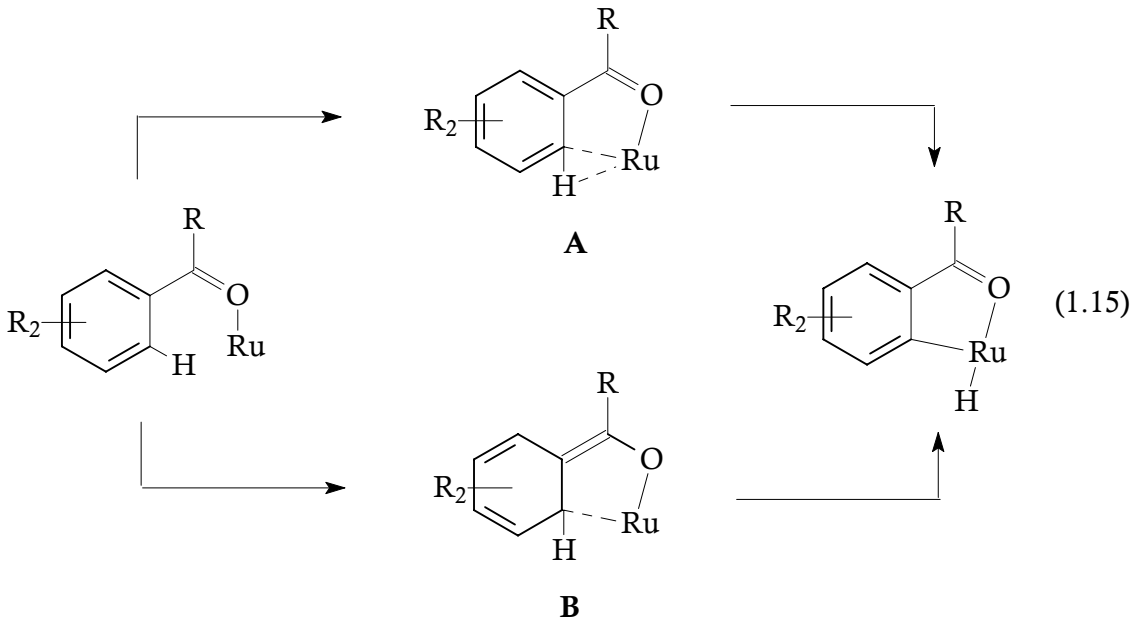

Subsequent to C-H addition, olefin insertion could be plausibly envisaged to proceed via two classes of mechanism involving: (a) initial insertion into the resulting Ru-C bond, or (b) insertion into the resulting Ru-H bond. In each case the appropriate reductive elimination would follow. *Murai* has presented strong evidence, some of which follows, for the hydrometalation path (b) and the overall mechanism of Figure 1.4.

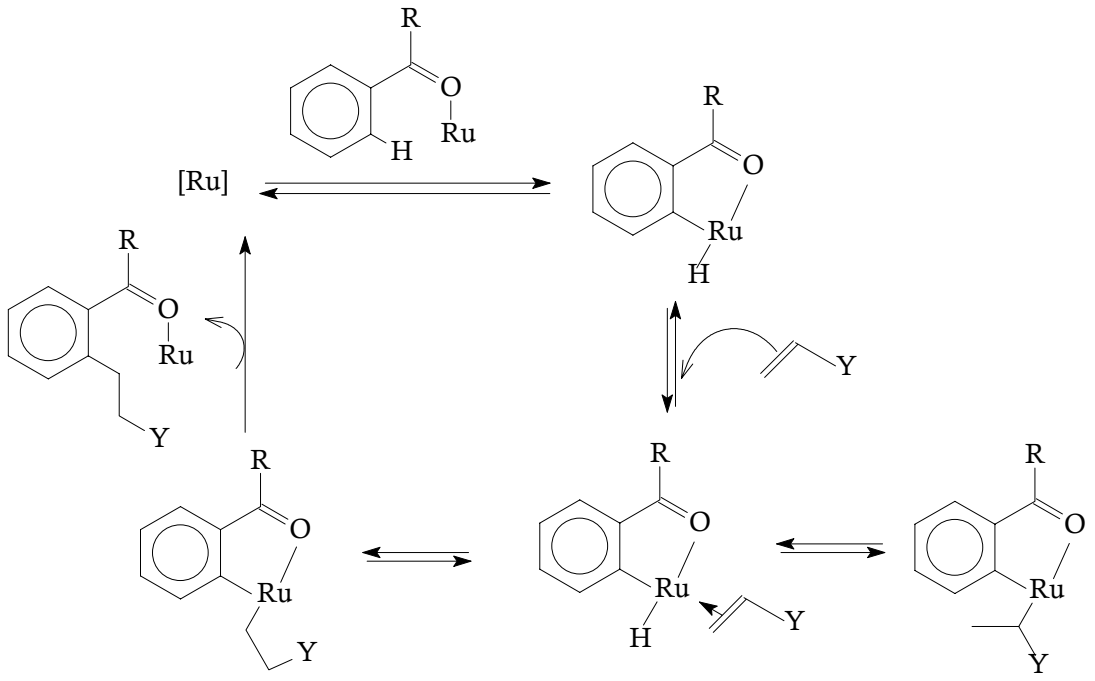

Figure 1.4 Mechanism proposed by Murai for Ru(0)-cataylzed "site-directed" addition of C-H bonds to olefins.

Reaction of Aromatic Imines with Olefins

An appropriate sp^2 nitrogen atom can also function as a directing group.[82,83] The catalytic reaction of aromatic imines with the olefin gives the corresponding 1:1 addition product [Eq. 1.16]. In addition, there is a side product, the unsaturated coupling product in the system. Although the phosphine complex $RuH_2(CO)(PPh_3)_3$ shows cataytic activity, $Ru_3(CO)_{12}$ which is an ineffective catalyst for the reaction of ketones with olefins, shows the highest activity of the various transition metal complexes screened. Aldimines react with some types of vinylsilanes, ethylene, *tert*-butylethylene, or aromatic olefins.

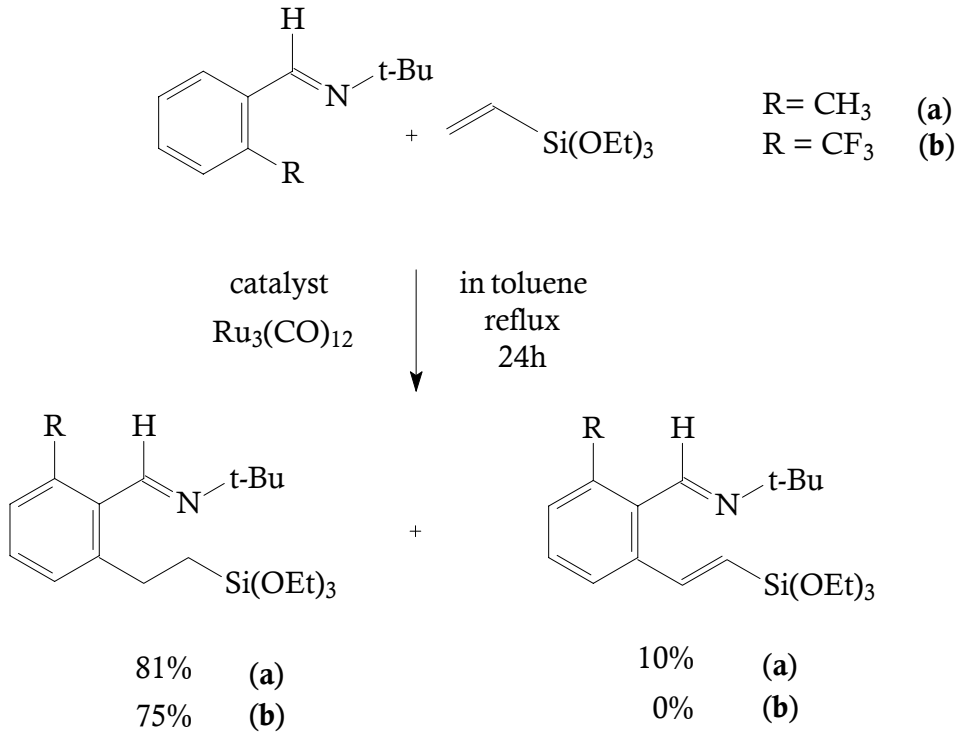

(1.16)

Jun et al. have reported a similar *ortho*-alkylation reaction of aromatic imines with olefins using *Wilkinson's* complex.[84] This *ortho*-alkylation is chelation-assisted and shows generality as well as regioselectivity, and high efficiency [Eq.1.17-1.18].

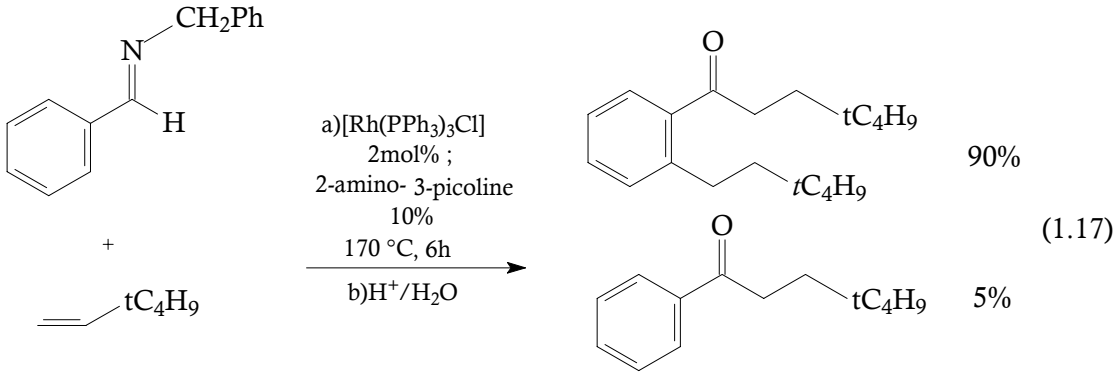

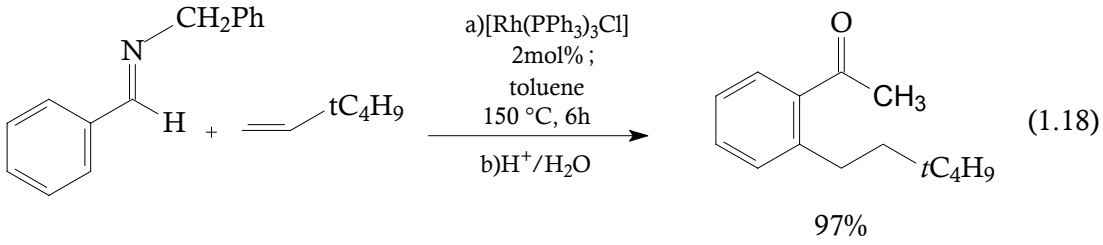

1.2.2 Suzuki Coupling

The coupling of aryl halides with aryl boronic acids, the *Suzuki* reaction (Figure 1.5 and Figure 1.6), is one of the most powerful and versatile methods for the synthesis of biaryls.[85-86]

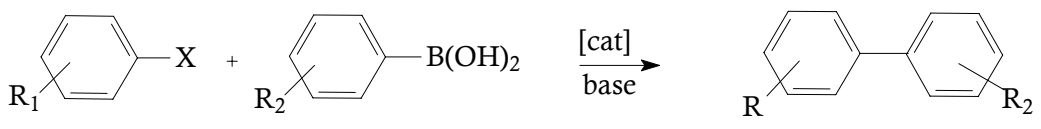

Figure 1.5 The Suzuki biaryl coupling reaction.

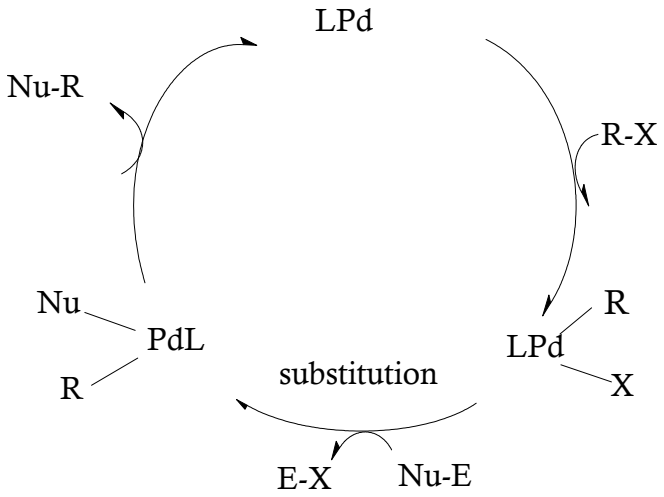

Figure 1.6 A schematic mechanism for the Suzuki coupling (R:aryl or vinyl; Nu:aryl; E: $B(OH)_2$; L:PPh_3).

There has recently been considerable interest in the development of new, high-activity catalysts that can be used in low loadings in such reactions, and palladacyclic complexes are believed to play a significant role. *Milstein* demonstrated that the *ortho*-metahalated imine complex **A** show excellent activity.[87] *Bedford* found that triarylphosphine adducts of imine-based palladacycles (**B**) show much greater reactivity than the parent dimers (**A**) in the *Suzuki* coupling of a deactivated aryl bromide.[88-91]

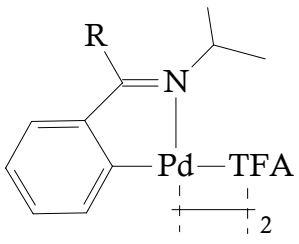

R= Me, H

A

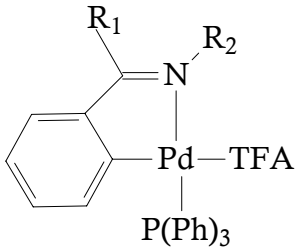

R_1= H, Me

R_2= ^{i}Pr, Ph

B

1.3 Catalysts of Fe, Co and Ni with C=N Functional Groups in Olefin Polymerization - Brookhart and Gibson Catalysts

Once it was recognized that coordinative unsaturation could facilitate insertion, the widely accepted rule of thumb that only early metals could give effcient polimerization catalysts seemed shortsighted. Brookhart and Gibson have exploited highly unsaturated, electrophilic late metal systems.[92-103] Electrophilicity is also important because it slows down β-elimination by limiting the extent of back donation into the β-C-H σ*orbital, required for the reaction to proceed.

Catalysts of the general type shown, once activated by MAO, were found to be extremely effective, with exact properties depending on the steric environment of the site, governed by the nature of the aryl group.

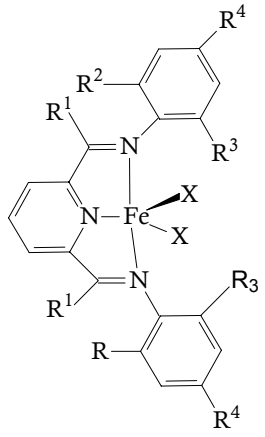

R^1= H, Me
R^2= R^3= iPr, R^4= H
R^2= R^3= Me, R^4= H, Me
R^2= R^4= Me, R^3= H

X = Cl^-, Br^-

planar.[N, N, N]

Brookhart

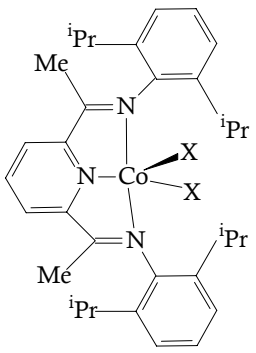

X = Cl^-, Br^-

planar.[N, N, N]

Brookhart

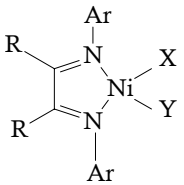

R= H, Me,

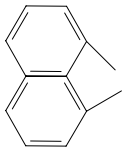

X= Y= Br
X= B[3,5-$(CF_3)_2C_6H_3]_4$.Et_2O, Y= Me
Ar= 2,6-*i*$Pr_2C_6H_3$, 2,6-$Me_2C_6H_3$, 2-*t*BuC_6H_4

Brookhart

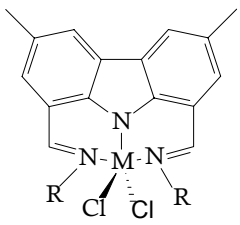

M = Co ; R = 2,4,6-$Me_3C_6H_2$
M = Fe ; R = Ph

Gibson

Study of the polymerization of olefins by soluble, well defined transition metal complexes is an ever growing area but it is already clear that these catalysts can produce polymers of quite different microstructures than previously seen and could become commercially important in future.[104]

1.4 Trimethylphosphine

Tertiary phosphines, PR_3, are important because they constitute one of the few series of ligands in which electronic and steric properties can be altered in a systematic and predictable way over a wide range by varying R. They also stabilize an exceptionally wide variety of ligands of interest to the organometallic chemist as their phosphine complexes $(R_3P)_nM\text{-}L$.[105]

Trimethylphosphine is the sterically least demanding of the triorganophosphanes. It forms stable metal complexes, reactions of the coordinated ligand are essentially unknown, and its high symmetry in complexes (local C_{3V}) facilitates spectroscopic investigations (IR, NMR).[106]

Tolman has defined the steric requirements of phosphane ligands by the vertex angle Θ of a cone with its vertex at the metal which encloses the *van der Waals* boundaries of the substituents at the phosphorus atom.[107] This sterically least demanding, basic trimethylphosphine is able to make backbonding to electron rich metal centers and able to stabilize low oxidation states. All these properties make it suitable for catalyst intermediate stages.

1.5 Purpose

The intramolecular C-H activation initiating a cyclometalation reaction is an important and intensely studied elementary step in homogenous catalysis. As known from the introduction, the cyclometalation reactions of 3rd row transition metals with imine anchoring groups via C-H activation, except manganese, are not known. When we take into account the great importance of *Murai* reaction, *Suzuki*

coupling and *Brookhart-Gibson* systems in catalysis field and the application of imine and ketone chelating systems as catalyst/catalyst precoursors in these reactions, the big gap in the late 3rd row transition metals shold be filled.

By means of this research the following contributions would be essential to make to the very limited knowledge on cyclometalation reactions of iron, cobalt, and nickel with imines:

- Synthesis of the new cyclometalated compounds from the reactions of ketimines and benzylic imines with trimethylphosphine supported iron, cobalt, and nickel adducts.

- Fully characterized iron and cobalt cyclometalated compounds could provide information on postulated reaction mechanisms in the literature.

- The reaction with isoelectronic ketones would illuminate this principle with parallel reactivity.

- Study of the preference for the C-H activation or C-F activation in benzophenone chelated systems.

- The reactivity of the synthesized complexes toward strong π-acceptor ligand carbon monoxide.

- Using iodomethane as a substrate, the interesting question arises as to whether attack by the metal would proceed as a regioselective addition or promote ring opening through a subsequent reductive C,C-coupling reaction.

- Bicyclometalation reactions of iron and cobalt would open a novel way of forming dianaionic [C, N, C]-ligands.

2 RESULTS AND DISCUSSION

This chapter mainly covers the first examples of cyclo- and bicyclometalation reactions which belong to Fe and Co with imine and carbonyl anchoring grous. Moreover, it includes the Ni reactions which resulted without any C-H activation with the same anchoring groups.

2.1 Cyclometalation Reactions

As it was explained in the introduction part, the cyclometalation reactions have been kown for a long time and they constitute one of the most important parts of modern metal-organic chemistry.[108-111] Cyclometalation transform barely activated or nonactivated C-H bonds of a coordinated ligand into C-metal bonds.[112] The compounds that contain a cyclometalated ligand continue to be of interest for the generation of catalysts, compounds with interesting material properties and antitumor agents.[113-120] In spite of more than 30 years work, other than some cyclomanganated, there are no examples of cyclometalated products of 3d row transition metals with imines [Eq. 2.1].[121-124]

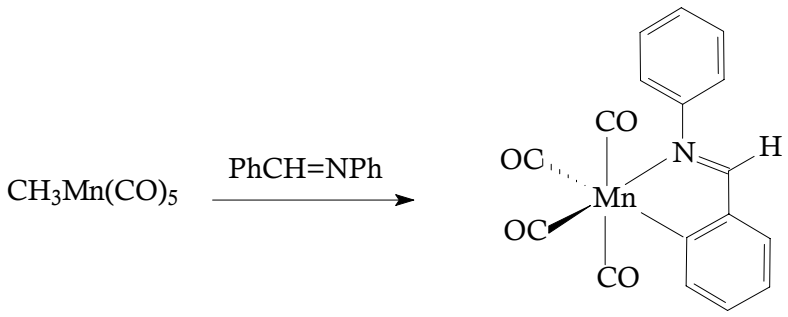

(2.1)

2.1.1 Cyclometalation Reactions via C-H Activation with Imine Anchoring Groups

In this section the activation and functionalization of C-H bonds by solution-phase transition metal-based systems are presented, with an emphasis on the activation of aromatic C-H bonds. Phenyl ketimines and benzlyic imines react smoothly under particularly mild conditions as well as their isoelectronic structural isomers having an azadiene topology (Figure 2.1).[125-126]

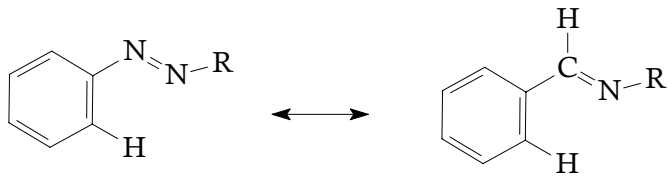

Azadiene Imine

Figure 2.1 Isoelectronic compounds with exchange of N for CH.

The new, stable, and structurally characterized compounds containing N,C-metallacycles can be viewed as models for the organometallic intermediates in ruthenium and rhodium catalyzed C,C-coupling reactions between aromatic imines and olefins utilized in organic synthesis.[60,127] In these reactions, typically conducted in refluxing toluene, the metalated species are not isolated but are converted into metal-free products in a catalytic process. [128]

2.1.1.1 Reactions of $Fe(PMe_3)_4$ with Phenyl Ketimines

Although *ortho*-metalated compounds of imines and other nitrogen donor ligands related to ketimines are known, the only examples for transition metals with *ortho*-metalated ketimines are some osmium complexes obtained with benzophenone-imine by Esteruelas et al.[129-130] These are the first examples of *ortho*-metalated iron compounds of N-donor functional ligands in the literature.

Synthesis and Characterization

Stoichiometric amounts of diphenyl- and *tert*-butylphenylketimine react with $Fe(PMe_3)_4$ in THF at –70 °C . During the warm up process to room temperature, the colour of the mixtures change from dark brown to violet for **1** and to reddish violet for **2** [Eq. 2.2].

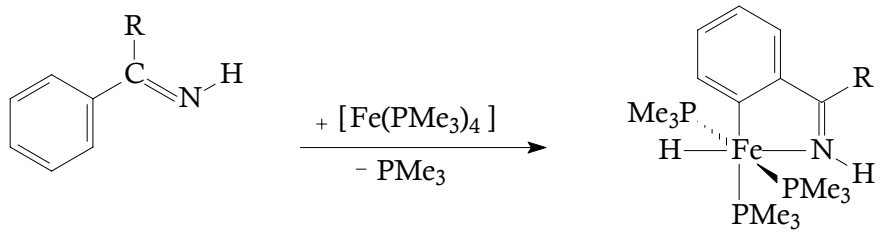

(2.2)

$R = C_6H_5$ **1**
$R = C(CH_3)_3$ **2**

Compounds **1** and **2** crytallize from pentane at –27 °C as dark violet prisms. The yields are 78% for **1** and 48% for **2** respectivelly. Compound **2** is moderately sensitivite while compound **1** is extremely hygroscopic. Under 1 bar argon decompose between 105-118 °C.

Spectroscopic Investigation

IR spectra of the compounds give evidence for hydrido-iron(II) complexes with ν(Fe-H) stretching frequencies at 1730 cm^{-1} for **1** and 1795 cm^{-1} for **2**. ν(N-H) bands are observed with bathochromic shifts between 45-70 cm^{-1} indicating coordination through the N atom. Both spectra show all characteristic bands of coordinated PMe_3 and the coordinated aromatic backbone (Figure 2.2).

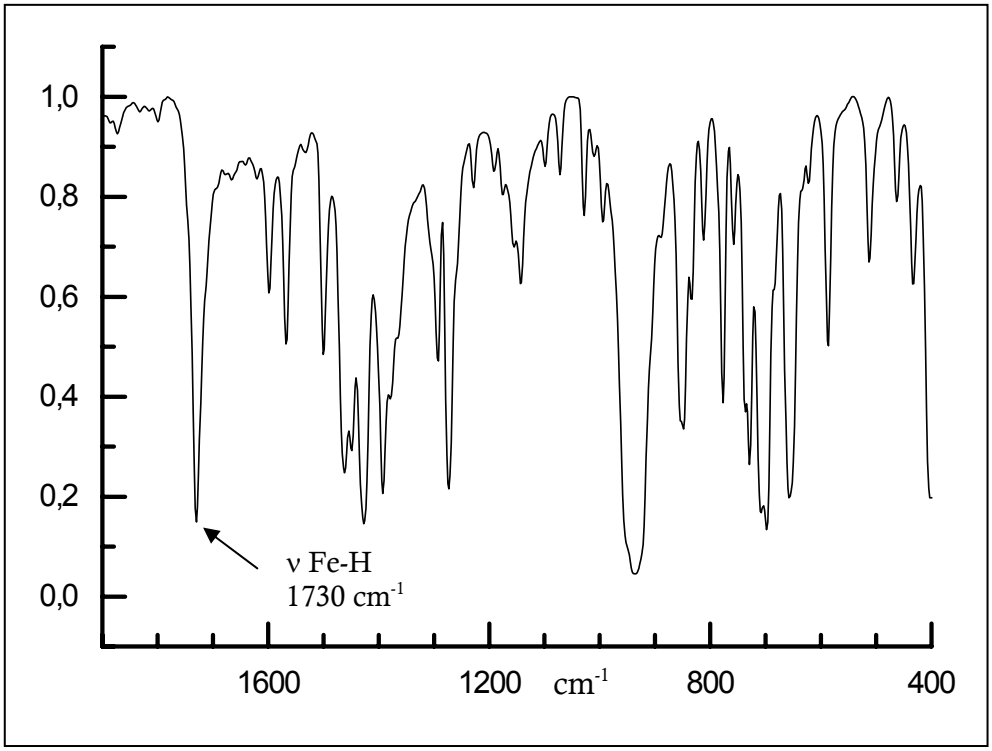

Figure 2.2 IR spectrum of **1** between 1900 - 400 cm^{-1}.

In ^{1}H NMR spectra, Fe-H resonances appear at –16.4 for **1** and –17.5 for **2** as doublets of triplets due to the coupling of hydride nucleus with *trans* and *cis* disposed trimethylphosphines. Both compounds show two sets of enviromentally different PMe_3 groups which indicate that the iron centers have an octahedral coordination environment made up of three PMe_3 ligands in meridional positions (Figure 2.3).

The presence of the *ortho*-metalated imine complexes is also supported by the ^{13}C NMR spectra. Compound **1** contains a doublet at 165.6 ppm ($J_{P,C}$=10.3 Hz) due to a coupling of imine carbon with one of PMe_3 group and a multiplet at 199.9 ppm assigned to metalated aromatic carbon. In compound **2**, they resonate as multiplets at 186.1 ppm (C=N) and 200.1 ppm (Fe-C). The ^{31}P NMR spectra of the two compounds, which are temperature invariant, show couplings of 37 Hz for two sets of PMe_3 groups. The PMe_3 group *trans* to the metalated carbon gives a triplet with a resonance at around 23 ppm and the two isochronic *trans* phosphines appears at 18 ppm as doublets in both cases.

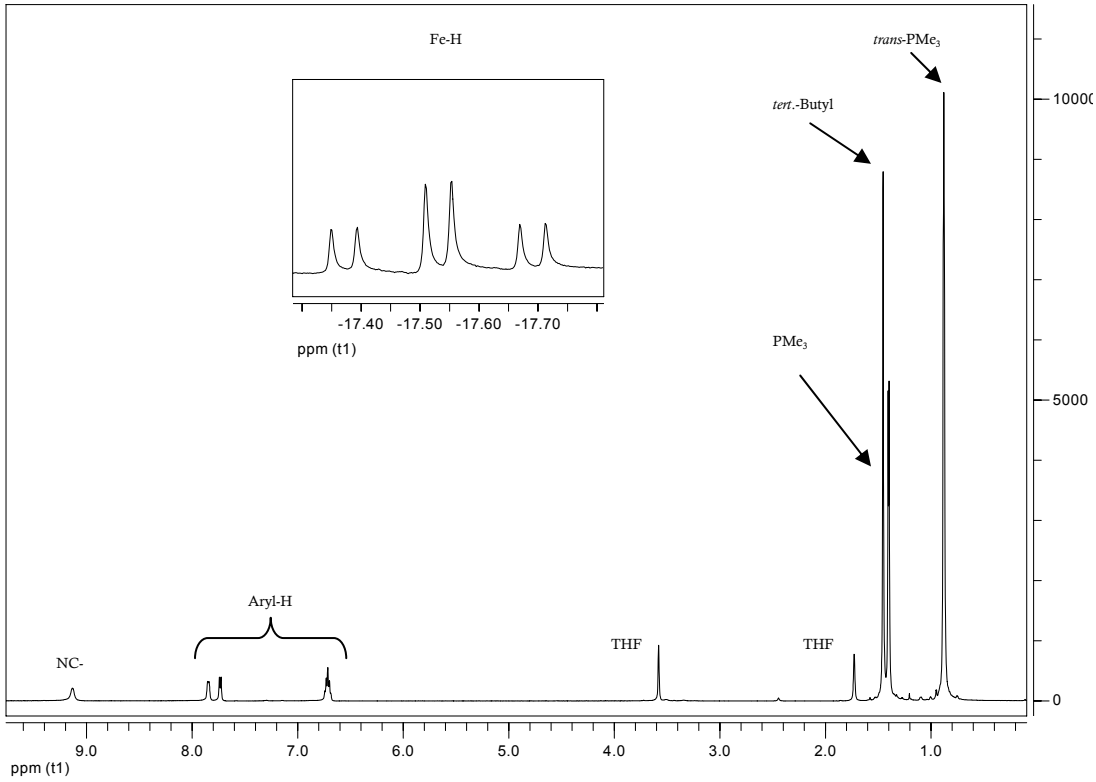

Figure 2.3 ^{1}H NMR spectra of **2** (500 MHz, [D_8]THF, 300 K).

Molecular Structure of 1

The structure was solved in a triclinic crystal system with the space group $P\bar{1}$ and R_1 value of 0.0294. The molecular structure of **1** shows a slightly distorted octahedral frame of donor atoms centered by an iron atom that bears three meridional P donor groups (Figure 2.4). Three remaining ligand positions are occupied by C, N and H atoms of the metalacycle. The angle P3-Fe1-P1=152.878 Å shows a significant deviation from 180° because the hydrogen atom requires very little space. The orthometalated imine ligand acts with a bite angle of 79.0(6)° and the sum of internal angle for the five-membered metallacycle (539.90°) approach as the ideal value for a planar five-membered ring (540°).

The Fe-P distances are in the typical range of 2.18 - 2.22 Å.[131] Fe1-P2 distances is lengthened due to the *trans* influence of the carbon donor. N1-Fe1 and C1-Fe1 distances are also in typical ranges.[132] The C=N bond is lengthened upon coordination from 1.237(3) to 1.314(2) Å. The Fe1-H1 1.480(19) Å is in typical range of a coordinated H to an Fe atom. [133-134]

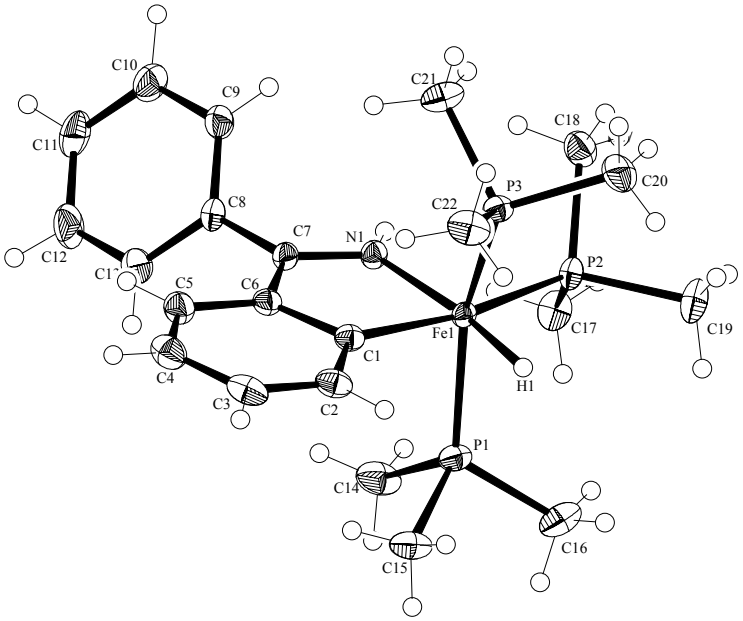

Figure 2.4 Molecular structure of **1**. Selected bond lenghts (Å) and angles (°): Fe1-H1 1.480(19), Fe1-N1 1.9434(13), Fe1-C1 1.9860(15), Fe1-P3 2.1803(5), Fe1-P1 2.1874(5), Fe1-P2 2.2146(5), N1-C7 1.314(2); N1-Fe1-C1 79.0(6); N1-Fe1-H1 172.8(7), P3-Fe1-P1 152.878(18), P3-Fe1-P2 95.320(19), P1-Fe1-P2 95.66(2), N1-Fe1-P3 103.01(4), C1-Fe1-P2 167.36(5).

Molecular Structure of 2

A view of the molecular geometry of **2** is shown in Figure 2.5. The structure was solved in a orthorhombic crystal system with the space group Pnma and a final R_1 value of 0.0378. All non-hydrogen atoms were refined anisotropically, hydrogen atoms with riding model at idealized positions and with isotropic parameters.

The X-ray diffraction study on a single crystal of **2** confirms the structure proposed in eq 1. The iron atom is coordinated in a distorted octahedral fashion with two trimethylphosphines in *trans* positions P1-Fe1-P1A = 153.16(3)°, the third trimethylphosphine is coplanar with the aromatic backbone C1-Fe1-P2 168.98(7)° and the hydrogen atom is *trans* to nitrogen. The coordination sphere is completed by a hydride ligand fixed in a calculated position. An ideal equatorial plane is formed by the atoms C1 and N1 of the *ortho*-metalated imine coordinating with the iron atom to form a five-membered ring with a bite angle N1-Fe1-C1 78.93(9)°. The

sum of the internal angles in the metallacycle (540°) equals that of a regular pentagon.

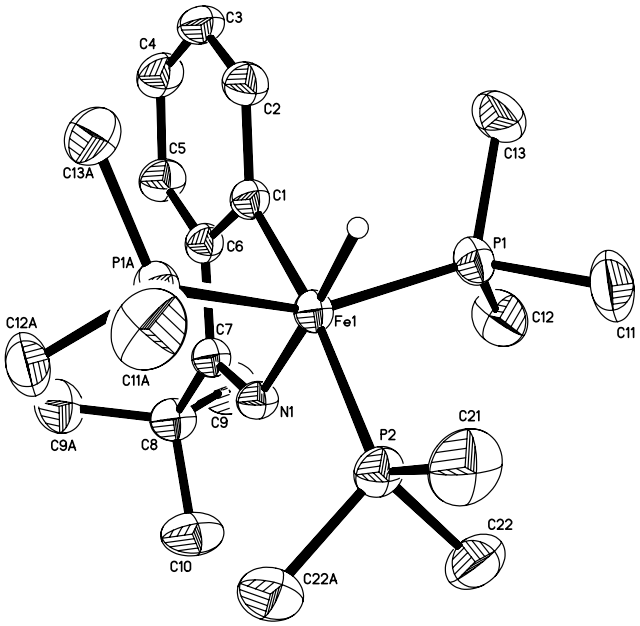

Figure 2.5 Molecular structure of **2** (ORTEP plot with hydrogen atoms omitted). Selected bond lenghts (Å) and angles (°): Fe1-N1 1.9316(19), Fe1-C1 1.966(2), Fe1-P1 2.1739(5), Fe1-P1A 2.1739(5), Fe1-P2 2.2064(8), N1-C7 1.297(3) ; N1-Fe1-C1 78.93(9), C1-Fe1-P2 168.98(7), N1-Fe1-P1 102.105(17), C1-Fe1-P1 68.71(2), P1-Fe1-P2 95.705(18).

The bond lengths Fe1-N1 = 1.9316(19) Å and the Fe1-C1 = 1.966(2) Å are typical for Fe-N and Fe-C(aryl) single bonds. The Fe-P distances are in between 2.17-2.20 Å, which are typical values for Fe(II) compounds.[135]

Discussion

$Fe(PMe_3)_4$ upon reaction with ketimines is transformed to Fe-H complexes under the same mild conditions. The M-H bond plays a very important role in organometallic chemistry because metal hydrides can undergo insertion with a wide variety of unsaturated compounds to give stable species or reaction intermediates

containing M-C bonds.[136] These are not only synthetically useful, but many of the catalytic reactions involve hydride insertion as the key step.[137-139] The discovery of molecular hydrogen complexes stimulated intense activity, which continues today. For such a simple ligand, H has a remarkably rich chemistry.

Elemental analysis and spectral data proves the suggested structures for compounds **1** and **2**. IR studies show Fe-H strecthing frequencies are over 1700 cm^{-1}, these are in the range of typical M-H frequencies 1500-2200 cm^{-1}.[140] Hydrides are usually detected by ^1H NMR because they resonate at high field in a region normally free of other ligand resonances. **1** and **2** show ^1H NMR resonances around -17 ppm. The couplings with *cis* and *trans* phosphines are useful for determining the stereochemistry of the complex. Crystallographic studies of M-H compounds are sometimes problematic like that compound **2** because the hydride when close to a metal atom is such a poor scatter of X rays. Hydrides may not be detected or may not be distinguishable with certanity from random electron density maxima in the neighborhood of the metal like in the case of *Manning's* compound $HFe(CO)_2\{P(OPh)_3\}\{(PhO)_2POC_6H_4\}$ which is obtained on photolysis of the bis (phosphite) complex $Fe(CO)_3\{P(OPh)_3\}_2$.[141-142]

The reaction [Eq. 2.2] may begin with the coordination of the iron adduct to the nitrogen by substituting one of the trimethylphosphines, which brings the metal closer to the *ortho* C-H bond. This chelation assistance results in easier, highly selective C-H bond cleavage to give the cyclometalated iron(II) complex.

2.1.1.2 Reactions of $Fe(CH_3)_2(PMe_3)_4$ with Ketimines

Synthesis and Characterization

When stoichiometric amounts of diphenylketimine or *tert*-butylphenylketimine are added to a THF solution of $Fe(CH_3)_2(PMe_3)_4$ at –70 °C, evolution of gas is observed in both cases during addition and warming up process. The reaction *with tert*-butylphenylketimine is faster than that of diphenylketimine being complete within 20 minutes. Compound **3** crystallizes from pentane at –27 °C as violet prisims with a yield of 74% percent and decomposes at 104°C [Eq. 2.3]. *tert*-Butylphenylketimine reaction gives an extremely low yield of violet crystals which are very air sensitive.

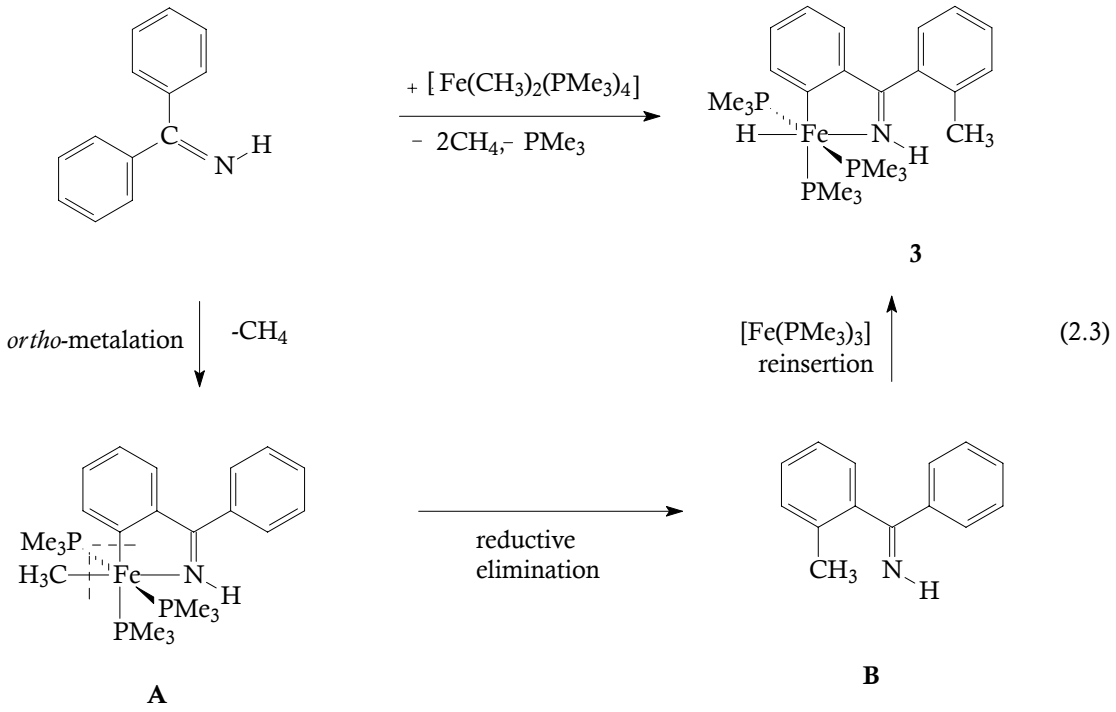

$Fe(CH_3)_2(PMe_3)_4$ reacts first with diphenylketimine to produce a methyl-iron(II) intermediate **A** by elimination of methane. C,C-coupling between methyl and phenyl groups and reductive elimination afford the new aromatic backbone **B**. The Fe(0) complex in solution reinserts into the *ortho* C-H bond of the unsubstituted phenyl ring and forms the hydrido-Fe(II) compound **3**.

Spectroscopic Investigation

IR and NMR data support the structure assigned for **3**. In the IR spectrum, the absorption bands at 3279cm^{-1} and 1761cm^{-1}, respectively, represent (ν N-H) and (ν Fe-H) vibrations. The ligand C=N stretching absorption occurs at significantly lower energy (1500 cm^{-1}) than the free imine C=N stretching absorption (1669 cm^{-1}). The 1300–650 cm^{-1} region of the spectrum shows all characteristic absoprtion bands of coordinated PMe_3, e.g. 935 cm^{-1} (ρ_1 PCH_3) and aromatic backbone e.g. 729 cm^{-1} (γ C-H_{arom}).

In the ^{1}H NMR spectrum (Figure 2.6) the H atom coordinated to the Fe atom gives rise to a doublet of triplets at –17.2 ppm. Two enviromentally different PMe_3 groups give singlet and doublet resonances at 0.99 ppm and 1.41 ppm ($^{2}J_{P,H}$ = 3.3 Hz). The CH_3 group formed by C,C-coupling appears as a singlet at 2.21 ppm. The aromatic protons resonate in the typical low field area between 6.65 and 7.89 ppm. In addition, we can clearly see the N-H signal at 9.25 ppm as singlet. ^{13}C NMR and ^{31}P NMR spectra support the suggested structure. The imine carbon atom and metalated carbon resonate as multiplets at 181.2 ppm and 203.1 ppm, respectively. The Ar-CH_3 protons appear as singlet at 21.1 ppm. Trans PMe_3 groups resonate as multiplet at 15.7 ppm and PMe_3 *cis* disposed to H appears as triplet with a coupling constant $^{2}J_{P,P}$ = 38.3 Hz. These data support an *mer*-octahedral hydrido-Fe(II) complex with three PMe_3 ligands and a coordinated imine backbone.

The product from the reaction of *tert*-butylphenylketimine with $Fe(CH_3)_2(PMe_3)_4$ is also a Fe-H complex. In the IR there is a strong metal hydride stretching band (ν Fe-H) at 1777 cm^{-1} but (ν C=N) and (ν C=C) signals are very weak. The ^{1}H NMR spectrum shows two broad different Fe-H resonances around –4.9 and –14.3 ppm which are assigned to two different products of unknown constitution.

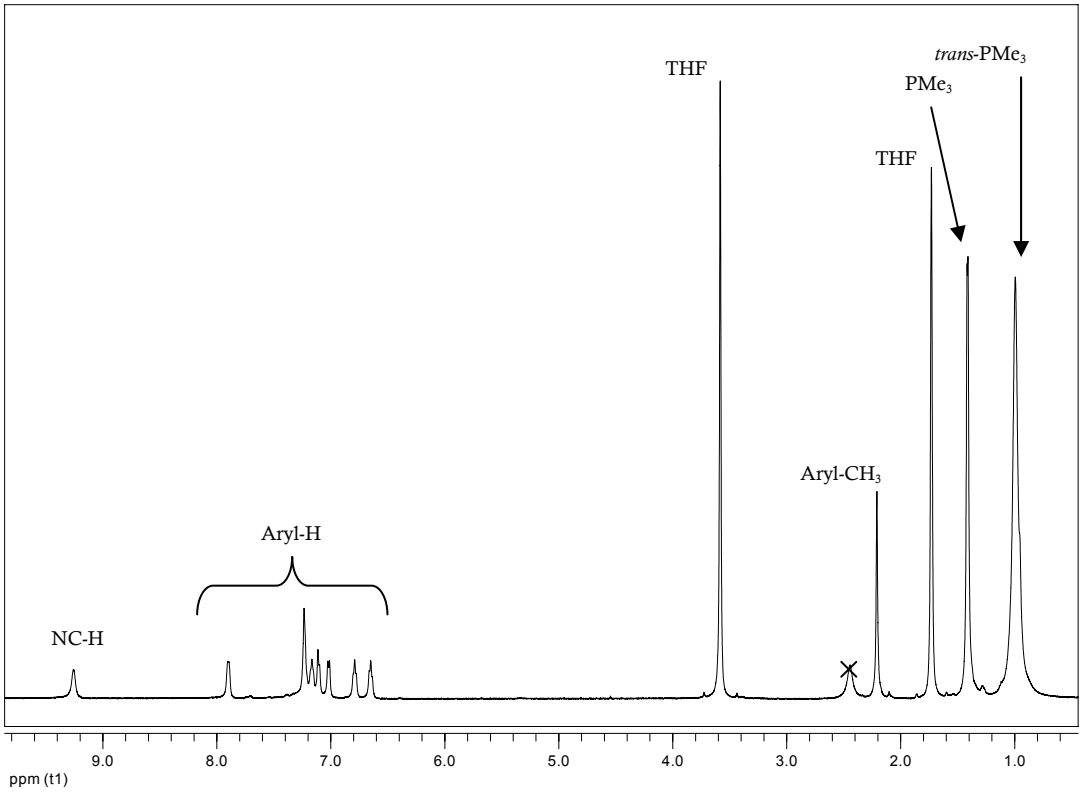

Figure 2.6 ^{1}H NMR spectra of **3** (500 MHz, [D_8]THF, 300 K).

Molecular Structure of 3

The crystal structure of compound **3,** Figure 2.7, was solved in a triclinic crystal system and the space group was determined as $P\bar{1}$. The refinement resulted in an R value of 0.0365. X-ray diffraction analysis of **3** indicates that the imine reactant binds to iron through two atoms (N1 and C1) and forms a five-membered metallacycle with a bite angle N1-Fe1-C1 = 79.52(6)°. The sum of internal angles is that of a planar five-membered ring. An octahedral coordination with three PMe_3 ligands in meridional positions and is completed by a hydride ligand in calculated position which is *trans* to nitrogen. Two trimethylphosphine groups are in opposite positions, P2-Fe1-P3 = 149.64(2)°, and one trimethylphosphine group is *cis* to nitrogen, N1-Fe1-P1 = 87.25(4)°.

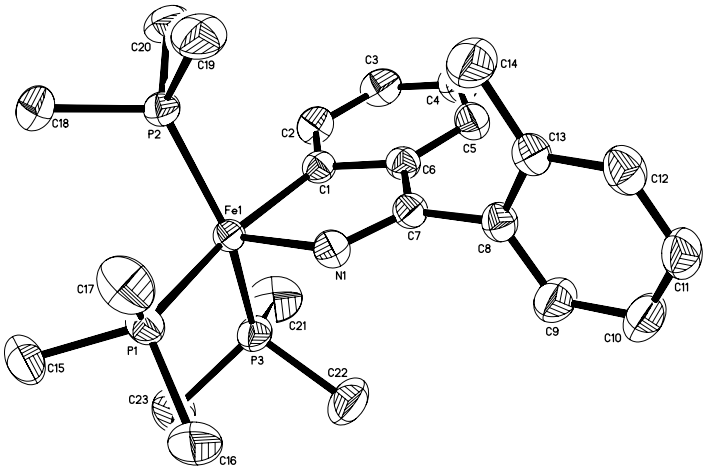

Figure 2.7 Molecular structure of **3** (ORTEP plot with hydrogen atoms omitted). Selected bond lenghts (Å) and angles (°): Fe1-C1 1.9820(17), Fe1-N1 1.9438(14), N1-C7 1.306(2), Fe1-P1 2.2180(5), Fe1-P2 2.1784(5); Fe1-P3 2.1751(5); N1-Fe1-C1 79.52(6), P2-Fe1-P3 149.64(2), C1-Fe1-P1 166.77(5), N1-Fe1-P3 102.82(5); N1-Fe1-P2 105.75(5) N1-Fe1-P1 87.25(4).

The molecular structure of **3** in particular confirms the new formed CH_3 group C8-C13-C14 = 121.01(17)° and C13-C14 = 1.498(3)Å. The bond length of Fe1-N1 = 1.9438(14) Å and the Fe1-C1 = 1.9820(17) Å are typical for Fe-N and Fe-C(aryl) single bonds, respectively, and are in agreement with the values found for compounds **1** and **2**. The Fe-P distances 2.17-2.20 Å, attain typical values for octahedral Fe(II) compounds.[143-146]

Discussion

The reaction of diphenylketimine with $Fe(CH_3)_2(PMe_3)_4$ presented an methyl-iron(II) complex with a C,C-coupling between an sp^2 carbon of the aromatic backbone and an sp^3 carbon of the CH_3 fragment. This novel type of coupling suggests a reaction pathway. The reaction sequence starts with the C-H activation in an *ortho* position affording a methyl-iron(II) intermediate. This undergoes a reductive C,C-coupling as second step. The iron adduct in solution cyclometalates again with the imine ligand and the final hydrido-iron(II) compounds formed.

Table 2.1 and Table 2.2 summarize the spectroscopic and structural properties of complexes **1**-**3**.

All three compounds display strong absorption bands between 1700-1800 cm^{-1} which arise from a stretching vibration of ν(Fe-H). Hyride resonances are observed around –17 ppm as expected. Because of the strong *trans* influence of aromatic sp^2 carbon, Fe-P bond length which is *trans* to metalated carbon is clearly longer than the other Fe-P distances in all three stuctures. They all attain a distorted octahedral geometry and the iron atom is part of a five-membered metallacycle of a chelating imine ligand.

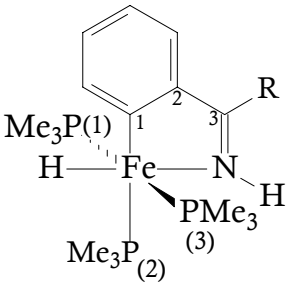

R : C_6H_5 **1**

R : $C(CH_3)_3$ **2**

R : o-C_6H_5-CH_3 **3**

IR, cm^{-1} :	**1**	**2**	**3**
ν (Fe-H)	1730	1795	1761
^{1}**H-NMR**, ppm :	**1**	**2**	**3**
δ FeH	-16.4; dt $^{2}J_{P,H}$ = 22.8 Hz, $^{2}J_{P,H}$ = 81.3 Hz	-17.5; dt $^{2}J_{P,H}$ = 21.8 Hz, $^{2}J_{P,H}$ = 80.0 Hz	-17.2; dt $^{2}J_{P,H}$ = 22.5 Hz, $^{2}J_{P,H}$ = 82.3 Hz
δ $P_{(1)}$Me, δ $P_{(3)}$PMe	0.94, s	0.88, s	0.99, s
δ $P_{(2)}$Me	1.42; d $^{2}J_{P,H}$ = 4.7 Hz	1.40; d $^{2}J_{P,H}$ = 4.5 Hz	1.41; d $^{2}J_{P,H}$ = 3.3 Hz
^{13}**C-NMR,** ppm :	**1**	**2**	**3**
δ C_3=N	180.2; d $^{3}J_{P,C}$ = 10.3 Hz	186.1; m	181.2; d $^{3}J_{P,C}$ = 10.3 Hz
δ Fe-C_1	204.1; m	200.1; m	203.1; m
^{31}**P-NMR**, ppm:	**1**	**2**	**3**
δ $P_{(1)}$Me, δ $P_{(3)}$Me	18.2; d $^{2}J_{P,P}$ = 37.4 Hz	18.2; d $^{2}J_{P,P}$ = 36.5 Hz,	15.7; m
δ $P_{(2)}$Me	22.5; t $^{2}J_{P,P}$ = 37.4 Hz	23.7; t $^{2}J_{P,P}$ = 36.5 Hz	21.2; t $^{2}J_{P,P}$ = 38.3 Hz

Table 2.1: Selected spectrocopic data of hydrido-Fe(II) complexes **1-3**.

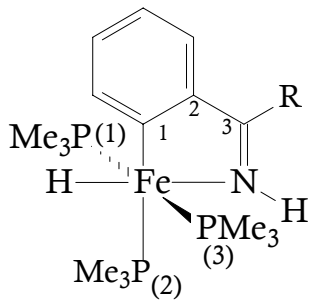

R : C_6H_5 **1**

R : $C(CH_3)_3$ **2**

R : o - C_6H_5 - CH_3 **3**

Bond lenghts, [Å]	**1**	**2**	**3**
Fe – C1	1.9860(15)	1.9660(2)	1.9820(17)
Fe – N	1.9434(13)	1.9316(19)	1.9438(14)
Fe – P1	2.1874(5)	2.1739(5)	2.1784(5)
Fe – P2	2.2146(5)	2.2146(5)	2.2180(5)
Fe – P3	2.1803(5)	2.1739(5)	2.1751(5)
Bond angles, [°]	**1**	**2**	**3**
C1 – Fe – N	79.60(6)	78.93(9)	79.52(6)
C1 – Fe – P1	87.08(4)	86.71(2)	88.23(5)
C1 – Fe – P2	167.36(5)	168.96(7)	166.77(5)
C1 – Fe – P3	87.59(4)	86.71(2)	87.04(5)
P1 – Fe – P3	152.878(18)	153.16(3)	149.64(2)
N – Fe – P1	102.13(4)	102.105(17)	105.75(5)
N – Fe – P2	87.76(4)	90.03(6)	87.25(4)
N – Fe – P3	103.01(4)	102.105(17)	102.82(5)
Σ (5-Ring)	**1**	**2**	**3**
	539.90°	540.00°	539.99°

Table 2.2 Selected bond lenghts and angles of hydrido-Fe(II) complexes **1-3**.

2.1.1.3 Reactions of $Fe(CH_3)_2(PMe_3)_4$ with Benzylic Imines

In this part, the reactions of $Fe(CH_3)_2(PMe_3)_4$ with *N*-methyl-, *N*-isopropyl- and *N*-phenylbenzylideneimines are demonstrated. Reactions of simple imines (R_2C=NR) with basic iron compounds have not been described to date although such reactions have been carried out with other transition metal complexes and have drawn much attention.[147-153] In most cases complexes with N-coordinated imine ligands,

bidentate *ortho*-metalated ligands, iminoacyl ligands, bridging amide ligands, and ligands have been obtained which result from coupling of the imine function with other unsaturated functional groups. Their particular activity is well-known from the palladium N-isopropylbenzylideneimine catalyst for the Suzuki reaction which catalyzes the coupling of aryl bromides and phenylboronic acid with extremely high efficieny.[87]

Synthesis and Characterization

Benzylic imines (N-methyl-, N-isopropyl-, and N-phenylbenzylideneimines) react with $Fe(CH_3)_2(PMe_3)_4$ in THF at –70 °C through the elimination of methane to afford the hexacoordinate iron(II) complexes **4-6** [Eq 2.4].

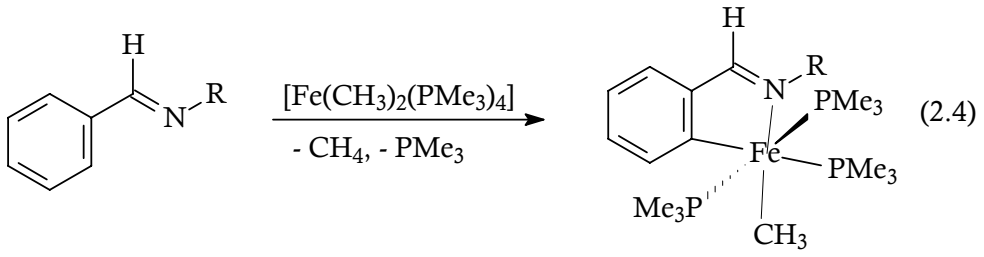

(2.4)

R = CH_3 **4**
R = $CH(CH_3)_2$ **5**
R = C_6H_5 **6**

While violet solutions of **4** and **5** in pentane deposite crystals at –27°C petroleum green **6** crystallizes at 4 °C. The solids have moderate air-sensitivity and under argon decompose at 115 °C, 116 °C, and 119 °C, respectively.
Elemental compositions show that the loss of methane and one of the trimethylphosphine groups during the reaction.

Spectroscopic Investigations

The infrared spectrum of each compound exhibits a ν (C=N) absorption of the coordinated imine ligand (R=CH_3, 1572 cm^{-1} (m); R= $CH(CH_3)_2$, 1519 cm^{-1} (m); R=C_6H_5, 1543 cm^{-1} (w)) which occur at significantly lower energies than the free

imine C=N stretching absorptions, the (ν C=N, 1651 cm^{-1}) in free PhCHNMe. In all three spectra, δ (Fe-CH_3) absorptions are recognized at 1180 cm^{-1} (**4**); 1162 cm^{-1} (**5**); 1193 cm^{-1}, 1170 cm^{-1} (**6**), although insenties are weak.

Complexes **5** and **6** decompose in THF solution. The ^{1}H NMR spectrum of **4** in d_8–THF exhibits a broad singlet resonance at 1.38 ppm due to the metal-coordinated methyl group along with the expected resonances for the protons of the metalated phenyl ring from 6.74 ppm to 7.87 ppm. The trimethylphosphine protons resonate at 0.71 ppm and 1.49 ppm as broad singlets. The ^{13}C NMR (Figure 2.8) data also agree well with the structure proposed in [Eq 2.3]. Fe-CH_3 carbon has a resonance at –16.6 ppm (dt, $^2J_{P,C}$ = 25.6 Hz, $^2J_{P,C}$ = 8.2 Hz) and the metalated carbon atom resonates at 206.6 ppm (dt, $^2J_{P,C}$ = 26.2 Hz, $^2J_{P,C}$ = 6.2 Hz) with expected chemical shifts.

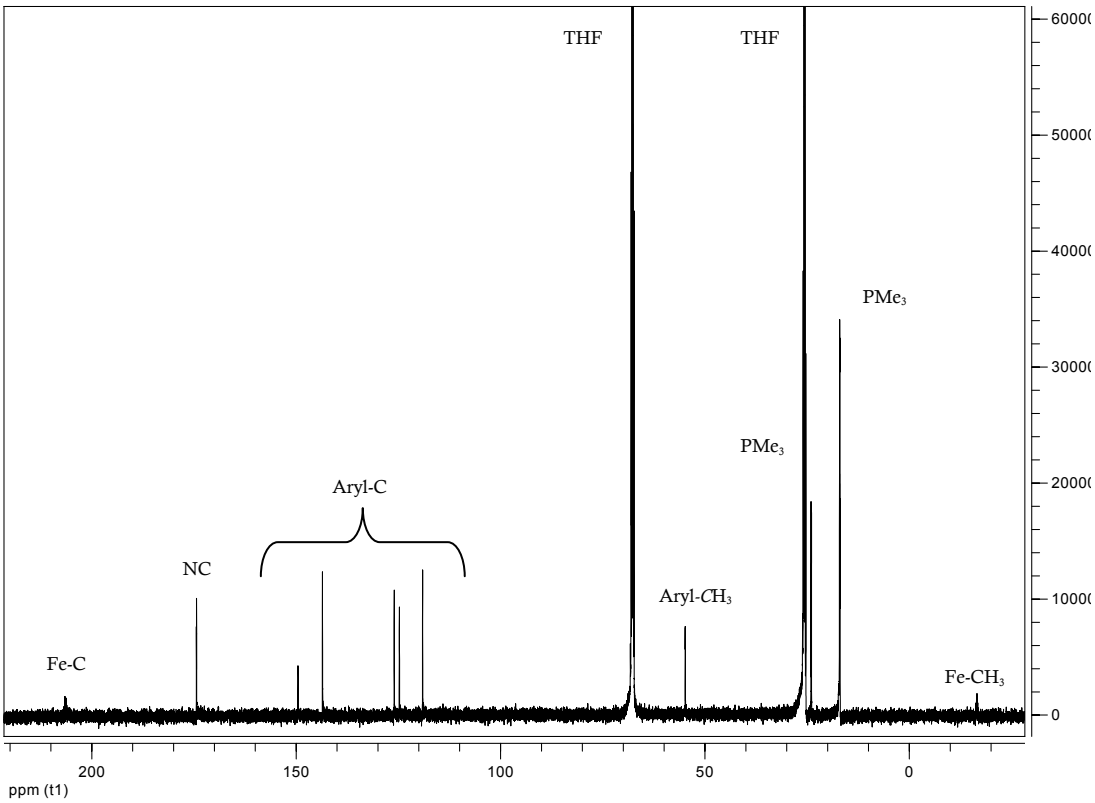

Figure 2.8 ^{13}C NMR spectra of **4** (125 MHz, [D_8]-THF, 300 K).

The ^{31}P NMR spectrum shows a triplet at 7.6 ppm ($^2J_{P,P}$ = 35.6 Hz) and a doublet at 16.7 pmm ($^2J_{P,P}$ = 35.6 Hz) with P-P coupling as expected for a mer configuration of **4** (Figure 2.9).

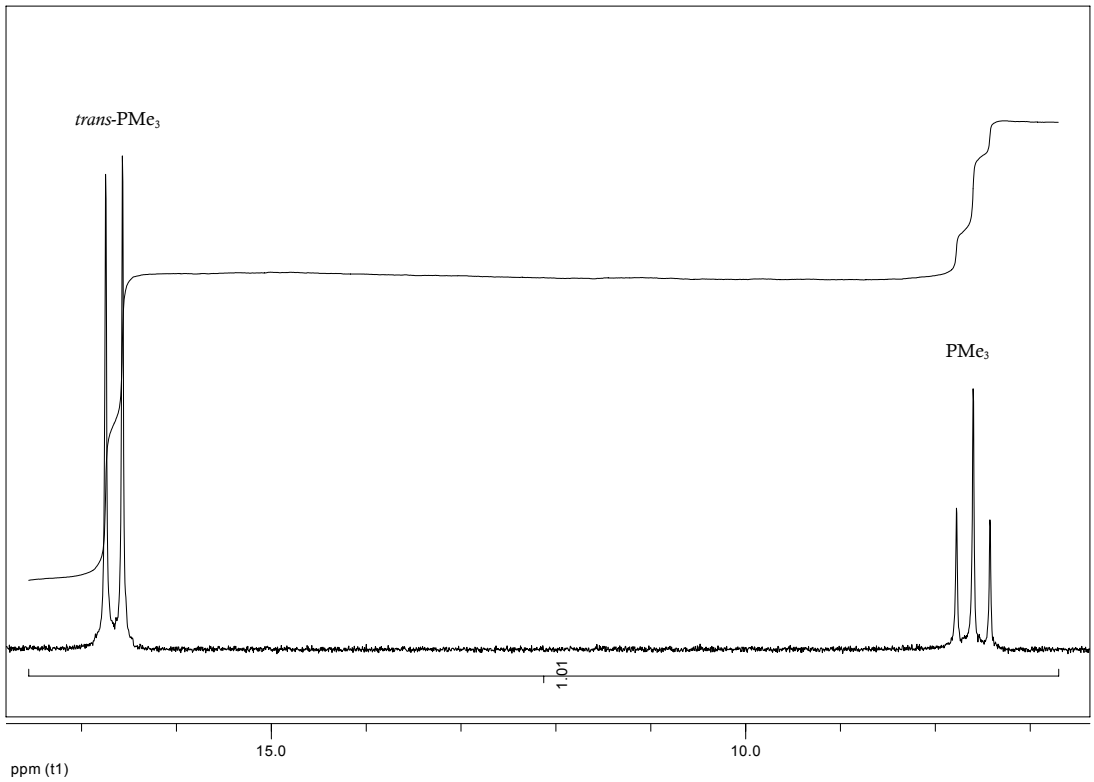

Figure 2.9 ^{31}P NMR spectra of **4** (202 MHz, $[D_8]$THF, 300 K).

Molecular Structure of 4

The definitive characterization of **4** as an ortho-metalated imine complex is derived from an X-ray diffraction experiment on a single crystal. The structure was solved in a triclinic crystal system with the space group of $P\bar{1}$ and a final R_1 value of 0.0526 was obtained. Figure 2.10 shows an ORTEP drawing of the molecule with selected bond distances and angles.

The coordination geometry around the iron atom octahedral with two P-donor atoms of the occupying *trans* positions: P1-Fe1-P3 = 168.04(4)°. The perpendicular plane is formed by the atoms C2 and N1 of the orthometalated *N*-methylbenzylideneimine (N1-Fe1-C2 = 80.34(13)°), defining a five-membered ring with the iron atom, the P2 atom of the trimethylphosphine group disposed *trans* to to C2 (C2-Fe1-P2 = 176.97(11)°) and the CH_3 ligand located in opposite position to the nitrogen atom (N1-Fe1-C1 = 169.91(16)°).

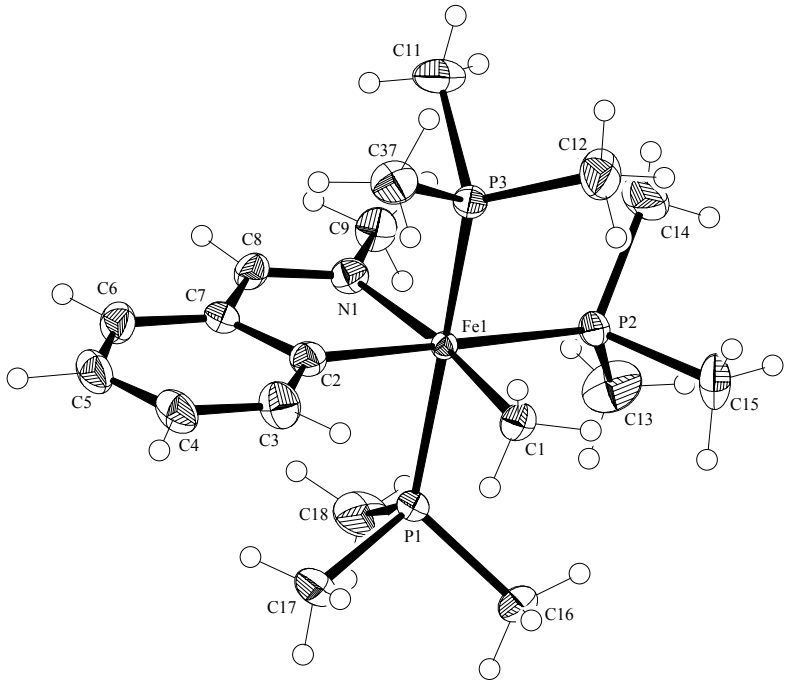

Figure 2.10 Molecular structure of **4**. Selected bond lenghts (Å) and angles (°):Fe1-C1 2.085(4), Fe1-C2 1.987(4), Fe1-N1 2.014(3), N1-C8 1.290(5), Fe1-P1 2.2241(11), Fe1-P2 2.2568(11), Fe1-P3 2.2037(11); N1-Fe1-C1 169.91(16), N1-Fe1-C2 80.34(13), C2-Fe1-P2 176.97(11), P1-Fe1-P3 168.04(4), N1-Fe1-P1 93.76(9), C1-Fe1-P3 85.08(15).

The Fe1-N1 bond length of 2.014(3) Å and the Fe1-C2 bond distance of 1.987(4) Å are typical for Fe-N and Fe-C_{aryl} single bonds. The Fe-P distances range between 2.20-2.26 Å and are in agreement with the values previously found in complexes **1-3**.

Molecular Structure of 6

The octahedral configuration of **6** has been confirmed in the crystal. The structure was solved in a monoclinic crystal system and the space group was determined as P21/n. The refinement resulted in an R value of 0.0290. Figure 2.11 shows the *ortho*-metalated iron(II) complex.

The configuration about the iron atom is close to octahedral; the principal distortions are related to the angle of 80.12(6)° subtended by the chelating atoms and to a nonlinearity of the P2-Fe-P3 vector. The chelate ligand coordinates via Fe-

N and M-C σ bonds in an *ortho* position of the benzylidene phenyl ring which is analogous to compound **5**.

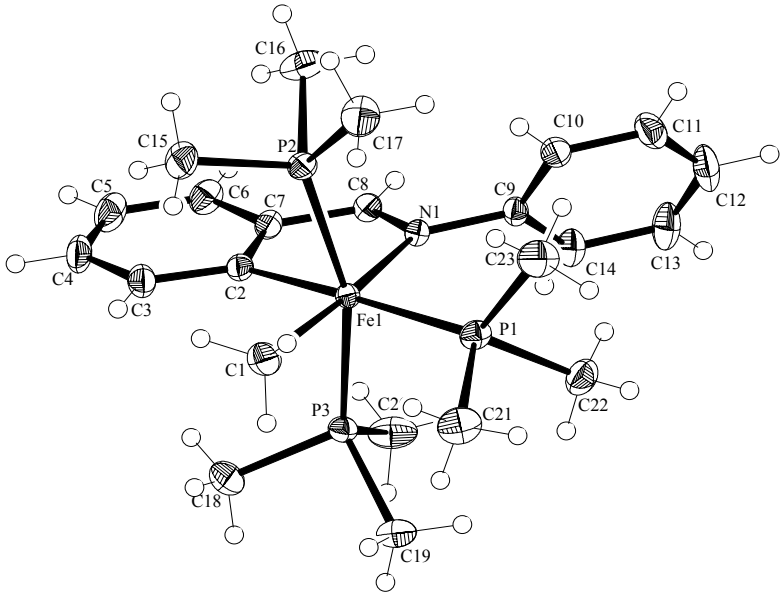

Figure 2.11 Molecular structure of **6**. Selected bond lenghts (Å) and angles (°):Fe1-C1 2.0972(17), Fe1-C2 2.0184(16), Fe1-N1 2.0130(13), N1-C8 1.317(2), Fe1-P1 2.2954(5), Fe1-P2 2.2500(5), Fe1-P3 2.2370(5); N1-Fe1-C1 175.05(6), N1-Fe1-C2 80.12(6), C2-Fe1-P1 175.15(4); P2-Fe1-P3 161.464(18); N1-Fe1-P3 94.68(4); C1-Fe1-P2 85.45(5).

On the whole, the confirmation of the coordinated imine ligand closely resembles that of free benzylideneimines.[154] The aniline phenyl ring is rotated by 61.2° away from the imine plane in the complex ; the corresponding twist in the free ligand is 55°. The other phenyl ring is coplanar with the imine grouping, forming a dihedral angle of 3.0° with the imine plane, as compared to a value of 10° in free imine. The C=N bond is lengthened upon coordination from 1.237(3) to 1.317(2) Å. The N-C9 and C7-C8 distances of 1.4434(19) Å and 1.437(2) Å are both mariginally shorter than the corresponding bond lengths of 1.460(3) Å and 1.496(3) Å in free imine. The Fe-N 2.0130(13) Å, Fe-C(sp^2) 2.0184(16) Å and Fe-P distances fall within the literature range and are compatible with compounds **1**- **4**.[155]

Discussion

Reactions of $Fe(CH_3)_2(PMe_3)_4$ with benzylic imines afford methyl-iron(II) complexes, **4**-**6**. The solids are moderately air sensitive but solutions of **5** or **6** undergo thermal decomposition in THF. The strucutre of **5** is proposed to bear in for **4** and **6** as models. Table 2.3 presents selected bond lenghts and angles of **4** and **6**.

Similar to the hyrido-iron(II) complexes, the reaction is believed to begin with coordination of the iron adduct to the nitrogen by substitution of one trimethylphosphine, bringing the metal closer to the *ortho* C-H bond. This chelation assistance facilitates highly selective C-H bond cleavage to give a cyclometalated iron(IV) intermediate. Reductive elimination of CH_4 results in an *ortho*-metalated methyl-iron(II) complex with three trimethylphosphine ligands. Alkyl complexes of iron(II) are usually coordinatively saturated, 18 electron species supported by cyclopentadienyl and carbonyl ligands.[156]

Transition metal alkyl complexes are of practical importance due to their role in numerous catalytic transformations such as olefin hydrogenation, hydroformylation, and polymerization.[157] It is the existence of several decomposition pathways that makes many transition metal alkyls unstable. Early efforts to prepare simple alkyls or aryls of transition metals showed that such compounds were generally unstable under ambient conditions. Despite the synthesis of $[Me_3PtI]_4$ by Pope and Peachy, it was assumed until quite recently that ,metal-carbon bonds are weak.[158] In fact, we now know that such M-C bonds are reasonably strong ranging 165-350 kJ mol^{-1}. When it was found that the presence of ligands such as η-C_5H_5, CO or PR_3 allowed the synthesis of thermally stable compounds, it was considered that the presence of such ligands provided better overlap between sp^3 hybridized carbon and metal orbitals implying increased bond strength. A lacking β-decomposition pathway by choice of a Fe-CH_3 group, ablocking imine ligand and a PMe_3 ligand are in favor of stable compounds **4**-**6**. At variance with the methyl-iron(II) intermediate of compound **3** [Eq. 2.3], there is no reductive C,C-coupling in the formation of compound **6**. The principles governing their stability make a useful starting point in order to understand some of the most important organometallic reactions.

Unexpectedly, no reaction was observed between $Fe(PMe_3)_4$ and benzylic imines.

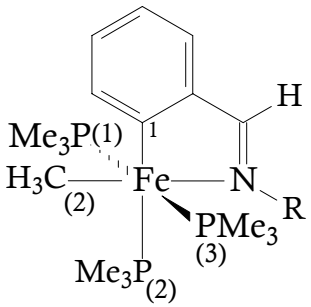

R : CH_3 **4**

R : C_6H_5 **6**

Bond lenghts, [Å]	**4**	**6**
Fe – C1	1.987(4)	2.0184(16)
Fe – C2	2.085(4)	2.0972(17)
Fe – N	2.014(3)	2.0130(13)
Fe – P1	2.2241(11)	2.2370(5)
Fe – P2	2.2568(11)	2.2954(5)
Fe – P3	2.2037(11)	2.2500(5)
Bond angles, [°]	**4**	**6**
C1 – Fe – N	80.34(13)	80.12(6)
C2 – Fe – N	169.91(16)	175.05(6)
N – Fe – P1	93.76(9)	94.68(4)
N – Fe – P3	94.53(9)	93.38(4)
C1 – Fe – P2	176.97(11)	175.15(4)
P1 – Fe – P3	168.04(4)	161.464(18)
Σ (5-Ring)	540.04	539.88

Table 2.3 Selected bond lenghts and angles of methyl-Fe(II) complexes **4** and **6**

2.1.1.4 Iodomethane Reactions of Hydrido-Iron(II) Complexes

The hydrido-iron(II) complexes **1-3** are good canditates for oxidative addition reactions. Potential ligands that do not have a lone pair or filled π type orbitals are still able to interact with transition metal complexes by breaking a σ bond. Using iodomethane as a substrate, the interesting question arises to whether attack by the

metal would proceed as a regioselective addition or promote ring opening through a subsequent reductive C,C-coupling reaction.

Synthesis and Characterization

Reactions of **1** – **3** in pentane proceeds as described in [Eq. 2.5].

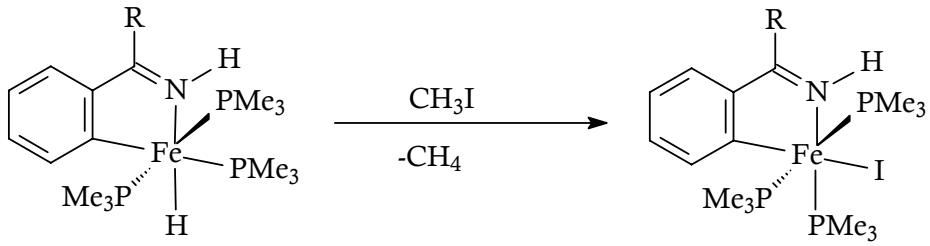

(2.5)

1, **2**, **3**

R = C_6H_5 **7**
R = $C(CH_3)_3$ **8**
R = o-$CH_3(C_6H_4)$ **9**

When iodomethane is added to the hydrido-iron(II) complexes at –70 °C, evolution of gas is observed during warm up process. Compounds **7** - **9** crystallize from pentane at 4 °C. Table 2.4 shows some important properties.

Metallacycle	Yield [%]	Color and shape of crystals	Decomposition [°C]
7	77	dark pink cubes	<143
8	75	dark purple rods	<160
9	72	reddish orange plates	<146

Table 2.4 Properties of **7** – **9**.

Spectroscopic Investigations

IR spectra give a first clue to the structures of **7**-**9**. Strong stretching absorptions of Fe-H over 1700 cm^{-1} are absent, and there is a bathochromic shift in all characteristic bands.

Table 2.5 shows some important NMR data of **7** - **9**. Parallel to IR, they show similar spectroscopic characteristics.

In the ^{1}H NMR spectra, there is no Fe-H resonance at high field and trimethylphosphine ^{1}H and ^{13}C resonances are shifted to low field. Phosphorus nuclei *trans* to each other resonate around 1.1 ppm and the third around 1.6 ppm. We can see clearly the metalated carbons in ^{13}C-NMR at 208.1 ppm, 208.4 ppm, and 209.3 ppm respectively which are shifted to lower field than in the hydrido-iron(II) compounds. The observed patterns in the ^{31}P NMR spectra are consistent with a meridional arrangement of the three trimethylphoshines. On the basis of chemical shifts, the electron density at the iron nucleus is subject to the σ-electron withdrawing power of the halides.[159]

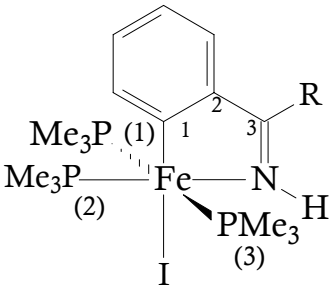

R : C_6H_5 **7**

R : $C(CH_3)_3$ **8**

R : o-C_6H_5-CH_3 **9**

^{1}H-NMR, ppm :	**7**	**8**	**9**
δ $P_{(1)}Me$+ δ $P_{(3)}PMe$	1.09; t' $\lvert {}^{2}J_{P,H} + {}^{4}J_{P,H} \rvert$ =6.6Hz	1.06; s	1.17; t' $\lvert {}^{2}J_{P,H} + {}^{4}J_{P,H} \rvert$ =6.4Hz
δ $P_{(2)}Me$	1.66; d $^{2}J_{P,H}$ = 6.6 Hz	1.61; d $^{2}J_{P,H}$ = 5.9 Hz	1.67; d $^{2}J_{P,H}$ = 6.4 Hz
^{13}C-NMR, ppm :	**7**	**8**	**9**
δ C_3=N	181.9; m	187.8, m	182.9; m
δ Fe-C_1	208.1; m	208.4; m	209.3; m
^{31}P-NMR, ppm:	**7**	**8**	**9**
δ $P_{(1)}Me$, δ $P_{(3)}PMe$	11.3; d $^{2}J_{P,P}$ = 57.0 Hz	13.1; d $^{2}J_{P,P}$ = 55.9 Hz,	10.8; d $^{2}J_{P,P}$ = 57.5 Hz
δ $P_{(2)}Me$	17.7; t $^{2}J_{P,P}$ = 57.0 Hz	19.9; t $^{2}J_{P,P}$ = 55.9 Hz	19.2; t $^{2}J_{P,P}$ = 57.5 Hz

Table 2.5 Some selected spectrocopic data of complexes **7-9**.

While elemental analyse confirm the composition of **7-9** and X-ray determination demonstrates the molecular structures.

Molecular Structure of 7

A molecule of the compound **7** is depicted in Figure 2.12. In an octahedral geometry, a meridional arrangement of the three trimethylphosphines is recognized. The remaining three coordination sites are occupied by an iodide and a chelating imine ligand. The iodide and one trimethylphosphine P-donor are coplanar with the metallacycle forming an angle P2-Fe1-I1 97.87(3)°. Because of its weak *trans* influence the iodide is coordinated *trans* to the metalated carbon C1-Fe1-I1 166.44(9)°. The five-membered metallacycle has a bite angle of 80.05(12)° and the sum of internal angles (539.85°) approach the ideal value of a planar five-membered ring. Complex **7** is distorted than **1** because iodine ligand restricts the flexibility of the trimethylphosphine groups.

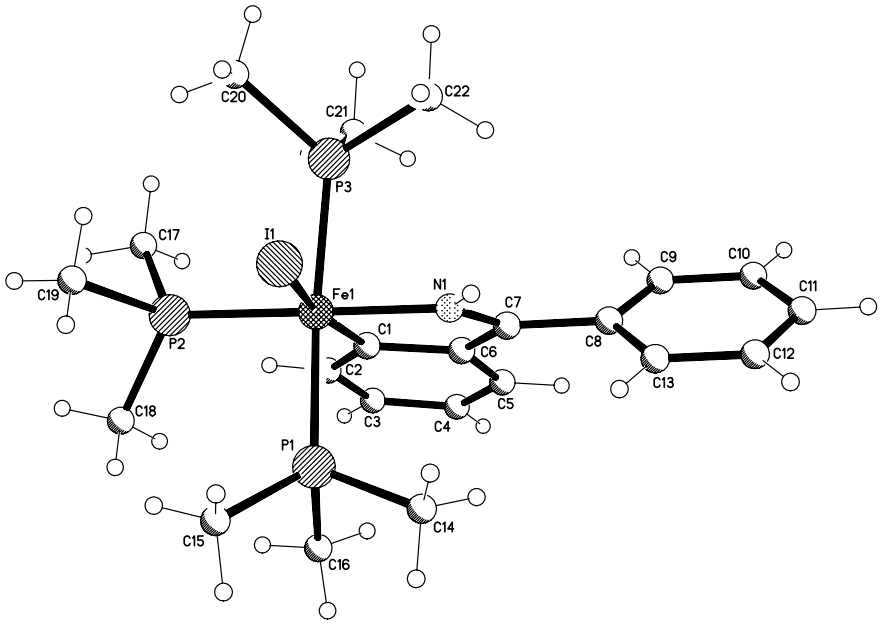

Figure 2.12 Molecular structure of **7**. Selected bond lenghts (Å) and angles (°):Fe1-C1 1.957(3), Fe1-N1 1.940(2), Fe1-I1 2.7616(5), N1-C8 1.294(4), Fe1-P1 2.2587(9), Fe1-P2 2.2350(9), Fe1-P3 2.2568(9); N1-Fe1-C1 80.05(12), C1-Fe1-I1 166.44(9), N1-Fe1-P1 88.68(8); N1-Fe1-P2175.24(9); N1-Fe1-P3 85.93(8); N1-Fe1-I 86.64(8); C1-Fe1-P2 95.51(9)

N1-Fe1 and C1-Fe1 distances are 1.940(2)Å and 1957(3)Å, respectively and fall in the expected range. The Fe1-I1 distance 2.7616(5)Å agrees with the Fe-I 2.6646Å distance in an *ortho*-metalated octahedral Fe(II) compound $Fe(CO)_2\{P(OPh)_3\}\{(PhO)_2POC_6H_4\}(I)$.[160] Because of the weak *trans* influence of iodine, the Fe1-C1 distance is 0.029 Å smaller than Fe1-C1 in compound **1**. The two mutually *trans* trimethylphosphine groups have long Fe-P distances (mean 2.25 Å) compared with the one that is *trans* to the N atom (Fe-P = 2.2350(9) Å) due to a sizeable *trans* influence of trialkylphosphines. All bond lengths are well-matched with the other structural features.[161-162]

Molecular Structure Analysis of 8

Figure 2.13 is a diagram of the structure of molecule **8**.

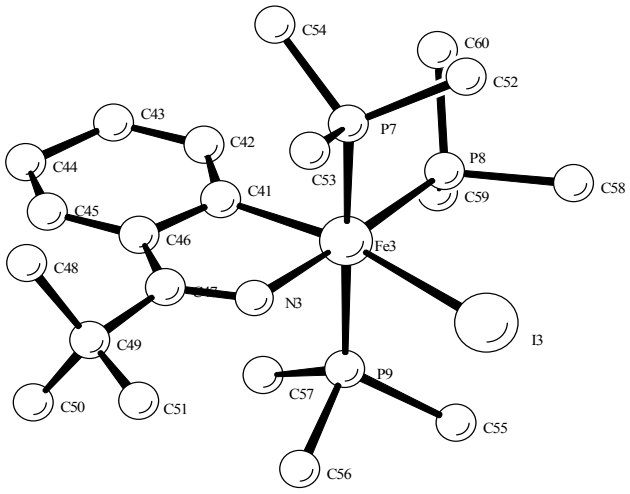

Figure 2.13 Molecular structure of **8**. Selected bond lenghts (Å) and angles (°): Fe3-C41 2.03(3), Fe3-N3 1.94(3), Fe3-I3 2.789(6), Fe-P7 2.261(13), Fe-P8 2.249(11), Fe-P9 2.253(13); C41-Fe3-N3 79.6(14), C41-Fe3-I3 165.1(9), C41-Fe3-P7 92.5(10), C41-Fe-P8 96.6(10), C41-Fe3-P9 91.8(10), N3-Fe3-I3 85.6(10), N3-Fe3-P8 176.1(11), P9-Fe3-P7 172.3(5).

A crystal of compound of the compound **8** contains three crystallographically independent molecules separated by van der Waals interactions. These are three molecules in the asymmetric unit that are related by a non-crystallographic pseudo-

center of symmetry. As a result of this pseudosymmetry, the refinement was really not satisfactory and the precision of the structure determination is low. Nevertheless, the molecular structure is unequivocally defined. Inspection of these three molecules shows that there are no major differences between them and the bond lenghts and bond angles are very similar and (see supplementary data).

The coordination around the cobalt atom is octahedral, the principal distortions being related to the chelate bite angle of 79.6(14)° and the non-linearity of the P7-Fe3-P9 arrangement forming an angle of 172.3(5)°. The other deviation arises from an angle C41-Fe3-I3 165.1(9)°.

Bond lenghts follow the same trend as in compound **7.** The Fe-P distance *trans* to nitrogen is slightly shorter than *trans* to a phoshorus atoms because of the weak *trans* influence of nitrogen. Fe3-N3 at 1.94(3) Å and Fe3-C1 at 2.03(3) Å are agree well with literature values e.g. Fe-C 2.042(3) Å and Fe1-N1 2.025(2) Å in four coordinate iron(II) complexes of *Chirik*.[163]

Discussion

Iodomethane reactions of hydrido-iron(II) compounds give iodo-iron(II) compounds. When we think of a possible mechanism for the formation of **7**-**9**, via oxidative addition of iodomethane, the subsequent step must be a reductive elimination of methane from an alkyl hydride intermediate. The resulting iodo-iron(II) complexes are interesting as versatile nucleophiles with applications in organometallic and organic synthesis. The recent independent reports by Brookhart and Gibson using five-coordinate Fe(II) dihalide complexes as precatalysts for the polymerization of ethylene and α-olefines suggest the idea that iron (II), when in an appropriate coordination environment, may be an active catalyst for C-C and C-H bond forming reactions.[164-166] Iron is an attractive metal for this purpose because of its low cost and relatively low risk of toxicity.

2.1.1.5 Iodomethane Reactions of Methyl-Iron(II) Complexes

Syhnthesis and Characterization

Compounds **4** and **5** react with iodomethane to afford iodo-iron(II) compounds [Eq. 2.6].

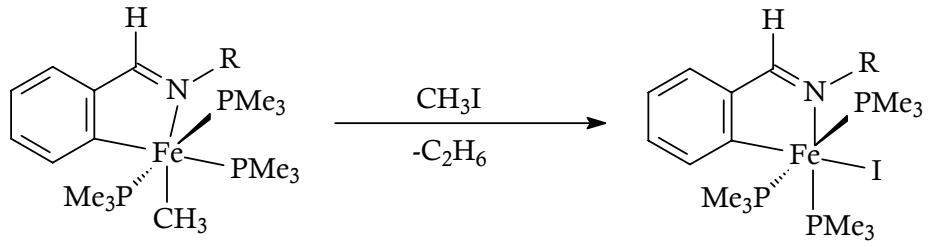

(2.6)

4, **5**

R = CH_3 **10**
R = $CH(CH_3)_2$ **11**

Pink crystals of **10** and light violet crystals of **11** are obtained from pentane at 4 °C. Elemental analyse show the expected decrease in carbon and hydrogen contents. Thermal stabilities of the solids are improved, as **10** melts at 142 °C and **11** decomposes at 145 °C.

Spectroscopic Investigation

IR spectra of **10** and **11** show the absence of characteristic deformation bands δ_s Fe-CH_3 of methyl-iron(II) complexes **4** and **5**. In ^{1}H NMR spectra, resonances at 1.14 ppm as singlet in **10** and at 0.84 ppm as pseudo-triplet ($|^2J_{P,H} + ^4J_{P,H}|$ = 5.9 Hz) in **11** are assigned to the trimethylphosphine ligands in mutual *trans* positions. Cis arranged trimethylphosphines resonate at 1.56 ppm as singlet in **10** and at 1.50 pmm as doublet ($^2J_{P,H}$= 6.4 Hz) in **11.** Aromatic protons typically appear at 6.7 – 7.7 ppm. In ^{13}C NMR metalated carbon nuclei resonate at 212.7 and 199.7 ppm, respectively. ^{31}P NMR resonances of **10** and **11** confirm the suggested structures of Eq. 2.7. Two phosphorus nuclei appear as a doublet at 5.8 ppm ($^2J_{P,P}$ = 54.3 Hz,

complex **10**) and 28.3 ppm ($^2J_{P,P}$ = 28.3 Hz, complex **11**), while the singular phosphorus nuclei form triplets at 14.9 ppm ($^2J_{P,P}$ = 54.3 Hz, complex **10**) and 21.8 ppm ($^2J_{P,P}$ = 28.3 Hz, complex **11**). This pattern is consistent with a *mer*-octahedral coordination geometry.

Molecular Structure of 10

An X-ray structural determination was performed on a single crystal of compound **10** grown from pentane. A view of the molecular structure is shown in Figure 2.14.

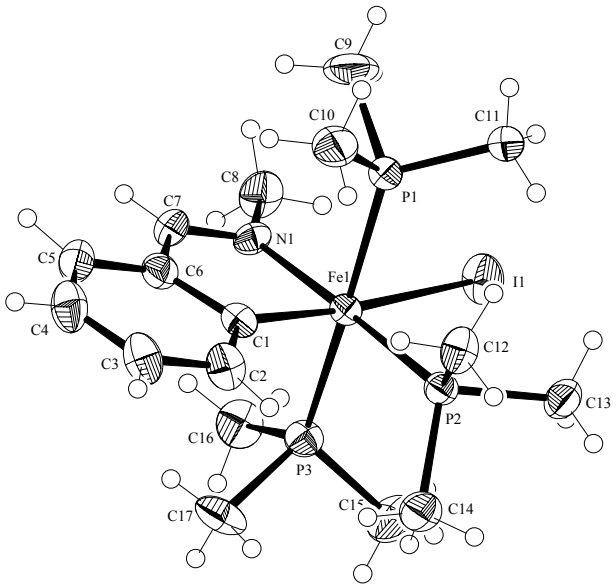

Figure 2.14 Molecular structure of **10**. Selected bond lenghts (Å) and angles (°): Fe1-C1 1.950(4), Fe1-N1 2.025(5), Fe1-I1 2.7973(8), Fe-P1 2.2638(16), Fe-P2 2.246(3), Fe-P3 2.2493(15); C1-Fe1-N1 81.4(2), C1-Fe1-I1 172.02(16), C1-Fe1-P1 90.44(14), C1-Fe1-P2 93.95(17), C1-Fe1-P3 91.30(14), N1-Fe1-I1 90.67(13), N1-Fe1-P2 175.26(13), P1-Fe1-P3 175.36(6), P2-Fe1-I1 94.01(6).

The Fe1-C1 and Fe1-N1 bond lengths (1.950(4)Å and 2.025(5)Å) fall in the range of values found in the related complexes **7** and **8**. The Fe1-I1 bond length 2.7973(8)

Å lies above the literature value e.g Fe-I distance 2.61(3) Å in *cis,trans*-$Fe(CO)_2(PMe_3)_2(p\text{-}C_6H_5)I$ complex synthesized by Cardaci because of the strong *trans* influence of the carbon atom.[167] The structure was solved in the orthorhombic crystal system with a space group $P2_1\ 2_1\ 2_1$. Refinement resulted in an R value of 0.0378. The structure shows no unexpected features; the iron center is coordinated in an octahedral configuration and is part of a five-membered metallacycle. The acute angle C1-Fe1-N1 81.4(2)° reflects the big bite of the *N*-methylbenzylideneimine ligand. The sum of the *cis* angles involving Fe and the atoms C1, N1, I2 and P2 (the equatorial plane) is 360.03° and the sum of the internal angles in the five-membered metallacycle is 539.80° consistent with planarity.

Discussion

Similar to the hydrido-iron(II) compounds **1**-**3**, methyl-iron compounds react with iodomethane to produce iodo-iron(II) compounds. In order to detect the iron(IV) intermediate, the stoichiometric ratios and conditions modified but resulted in the same products. Instead of methane loss, products of oxidative addition reductively eliminate ethane. Like compounds **7**-**9**, complexes **10**-**11** form thermally stable solids. In contrary to its parent complex, **10** does not decompose in deuterated solvents, and full characterization of its structure confirms that of **5**, too. Table 2.6 summarizes some crystallographic data which belong to **7**, **8** and **10**.

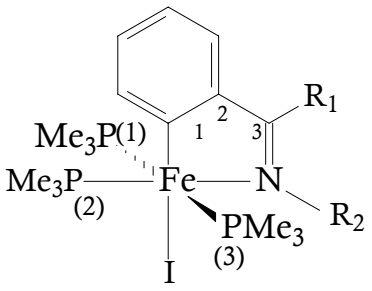

R_1 : C_6H_5 R_2 : H **7**

R_1 : $C(CH_3)_3$ R_2 : H **8**

R_1 : H R_2 : CH_3 **10**

Bond lenghts, [Å]	**7**	**8**	**10**
Fe – C1	1.957(3)	2.03(3)	1.950(4)
Fe – N	1.940(2)	1.94(3)	2.025(5)
Fe– I	2.7616(5)	2.789(6)	2.7973(9)
Fe – P1	2.2587(9)	2.261(13)	2.2638(16)
Fe – P2	2.2350(9)	2.249(11)	2.246(3)
Fe – P3	2.2568(9)	2.253(13)	2.2493(15)
Bond angles, [°]	**7**	**8**	**10**
C1 – Fe – N	80.05(12)	79.6(14)	81.4(2)
C1 – Fe – I	166.44(9)	165.1(9)	172.02(16)
N – Fe – P2	175.24(9)	176.1(11)	175.26(13)
P1 – Fe – P3	172.52(4)	172.3(5)	175.36(6)
Σ (5-Ring)	539.85	539.60	539.80

Table 2.6 Selected bond lenghts and angles of **7, 8, 10**.

2.1.1.6 Carbon Monoxide Reactions of Methyl-Iron(II) Complexes

Synthesis and Characterization

Under 1 bar of CO, methyl-iron(II) compounds **4**-6 in THF solution form the monocarbonyl complexes **12**-**14** [Eq 2.7]. Carbon monoxide substitutes one of the trimethylphosphines, selectively occupying the ligand position opposite the nitrogen atom of the imine group.

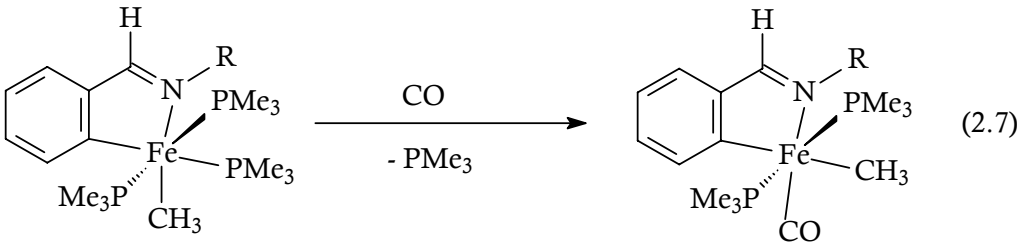

(2.7)

4, **5**, **6**

R = CH_3 **12**
R = $CH(CH_3)_2$ **13**
R = C_6H_5 **14**

12 and **13** form dark pink, **14** forms light green crystals. Whe compared with parent methyl-trimethylphosphine complexes and they show increased thermal stability but decompose at 134 °C, 135 °C and 138 °C, respectively. Elemental anaylse confirm the substitution of a trimethylphosphine group by a carbon monoxide ligand (Table 2.7).

Compound	Yield (%)	M.P. (°C)	Analyses [a]			
			%C	%H	%N	%P
12	66	134	52.30 (52.05)	7.91 (7.92)	3.10 (3.79)	17.32 (16.78)
13	58	135	54.46 (54.42)	8.41 (8.37)	3.65 (3.53)	16.54 (15.59)
14	73	138	58.85 (58.48)	6.81 (7.25)	3.24 (3.25)	14.35 (14.36)

Table 2.7 Yields, melting points, and analyses data for **12-14.**[a] Found with calculated values in parentheses.

Spectroscopic Investigation

The complexes **12-14** show very strong terminal CO stretching bands at 1869 cm^{-1}, 1879 cm^{-1}, and 1870 cm^{-1} which are at lower energies reflecting strong back-bonding and weaken the C-O bonds. Fe-CH_3 stretching absorptions bands are observed at 1153 cm^{-1}, 1151 cm^{-1} and 1193 cm^{-1} for **12-14,** respectively. In contrast to their parent methyl-complexes, **13** and **14** do not decompose in deuterated

solvents. So the spectrocopic characterization of **13** gives the structure solution of **5**. Figure 2.15 shows the ^{1}H NMR spectrum of **1**.

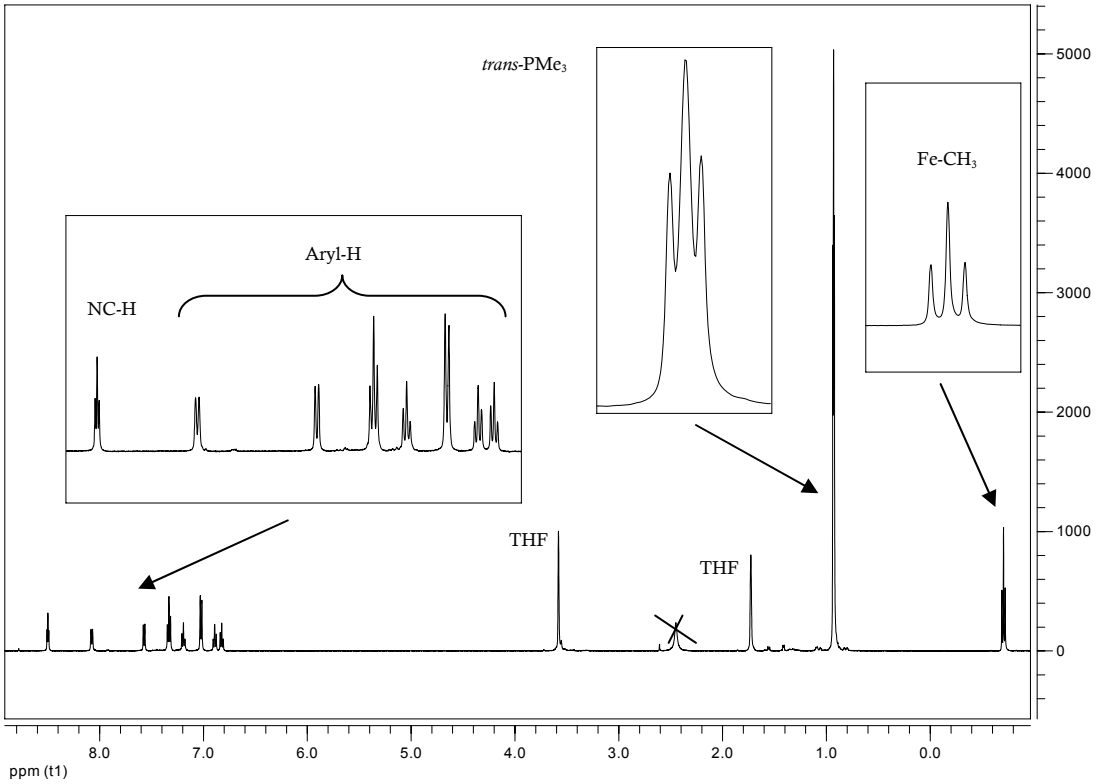

Figure 2.15 ^{1}H NMR spectra of **14** (500 MHz, [D_8]THF, 300 K)

In ^{1}H NMR spectra metal coordinated CH_3 groups show triplets at –0.71 ppm ($^{3}J_{P,H}$= 8.1 Hz for **12**), –0.59 ppm ($^{3}J_{P,H}$= 7.3 Hz for **13**) and -0.67 ppm (6.8 Hz for **14**). For compound **14**, we can observe the expected pseudo triplet at 0.93 ppm ($|^{2}J_{P,H} + {}^{4}J_{P,H}|$= 4.7 Hz) while PMe_3 groups in *trans* positions appear as broad singlets around 0.9 ppm for **12** and **13**. ^{31}P NMR spectra display singlets for *trans*-trimethylphosphine groups. The carbonyl region of the ^{13}C NMR spectra of **13**-**14** comprises triplet resonances consistent with CO groups coupled to two equivalent P nuclei. Table 2.8 summarizes the spectroscopic data of **12**-**14**.

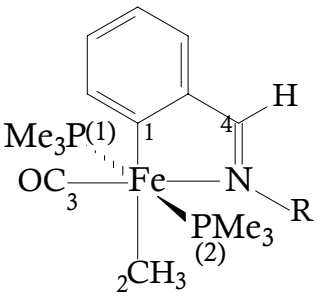

R : CH_3 **12**
R : $CH(CH_3)_2$ **13**
R : C_6H_5 **14**

IR, cm^{-1} :	**12**	**13**	**14**
ν (Fe-CO)	1730	1795	1761
^{1}**H-NMR**, ppm :	**12**	**13**	**14**
δ Fe-CH_3	-0.67; t $^3J_{P,H}$ = 6.8 Hz	-0.59; t $^3J_{P,H}$ = 7.3 Hz	-0.71; t $^3J_{P,H}$ = 8.1 Hz
δ $P_{(1)}$Me, δ $P_{(2)}$PMe	0.89; s	0.90; s	0.93; t' $\lvert {}^2J_{P,H} + {}^4J_{P,H} \rvert$ = 4.7 Hz
^{13}**C-NMR,** ppm :	**12**	**13**	**14**
δ C_4=N	175.8; t $^3J_{P,C}$ = 6.8 Hz	168.0; t $^3J_{P,C}$= 3.6 Hz	175.8; t $^3J_{P,C}$= 4.5 Hz
δ Fe-C_1	211.6; m	207.3; t $^2J_{P,C}$= 21.8 Hz	215.8; m
δ Fe-C_3O	224.2; m	222.6; t $^2J_{P,C}$= 35.6 Hz	224.9; t $^2J_{P,C}$= 35.6 Hz
^{31}**P-NMR**	**12**	**13**	**14**
δ$P_{(1)}$Me, δ $P_{(2)}$PMe	19.1; s	18.7; s	18.3; s

Table 2.8: Selected spectrocopic data of **12-14**.

Molecular Strucutre of 14

In order to elucidate the solid-state structure of **14,** an X-ray crystal diffraction analysis was performed. The ORTEP drawing of molecular structure of **14** is shown in Figure 2.16.

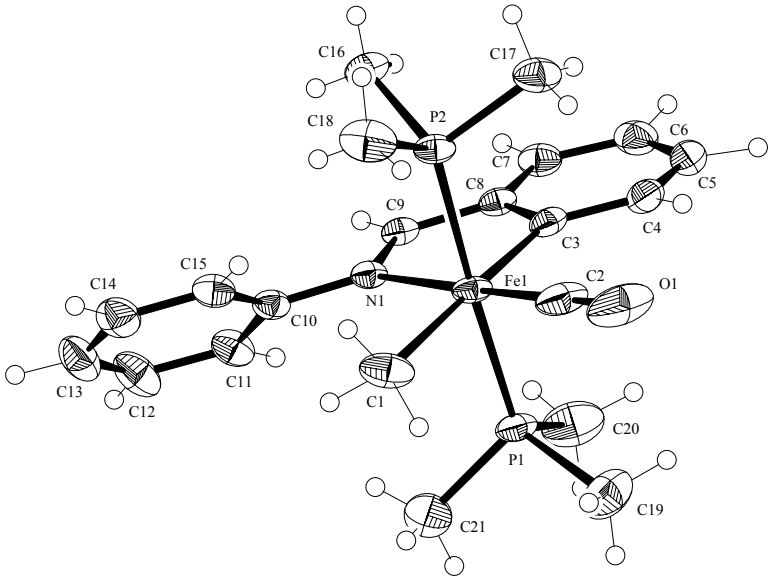

Figure 2.16 Molecular structure of **14**. Selected bond lenghts (Å) and angles (°): Fe1-C1 2.093(3), Fe1-C2 1.715(3), C(2)-O1 1.158(4), Fe1-C3 1.972(3), N1-C9 1.303(3), Fe1-N1 2.081(2), Fe1-P1 2.2259(9), Fe1-P2 2.2229(8); C3-Fe1-N1 80.73(10), N1-Fe1-C2 176.96(14), Fe1-C2-O1 178.1(4), C3-Fe1-C1 174.22(12), P2-Fe1-P1 177.28(3), N1-Fe1-P2 91.34(6), C3-Fe1-P1 89.25(8), C1-Fe1-C2 87.79(16), C1-Fe1-P1 86.56(10), C1-Fe1-P2 95.92(10), C2-Fe1-P1 90.49(10), C2-Fe1-P2 88.50(10).

The coordination sphere about the Fe^{II} atom is octahedral and slight distortions may be illustrated by angles for some *trans*-arrangements: P2-Fe1-P1 177.28(3)°, N1-Fe1-C2 176.96(14) °, C3-Fe1-C1 174.22(12) °. The main feature of this structure is the five-membered metallacycle derived from *ortho*-metalation of the imine ligand, and the bite angle N1-Fe1-C3 is 80.73(10)°. The constrained bite angle of the chealate ligand is considered to be the ultimate source of the distortions from octahedral geometry exhibited by **14**. The sum of internal angles in the five-membered ring is 540.04° indicating planarity.

The P donor atoms adopt mutually *trans* positions. The Fe-P1 (2.2259(9) Å) and Fe-P2 (2.2229(8) Å) bond lengths are in the normal range for such bonds.[168] Fe-CH_3, Fe-CO and C2-O1 bond lenghts (2.093(3) Å, 1.715(3) Å and C(2)-O1 1.158(4) Å respectively) are in literature ranges as compared with isoelectronic benzoyl-acetones.[169]

Discussion

Carbon monoxide reactions of methyl-iron complexes **4**-**6** afforded monocarbonyl derivatives.[170-172] Possible insertion reactions of CO into metal-carbon or metal-methyl bonds were not observed. The substitution of one trimethylphosphine ligand and the coordination of the CO stabilize the complexes. **13** and **14** do not decompose in deuterated solvents and their melting points lie above those of their parent complexes. Full characterization of their structure would support the suggested structure of **5**.

2.1.1.7 Reactions of $CoCH_3(PMe_3)_4$ with Phenyl Ketimines

In addition to the iron complexes presented **1** -**14**, the cobalt complexes introduced here are the first isolated and fully characterized orthometalated cobalt complexes obtained from imines via C-H activation that exist in literature.[127] They form trigonal bipyramidal Co(I) complexes with C,N-coordinated ketimines.

Synthesis and Characterization

Reactions of $CoCH_3(PMe_3)_4$ with diphenyl- and *tert*-butylphenylketimines result in *ortho*-metalated Co(I) complexes **15** and **16** [Eq. 2.8].

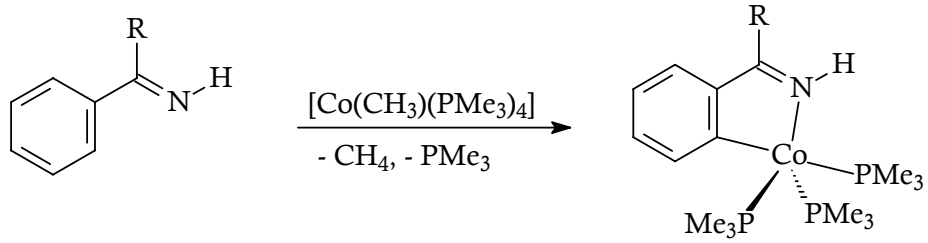

(2.8)

R = C_6H_5 **15**
R = $C(CH_3)_3$ **16**

Dark green crystals of **15** and **16** are grown in pentane at –28°C. Under argon they decompose at 106 °C (**15**) and 116 °C (**16**). At 20 °C in air the crystal surfaces remain unchanged for at least 15 minutes. Elemental analyse (table 2.9) are consistent with the loss of methane and one trimethylphosphine group.

	Analyses[a]			
Compound	%C	%H	%N	%P
15	56.54 (56.53)	8.15 (7.98)	3.04 (3.00)	19.78 (19.88)
16	53.65 (53.69)	9.04 (9.24)	3.08 (3.13)	21.06 (20.77)

Table 2.9 Elemental analyses for **15**-**16.** [a] Found with calculated values in parentheses.

Spectroscopic Investigation

In ^{1}H NMR spectra, three trimethylphosphine groups appear as a doublet (1.23 ppm, $^{2}J_{P,H}$=6.2 Hz; **15** and 1.16 ppm, $^{2}J_{P,H}$=5.8 Hz; **16**) due to fast pseudorotation of ligands as often observed in penta-coordinate complex molecules.[173] We can see this effect also in ^{31}P NMR; two environmentally different phosphorus atoms resonate as singlet at –0.26 ppm (**15**) and –4.5 ppm (**16**). N–H protons appear around 8 ppm as broad singlets. The reason of this broadening can be an exchange of the proton. Aromatic protons appear typically between 6.7 ppm and 8.0 ppm. In ^{13}C NMR, imine carbon nuclei of **15** resonate as quartet due to coupling with three phosphorus nuclei, and the metalated carbon gives a singlet. In **16**, both are multiplet resonances 167.1 ppm (C=N) and 181.3 ppm (Co–C). Table 2.10 makes the summary of the spectroscopic data for **15** and **16**.

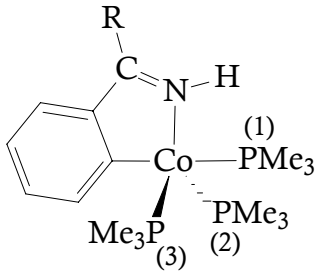

R : C_6H_5 **15**

R : $C(CH_3)_3$ **16**

IR, cm^{-1} :	**15**	**16**
ν (N–H)	3301	3358
^{1}H-NMR, ppm :		
δ $P_{(1)}$Me+ δ $P_{(2)}$PMe+ $P_{(3)}$PMe	1.23; d $^2J_{P,H}$ = 6.2 Hz	1.16; d $^2J_{P,H}$ = 5.8 Hz
δ N– H	7.97; s_{br}	8.26; s_{br}
^{13}C-NMR, ppm :	**15**	**16**
δ $P_{(1)}$Me, δ $P_{(2)}$PMe, $P_{(3)}$PMe	22.5; q' $^1J_{P,C}$ = 24.2 Hz, $^1J_{P,C}$ = 4.5 Hz	20.4; q' $^1J_{P,C}$ = 24.1 Hz, $^1J_{P,C}$ = 4.5 Hz
δ C=N	160.6; q $^3J_{P,C}$ = 8.0 Hz	167.1; m
δ Co–C	179.2; s	181.3; m
^{31}P-NMR, ppm :	**15**	**16**
δ $P_{(1)}$Me, δ $P_{(2)}$PMe, $P_{(3)}$PMe	-0.26; s_{br}	-4.5; s_{br}

Table 2.10 Selected spectrocopic data complexes **15** and **16**.

Molecular Structure of 15

Single crystals were obtained by keeping a solution of **15** in pentane at – 27 °C. Selected crystal data and data collection parameters are given at the index. Data were collected on a STOE IPDS diffractometer. X-ray data reduction and structure solution and refinement were done using SHELXS-97 and SHELXL-97 programs.[174-175]

The crystal was affixed to a glass fiber using silicone grease and transferred to the goniostat, where it was cooled to -123 °C using a gas flow cooling system of local design. Standard inert atmosphere techniques were used during the handling and

mounting process. The X-ray structure could be solved in the orthorhombic crystal system with a space group Pn a 2_1.

The molecular structure of **15** is shown in figure 2.17. The cobalt atom resides in the center of a trigonal bipyramid of donor atoms where the carbon atom of the aromatic backbone and one trimethylphosphine occupying axial positions. The nitrogen donor atom and the two remaining PMe_3 ligands reside in equatorial positions. The main axis in the trigonal bipyramid (C12-Co1-P1 = 168.15(19)°) is slightly bent from idealized geometry (180°).The angles from the axial (P1) to the equatorial phosphorus atoms are similar with 96.69(7)° for (P2) and 97.51(8)° for (P3) respectively.

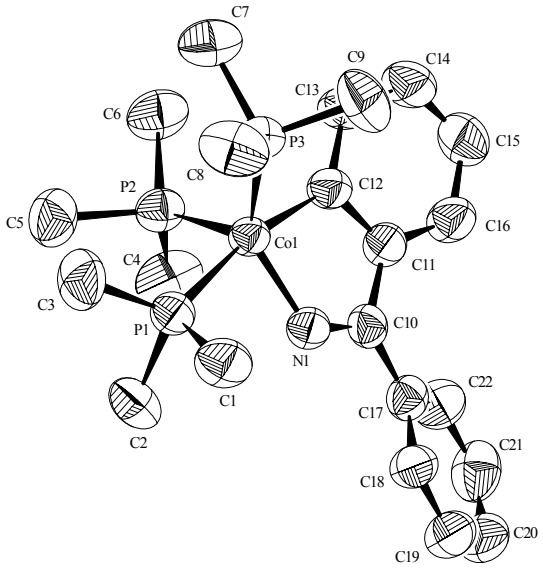

Figure 2.17 Molecular structure of **15** (ORTEP plot with hydrogen atoms omitted). Selected bond lenghts (Å) and angles (°):Co1-C12 1.959(6), Co1-N1 1.882(5), Co1-P1 2.2178(18), Co1-P2 2.1858(19), Co1-P3 2.189(2), N1-C10 1.337(8), C10-C11 1.451(9); N1-Co1-C12 80.6(2), C12-Co1-P1 168.15(19), N1-Co1-P3 135.41(17), N1-Co1-P2 111.98(18), P3-Co1-P2 111.34(7), C12-Co1-P2 88.5(2), C12-Co1-P3 90.4(2), P2-Co1-P1 96.69(7), P3-Co1-P1 97.51(8).

The two equatorial cobalt phosphorus distances (Co1-P2 = 2.1858(19) and Co1-P3 = 2.189(2) Å) are shorter than those opposite the σ-bonded aryl group (Co1-P1 = Co1-P1 2.2178(18) Å) due to its strong *trans* influence of the carbon atom. The distance between cobalt and nitrogen (1.882(5) Å) and as for cobalt carbon (Co1-

C12 = 1.959(6) Å) is in the range for single bonds.[173] The sum of internal angles in the five membered metallacycle (539.4°) equals that of a regular pentagon. And the sum of the inner angles in the trigonal plane which is formed by N1, Co1, P2 and P3 is 358.7 °.

Molecular Structure of 16

Compound **16** as obtained from pentane was formed to crystallize in the space group P21/c; no close intermolecular contacts were observed. Figure 2.18 shows an ORTEP drawing of **16**.

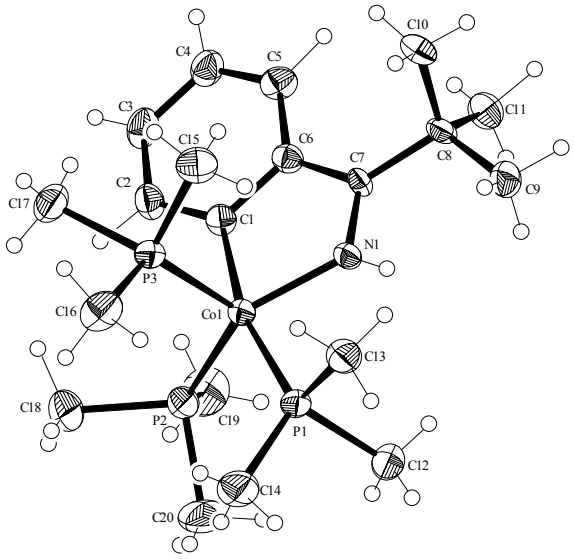

Figure 2.18 Molecular structure of **16**. Selected bond lenghts (Å) and angles (°): C1-Co1 1.948(6), Co1-N1 1.902(5), C7-N1 1.323(8), 1.437(9), Co1-P1 2.210(2), Co1-P2 2.1740(18), Co1-P3 2.1716(17); N1-Co1-C1 79.7(3), C1-Co1-P1 166.1(2), C1-Co1-P2 92.13(19), C1-Co1-P3 87.25(18), N1-Co1-P1 86.43(18), N1-Co1-P2 135.73(16), N1-Co1-P3 110.77(15), P2-Co1-P3 112.20(8).

The coordination around cobalt atom is a distorted trigonal bipyramid. Axial positions are occupied by metalated aromatic carbon atom and one trimethylphosphine group; equatorial positions occupied by nitrogen and two trimethylphosphine groups. The main axis C1-Co1-P1 166.1(2)° shows a deviation from 180°. The sum of the internal angles in the five membered metallacycle (539.4°) equals that of a regular pentagon. There are also deviations from 120 ° on the trigonal plane in equatorial position; N1-Co1-P2 135.73°, N1-Co1-P3 110.77°

and P2-Co-P3 112.20°. And the sum of the inner angles in the trigonal plane which is formed by N1, Co1, P2 and P3 is 358.7°. Changing of the substituent on imine carbon affects the C7-N1 1.323(8) Å and C6-C7 1.437(9) Å (imine carbon-aromatic carbon) bond lenghts which are 0.014 Å shorter than the ones in compound **15**. Co1-N1 1.902(5) Å, C1-Co1 1.948(6) Å and Co1-P1 2.210(2) Å bond lenghts are well-adjusted with the distances in compound **15** and with the literature.[176-177] As expected, Co1-P1 2.2178(18) Å bond length is slightly longer than the equatorial phosphines due to the strong *trans* influence of aromatic carbon atom. Table 2.11 shows some selected crystallographic data of **15** and **16**.

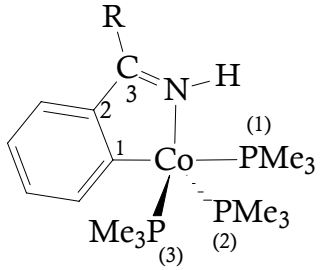

R : C_6H_5 **15**

R : $C(CH_3)_3$ **16**

Bond lenghts, [Å]	**15**	**16**
Co – C1	1.959(6)	1.948(6)
Co – N	1.882(5)	1.902(5)
Co – P1	2.2178(18)	2.210(2)
Co – P2	2.189(2)	2.1740(18)
Co – P3	2.1858(19)	2.1716(17)
Bond angles, [°]	**15**	**16**
C1 – Co – N	80.6(2)	79.7(3)
C1 – Co – P1	168.15(19)	166.1(2)
N – Co – P2	111.98(18)	135.73(16)
N – Co – P3	135.41(17)	110.77(15)
P3 – Co – P2	111.34(7)	112.20(8)
Σ (5-Ring)	539.40	539.40
Σ (Triangular Plane)	358.70	358.70

Table 2.11 Selected bond lenghts and angles of complexes **15** and **16**.

Discussion

Reactions of diazenes, particularly azobenzene, with transition metal compounds are known. *Ortho*-metalated Co(I) azobenzene complexes are isoelectronic with **15** [Eq. 2.10] but there is no structural information on this type of compound.[178] Only *trans* aryl diazenes adopt conformations suitable for *ortho*-metalation reactions.[179-183] Azobenzene ($C_6H_5N=NC_6H_5$) is isoelectronic with N-phenylbenzylideneimine ($C_6H_5HC=NC_6H_5$) but the reaction of $CoCH_3(PMe_3)_4$ with N-phenylbenzylideneimine gave a dark green solution without any crystallization. No isolation could have been done too. And N-methyl- and N-isopropyl-benzylideneimines gave no reaction with $CoCH_3(PMe_3)_4$.

Diphenylketimine and *tert*-butylphenylketimine react with $CoCH_3(PMe_3)_4$ to give *ortho*-metalated Co(I) compounds. These are the first *ortho*-metalated cobalt complexes with an imine in literature. A possible mechanism of the reaction, like in the iron cases, may start by dissociation of a phosphine group and coordination of cobalt to the nitrogen atom. Proximity of the cobalt atom towards the *ortho* C-H bond is effected by σ- or π-cooordination. Activation and regiospecific cleavage of the C-H bond forms a hydrido-cobalt(III) compound which eliminates methane.

2.1.1.8 Iodomethane Reactions of Cobalt(I) Compounds

Synthesis and Characterization

Complexes **15** and **16** react with two molar equivalents of iodomethane in pentane to form the iodo-methyl-cobalt (III) complexes **17** and **18** with substitution and quaternization of a trimethylphosphine ligand [Eq. 2.9].

The dark orange crystals of **17** and **18** melt at 138 °C and 141 °C, respectively. The steric influence of the alkylimino group in **17** and **18** does not affect the coordination sphere of cobalt, therefore the streoselective oxidative cis-addition proceeds with retention of the metallacycle, as with other ring substituents.[184]

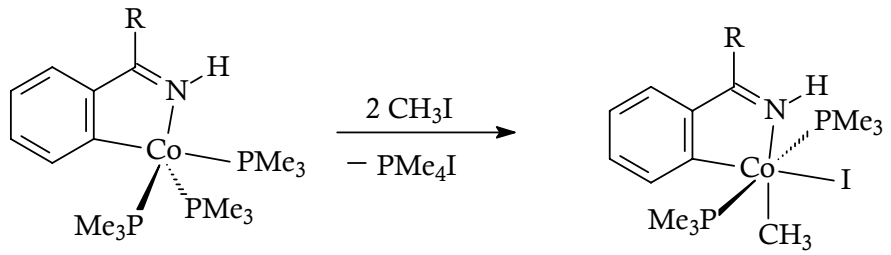

(2.9)

15, 16

R = C_6H_5 **17**
R = $C(CH_3)_3$ **18**

Spectroscopic Investigation

The presence of a Co-CH_3 group is recognized in the IR spectra of **17** and **18** by medium intensity absorbances at 1155 cm^{-1} and 1157 cm^{-1}. Table 2.12 shows some important IR frequencies of the compounds **17** and **18**.

In ^1H NMR the coordinated methyl groups resonate as multiplets at 0.30 ppm (**17**) and 0.54 ppm (**18**). Mutually *trans*-disposed trimethylphosphine groups resonate as virtual triplets due to phosphorus-hydrogen coupling at 1.09 ppm (t, $|^2J_{P,H} + {}^4J_{P,H}|$ =

IR, cm^{-1}	17	18	IR, cm^{-1}	17	18
ν (C=N-H)	3298; w	3329; w	δs (Co-CH_3)	1155; m	1157; m
ν (C=C)	1571,1554; w	1568; w	ρ_1 (PCH_3)	944; vs	948; vs
ν (C=N)	1528; w	1537; vw	γ (C-H)	728; vs	718; vs

Table 2.12 Selected IR frequencies of **17** and **18**.

7.41 Hz) in **17** and 1.45 ppm (t', $|^2J_{P,H} + {}^4J_{P,H}|$ = 7.46 Hz) in **18**. ^{13}C NMR and ^{31}PNMR data are also consistent with *trans* positions of two trimethylphosphine groups. In ^{31}P NMR they resonate as singlets at 2.2 ppm and 3.6 ppm, respectively. In ^{13}C NMR virtual triplets at 15.2 ppm (t', $|^1J_{P,C} + {}^3J_{P,C}|$ = 28.1 Hz; **17**) and 14.8 ppm (t', $|^1J_{P,C} + {}^3J_{P,C}|$ = 26.8 Hz; **18**) are observed. Imine carbon C=N resonances found at 166.5 (m; **17**) and 167.1 (m; **18**). The metalated aromatic carbon nuclei resonate at 183.4 ppm and 187.9 ppm.

Molecular Structure of 17

Crystals of **17** proved to be stable in air for more than two days and could thus be mounted on an X-ray diffractometer without inert gas protection. The molecular structure (Figure 2.19) confirms the configuration of **17** as derived from the spectroscopic data. The iodo and methyl ligands lie in the plane of the chelate ring and the two Co-C bonds are mutually cis (C2-Co1-C1 = 94.52(14)°). The trimethylphosphine ligands are positioned in an axis perpendicular to the chelate ring and appear slightly bent (P2-Co1-P1 = 170.84(4)°) towards the Co-CH_3 group. This bending and the bite angle of the chelating ligand (N1-Co1-C2 = 81.24(14)°) reflect the spatial requirements of the iodo ligand. The sum of the internal angles (549.7°) indicates a slightly distorted five membered metallacycle. The strong *trans* influence of the Co-CH_3 group causes an elongation of Co1-N1 by 0.8 A compared to corresponding parental compound **15** Co(I). The Co-Csp^3 distance is 0.14 A longer than the distance between cobalt and the aryl carbon but still in the range of cobalt carbon distances cited in literature.[185] The Co-P1 and Co-P2 distances fall in the usual ranges of bond lengths in trimethylphosphine stabilized cobalt(III) complexes.[186]

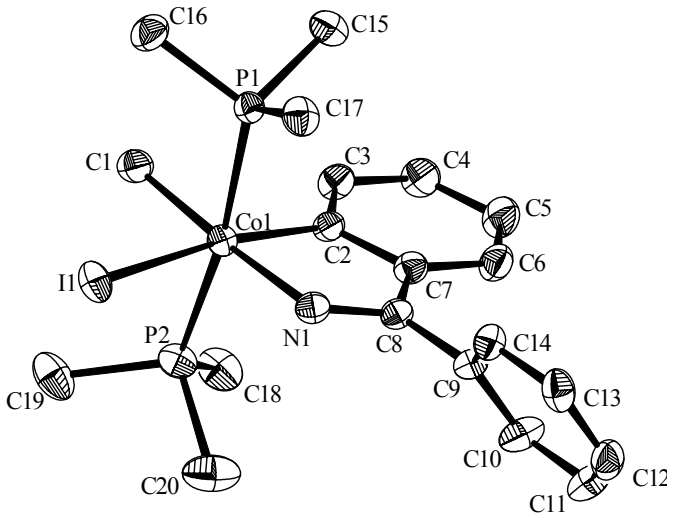

Figure 2.19 Molecular structure of **17** (ORTEP plot with hydrogen atoms omitted). Selected bond lengths (Å) and angles (°): Co1-C1 2.067(4), Co1-C2 1.923(3), Co1-I1 2.7227(5), Co1-N1 1.963(3), Co1-P1 2.2162(10), Co1-P2 2.2108(11), N1-C8 1.295(5), C7-C8 1.459(5), C7-C2 1.426(5); N1-Co1-C2 81.24(14), P2-Co1-P1 170.84(4), N1-Co1-C1 175.69(13), C2-Co1-I1 168.17(10), C2-Co1-P1 92.08(11), N1-Co1-P2 95.61(10).

Discussion

The reactions of iodomethane with low-valent cobalt complexes **15** and **16** proceed under bond cleavage forming two new bonds. As two previously nonbonding electrons of the metal are involved in the new bonding, the metal increases its formal oxidation state by two units, namely Co^{I} is oxidized to Co^{III} and increases the coordination number of the cobalt center by two. The trends toward decreased stability of the II state relative to the III state which have been noted through the series Ti, V, Cr, Mn and Fe persist with cobalt. The III states are exceedingly stable especially where the donor atoms (usually N) make strong contributions to the ligand field. Oxidative addition expected to be facilitated by higher electron density on cobalt brought about by σ-donor trimethylphosphine ligands.

2.1.1.9 Carbon Monoxide Reaction of 15

While in four-membered cobaltacycles monosubstituion is commonly accompanied by insertion of CO into the Co-C bond under ring expansion to give aroylcobalt complexes, five-membered cobaltocycles react with carbon monoxide to give monocarbonyl derivativeswithout insertion.[185, 187]

Synthesis and Characterization

In a pentane solution under 1 bar CO at 20 °C, **15** smoothyl forms a monocarbonyl complex **19** [Eq. 2.10].

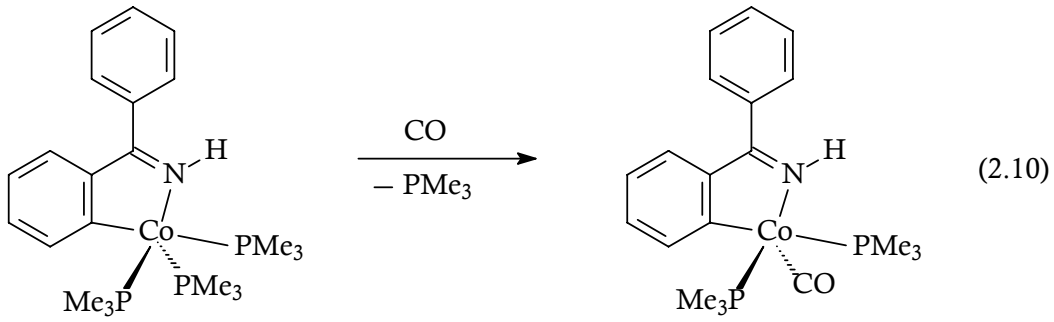

(2.10)

15 **19**

The redish – orange crystals of **19** are more stable than the crystals of their parent trimethylphosphine compouns and they melt at 126 °C.

Spectroscopic Identification

The IR spectra display characteristic bands at 1883 cm^{-1} for terminal carbonyl ligand and at 1497 cm^{-1} for the coordinated C=N group. ^{1}H NMR data suggest an equatorial position for the carbonyl ligand. There are two different trimethylphosphine resonances as doublet due to P,H coupling at 1.33 ppm ($^{2}J_{P,H}$ = 12.9 Hz, 9H) and at 1.57 ppm ($^{2}J_{P,H}$ = 9.5 Hz, 9H). ^{31}P NMR spectra show equatorial and axial phosphorus nuclei as singlets at 14.9 and 31.9 ppm. In the ^{13}C NMR spectrum metalated carbon and coordinated CO resonate at downfield around 181 and 215 ppm, respectively.

Molecular Strucutre of 19

In Figure 2.20 a molecule of **19** is shown, containing a cobalt atom centred in a trigonal bipyramid.

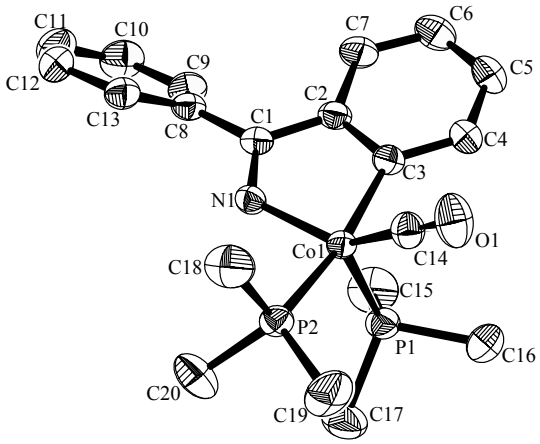

Figure 2.20 Molecular structure of **19** (ORTEP plot with hydrogen atoms omitted). Selected bond lengths (Å) and angles (°): Co1-N1 1.9149(12), Co1-C3 1.942(2), Co1-C14 1.7115(2), Co1-P1 2.1944(4), Co1-P2 2.1963(4), C14-O1 1.160(2), N1-C1 1.321(2), C1-C2 1.440(2), C2-C3 1.425(2); N1-Co1-C3 81.38(6), N1-Co1-P1 104.93(4), P1-Co1-P2 102.75(2), C3-Co1-P2 167.64(5), C3-Co1-P1 89.33(5), N1-Co1-P2 92.84(4), C14-Co1-C3 87.87(7), C14-Co1-N1 140.58(7).

The structure confirms the presence of two trimethylphosphine ligands: one PMe_3 group in axial position and the other in equatorial position. The incoming carbonyl ligand has substituted the formerly equatorial PMe_3 ligand. The third equatorial position is coordinated by the nitrogen atom and the second axial position by the carbon atom of the aromatic imine backbone.

A slightly distorted [C,N] metallacycle (sum of internal angles = 553°) spans axial and equatorial positions wth a bite angle (N1-Co1-C3 = 81.38(6)°). The sum of angles in the equatorial plane (358°) perfectly fits a trigonal bipyramid. The Co-P bond lengths (2.1944(4) and 2.1963(4) Å) fall within the range of for other Co(I) complexes containing aryl and carbonyl groups. The complex contains two different Co-C bonds: a shorter one to carbonyl ligand (Co1-C14 = 1.7115(2) Å) and a longer one the (Co1-C3 = 1.942(2) Å) which is typical for a cobalt aryl carbon distance.[188]

In compound **19** a deviation in the sum of the internal angles in the five memberd metallacycle (553.7°) is recognized which exceeds that of a regular pentagon (540°).

Discussion

Five-membered Co(I) metallacycle react with carbon monoxide under ambient conditions to form mono carbonyl complexes without insertion of the CO ligand into cobalt-carbon bond. Compound **19** has a very strong stretching absorption of CO at a low energy (1883 cm^{-1}) than in free CO (2149 cm^{-1}). This is consistent with the weakning of the C-O bond. N-donor ligands which lack π orbitals cause significantly lower frequencies of CO vibrations. PMe_3 can easily be replaced by CO because the metal can donate its electron density in an empty π^* orbital of carbon monoxide, becoming more stabilized and less reactive.

In compound **19**, CO occupies an equatorial position as expected. The diphenylketimine ligand does not impose a crowding problem onto the coordinated ligands.

2.1.1.10 Carbon Monoxide Reaction of 16

In the reaction of **16** with carbon monoxide, monosubstituted and disubstituted carbonyl complexes are formed.

Synthesis and Characterization

Under 1 bar CO, a pentane solution of **16** fast and smoothly forms compounds **20** and **21** [Eq. 2.11 and 2.12].

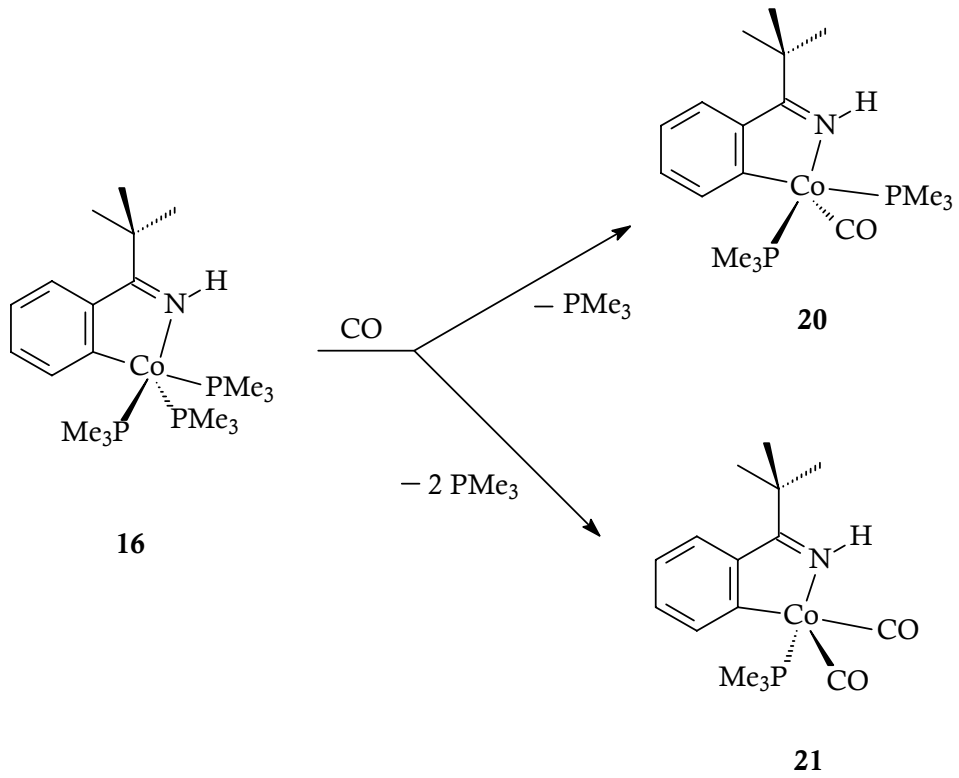

16 **20** **21**

(2.11)

(2.12)

At –27 °C claret red crystals of **20** and orange crystals of **21** crystallize together. They melt at 129 °C (**20**) and 135 °C (**21)** and are quite air-stable. Complete separation of **20** and **21** has not been achieved.

Spectroscopic Identification

The IR spectrum of **21** contains two conspicuous bands which are assigned to the terminal carbonyl ligands; 1945 cm^{-1} (ν CO) and 1896 cm^{-1} (ν CO). On the other

side, **20** has only one absorption as predicted at 1893 (ν CO) which is assigned to a terminal carbonyl. Some important IR data of 20 and 21 are given in Table 2.13.

IR, cm^{-1}	20	21	IR, cm^{-1}	20	21
ν (C=N-H)	3362; vw	3347; w	ν (C=N)	1565; m	1517; w
ν (Co–CO)	1893; vs	1945; vs 1896; vs	ρ_1 (PCH_3)	941; vs	950; vs
ν (C=C)	1584; m	1572; m	γ (C-H)	766; w	777; m

Table 2.13 Selected IR frequencies of **20** and **21**.

The ^{1}H NMR spectrum shows all expected resonances of **21**. PMe_3 protons resonate at 1.53 ppm as doublet due to P,H coupling and *tert*-butyl protons resonate as singlet at 1.49 ppm. Four aromatic protons appear at 6.93 ppm (dt, $^4J_{H,H}$ = 1.4 Hz, $^3J_{H,H}$ = 7.9 Hz), 6.98 ppm (tt, $^4J_{H,H}$ = 1.1 Hz, $^3J_{H,H}$ = 7.1 Hz), 7.93 ppm (td, $^4J_{H,H}$ = 1.5 Hz, $^3J_{H,H}$ = 7.8 Hz) and 7.98 ppm (ddd, $^4J_{H,H}$ = 1.2 Hz, $^3J_{H,H}$ = 3.8 Hz, $^3J_{H,H}$ = 7.5 Hz) respectively. The imine proton forms a broad singlet at 9.10 ppm. Because of axial and equatorial carbon atoms, **21** has C_S symmetry generating two different CO resonances in the low field region at 204.4 and 228.2 ppm as multiplets.
The ^{31}P NMR spectrum of **21** in d_8-THF solution is less specific showing a broad singlet at 21.7 ppm.

Discussion

The reaction of **16** with CO produces two carbonyl complexes, **20** and **21**. When the reaction times are longer, the backbone is removed completely and $Co(CO)_2(PMe_3)_2$ is formed. Optimization of the reaction conditions were impossible for the product **20.** Both compounds crystallize just from pentane. Significantly low yield of **20** and a high rate of the reaction point to the formation of **21** in a two step processes.

2.1.1.11 Reaction of $Ni(CH_3)_2(PMe_3)_4$ with Diphenylketimine

Methyl-nickel complexes are known to effect C-H activation and give cyclometalated products when anchoring groups containing phosphorus, carbonyl, or hydroxyl donor functions.[173, 189] Nickelacycles containing N-C anionic ligands have been described by *Granell* and *Muller* to arise as five-membered nickelacycles from an oxidative addition of *ortho*-halogenated amines or imines to $[Ni(cod)_2]$ in the presence of heterocyclic amines or $PhMe_2$ as supporting ligands.[190-191] Succesful *ortho*-metalation with iron and cobalt suggested to investigate reactions of methyl-nickel complexes with ketimines under similar reaction conditions.

Synthesis and Characterization

Diphenylimine reacts with $Ni(CH_3)_2(PMe_3)_3$ at -70 °C in THF according equation 2.13. During warm up an evolution of gas is detected, and a color change from yellow to red takes place. After typical work up octahedral shaped orange red crystals are formed in pentane at -27 in 68 % yield.

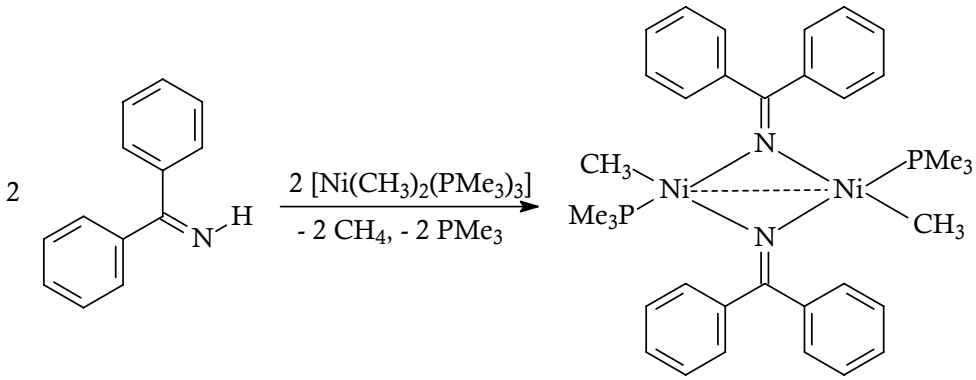

(2.13)

22

Spectroscopic Investigation

The NMR spectra of THF solutions of **22** display a set of more than one resonance in the area of coordinated trimethylphosphine groups which is probably due to its dynamical behaviour in solution and/or formation of *cis*/*trans* isomers. This

unexpected feature is supported by a weak absorption band at 2252 cm^{-1} in the IR spectrum. In the $^{13}C\{^1H\}$ NMR spectrum of **22**, the most distinctive spectroscopic data are a doublet at 13.7 ppm ($^1J_{P,C}$ = 28.0 Hz) due to the phosphine group and singlet at 177.7 ppm which is assigned to the C=N carbon atoms of the bridging diphenylimine group. The ^{31}P NMR spectrum contains singlets at -23.5 ppm, -9.4 ppm, -8.4 ppm and – 7.9 ppm indicating again dynamic behaviour.

Molecular Structure of 22

An ORTEP representation of a molecule of **22** is represented in Figure 2.21. The coordination around each nickel atom is in between tigonal bipyramidal and octahedral when taking the agostic hydrogen atoms H1 and H2 into an account. The dihedral angle between the two coordination planes, 109.23° gives a bent configuration to the molecule as is predicted by the ^1H NMR spectrum. This butterfly-type geometry seems to be an intrinsic salient feature of molecules containing a four-membered core M_2L_2 (M = Rh, Ir, Co,).[192-193]

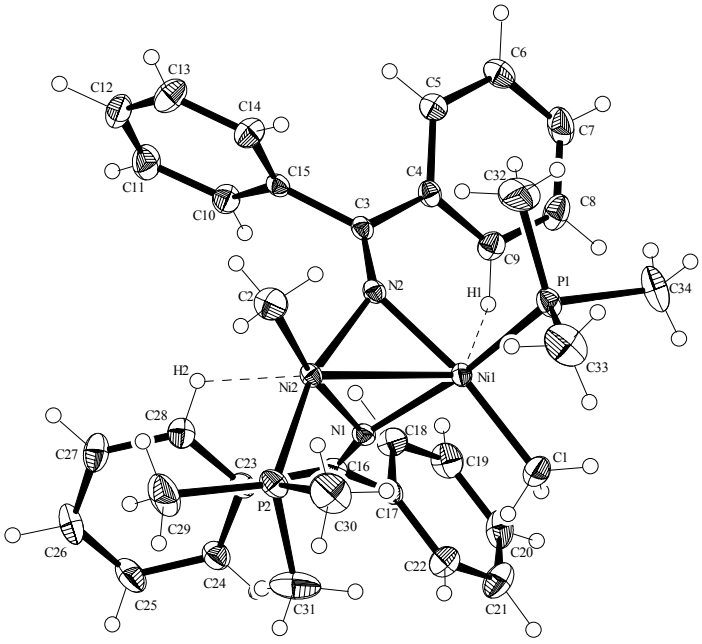

Figure 2.21 Molecular structure of **22**. Selected bond lengths (Å) and angles (°): Ni2-Ni1 2.5356(6), Ni1-H1 2.455, Ni2-H2 2.432, Ni1-C1 1.942(4), Ni2-C2 1.943(2), Ni1-N1 1.9099(14), Ni2-N2 1.9182(15), Ni1-P1 2.1252(6), Ni2-P2 2.1243(8), N2-C3 1.269(2), N1-C16 1.270(2), C3-C4 1.503(2), C3-C15 1.504(2), C16-C17 1.504(2), C23-C16 1.502(2); N1-Ni1-N2 75.29(6), N1-Ni1-C1 97.15(8), N2-Ni1-C1 171.71(8), N1-Ni1-P1 164.26(5), N2-Ni1-P1 96.64(5), C1-Ni1-P1 89.89(7), N1-Ni1-Ni2 48.66(5), N2-Ni1-Ni2 48.37(6).

Figure 2.22 focuses on the coordination around the nickel atom and shows the Ni-Ni axis more clearly. The Ni-Ni distance (2.5356(6) Å) lies close to the average of distances (2.36 – 2.69 Å) observed in other dinickel complexes where a single bond is believed to exist.[194-195] The Ni-N bond lengths (about 1.92 Å) are comparable with those reported for complexes with ligands containing bridging nitrogen atoms. Distances within the diphenylimine ligands are as expected. The nitrogen-carbon distances N1-C16 = 1.270(2) Å and N2-C3 = 1.269(2) Å, are consistent with the formulation of these linkages as N=C.[192-193] The suggested Ni1-H1 and Ni-H2 agostic distances are about 2.45 Å represent reasonable values although H positions are less accurate.

The metal atom deviates remarkably from the N1, C16, C17, C23 mean plane. The phenyl rings, forming a dihedral angle of 109.7°, are rotated by 34.62 and 74.05° respectively around the C17-C23 and C16-C17 bonds.

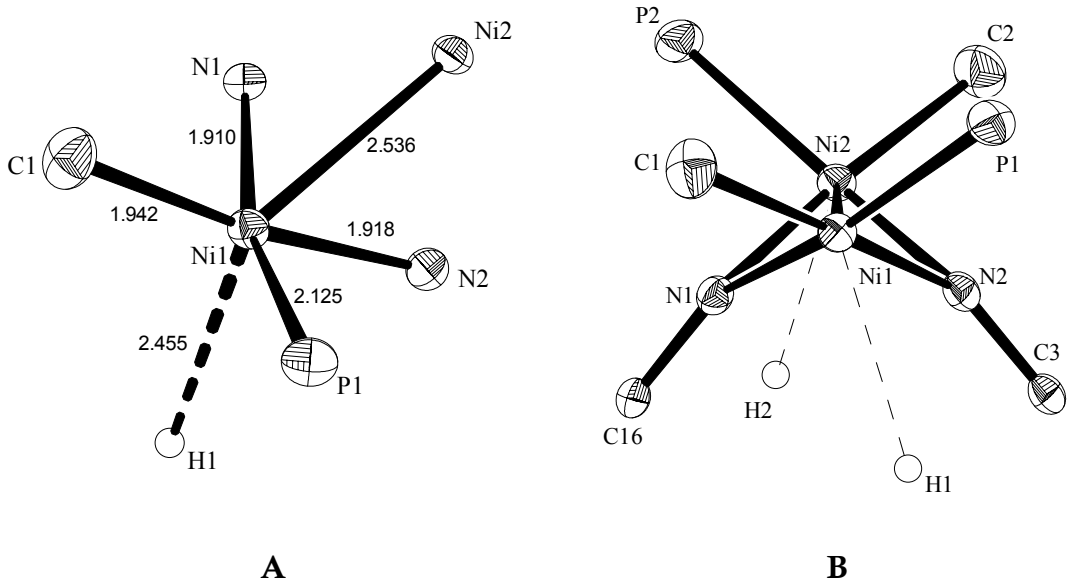

Figure 2.22 a) Coordination sphere of the nickel atoms in **22**. **b)** View along the Ni-Ni axis indicating agostic C-H-Ni interactions in **22.**

Discussion

In the previously reported *ortho*-metalation reactions with methyl complexes of iron and cobalt, the proton of the imine function of the ligand is not deprotonated by N-coordination compounds. In dimethylnickel compounds, only one methyl group is strongly basic. Even in dilute hydrochloric acid the second methyl group is not cleaved from the nickel complex. The first step of the reaction is a deprotonating step involving the imine function, whereby the metal is no longer able to activate the phenyl groups.

Complex **22** appears to be the first example of a diphenylamine bridged nickel dimer. The agostic distance observed in Ni-H-C fragment with a distance Ni-H = 2.45 Å is the middle of the reported values. Typical agostic cobalt interactions seem to be the farest known by literature with aliphatic or aromatic C-H groups fall between 2.31 – 2.79 Å.[192]

Recently Strassner et al. reported agostic interactions of beta hydrogen atoms in ethyl groups. In these molecular structures the protons were calculated as fixed in idealized positions. [197]

N-briged dinuclear complexes are known for iridium, cobalt and molybdenum. In none of these molecules, an agostic interaction between the metal center and an aromatic C-H bond has been reported.[198-199]

2.1.1.12 Reaction of $NiClCH_3(PMe_3)_2$ with Diphenylketimine

Synthesis and Characterization

Diphenylimine reacts with $NiCl(CH_3)_2(PMe_3)_2$ at -70 °C in THF according to equation 2.14. During warm up a color change from brown to orange red takes place. After 10 h typical work up affords dark red rods from pentane at -27 °C in 72 % yield.

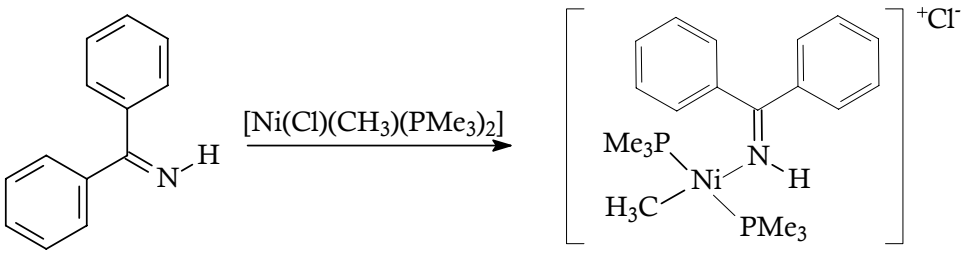

(2.14)

23

Spectroscopic Investigation

In agreement with the postulated reaction pathway of complex **23** [Eq. 2.14] an absorption band was detected at 1567 cm^{-1} indicating C=N coordination to the nickel. The $NiCH_3$ group resonates at 0.81 ppm as a singlet. Typically for square planar nickel(II) complexes, the trimethylphosphine groups give rise to a singlet because ligand dissociation breaks down the P-coupling. The aromatic protons appear in the area of 7.35 – 7.74 ppm. The imine proton resonates at 10.12 ppm as a broad singlet. In the ^{31}P NMR spectrum, the absorption of two isochronic phosphine ligands lies at -16.6 ppm.

Discussion

Under similar reaction conditions as with $Ni(CH_3)_2(PMe_3)_3$, diphenylimine does not undergoes a C-H activation step, because opposite to the $Ni\text{-}CH_3$ the nitrogen donor just substitutes the chloride ligand leading to a cationic methyl-nickel(II) species. This type of reaction pathway is well described in the literature.[200-201]

2.1.2 Cyclometalation Reactions via C-H Activation with Carbonyl Anchoring Groups

As imine is the isoelectronic nitrogen analog of a carbonyl group, imines and ketones are isoelectronic ligands, and the same number of electrons are distributed in very similar molecular structures (Figure 2.19).[202] A comparison of isoelectronic complexes or ligands in reaction can be useful pointing out analogies contrasts.[203]

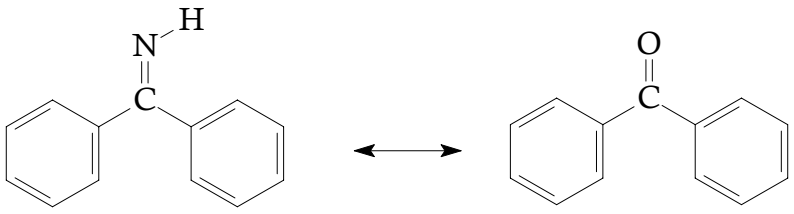

Benzophenoneimine **Benzophenone**

Figure 2.19 Isoelectronic benzophenoneimine and benzophenone compounds

Ketones play an important role in the field of organic chemistry, and much is known about the reactivity of these carbonyl compounds. One of the great utilities of transition metal chemistry is the ability to enhance the reactivity of organic compounds. The most significant breakthrough in this field was reported by *Murai* (see Introduction part for detalis).

Except for Mn, *ortho*-metalation reactions of aromatic ketones with first row transition metals have not been reported to date. Complexes $RMn(CO)_5$ (R = Me, Et, Ph, CH_2Ph) give *ortho*-metalated products in a very general reaction and the manganese derivatives have in turn found applications in organic synthesis.[204-207] The only known cyclometalated Fe compound was synthesized by *Green* in an unexpected reaction between the Lewis acid $B(C_6F_5)_3$ and $[Fe(\eta^5\text{-}C_5H_5)(CO)_2Me]$. The ketone function and the product is formed by insertion of CO group into Fe-Me bond followed by insertion of the C_6F_4 fragment into the metal acetyl bond.[208]

2.1.2.1 Reaction of $CoCH_3(PMe_3)_4$ with Benzophenone and Benzyl Phenyl Ketone

An important part of organometallic chemistry is dominated by soft-soft interactions. Very interestingly again, the hard donor atom oxygen like in the case medium hard nitrogen donor can activate the soft Co^I center [Eq. 2.8] to form *ortho*-metalated complexes **24** and **25**.

Synthesis and Characterization

Combining THF solutions of $CoCH_3(PMe_3)_4$ with benzophenone or benzylphenylketone at –70°C after 16 h affords dark brown solutions from which the compounds **24** and **25** were isolated as dark brown crystals in about 81% and 66% yields, respectively [Eq. 2.15].

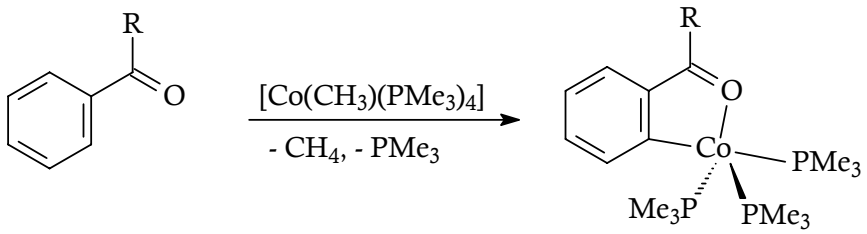

(2.15)

R = C_6H_5 **24**
R = $CH_2(C_6H_5)$ **25**

Similar to their analogue compound **15**, **24** and **25** they form pentacoordinate molecular complexes which decompose around 110 °C. Elemental analyse confirm the composition after elimination of methane and one of the trimethylphosphine ligands (Table 2.14).

	Analyses[a]		
Compound	%C	%H	%P
24	56.95 (56.42)	7.53 (7.75)	20.68 (19.84)
25	56.49 (57.27)	7.39 (7.94)	19.53 (19.26)

Table 2.14 Elemental analyses for **24 - 25.**[a] Found with calculated values in parentheses.

Spectroscopic Identification

The infrared absorptions of the acyl groups coordinated through oxygen to the cobalt show the expected bathochromic shifts. They have absorbances in lower energies than the free ketone, 1484 cm^{-1}(ν C=O; **24**) and 1483 cm^{-1} (ν C=O; **25**). In

^{1}H NMR experiment trimethylphosphine protons resonate at 1.30 ppm as a doublet ($^{2}J_{P,H}$ = 6.5 Hz, 27 H; **24**) and at 1.05 ppm as a broad singlet (27H; **25**) due to the ligand dynamics in trigonal bipyramidal systems. In the ^{31}P NMR spectrum three phosphorus nuclei resonate at 5.1 ppm in **24** and at 1.5 ppm in **25** as broad singlets. There can be two reasons for this exchange broadening in trigonal bipyramidal systems: we have either dissociation of trimethylphosphine groups or fast exchange of ligand positions in a pseudorotation process. In the slow exchange limit, we should observe in the ^{13}C spectrum a quartet due to P,C coupling. Only in **24** we can clearly locate the C=O resonance as quartet at 170.8 ppm ($^{3}J_{P,C}$ = 11.8 Hz). The acyl group in **25** resonates at 166.1 ppm as singlet. Coordinated acyl groups appear at higher energies in both compounds than in the free ketones; C=O resonates in benzophenone at 196.50 ppm and in benzyl phenyl ketone at 197.43 ppm.[209]

^{13}C NMR data confirms the cyclometalation, as metalated carbon atoms resonate at 173.9 ppm (**24**) and 183.7 ppm (**25**).

Molecular Structure of 24

The structural data for complex **24** closely resemble those of the isoelectronic compound **15** (see Figure 2.17 and Table 2.10). Both complexes adopt a trigonal bipyramidal geometry (C-Co1-P angles near 163° and 168° respectively). The two axial positions are occupied by the metallated carbon atom and a phosphine ligand while two PMe_3 groups and the oxygen donor of the benzophenone anchoring group reside in equatorial positions.

The Co-O and Co-C distances (Co1-O1 = 1.9051(12) and Co1-C1 = 1.9339(18) Å) correspond with literature values.[210] The Co1-P2 distance is elongated (Co1-P2 = 2.2401(5) Å), due to the *trans* influence of the carbon atom while the other Co-P and P-C bond lengths are close to the average of reported values in arylcobalt compounds. The bond lengths and angles resemble those found in the isoelectronic cyclometalated diphenylimine compound **15**.

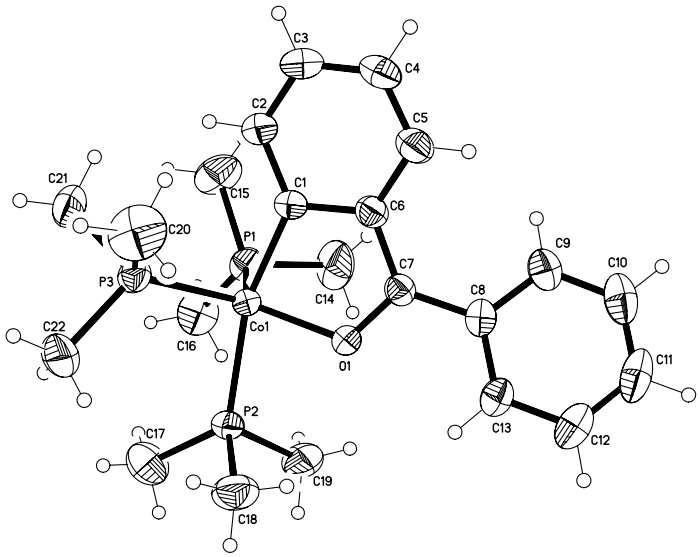

Figure 2.23 Molecular structure of **24**. Selected bond lengths (Å) and angles (°): Co1-O1 1.9051(12), Co1-C1 1.9339(18), Co1-P1 2.1786(6), Co1-P3 2.1852(6), Co1-P2 2.2401(5), C7-O1 1.297(2), C6-C7 1.430(3), C7-C8 1.460(3); O1-Co1-C1 83.49(7), C1-Co1-P2 163.52(6), C1-Co1-P1 90.33(6), O1-Co1-P3 137.94(5), C1-Co1-P3 91.46(6), P1-Co1-P3 110.77(2), P1-Co1-P2 97.73(2), P3-Co1-P2 99.01(2), O1-Co1-P2 81.21(4), O1-Co1-P1 110.84(5), C7-O1-Co1 117.51(11).

The bite angle of the chelating benzophenone ligand (O1-Co1-C1 = 83.49(7)°) is within experimental error equals those of the acylphenolato dianionic ligands (85.5(2)°) or monoanionic phosphinobenzoyl ligands (85.5(2)°).[211-212] The sum of the internal angles in the five membered metallacycle (540°) equals that of a regular pentagon.

Discussion

Benzophenone and benzyl phenyl ketone react with $Co(CH_3)(PMe_3)_4$ to give *ortho*-metalated Co(I) complexes **24** and **25**. Mechanistic details can be understood by taking into account Murai's reaction. A sequence of possible reactions for the formation of **24** and **25** is given below (Scheme 2.1). Coordination of the carbonyl oxygen of aromatic ketones to cobalt is the origin of the high ortho selectivity, which induces breaking of the closest ortho C-H bond.

Scheme 2.1

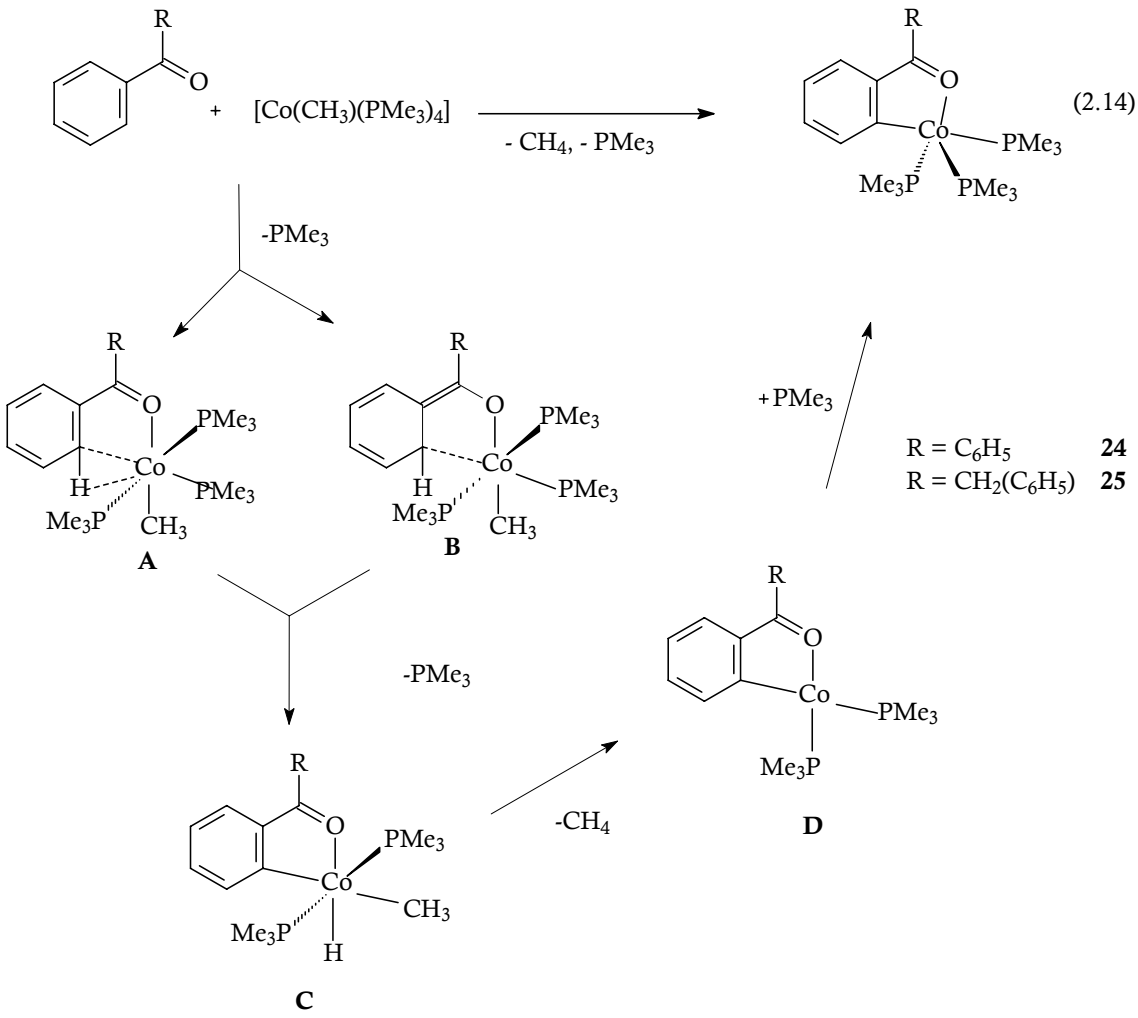

Two mechanisms are possible for the C-H bond cleavage process: the conventional CH bond breaking through σ complex **A** and the 1,2-H shift through the intermediate **B**. Theoretical studies suggest that the stable metallacycle intermediate B plays an important role in the high ortho selectivity.[213] Intermediate **C** has Co-C, Co-H bonds and Co-CH_3 bonds from which the 16 e^-s intermediate **D** is formed via reductive elimination of the methane. The reductive elimination of the methane forms. Coordination of the trimethylphosphine affords the 18 e^-s cobalt (I) complex.

2.1.2.2 Iodomethane Reaction of 24

Synthesis and Characterization

Complex **24** reacts with iodomethane in pentane by dissociation and quarternization of a trimethylphosphine [Eq. 2.16] to afford the octahedral Co(III) complex **26**.

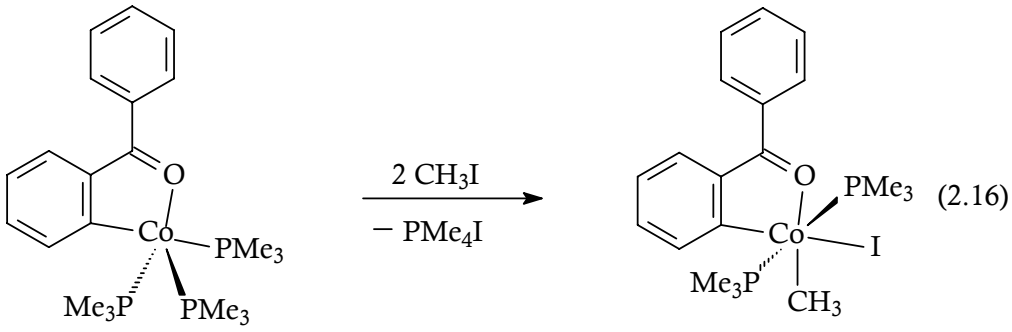

(2.16)

24 **26**

The dark orange crystals of **26** are air-stable and under argon decompose above 133 °C. Elemental analysis data support the loss of trimethylphosphine group and coordination of iodomethane (see Experimental Part).

Spectroscopic Identification

Sprectroscopic data are consistent with an octahedral coordination around the cobalt atom. In the IR spectrum, Co-CH_3 group shows a bending vibration at 1158 cm^{-1} (δ_s Co–CH_3). In the ^1H NMR spectrum, they resonate as a triplet at 0.21 ppm ($^3J_{P,H}$ = 9.4 Hz) and as a multiplet at –10.1 ppm in ^{13}C NMR spectrum. The protons of *trans* trimethylphosphine groups give a resonance as pseudo triplet at 1.11 ppm (t', $|^2J_{P,H} + {}^4J_{P,H}|$ = 7.8 Hz, 18H, PCH_3) in ^1H NMR and at 14.6 ppm (t', $|^1J_{P,C} + {}^3J_{P,C}|$ = 27.6 Hz, PCH_3) in ^{13}C NMR. In the ^{31}P NMR spectrum a broad singlet at 2.03 ppm is observed for them. Acyl carbon and metalated carbon have ^{13}C NMR multiplets at 171.8 ppm and 188.6 ppm.

Discussion

Oxidative addition reactions of **24** forms a Co(III) complex **26** which has spectroscopic characteristics closely related with the isoelectronic imine analogue **17** (Table 2.15). Both compounds are very stable solids and their spectra fully consistent with octahedral geometry and two *trans* disposed trimethylphosphine groups. In both cases CH_3 and I groups occupy *cis* positions and are coplanar with the metallacycle.

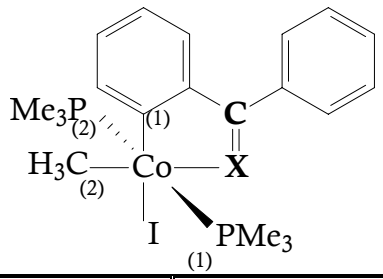

X : O **26**
X : NH **17**

^{1}H-NMR, ppm :	**26**	**17**
δ Co-CH_3	0.21; t $^{3}J_{P,H}$ = 9.4 Hz	0.30; t $^{3}J_{P,H}$ = 9.7 Hz
δ $P_{(1)}Me$, δ $P_{(2)}Me$	1.11; t' $\lvert {}^{2}J_{P,H} + {}^{4}J_{P,H} \rvert$ = 7.8 Hz	1.11; t' $\lvert {}^{2}J_{P,H} + {}^{4}J_{P,H} \rvert$ = 7.4 Hz
^{13}C-NMR, ppm :	**26**	**17**
δ Co-$C_{(1)}$	-10.1; m	-7.5; m
δ $P_{(1)}Me$, δ $P_{(2)}Me$	14.6; t' $\lvert {}^{1}J_{P,C} + {}^{3}J_{P,C} \rvert$ = 27.6Hz,	15.2; t' $\lvert {}^{1}J_{P,C} + {}^{3}J_{P,C} \rvert$ = 28.1 Hz
δ C=X	171.8; m	166.5; m
δ Co–$C_{(2)}$	188.6; m	183.4; m
^{31}P-NMR, ppm :	**26**	**17**
δ $P_{(1)}Me$, δ $P_{(2)}Me$	2.03; s	2.20; s

Table 2.15 Selected spectrocopic data of complexes **26** and **17**.

2.1.2.3 Reaction of $Ni(CH_3)_2(PMe_3)_4$ with Benzophenone

Ortho-metalated compounds of nickel with aryl ketones are not known. In an attempt to obtain an *ortho*-metalated complex, a π-complex of nickel(0) (**27**) was formed.

Synthesis and Characterization

The addition of one equivalent of benzophenone to a THF solution of $Ni(CH_3)_2(PMe_3)_3$ at –70 °C affrods a red solution of **27** after 18 hours mixing [Eq. 2.17].

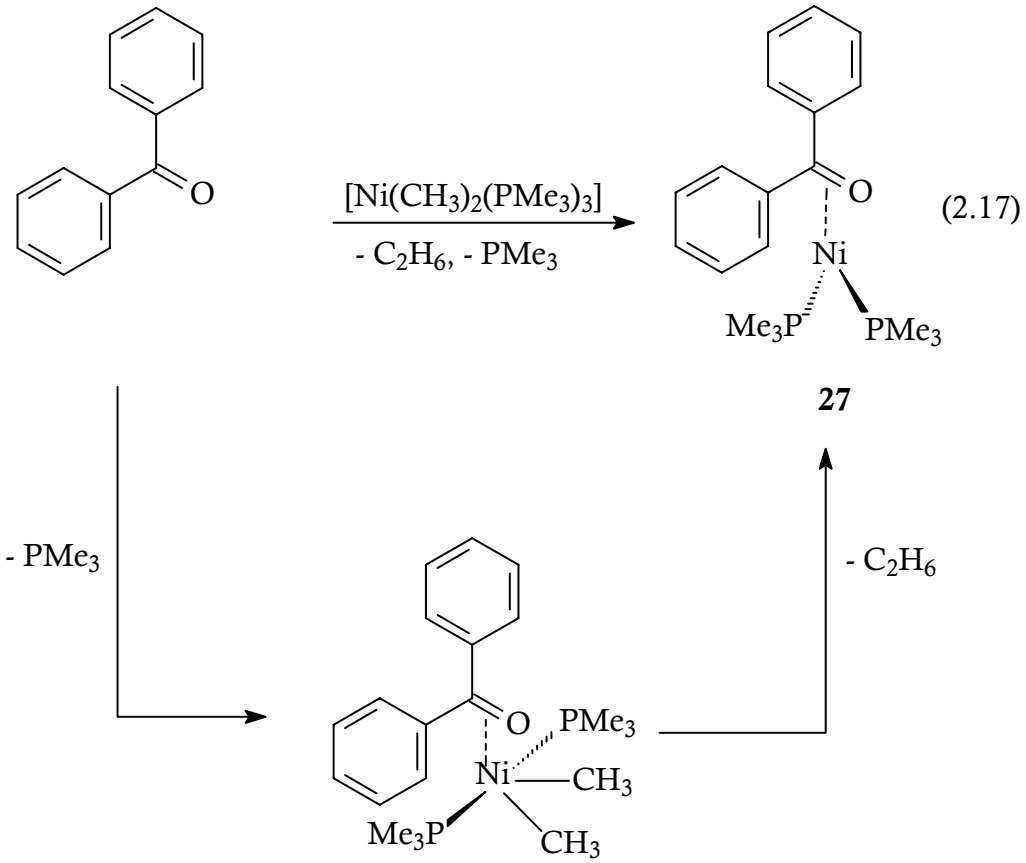

(2.17)

After substitution of trimethylphosphine group in **27**, a $Ni(CH_3)_2(PMe_3)_2$ fragment coordinates to the carbonyl group. Upon reductive elimination of ethane, π-complex **27** is formed which crystallize from pentane at 4 °C. Under argon these melt at 78 °C and suprisingly for a π-coordinated Ni(0) complex, they are air-stable for at least 30 minutes.

Spectroscopic Identification

Upon coordination to the nickel (0) center, the infrared streching frequencies of the carbonyl group of benzophenone is shifted to 1485 cm^{-1}.[214-215] The ^{1}H- NMR shows two different signals for protons of trimethylphosphine groups as doublets at 0.86 ppm ($^{3}J_{P,H}$ = 5.6 Hz) and 1.31 ppm ($^{3}J_{P,H}$ = 6.2 Hz). This shows that the coordination of the carbonyl group to nickel is not symmetrical. One reason can be the *trans* influence of carbon which is more powerful on *trans* positioned trimethylphosphine than that of an oxygen. Another reason can be the coordination of benzophenone to nickel destroys the coplanarity of the carbonyl group in the free ligand. ^{31}P NMR data confirm this situation with two phosphorus resonances at –11.9 ppm and –14.5 ppm as doublets due to P,P-coupling and ($^{2}J_{P,P}$ = 62.7 Hz).
In ^{13}C NMR, the carbonyl carbon resonates at 147.1 ppm which is at higher field than in σ-coordinated complexes (166.1 ppm; **25** and 170.8 ppm; **24**). We can see clearly all aromatic carbon resonances at 122.5-131.1 ppm.

Discussion

π-Coordinated nickel (0) complexes of ketones are well-known. Benzophenone forms stable complexes of a bis(triphenylphoshine)nickel(0) moiety.[216] Kochi prepared an analogoue triethylphosphine complex in which benzophenone reacts with tetrakis-(triethylphosphine)nickel(0) to give the π-coordinated nickel(0) complex.[217] These red nickel (0) compounds are very air-sensitive. In all cases, the presence of an electron-withdrawing substituent (oxygen), which lowers the energy of the antibonding π* orbital of the unsaturated ligand, favors the formation of the π complex.

2.1.3 Cyclometalation Reactions via C-F Activation with Carbonyl Anchoring Gropus

Compounds containing aromatic C-F bonds have considerable interest as solvents, agrochemicals, pharmaceuticals and dyes.[218] However, their extensive use is

constrained in part by the difficulty in eliminating them from the environment.[219-223] The selective cleavage of C-F bonds, or C-F bond activation, offers potential both in synthesis and disposal of fluorocarbons and has therefore become an important goal in the chemical community.

Activation of C-F bonds provides a chemical challenge akin to that of C-H activation in analogous hydrocarbon compounds. Even though C-F bonds are about 30 kcal mol^{-1} stronger than C-H bonds, a number of transition metal compounds, with the metal in a low oxidation state, have shown to be capable of intermolecular activation of aromatic C-F bonds, including catalysis.[224-226] The selectivity of the C-F versus C-H activation has received scare attention, and the underlying trend is not clear. The ability to produce aryl C-F oxidative-addition processes has been attributed to the nature of the transition metal systems.[227-229]

2.1.3.1 Reaction of $CoCH_3(PMe_3)_4$ with 2,3,4,5,6-pentafluorobenzophenone

An intramolecular C-F activation by cobalt complexes has not been reported. After obtaining the first *ortho*-metalated complex of cobalt **24** with benzopheneone, 2,3,4,5,6-decafluoro-benzophenone was used to study the preference for the C-H or C-F activation in aromatic ketones.

Synthesis and Characterization

$CoCH_3(PMe_3)_4$ was combined with 2,3,4,5,6-pentafluorobenzophenone to afford pentacoordinate cobalt(I) complex **28** which crystallizes from pentane at -27 °C [Eq. 2.18].

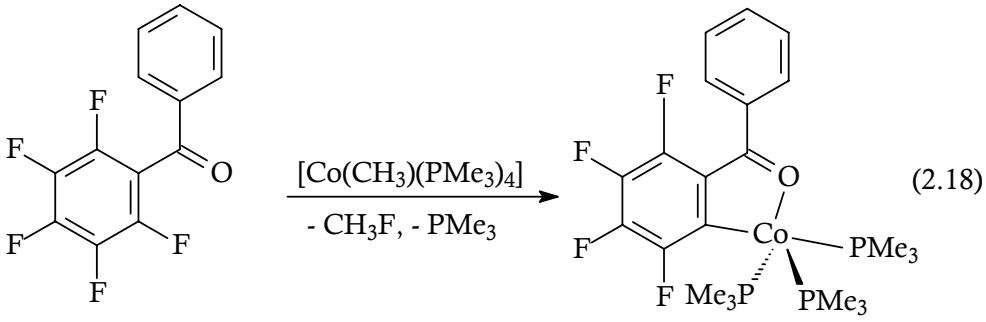

(2.18)

28

The brown crystals of **28** start to decompose at 152 °C which is 40 °C higher than **24.** Elemental analysis confirms the expected constitution of **28** (Table 2.16) with three trimethylphosphine groups and loss of one fluorine atom.

28	%C	%H	%P
Calculated	48.90	5.97	17.20
Found	48.58	5.70	16.88

Table 2.16 Elemental analysis data for **28**.

Spectrocopic Investigation

The IR spectra show a ν(C=O) vibration at 1490 cm^{-1} which lies by 6 cm^{-1} to higher energy than that in **24,** along with a strong ν(F-C) vibration at 1339 cm^{-1}. In the ^{1}H NMR spectrum the protons of trimethylphosphine groups resonate at 1.32 ppm as a doublet ($^{2}J_{P,H}$ = 6.1 Hz) indicating ligand mobility. In ^{31}P NMR as a broad singlet at 3.6 ppm is recorded. Five aromatic protons on the phenyl ring resonate at 7.09 ppm (t, $^{3}J_{H,H}$ = 7.2 Hz, 2H), 7.48 ppm (t, $^{3}J_{H,H}$ = 7.0 Hz, 1H) and 7.81 ppm (t, $^{3}J_{H,H}$ = 6.5 Hz, 2H), respectively. Highly concentrated solution of **28** was prepared in order to see the fluorinated carbon atoms in a $^{13}C\{^{1}H\}$NMR spectrum (see Experimental Part). The metalated carbon atom is detected resonates at 168.7 ppm as multiplet and the coordinated C=O group resonates at 167.9 ppm as a singlet.

Molecular Structure of 28

A view of the molecular geometry of **28** is shown in Figure 2.24 which confirms the geometry predicted from spectroscopic and analytical data. The unit cell contains two discrete molecules

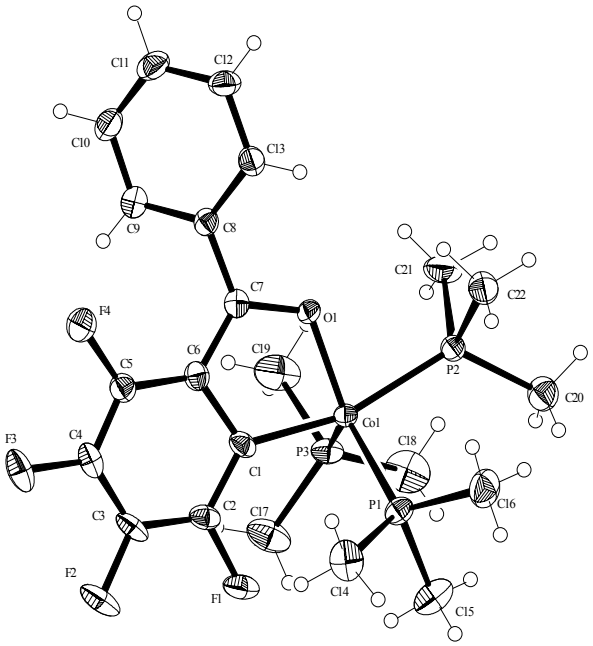

Figure 2.24 Molecular structure of **28**. Selected bond lengths (Å) and angles (°): Co1-O1 1.903(3), Co1-C1 1.934(4), Co1-P1 2.2038(14), Co1-P3 2.2.1958(13), Co1-P2 2.2294(13), C7-O1 1.297(5), C6-C7 1.419(6), C7-C8 1.472(6); O1-Co1-C1 82.28(16), C1-Co1-P2 163.89(14), C1-Co1-P1 94.71(14), O1-Co1-P3 112.87(10), C1-Co1-P3 91.35(13), P1-Co1-P3 112.06(5), P1-Co1-P2 96.14(5), P3-Co1-P2 95.56(5), O1-Co1-P2 81.62(9), O1-Co1-P1 135.02(10), C7-O1-Co1 117.9(3).

The coordination geometry around the cobalt atom can be rationalized as a distorted trigonal bipyramid with three phosphorus atoms of the trimethylphosphine ligands occupying axial and equatorial positions; C1-Co1-P2 163.89(14)°, O1-Co1-P1 135.02(10)°, and O1-Co1-P3 112.87(10)°. The cobalt sphere is completed by the *ortho*-metalated ketone, which acts with a bite angle of 82.28(16)°. The sum of the inner angles of the five membered metalacycle is 539.28° and in the trigonal plane (formed by O1, P1, P3 and Co1) we have a sum of 359.95°. The main axis lies along C1-Co1-P2 °= 163.89(14)°. The plane of the phenyl ring which is not *ortho*-metalated forms an angle with that of the fluorinated phenyl ring about 40°.

The bond lengths Co1-O1=1.903(3) Å and Co1-C1=1.934(4) Å in **24** agree well with those in the imine analogue **15.** The distance Co1-P2=2.2294(13) Å is longer than the equatorial bonds Co1-P1=2.2038(14) Å and Co1-P3=2.1958(13) Å. Due to the coordination and chelation, the bond C6-C7=1.419(6) Å is shorter than the C7-C8=1.472(6) Å.

Discussion

Thermodynamic and kinetic factors affect the selectivity of the activation in partially fluorinated systems.[230] A simple way to picture the whole process arises from bonding energy arguments. Intramolecular activation of the C-F bond has been carried out with Pt(II) and W(0) complexes and it has been demonstrated that the C-F bond is cleaved selectively in the presence of weaker C-H bonds if the ligands are designed with steric constraints; otherwise C-H attack is preferred. The kinetic analysis of these reactions supports a conventional oxidative addition mechanism.[231-236]

Assuming that Co-C bonding energy is similar in all cases (the bond formed by C-H or C-F activation), the difference between both C-H and C-F activation processes can be traced to the realtive bond energies C-F, C-H, H_3C-F and H_3C-H in **28**. Thus, while the C-F activation process would be disfavored because of the higher energy required to break a C-F bond, this should be largely compensated by the H_3C-F formation energy. But on the other side C-F bond of CH_3F is weaker than C-H bond of CH_4 to compansate the energy difference. Caulton stated that the coordination site strongly influences thermodynamics.[228] If coordination to the oxygen brings the metal close to the fluorinated aromatic ring, C-F activation is prefered. So this will be the one which needs less activation energy in the transition state. This is a case where the traditionally defined bond dissociation energies may be of little use for determining reaction thermodynamics. A similar situation has been reported by Su and Chu who found that the oxidative addition of the C-F bond in CH_3-F to 3-coordinated 14-electron complexes $M(X)(PH_3)_2$ (M= Rh, Ir; X = CH_3, H, Cl) is thermodynamically favorable.[237] However, the C-F bond of CH_3F is exceptionally weak compared with an aromatic C-H bond. If the concerted oxidative addition to a C-F bond is kinetically unfavorable, the reductive elimination of R-F is even more unfavorable because of microscopic reversibility.

The compounds **15** and **24** which are formed by C-H activation have the same structural characteristics with C-F activated **28**. Table 2.17 gives a short summary of crystallographic properties of **15**, **24** and **28**. All three compounds show the same deviations from the ideal trigonal bipyramidal geometry. The least deviation in the main axis C1-Co-P1 is obseved in **15**, 168.15(19)°. The five-membered metallacycle is very close to the ideal value in all three compounds.

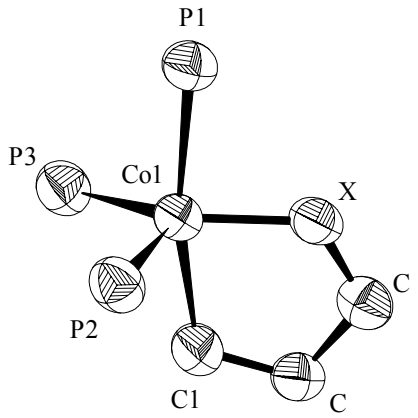

	X = O **28**	X = O **24**	X = NH **15**
Bond lengths (Å)			
Co-X	1.903(3)	1.9051(12)	1.882(5)
Co-C1	1.934(4)	1.9339(18)	1.959(6)
Co-P1	2.2294(13)	2.2401(5)	2.2178(18)
Co-P2	2.1958(13)	2.1852(6)	2.1858(19)
Co-P3	2.2038(14)	2.1786(6)	2.189(2)
C-X	1.297(5)	1.297(2)	1.337(8)
Bond angles (°)			
X-Co-C1	82.28(16)	83.49(7)	80.6(2)
C1-Co-P1	163.89(14)	163.52(6)	168.15(19)
X-Co-P3	135.02(10)	137.94(5)	135.41(17)
P2-Co-P3	112.06(5)	110.77(2)	111.34(7)
P1-Co-P3	96.14(5)	97.73(2)	96.69(7)
Sum internal angles Σ	539.28	540.2	539.4

Table 2.17 Selected structural characteristics of **28**, **24**, and **15**.

2.2 Biyclometalation Reactions via double C-H Activation with Imine Anchoring Groups: A Novel Way of Forming Dianaonic [C,N,C]-Ligands

In the cyclometalation of iron and cobalt described here, the metals retain their low oxidation states in the products and since the effects of donor ligands are similar before and after reaction, except for the chelate effect, it should be possible to perform a second C-H activation. Subsequent elimination accompanied by C,C-coupling would facilitate a catalytic reaction mode. Using complexes of low-valent iron and cobalt with imines which have exactly the proper positions for a second C-H activation, bicyclometalation reactions have been performed for the first time at the same central atom.[238]

2.2.1 Biyclometalation Reaction of $Fe(CH_3)_2(PMe_3)_4$ with N-Benzylidene-1-naphthylamine

Upon combining a dimethyliron compound with certain diarylated imines, a reaction sequence is observed which consists of a double metalation at the same complex center and, for the first time, leads to a metallabicycle.

Synthesis and Characterization

N-Benzylidene-1-naphthylamine reacted with dimethyltetrakis(trimethylphosphine) iron at –70 °C to afford the diaryliron compound **29** which was isolated from pentane in 72% yield [Eq. 2.19].

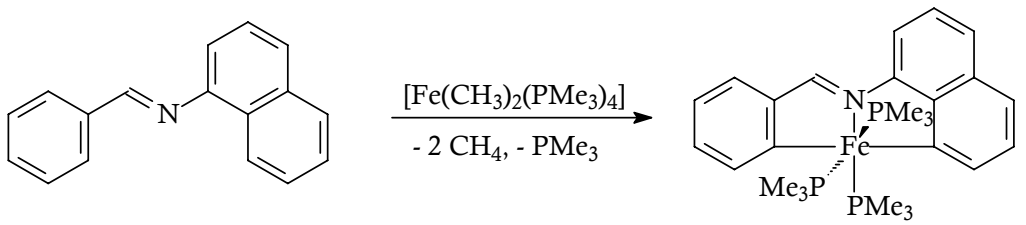

(2.19)

29

The solvent is very important in the synthesis of **29**. When *N*-Benzylidene-1-naphthylamine was combined with $Fe(CH_3)_2(PMe_3)_4$ in THF, total decomposition was observed. The green crystals of **29** start to decompose at 120 °C, and in air their surface remains unaltered at least for 10 minutes. Elemental analysis confirms a complete loss of methane and the presence of three trimethylphosphine groups.

29	%C	%H	%N	%P
Calculated	60.83	7.46	2.73	18.10
Found	60.38	6.68	2.73	18.79

Table 2.18 Elemental analysis data for **29.**

Spectroscopic Identification

The spectrocopic data are compatible with the presence of a mononuclear complex and the absence of isomers or polynuclear compounds as by-products. The IR spectrum of **29** contains in nujol has a strong imine stretching vibration band (ν C=N) at 1509 cm^{-1}. Figure 2.25 shows the ^{1}H NMR resonances of **29**.

In the ^{13}C NMR spectrum (Figure 2.26) virtual triplet at 17.1 ppm for *trans* trimethylphosphine carbons and a resonate as a triplet of doublets at 23.9 ppm for the third trimethylphosphine ligand are observed. This pattern arises from coupling of carbon nuclei with both *cis* and *trans* positioned phophorus nuclei.

The imine carbon appears as a triplet at 161.6 ppm ($^{4}J_{P,C}$ = 3.5 Hz). Most importantly the metalated carbon resonances appear at 194.3 ppm (dt, $^{2}J_{P,C}$ = 24.0 Hz, $^{2}J_{P,C}$ = 11.0 Hz, Fe–C) and 212.1 ppm (dq, $^{2}J_{P,C}$ = 19.5 Hz, $^{2}J_{P,C}$ = 5.7 Hz, Fe–C), respectively. ^{31}P NMR data confirms the *mer*-octahedral coordination with two phosphorus resonances at 16.8 ppm (d, $^{2}J_{P,P}$ = 61.2 Hz, 2P) and 22.9 ppm (t, $^{2}J_{P,P}$ = 61.2 Hz, 1P).

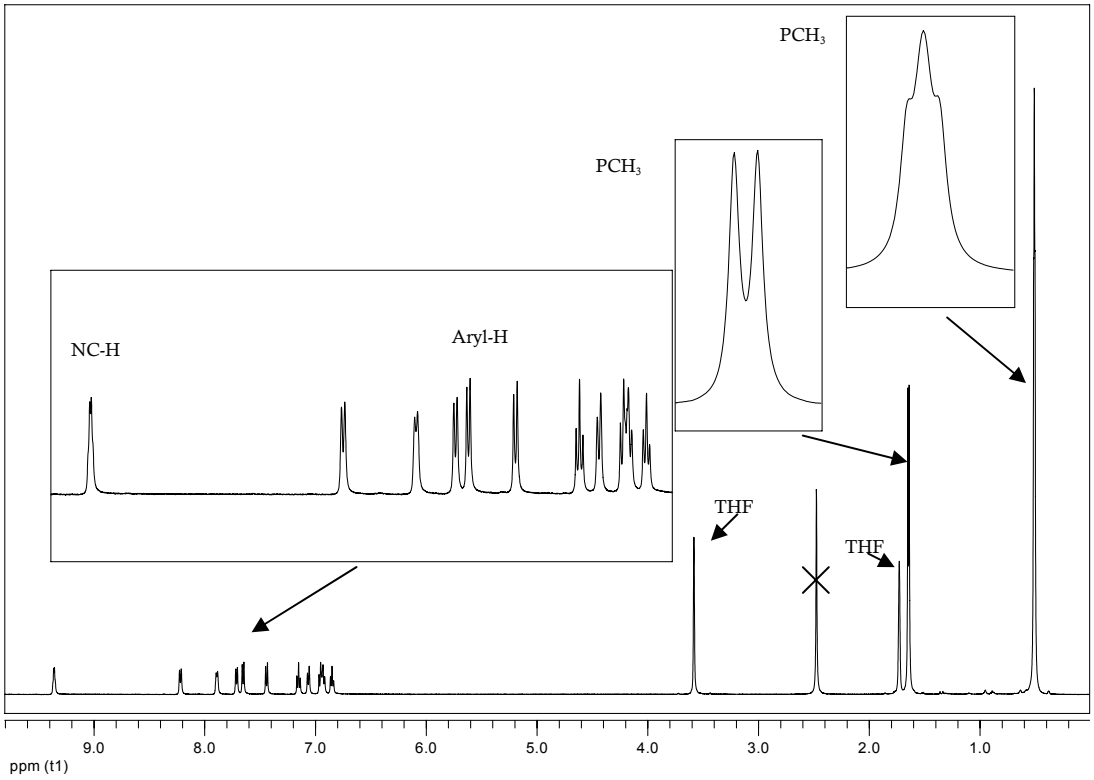

Figure 2.25 ^{1}H NMR spectra of ***29*** (500 MHz, [D_8]THF, 300 K).

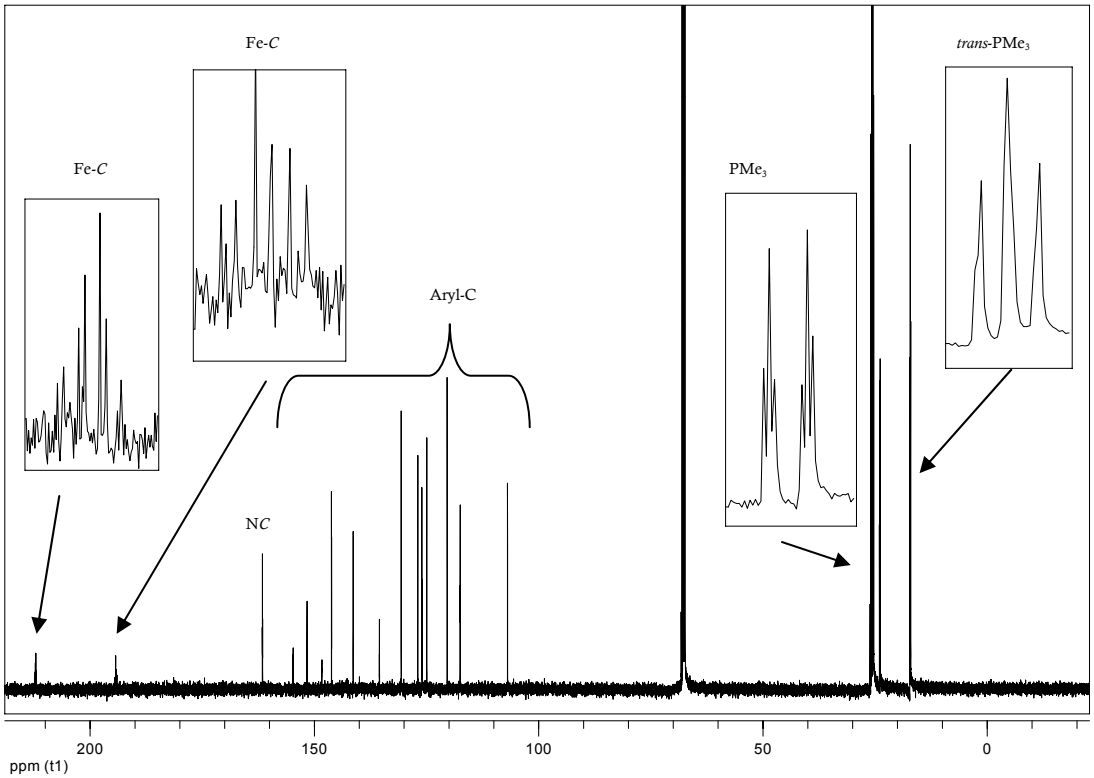

Figure 2.26 ^{13}C NMR spectra of ***29*** (125 MHz, [D_8]-THF, 300 K).

Molecular Structure of 29

The molecular structure of **29** shows a slightly distorted octahedron centered by an iron atom bearing three meridional P donor groups (Figure 2.27). The three remaining ligand positions are occupied by C and N atoms of the metallocycle. The Fe atom deviates from the P_3 and from the C(1)N(1)C(17) plane by 0.135(1) and 0.005(1) Å, respectively. The normals of these planes point at an angle 89.6(1)°. In particular, the sums of internal angles for both five-membered metallacycles (540.0(5)° and 540.0(5)°) approach the ideal value for a planar five-membered ring. This optimum fit consisting of typical bite angles (N1-Fe1-C1 81.21(6)and N1-Fe1-C17 80.47(6)) leads one to conclude, that in the formation of **29** both subsequent metalation steps are initiated by two equally suitable proximity conformations, where at the target point of metallation electron density is transferred from the metal into antibonding σ*(C–H) molecular orbitals.

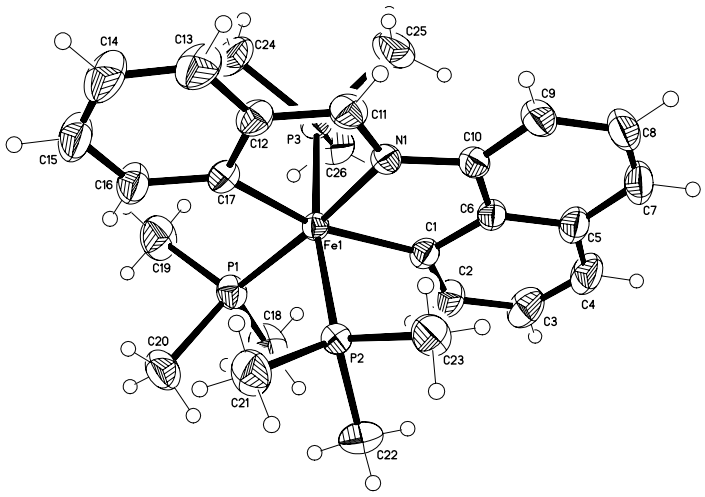

Figure 2.27 Molecular structure of **29**. Selected bond lengths (Å) and angles (°): Fe1-C1 2.0290(14), Fe1-C17 2.0045(14), Fe1-N1 1.9634(12), Fe1-P1 2.2247(4), Fe1-P2 2.2373(4), Fe1-P3 2.2393(4), N1-C10 1.4098(18), N1-C11 1.303(2), C11-C12 1.422(2); N1-Fe1-C1 81.21(6), N1-Fe1-C17 80.47(6), C1-Fe1-C17 161.68(6), C1-Fe-P2 85.39(4), C10-N1-C11 124.19(13), N1-Fe1-P1 174.31(4), P1-Fe1-P3 92.336(17), P2-Fe1-P3 171.245(16).

Discussion

In the wide varity of imines used as substrates in transition metal complexes to form cyclometalated products, naphthyl imines are rarely found. Platinum and palladium form cyclometalated compounds with naphthyl imine either as endo- or exo-metallacycles.[239-240] The reaction unlike in the synthesis of **29** require 7 to 21 days reflux in toluene which results in decomposition and gives very low yield. Complex **29** is the first example for a double metalation at the same metal center. The reaction proceeds under mild conditions and in high yields.

2.2.2 Reaction of $Fe(CH_3)_2(PMe_3)_4$ with *N*-(1-naphthylmethylene)-aniline

With an isostructural imine ligand the question of the reaction pathway is addressed: Is there an influence of steric demand on the ring size in the bicylometalated product?

Synthesis and Characterization

A pentane solution of $Fe(CH_3)_2(PMe_3)_4$ reacts with *N*-(1-naphthylmethylene)aniline at –70 °C to form η^4-iron(0) complex **30** [Eq. 2.20].

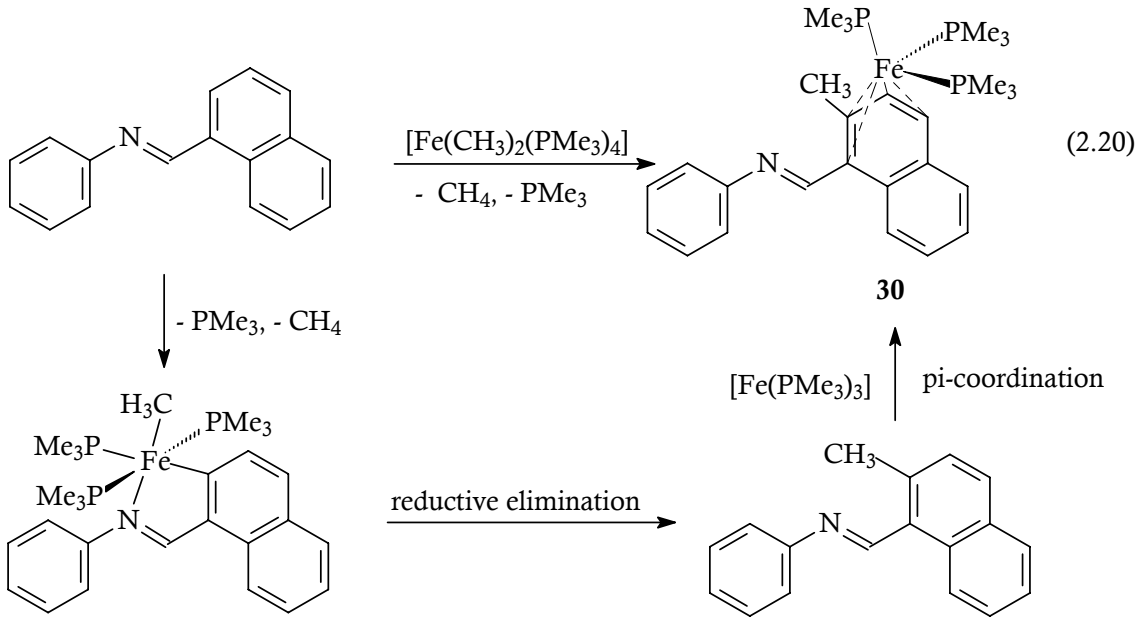

(2.20)

At varience with compound **29**, reaction starts with a β C-H activation step. $Fe(CH_3)_2(PMe_3)_3$ coordinates to the nitrogen atom of the imine ligand dissociating a PMe_3 group which is followed by C-H activation (β-position in the naphthalene group), and elimination of CH_4. The remaining methyl group in the octahedral Fe(II) compound undergoes C,C-coupling with the β-carbon of the naphthalene group and the aromatic backbone reductively couples with the Fe-CH_3 group. $Fe(PMe_3)_3$ is attached to the diene system to form π-coordinated complex **30**.

Spectroscopic investigations

Compound **30** is a paramagentic substance. The IR spectrum shows the typical absorption bands in the region for C=C and C=N stretching frequencies indicating coordination to the metal (Table 2.19).

IR, cm^{-1}	**30**	**IR, cm^{-1}**	**30**
ν (H–C=N)	3049 vw, 3030 vw	ρ_1 (PCH_3)	952 s, 937 vs
ν (H–C=N)	1603 m	ρ_2 (PCH_3)	850 m
ν (C=C)	1567 vs	γ (C-H)	743 s
δ_{as} (PCH_3)	1451 s	ν_{as} PC_3	705 s, 694 s
δ_s (PCH_3)	1296m, 1277 m	ν_s PC_3	658 s

Table 2.19 Selected IR frequencies of **30**.

Molecular Structure of 30

In the mononuclear complex **30** a $Fe(PMe_3)_3$ group is η^4-coordinated to the α-ring in the naphthyl-part of N-naphthylidenphenylimine (Figure 2.28). The carbon atoms C13 and C18 of the α-C_6 ring in the naphthyl part are held at a nonbonding distance and are located of the plane C1, C2, C3, C5 and away from the metal at an angle of 18° with respect to that plane. The iron phosphorus distances (2.21 – 2.24 Å) and also the iron carbon distances (2.02 – 2.10 Å) and angles are as expected, except for the very long Fe1-C5 distance (2.248(3) Å) which is the longest cited in literature so far. The reason is seen in the spatial requirement of the methyl group

C4. In the structure of **30** the β-position of the naphthyl part of the ligand contains the methyl group throughout the reducvive elimination step with a typical single bond distance C3-C4 = 1.516(4) Å. Typical distances between iron and aromatic or aliphatic carbons are (1.95 – 2.15 Å).[241] For instance complex **30** closely resembles the structure of a trimethylphosphine stabilized pyridine-iron(0) complex.[242] The N-C distance (1.142(4) Å) maintains essentially a double bond character in agreement with the IR spectrum showing the imino band at 1603 cm^{-1}.

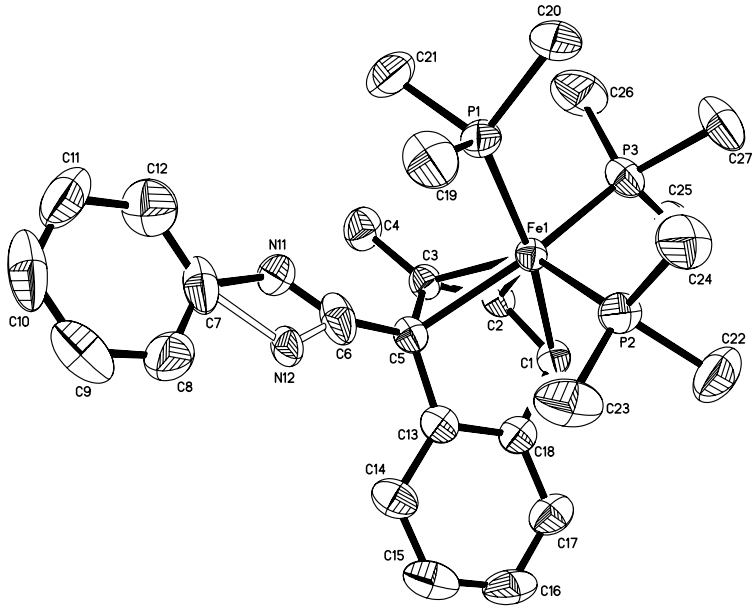

Figure 2.28 Molecular structure of **30** (ORTEP plot with hydrogen atoms omitted). Selected bond lengths (Å) and angles (°): Fe1-C1 2.109(3), Fe1-C2 2.027(3), Fe1-C3 2.074(3), Fe1-C5 2.248(3), Fe1-P1 2.2451(9), Fe1-P2 2.2053(9), Fe1-P3 2.2087(9), C1-C2 1.432(4), C2-C3 1.395(4), C3-C5 1.464(4), C3-C4 1.516(4), C5-C6 1.449(4) N11-C6 1.149(4); P1-Fe1-C1 170.28(8), P1-Fe-C2 132.03(9), P1-Fe1-P2 96.78(3), P1-Fe1-P3 93.12(4), P2-Fe1-P3 99.21(4), P2-Fe1-C5 103.81(8), C3-Fe1-P3 114.69(8), C1-Fe1-P2 90.14(8), C2-Fe1-P2 130.58(9), P1-Fe1-C3 100.02(8), P1-Fe1-C5 97.06(7), P3-Fe1-C5 153.46(7).

If we define the atoms P1, P2, P3 and the midpoints of the bonds C1-C2 and C3-C5 as ligand positions, the geometry around the iron is trigonal bipyramidal. P2, P3 and the midpoint C3-C5 occupy equatorial positions and the trimethylphosphine group (P1) is in one of the axial positions. Certainly in the other axial position the midpoint C1-C2 deviates from an ideal trigonal bipyramidal geometry by an angle of 28.8° which is due to the rigid diene geometry of the naphthyl ring.

Discussion

The β-position of the naphthyl part containing a new methyl group must arise from an intermediate *ortho*-metalation step with $FeMe_2(PMe_3)_4$ followed by a reductive elimination with

C,C-coupling. $Fe(PMe_3)_3$ fragment thaen coordinates in a η^4-fashion to the α-part of the N-naphthylidenphenylimine ligand. The reaction product suggests that in the switched coordination mode from the N=C part in the imine ligand there is no reaction with the phenyl part of the imine ligand which might lead to a bicylometalated product. The only possibility would be a second C-H activation in the phenyl ring forming a four-membered metallacyle. So far such C-H activation step has not been observed with iron.

2.2.3 Reaction of $Fe(CH_3)_2(PMe_3)_4$ with *N*-Benzylbenzylideneimine

Cyclopalladation, cyclomanganation and cycloplatination reactions of *N*-benzylbenzylideneimine are known.[243-249]. Generally two different metallacycles, are formed, either with an endocyclic structure (containing the C=N group) or with an exocyclic structure (Figure 2.29).

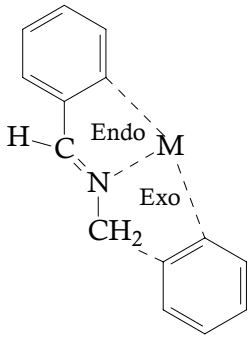

Figure 2.29 Possible endo and exo structures of metallacycles.

N-Benzylbenzylideneimine reacts with $Fe(CH_3)_2(PMe_3)_4$ to give a bicyclometalated iron(II) compound formed by two five-membered metallacycles which share one metal atom.

Synthesis and Characterization

The bicyclometalated iron(II) compound **31** was obtained by the reaction of $Fe(CH_3)_2(PMe_3)_4$ with *N*-benzylbenzlideneimine at -70 °C [Eq. 2.21].

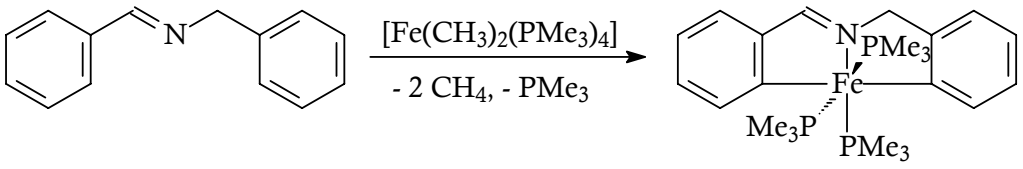

(2.21)

31

31 was isolated from pentane as reddish brown crystals, which under argon are stable up to 107 °C. Analytical characterization confirms the constitution of **31** (see Experimental Part).

Spectroscopic Identification

We can see all characteristic vibrations in the IR spectrum. At 1527 cm^{-1} we observe the C=N streching vibration. The deformation mode of PCH_3 absorbs at 941 cm^{-1}. In the ^1H NMR spectrum the protons of *trans* trimethylphosphine groups resonate at 0.7 ppm as a singlet. The singular trimethylphosphine protons resonate at 1.58 ppm as doublet ($^2J_{P,H}$ = 4.3 Hz). At 5.04 ppm, the -CH_2- group appears as singlet, while ten aromatic protons resonate between 6.85 ppm and 8.00 ppm. The imine group proton resonates at 8.52 ppm as a singlet as expected. The ^{13}C NMR spectrum confirms the proposed coordination: two metalated carbon atoms resonate at 184.8 ppm (m, Fe–C) and 204.8 ppm (q, $^2J_{P,C}$ = 9.2 Hz, Fe–C). In the ^{31}P NMR spectrum, figure 2.30, trimethylphosphine groups show resonances as expected from the octahedral geomerty at 16.1 ppm (dd, $^2J_{P,P}$ = 60.0 Hz, $^2J_{P,P}$ = 63.0 Hz 2P, PCH_3) and 20.5 ppm (dd, $^2J_{P,P}$ = 60.0 Hz, $^2J_{P,P}$ = 63.0 Hz, 1P, PCH_3).

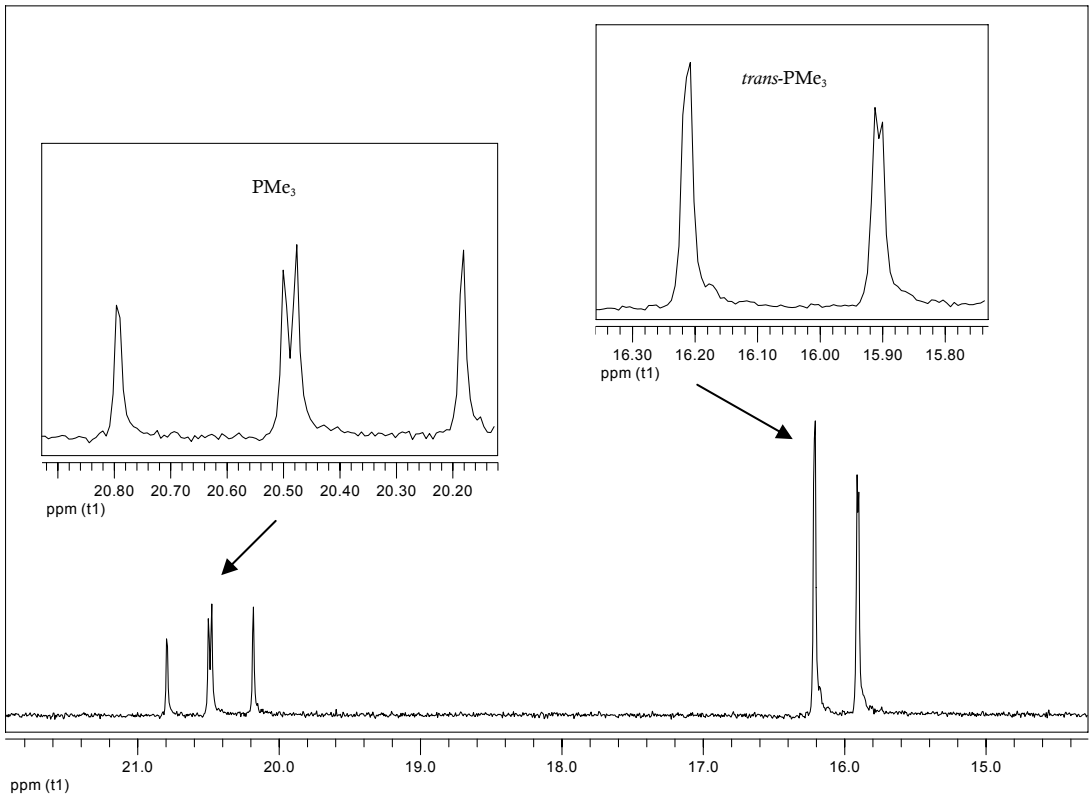

Figure 2.30 ^{31}P NMR spectrum of **31** (202 MHz, [D_8]THF, 300 K).

Molecular Strucutre of 31

An X-ray diffraction analysis was performed on a single crystal obtained by keeping a pentane solution of **31** at 4 °C. Figure 2.31 shows the molecular structure of **31**. The molecule attains an octahedral geometry with a *mer* arrangement of the three PMe_3 ligands. The remaining three sites are occupied by two σ-bonded carbon atoms and the nitrogen donor of the chelating arylimino ligand.

The angle at nitrogen (C8-N1-C1 = 120.83(16)°) and the N1-C8 distance of 1.339(2) Å are consistent with the presence of a double bond in this position. The frame characterized by N1-Fe1-P2 175.45(5)°, C14-Fe1-C7 161.43(7)°, and P3-Fe1-P1 173.30(2)° is bent. The bite angle in the C=N five-membered metalacycle 80.27 (7)° is slightly smaller than the second five-membered metallacycle 81.18(7)°.

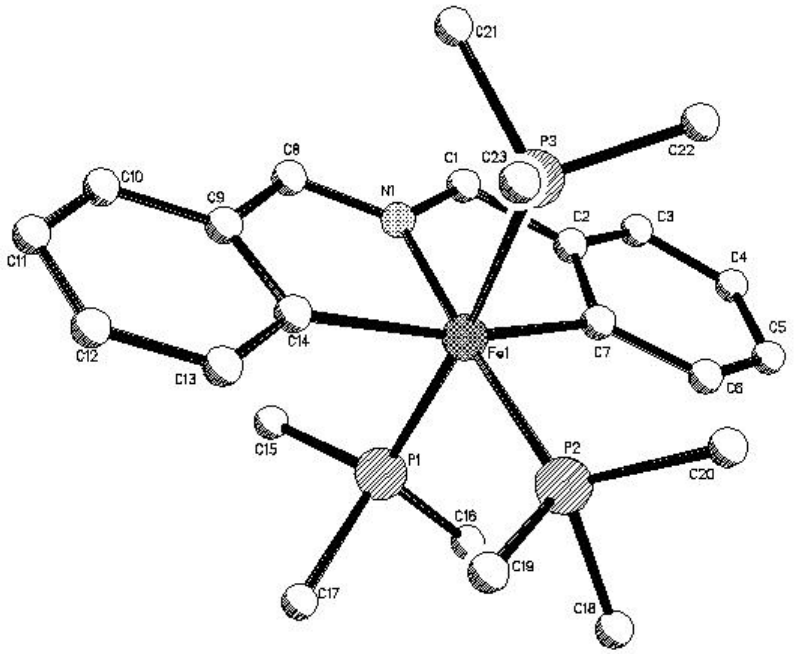

Figure 2.31 Molecular structure of **31**. Selected bond lengths (Å) and angles (°): Fe1-C7 2.0286(17), Fe1-C14 2.0397(17), Fe1-N1 1.9440(15), Fe1-P1 2.2239(5), Fe1-P3 2.224(5), Fe1-P2 2.2397(5), N1-C1 1.408(2), N1-C8 1.339(2), C1-C2 1.471(3), C8-C9 1.455(3); N1-Fe1-C7 81.18(7), N1-Fe1-C14 80.27(7), C7-Fe1-C14 161.43(7), N1-Fe1-P1 88.67(5), N1-Fe1-P3 88.67(5), N1-Fe1-P2 175.45(5), C7-Fe1-P1 91.72(5), C14-Fe1-P3 86.54(5), P1-Fe1-P2 91.75(2), P3-Fe1-P2 91.38(2), C8-N1-C1 120.83(16).

The Fe-C distances to the σ- bonded aryls of the aromatic backbone are similar to those in the structure of **29** (Fe1-C7 = 2.0286(17) Å and Fe1-C14 = 2.0397(17) Å). Because of the symmetry in **31**, both metallacycles have very close structural characteristics and they are compatible with the ones in **29**. The sum of internal angles in the both five-membered metalacycles are 540° and they are exactly coplanar.

Discussion

Like *N*-(1-naphthylmethylene)-aniline, *N*-Benzylbenzylideneimine reacts with $Fe(CH_3)_2(PMe_3)_4$ to give a symmetric, bicyclometalated iron(II) compound. Both compounds have very similar spectroscopic and structural characteristics (Table 2.20 and 2.21).

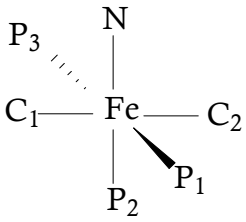

^{1}H-NMR, ppm :	**29**	**31**
δ $P_{(1)}Me$, δ $P_{(3)}Me$	0.51; t' $\lvert {}^{2}J_{P,H} + {}^{4}J_{P,H} \rvert$ = 5.4 Hz	0.70 ; s
δ $P_{(2)}Me$	1.64 ; d $^{2}J_{P,H}$ = 5.9 Hz	1.58 ; d $^{2}J_{P,H}$ = 4.3 Hz
δ H–C=N	9.36; s	8.52; s
^{13}C-NMR, ppm :	**29**	**31**
δ C=N	161.6; t $^{4}J_{P,C}$ = 3.5 Hz	170.5; t $^{4}J_{P,C}$ = 4.5 Hz
δ Fe-C_1	194.3; dt $^{2}J_{P,C}$ = 24.0 Hz $^{2}J_{P,C}$ = 11.0 Hz	184.8; m
δ Fe-C_2	212.1; dq $^{2}J_{P,C}$ = 19.5 Hz $^{2}J_{P,C}$ = 5.7 Hz	204.8; q $^{2}J_{P,C}$ = 9.2 Hz
^{31}P-NMR, ppm :	**29**	**31**
δ $P_{(1)}Me$, δ $P_{(3)}Me$	16.8; dd $^{2}J_{P,P}$ = 59.9 Hz $^{2}J_{P,P}$ = 63.2 Hz	16.1; dd $^{2}J_{P,P}$ = 60.0 Hz $^{2}J_{P,P}$ = 63.0 Hz
δ $P_{(2)}Me$	22.9; t $^{2}J_{P,P}$ = 59.9Hz $^{2}J_{P,P}$ = 63.2 Hz	20.5; dd $^{2}J_{P,P}$ = 60.0 Hz $^{2}J_{P,P}$ = 63.0 Hz

Table 2.20: Selected spectrocopic data of complexes **29** and **31.**

As complex **31** is more symmetric than **29** so we can see a different pattern in the spectroscopic data. Both form two identical five-membered metallacycles. Naphthalene and phenyl rings in **29** and both phenyl rings in **31** are coplanar with each other. Even though we cannot see P,H coupling for two *trans* trimethylphosphine groups in the ^{1}H-NMR spectrum of **31** (it is recorded as singlet), **29** and **31** show ^{31}P NMR resonaces with the same couplings. And crystallographically, they are closely related to each other.

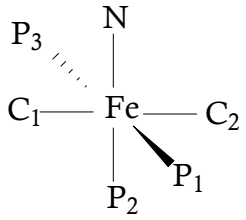

Bond lenghts, [Å]	**29**	**31**
N–Fe	1.9634(12)	1.9440(15)
Fe–C_1	2.0045(14)	2.0397(17)
Fe–C_2	2.0290(14)	2.0286(17)
Fe–P_1	2.2373(4)	2.224(5)
Fe–P_2	2.2474(4)	2.2397(5)
Fe–P_3	2.2393(4)	2.223985)
Bond angles, [°]	**29**	**31**
N–Fe–C1	80.47(6)	80.27(7)
N–Fe–C2	81.21(6)	81.18(7)
N–Fe1–P2	174.31(4)	175.45(5)
C1–Fe–C2	161.68(6)	161.43(7)
P1–Fe–P3	92.336(17)	91.38(2)
Σ (5-Ring)	**29**	**31**
N–Fe–C1 cycle	539.98	540
N–Fe–C2 cycle	539.98	539.86

Table 2.19 : Selected structural data of **29** and **31.**

2.2.4 Iodomethane Reaction of the Bicyclometalated Compound 31

Synthesis and Characterization

Iodomethane oxidizes **31** to form an iron(III) complex. Combining at low temperature **31** with iodomethane in pentane according to equation 2.22 the color of the solution changes immiedately.

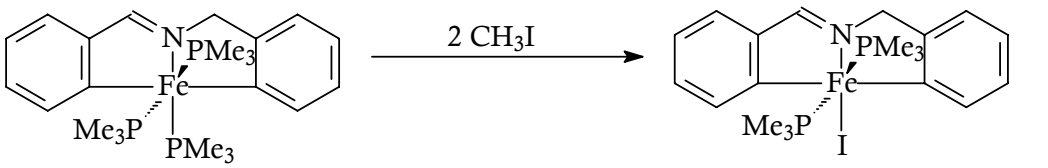

(2.22)

31 **32**

After 16 h reaction time **32** crystallizes at 4 °C. Solid **32** decomposes under argon between 144 – 146 °C. Crystals of **32** were suitable for X-ray diffraction.

Spectroscopic Investigation

In the IR spectrum no unusual coordination mode is indicated. The absorption bands of the coordinated imine backbone and trimethylphosphine ligands are found at typical wavelengths. For complex **32** no conspicuous line broadening in the ^{1}H NMR spectrum is present possibly caused by paramagnetism. The two trimethylphosphine ligands resonate at 0.93 ppm as a pseudo triplet ($|{}^{2}J_{P,H} + {}^{4}J_{P,H}|$ = 14.3 Hz). Most interesting, the aromatic and imine protons are shifted to low field. The aromatic protons are found between 12.92 and 13.43 ppm and the imine proton is shifted from 9.5 ppm in the iron(II) complex to 18.2 ppm when compared with previously discussed bicycylometalated compounds of cobalt(III) and iron(II). The reason for only six carbon resonances in the ^{13}C NMR spectrum arises from the delocalized double bond, which results in a C_s-symmetry for complex **32**. In the ^{31}P NMR one singlet is recorded at 2.5 ppm indicating two coordinated isochronic trimethylphosphine ligands.

Molecular Structure of 32

Figure 2.32 shows a view of the molecular geometry of **32** with selected bond lenghts and angles.

The coordination geometry around the iron atom can be rationalized as a distorted octahedron, with the two trimethylphosphine ligands occupying apical positions (P1-Fe1-P2 = 176.13(9)°). The nitrogen donor atom of the aromatic backbone is *trans* to the iodine group (I1-Fe1-N1 = 179.53(17)°).

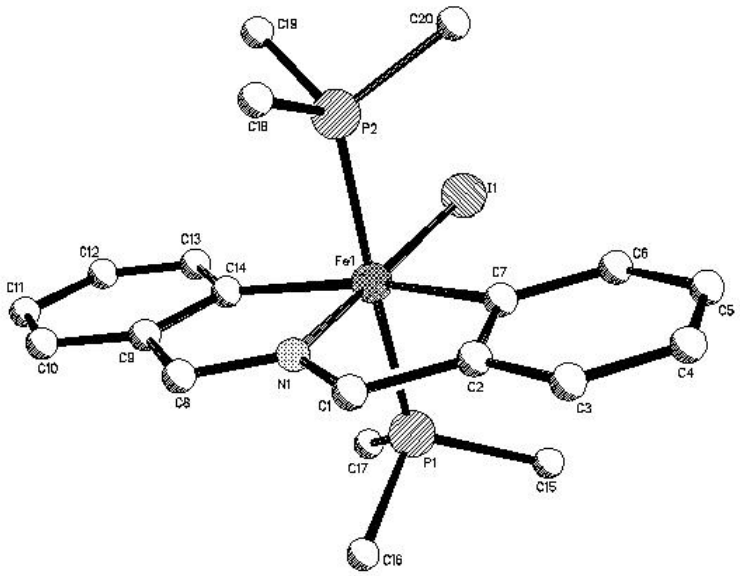

Figure 2.32 Molecular structure of **32**. Selected bond lengths (Å) and angles (°): Fe1-I1 2.6119(12), Fe1-N1 1.933(5), Fe1-C7 2.008(7), Fe1-C14 2.023(8), Fe1-P1 2.243(2), Fe1-P2 2.244(2), N1-C8 1.386(8), N1-C1 1.361(8), C1-C2 1.448(9), C8-C9 1.479(9); N1-Fe1-C7 80.2(3), N1-Fe1-C14 79.8(3), C7-Fe1-C14 160.0(4), N1-Fe1-P1 92.61(17), C7-Fe1-P1 90.35(19), C14-Fe1-P1 90.1(2), C14-Fe1-P2 91.1(2), C7-Fe1-P2 89.70(19), P1-Fe1-P2 176.13(9), N1-Fe1-I1 179.53(17).

The Fe-I distance (2.6119(12) Å) is well-fit with other mononuclear iron-iodine derivatives.[250] The iron sphere is completed by the metalabicycle, which acts with bite angles of 80.2(3) and 79.8(3)°. The two Fe-C bond lengths (2.008(7) and 2.023(8) Å) are as expected for an Fe-C(sp^2) single bonds which are similar to those found in complexes **4** and compatible with other aryl-iron complexes.[251]. The bond lengths C1-C2 = 1.448(9) Å and C8-C9 = 1.479(9) Å agree well with the average carbon carbon single bond distances in imino groups despite of similar distances N1-C1 = 1.361(8) Å and N1-C8 = 1.386(8) Å.

Discussion

With iodomethane, **31** is oxidized and an iodo ligand is attached *trans* to the nitrogen donor atom forming **32**. The fate of the methyl group is uncertain. One possibility is the loss of ethane from two molecules of **32** as described for other halogen bridged dinuclear complexes containing methyl groups.

Instead of an iron(III) complex with an imine coordinated backbone to the metal, **32** can be described as iron(IV) nitrene type complex. The resonance structures (figure 2.33) show the delocalization of the double bond in **32**.

2.2.5 Carbon Monoxide Reactions of the Bicyclometalated Iron Compound *29*

In solution under 1 bar of CO at 20 °C, ***29*** forms a monocarbonyl complex **33** [Eq. 2.23]. The dark green crystals of **33** are thermally by about 60 K more stable than their parent trimethylphosphine compound ***29*** and are less air sensitive. Complex **33** crystallizes in 61 % yield and proved suitable for an X-ray diffraction.

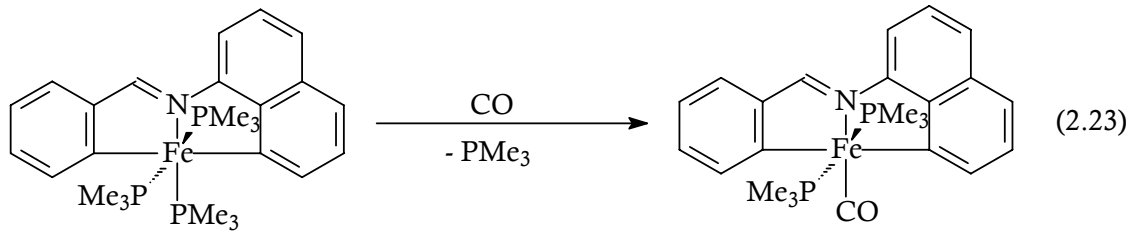

(2.23)

29 **33**

Spectroscopic Investigation

In the IR spectrum the coordination of a terminal carbonyl group is indicated by a strong absorption at 1883 cm^{-1}. In the ^{1}H NMR spectrum the trimethylphosphine ligands appears as a pseudo triplet at 0.63 ppm ($|^{2}J_{P,H} + {}^{4}J_{P,H}| = 7.9$ Hz). This spectrum also contains eight resonances for the aromatic protons between 6.89 and 8.13 ppm. The imine proton is observed as a triplet at 9.28 ppm with a coupling constant of 4.9 Hz. In the ^{13}C NMR spectrum the two metalated carbon nuclei arise as triplets with a P-C couplings of 22.5 Hz and 33.2 Hz, respectively. With a similar coupling of 32.5 Hz the carbon of the carbonyl group is detected at 218.7 ppm. The ^{31}P NMR spectrum contains one singlet at 19.2 ppm, which is assigned to the isochronic trimethylphosphine ligands.

Molecular Structure of 33

The structure solution of **33**, which was deduced by NMR spectroscopy in solution, was supported by an X-ray structure analysis in the solid state. A representation of the molecular structure of **33** is given in Figure 2.33; selected bond length and angles are collected beneath.

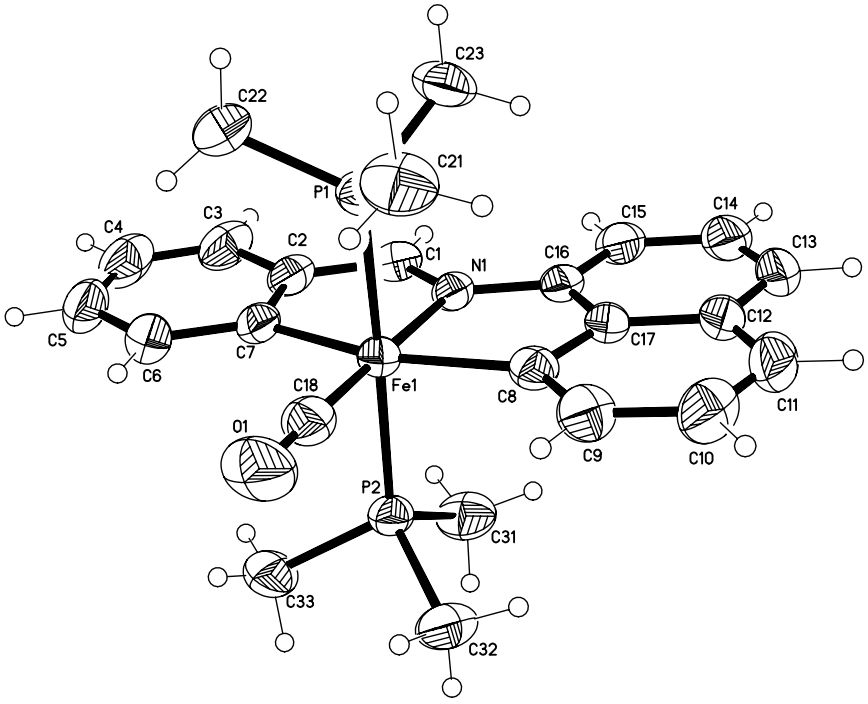

Figure 2.33 Molecular structure of **33**. Selected bond lengths (Å) and angles (°): Fe1-C18 1.718(2), Fe1-C7 1.976(2), Fe1-C8 2.0002(19), Fe1-N1 1.9767(14), Fe1-P1 2.2160(5), Fe1-P2 2.2167(5), C18-O1 1.160(2), N1-C1 1.301(2), N1-C16 1.410(2); N1-Fe1-C8 81.03(7), C7-Fe1-N1 80.66(7), C7-Fe1-C8 161.67(8), N1-Fe1-C18 179.13(8), C7-Fe1-P1 90.71(5), C18-Fe1-P2 86.74(7), N1-Fe1-P2 92.39(4), C8-Fe1-P2 91.04(5), P1-Fe1-P2 176.04(2).

Crystals of the carbonyl derivative **33** were obtained by slow crystallization of concentrated solution of **33** in pentane at 4 °C. The geometry around the iron center is octahedral. The two PMe_3 ligands are *trans* to each other and the incoming carbonyl ligand is *trans* to the nitrogen donor as suggested by the solution NMR data.

The two planes formed by the metal Fe1, the carbon atoms C7, C2, C1, C8, C17, and C16 and the nitrogen atom N1 enclose an angle of 161.67(8)°. All these crystal data are closely comparable to reported iron complexes described above.

Discussion

As expected, carbon monoxide easily replaces one of the trimethylphosphine ligands. Substitution occurs regiospecifically *trans* to nitrogen. From the NMR spectra there are no hints for insertion reactions into the iron carbon or iron nitrogen bonds.

2.2.6 Carbon Monoxide Reactions of Bicyclometalated Iron Compound 31

Synthesis and Characterization

In solution under 1 bar of CO at 20 °C, **31** forms a monocarbonyl complex **34** and a dicarbonyl complex **35** [Eqs. 2.24 and 2.25]. The dark crystals of **34** are thermally stable up to 117 °C and dark violet **35** up to 127 °C. Both complexes **34** and **35** crystallize from the same solution in a combined yield of 67%.

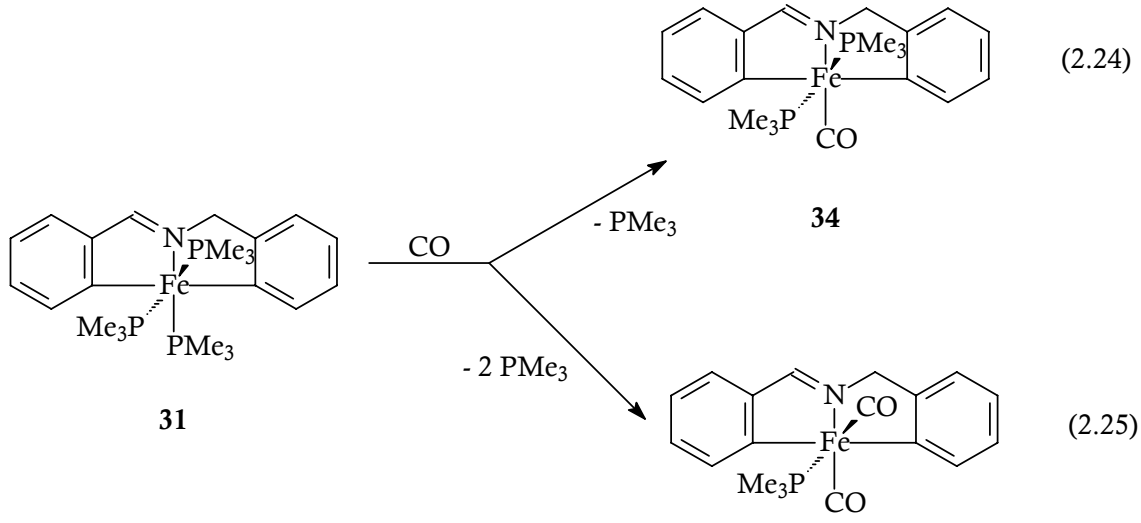

31 **34** **35**

Spectroscopic Investigation

IR spectra (Figure 2.34 and 2.35) displays characteristic bands around 1882 cm^{-1} for **34** and 1922 cm^{-1} for **35** indicating terminal carbonyl ligands and around 1531 cm^{-1} for endocyclic C=N groups. These are bathochromically shifted by about 13 cm^{-1} with respect to the parental complex **31**. As expected for a monocarbonyl complex **34** the trimethylphosphine ligands in the ^{1}H NMR spectrum give rise a pseudotriplet at 0.76 ppm with a $|^{2}J_{P,H} + {}^{4}J_{P,H}| = 7.8$ Hz.The dicarbonyl complex **35** diplays the phosphine resonance as the expected doublet at 0.78 with $^{2}J_{P,H} = 9.5$ Hz. The same pattern for the phosphine resonances is found in the ^{13}C NMR spectra. In the remaining aromatic carbon signals is nothing remarkable displayed. The ^{31}P NMR spectra show two resonances as singlets which are compatible with a first isomer with substitution of *trans* position of nitrogen and a second product where two trimethylphosphine ligands are substituted by carbon monoxide.

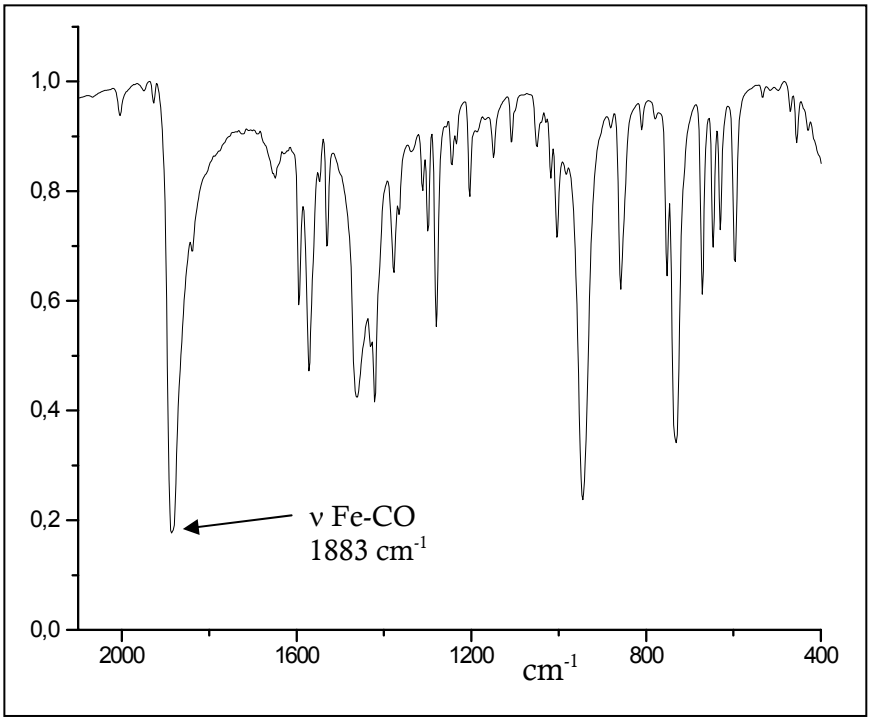

Figure 2.34 IR spectrum of **34** between 2000 and 400 cm^{-1}.

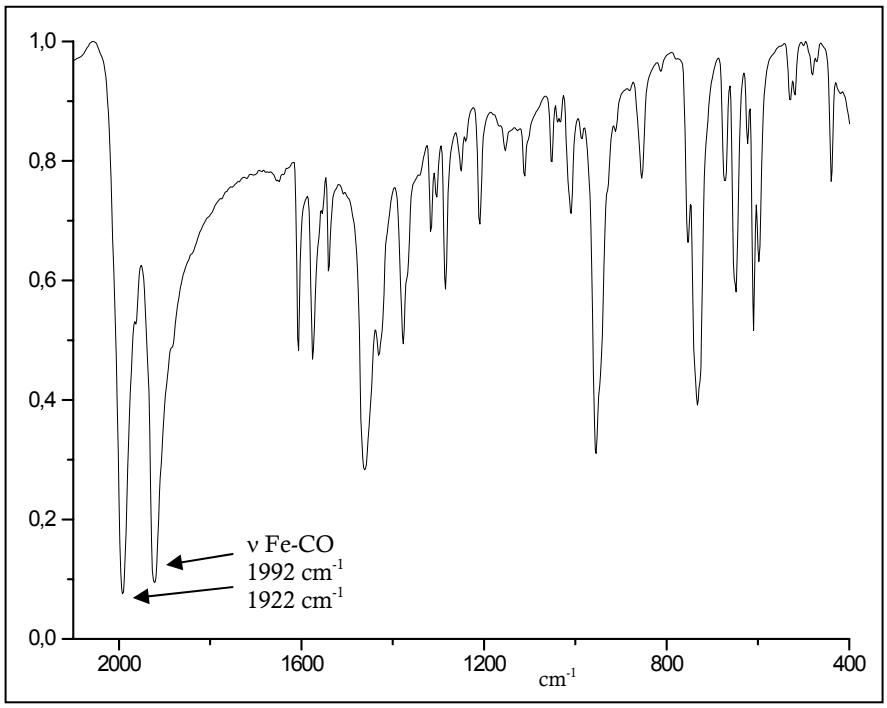

Figure 2.35 IR spectrum of **35** between 2000 and 400 cm^{-1}.

Discussion

When increased reaction time is allowed for **31** under an atmosphere of carbon monoxide affords two products. Complexes **34** and **35** contain terminal carbonyl groups and are less air sensitive than the parentcompound **31**. The resulting two products cannot be separated by fractional crystallization or by separating the crystals manually due to the same appearance of crystal color and shape. The mixture gave no a satisfactory elemental analysis.

2.2.7 Reaction of $Co(CH_3)(PMe_3)_4$ with N-Benzylidene-1-naphthylamine

In this thesis a dimethyl iron complex was found to bicyclometalate *N*-benzylidene-1-naphthylamine for the first time. In the reaction pathway an iron(IV) intermediate is considered which spontanously eliminates methane. In order to shed more light on this it is neccessary to conduct a reaction with $Co(CH_3)(PMe_3)_4$ under same conditions which should result in an isolelectronic cobalt(III) d^6 intermediate.

Synthesis and Characterization

Equimolar amounts of *N*-benzylidene-1-naphthylamine react with $Co(CH_3)(PMe_3)_4$ at -70 °C in THF. During slow warm up an evolution of gas is detected and a color change from orange red to dark red is observed. The reaction affords **36** exclusively, isolated in 67% yield [Eq 2.26]. Red crystals of **36**, melting with decomposition between 109 and 111 °C, were obtained from pentane at -27 °C.

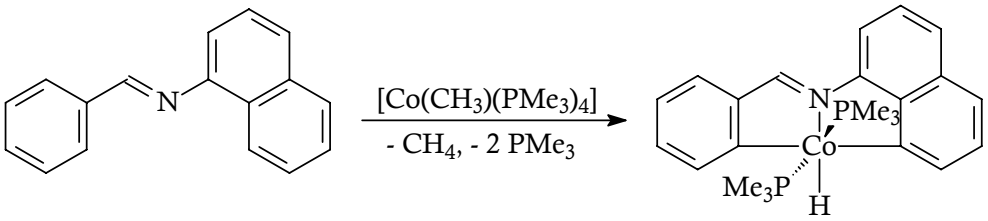

(2.26)

36

Spectroscopic investigations

The coordination of a hydrido ligand is indicated by the IR spectrum (figure 2.36) with a strong band at 1860 $cm^{-1}$and a triplet is arising in the ^{1}H NMR with a coupling $^{2}J(PH)$ = 71.1 Hz to two isochronic phosphorus nuclei.

In the $^{13}C\{^{1}H\}$ NMR spectrum of **36** (figure 2.38), the most distinctive spectroscopic data are two multipletts at 181.1 and 197.9 ppm indicating metallated carbon. Broadening is due to the nuclear spin of cobalt (I= 7/2).

In the ^{31}P NMR spectrum, the observed singlet resonance at 9.50 ppm is only compatible with two trimethyphosphines ligands mutual *trans* positions.

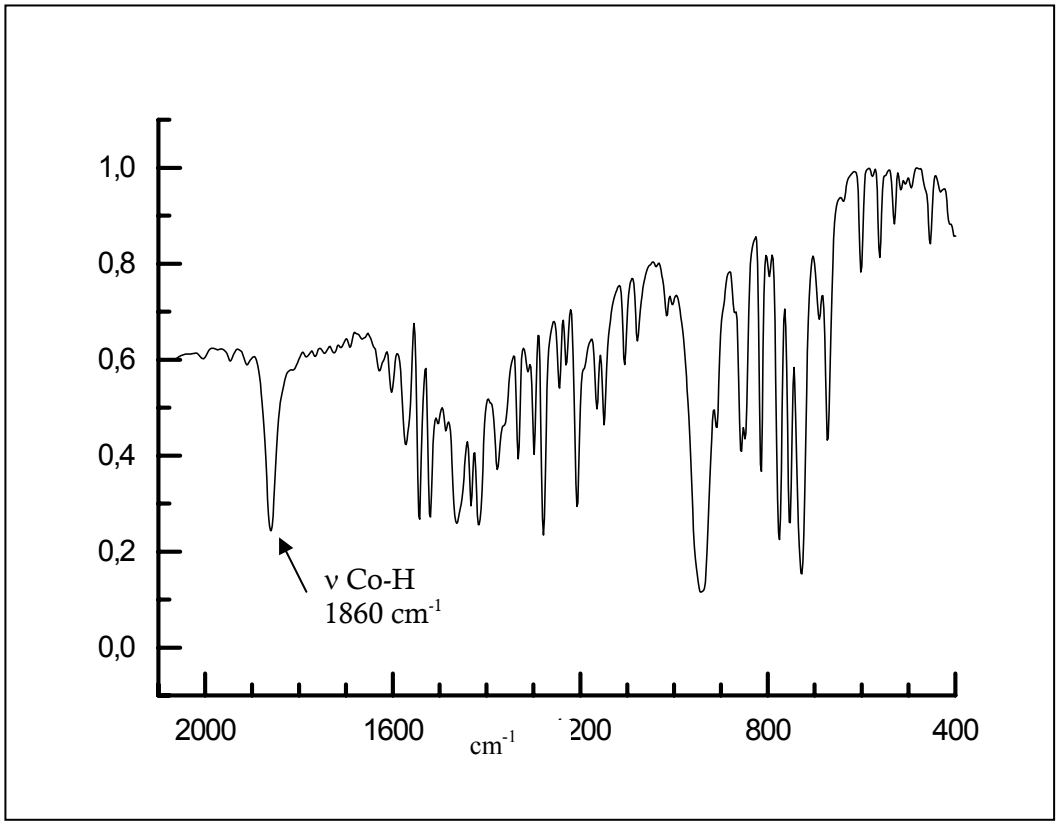

Figure 2.36 IR spectrum of **36**.

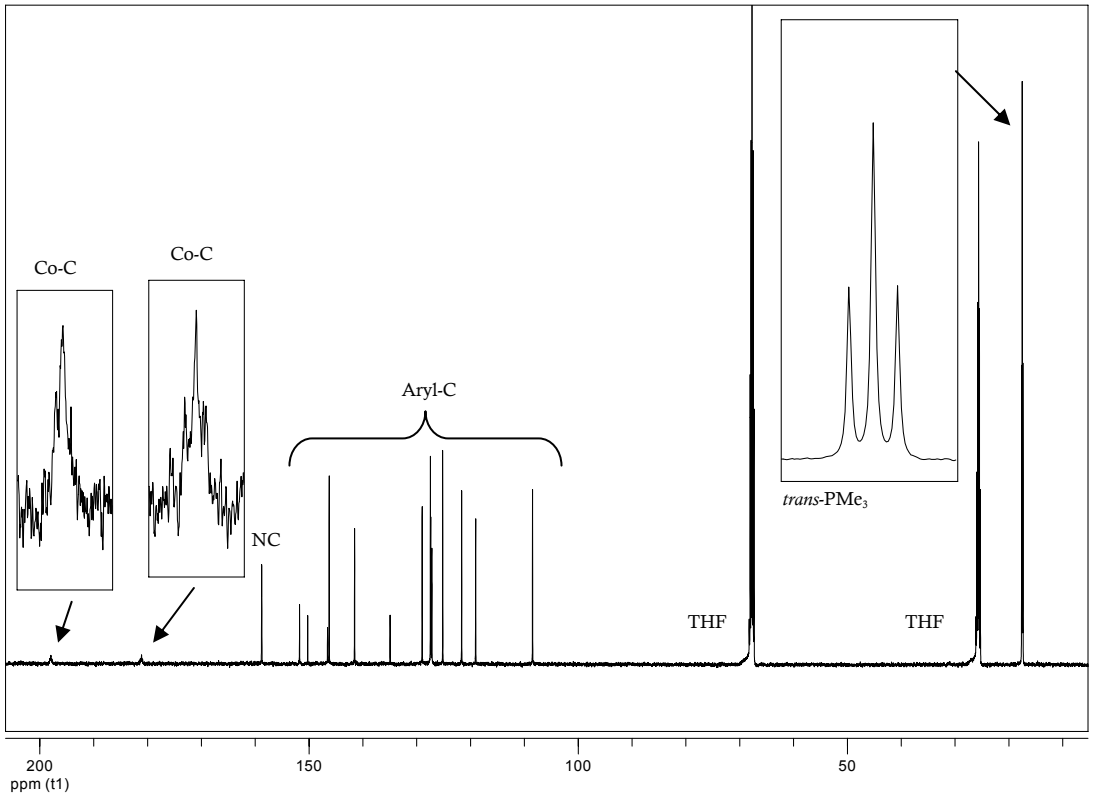

Figure 2.37 ^{13}C NMR spectra of **36** (125 MHz, [D_8]-THF, 300 K).

Discussion

Under same reaction conditions as with $Fe(CH_3)_2(PMe_3)_4$ and the imine ligand, a stable isoelectronic hydrido cobalt(III) complex is isolated. The predicted coordination geometry is the same as i the bicyclometalated iron complex **29**, with the difference of a hydrido ligand instead of a trimethylphosphine in **36**.
Compound **36** is the first bicyclometallated hydrido-cobalt(III) complex and also provides evidence for an iron(IV) intermediate in the formation of **29** [Eq. 2.19]. Interestingly, no reductive elimination is observed of the stable complex **36,** which could involve the coordinated phenyl group or the hydrido ligand.

2.2.8 Reaction of $Co(PMe_3)_4$ with N-Benzylidene-1-naphthylamine Synthesis and Characterization

Combining equimolar solutions of $Co(PMe_3)_4$ with *N*-benzylidene-1-napthylamine in THF at -80 °C shows a color change from dark brown to red brown [Eq. 2.27] Concentrated pentane solutions of **37** afforded in 55 % yield brown crystals, which were suitable for X-ray diffraction.

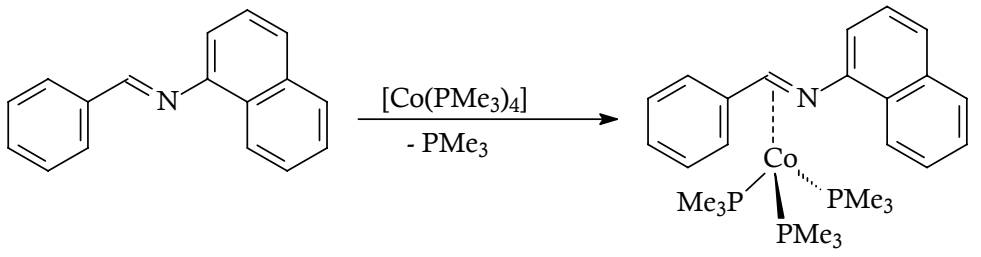

(2.27)

37

Spectroscopic investigations

The infrared spectrum of **37** contains all bands characteristic for coordinated trimethylphosphine, while the fingerprint of the hydrocarbon ligand does not clearly indicate the type of metal coordination. The ^1H NMR spectrum of **37** is totally different than all the previously reported complexes in this thesis. There are

unusual shifts and line broadenings that can be connected with the paramagnetic valence state.

Molecular Structure of 37

In the molecular structure of complex **37** a Co(PMe$_3$)- fragment is η^2-coordinated to the C=N group of the imine (Figure 2.39). If we define the midpoint of the C1-N1 bonds and P1, P2 and P3 as ligand positions, the geometry around the cobalt is tetrahedral. The coordination geometry is best represented by the angles N1-Co1-P1 = 127.38(6)°, N1-Co1-P2 107.40(5)° and N1-Co1-P3 118.78(5)° which slightly deviate from an ideal of 109° due to the spatial requirement of the aromatic backbone and the trimethylphosphine ligands. The π-coordinated imine ligand shows the expected increase of 14 ppm in the C1-N1 bond length relative to the free imine ligand.[185]

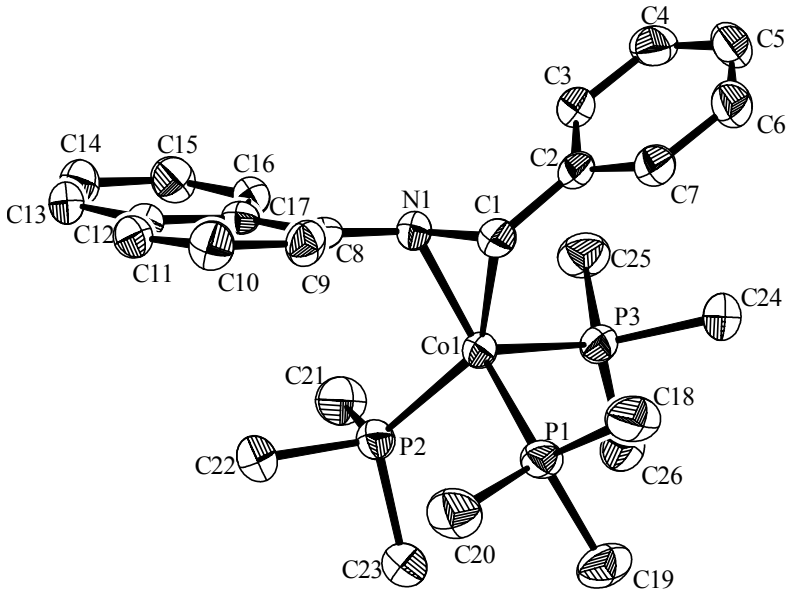

Figure 2.38 Molecular structure of **37** (ORTEP plot with hydrogen atoms omitted). Selected bond lengths (Å) and angles (°): Co1-N1 1.968(2), Co1-C1 2.019(2), Co1-P1 2.2142(13), Co1-P2 2.2167(10), Co1-P3 2.2546(9), N1-C1 1.381(3), N1-C8 1.396(3), C2-C1 1.473(3); N1-Co1-P1 127.38(6), C1-Co1-P1 96.10(7), N1-Co1-P2 107.40(5), C1-Co1-P2 145.79(6), P1-Co1-P2 100.34(2), N1-Co1-P3 118.78(5), C1-Co1-P3 107.87(7), P1-Co1-P3 99.19(3), P2-Co1-P3 98.88(4).

The Co1-N1 (1.968(2) Å) and Co1-C1 (2.019(2) Å) bond lengths fall in the typical range reported for imine-fragments π-coordinated to zero-valent cobalt complexes, the Co-P distances range accordingly (2.21 – 2.25 Å). The structure is comparable with a complex prepared by *König* with $Co(PMe_3)_4$ in reaction with phenylisocyanate leading to a similar coordination geometry.[252]

Discussion

The isolated compound **37** is the most air sensitive complex containing an aromatic imine backbone in solution and easily decomposes when in contact with air. This proximity is easy to understand because of its low oxidation state. Without Co-CH_3 group in the starting cobalt complex an *ortho*-metalation or bicyclometalation reaction cannot be observed.

2.2.9 Reaction of $Co(CH_3)(PMe_3)_4$ with *N*-(1-naphthylmethylene)aniline

The reaction sequence of an isostructural imine ligand with $FeMe_2(PMe_3)_4$ started with an *ortho*-metalation followed by a reductive elimination with C,C-coupling and release of a $Fe(PMe_3)_3$ fragment that coordinates in an η^4-fashion to the α-part of the imine ligand.
Now the question rises, if under same conditions the isostructural imine ligand can react with with $Co(CH_3)(PMe_3)_4$ in a similar reaction pathway.

Synthesis and Characterization

N-(1naphthylmethylene)aniline reacts with $Co(CH_3)(PMe_3)_4$ at -70 °C [Eq. 2.28] to afford **38** exclusively, isolated in 82 % yield. Concentrated pentane solutions afforded at – 27 °C dark green crystals of **38**.

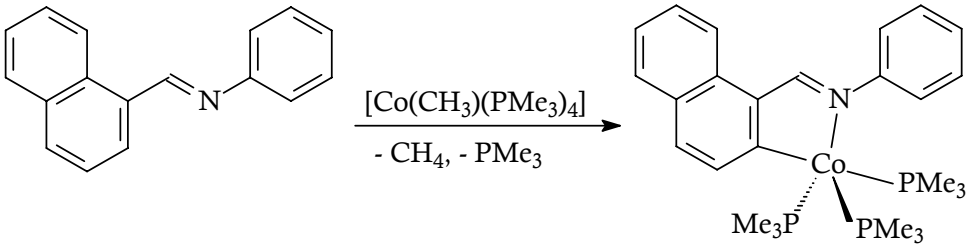

(2.28)

38

Spectroscopic investigations

The most distinctive spectroscopic data in the IR spectrum are a bathochromic shift of 127 cm $^{-1}$ for the imine band in comparison with the free ligand. In the ^{13}C NMR spectrum of the *ortho*-metalated complex **38** only one metallated carbon can be detected at 197.2 ppm as a multiplet. The ^{31}P NMR shows two resonances at -16.3 ppm and -3.8 ppm as multiplets. Even at -100 °C the coupling pattern cannot be resolved, which is either due to dynamic behaviour of the complex or quadropol broadening (I_{Co}=7/2). All spectroscopic data are similar to the previously rdescribed complexes **15** and **16**. The only difference is that in ^{31}P NMR the phosphorus nuclei appear as two resonances because of the low symmetry of the chelating ligand.

Discussion

The switched [C,N] coordination mode in the imine ligand gives the same result as observed in the reaction with a dimethyliron complex. Again no bicyclometallation is observed which is due to the steric demand in the second C-H activation step forming a four-membered metallacycle.

Here the reaction sequence does not involve a reductive elimination step because the methyl group is eliminated in the first step of the cobalt complex whereas a methyl group remains in the iron case [Eq. 2.19]

The specroscopic data and the coordination geometry are very similar with the first *ortho*-metalated complexes **15** and **16**.

2.2.10 Reaction of $Co(CH_3)(PMe_3)_4$ with *N*-(1-naphthylmethylene)-2,6-dimethylaniline

In a bicyclometalation reactions with iron and cobalt carried out, so far aromatic C-H bonds are activated to form five-membered metallacycles. Proximity of a C-H bond of the metal and a perpendicular orientation are believed to be necessary psrequisite for a cyclometalation to occur. It has been already shown that with *N*-phenylbenzylideneimine the small bite angle required for a second step metalation represents a limit. With a derivative of *N*-benzylidene-1-naphthylamine containing two methyl groups in ortho positions of the phenyl part of the imine ligand, the C-H proximity is believed to fullfill.

Synthesis and Characterization

N-(1-naphthylmetylene)-2,6-dimethylaniline providing one in plane *ortho*-C(sp^2)-H and one *ortho*-C(sp^3)-H bond out of plane, reacts with $Co(CH_3)(PMe_3)_4$ at -70 °C with a gas evolution [Eq. 2.29] to afford **39** exclusively, isolated in 60 % yield. The dark green crystals were suitable for X-ray diffraction.

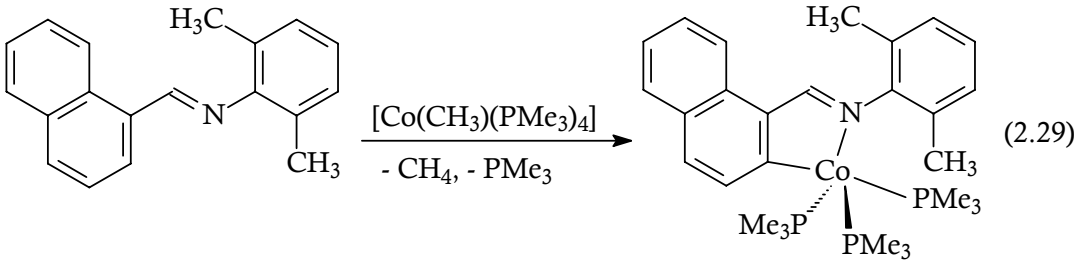

(2.29)

39

Spectroscopic Investigation

The coordinated imine band is present at 1531 cm^{-1} with a bathochromic shift of 91 cm^{-1} in comparison with the free imine ligand. The NMR spectroscopical data are very similar with complex **15** and **16**. The coordinated trimethylphosphine ligands are indicated by two broad singlet resonances at 1.01 ppm and 1.07 ppm. The six methyl protons appear at 2.14 ppm indicating no C-H activation of the methyl

group. A typical low field shift is recognized for the imine proton at 9.34 ppm. In the ^{13}C NMR spectrum all resonances are found to be consistent with an *ortho*-metalated coordination sphere. The metallated aromatic carbon is shifted to 181.2 ppm and forms a multiplet. Due to the asymmetric aromatic backbone the trimethylphosphine ligands are anisochronic in solution [compare **15** and **16**], indicated by two resonces at –14.9 ppm for the two equatorial trimethylphosphine ligands and at -4.5 for the axial phosphine ligand.

Molecular Structure of 39

Single crystals of **39** suitable for X-ray diffraction were obtained by crystallization from pentane at – 27 °C. The crystal belongs to the space group *P*bca. The coordination of the cobalt atom can be described as a trigonal bipyramid with an axial C1 atom and an axial PMe_3 group (P3). The equatorial positions are occupied by the nitrogen atom (N1) next to the other remaining phosphine groups with the phosphorus atoms (P1 and P2).The structural data found for **39** is very similar to that of **15** (See Figure 2.18).

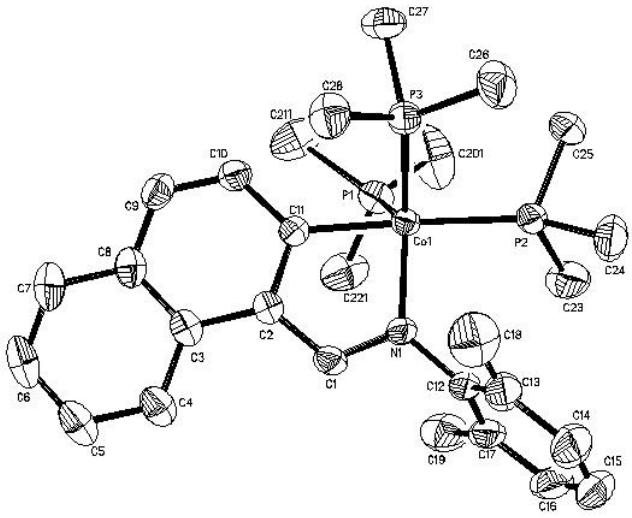

Figure 2.39 Molecular structure of **39** (ORTEP plot with hydrogen atoms omitted). Selected bond lengths (Å) and angles (°): Co1-C11 1.9536(18), Co1-N1 1.9552(14), Co1-P1 2.1915(6), Co1-P3 2.2030(6), Co1-P2 2.2401(6), N1-C1 1.318(2); C11-Co1-N1 81.06(7), C11-Co1-P2 177.17(6),C11-Co1-P1 84.86(6), N1-Co1-P1 118.84(5), C11-Co1-P3 87.82(6), N1-Co1-P3 123.97(5), P1-Co1-P2 95.22(2), P3-Co1-P2 94.71(2) P1-Co1-P3 114.47(2).

The angles from the axial (P2) to the equatorial phosphorus atoms are similar with 95.22(2)° for (P1) and 94.71(2)° for (P3), respectively.
The two equatorial cobalt phosphorus distances (Co1-P1 = 2.1915(15) and Co1-P3 = 2.2030(6) Å) are shorter than those opposite the σ-bonded aryl group (Co1-P2 = 2.2401(6) due to a strong *trans* influence of the carbon atom.
The distance between cobalt and nitrogen (1.9552(14) Å) is in the range for single bonds.[253]
The Co-C, Co-P and P-C bond lengths are close to the average of reported values in arylcobalt compounds. The bond lengths and angles resemble those found in the parent cyclometallated diphenylamine compound **15**. The sum of internal angles in the metallacycle (539.7°) equals that of a regular pentagon.

Discussion

With N-(1-naphthylmetylene)-2,6-dimethylaniline in reaction with $Co(CH_3)(PMe_3)_4$ a bicyclometallation is not possible. The reaction stops at the ortho-metallation of the β-position in the naphthyl part forming a five-membered metallacycle and no further C-H activation step of the methyl groups in the aromatic backbone occurs. Bicyclometallation reactions only occur when the two C-H bonds, which will be activated, are aromatic.
It is known that many transition metals predominantly activate the stronger aryl C-H bond (110 kcal/mol), instead of the weaker aliphatic C-H bond (96 – 102 kcal/mol).[254] Figure 2.41 shows the decrease in C-H bond energies according to substituted carbon atoms.

H- Ph > H-vinyl > $H\text{-}CH_3$ > $H\text{-}CH_2R$ > $H\text{-}CHR_2$ > $H\text{-}CR_3$ > $H\text{-}CH_2Ph$

Figure 2.41 C-H bond strengths.

It is crucial that the new formed metal carbon bond strength dominates the reaction pathway and not the C-H bond strength. The row in Figure 2.42 displays the metal carbon bond energies according to decreasing bond energies. The strongest belongs to phenyl-metal bond and the weakest to the benzylic metal bond.[255-256]

M-Ph >> M-vinyl >> M-CH_3 >> M-CH_2R >> M-CHR_2 >> M-CR_3 >> M-CH_2R

Figure 2.42 Metal-carbon bond energies.

Interestingly Halpern reported a C-H bond breaking by cobalt complex should not be possible, because the sum of the Co-C and C-H bondenergies are not enough to initiate a C-H bond breaking.[257]

2.2.11 Reaction of $Co(CH_3)(PMe_3)_4$ with *N*-Benzylbenzylideneimine

As previously described only with *N*-benzyliden-1-naphthylamine bicyclometalation reactions occur. With a sterically less demanding and more flexibile aromatic backbone the question arises if again just *ortho*-metalation will occur like in the N-(1naphthylmethylene)aniline case or again a second C-H activation step is brought about with the benzyl group of the ligand.
Also *N*-Benzylbenzylideneimine contains a methylene group next to the imine function which increase the acidity of these protons and gives the idea for a new reaction pathway other than a *ortho*-metallation or biycyclometallation.

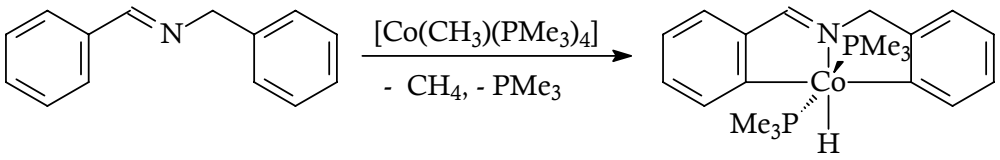

40

(2.30)

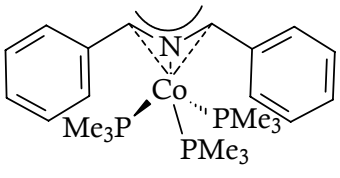

41

Synthesis and Characterization of 40 and 41

The reaction between $Co(CH_3)(PMe_3)_4$ and N-benzylbenzylideneimine proceeds below 20 °C according equation 2.30. The first step of the reaction is a bicyclometalation by a loss of methane and trimethylphosphine generating a hydrido-cobalt(III) complex **40**, followed by a reductive elimination producing a π-allylic η^3-cobalt(I) complex **41**.

The reaction sequence is depending on increased reaction time and polarity of the solvent. Predominantly long reaction times and polar solvent e.g. THF provides compound **41**. Both complexes crystallize from pentane at -27 °C in 11 % yield for **40** and 58 % yield for **41**. The two products formed large crystals which were separated manually. Crystals of **41** were suitable for an X-ray structure determination (Figure 2.40)

Spectroscopic Investigation of 40

Most remarkable, the IR spectrum of **40** shows a broad signal at 1879 cm^{-1} indicating a cobalt-hydrid stretching frequency. Corresponding to the IR, in the ^1H NMR spectrum with a high field shift a triplet arises for the hydrid resonance at -18.7 ppm with a $^2J(PH)$ coupling of 72.4 Hz. The two isochronic trimethylphosphine ligands resonate at 0.80 ppm as a singlet, the methylene protons at 5.08 ppm as a singlet and the imine proton with a typical low field shift to 8.56 ppm, next to the remaining aromatic proton signals at 6.69 – 7.39 ppm.

Spectroscopic Investigation of 41

Most significantly in the ^1H NMR of complex **41**, is the absence of a hydrid resonance at high field and accordingly the Co-H band in the IR spectrum is not present anymore. The ^1H NMR and ^{13}C NMR pattern in the aromatic region suggest a more symmetric molecule. The ratio of trimethylphosphine and aromatic protons has changed from 2:1 in complex **40,** to 3:1 in **41**. Table 2.22 gives the characteristic spectroscopic data of the biycyclometalated hydrido-cobalt complexes **36** and **40**.

	40	**36**
IR [cm^{-1}]		
ν (C=N)	1531 w	1521 m
ν (Co-H)	1879 m	1860 s
^{1}H NMR [ppm]	18.73	19.05
δ Co-*H*	t, ^{2}J(PH) = 72.4 Hz	t, ^{2}J(PH) = 71.7 Hz
δ PMe_3	0.80, singlet	0.72, t', $\lvert {}^{2}J(PH)+{}^{4}J(PH)\rvert$=7.4Hz
^{13}C NMR [ppm]	17.7	17.5
δ PMe_3	t', $\lvert {}^{1}J(PC)+{}^{3}J(PC)\rvert$=29.6 Hz	t', $\lvert {}^{1}J(PC)+{}^{3}J(PC)\rvert$= 29.7 Hz
δ Co-*C*	176.7, multiplet	181.1, multiplet
δ Co-*C*	194.6, multiplet	197.1, multiplet
^{31}P NMR [ppm]		
δ Co-*P*	9.98, singlet	9.50, singlet
Meltingpoint	115 – 117 °C	109 – 111 °C
Color	red	red

Table 2.22 Selected spectroscopic and physical data of **40** and **36**

Molecular Structure of 41

An X-ray structure analysis of **41** was carried out using a single crystal sealed in a capillary. The structure was solved by direct methods using SHELXS-97 and refined on F^2 by full-matrix least-squares techniques using SHELXL-97. Cobalt, phosphorus and carbon atoms were refined anisotropically and all nitrogen atoms isotropically. The sturucture was solved with the space group $P\bar{1}$ with a R-value 0.1606.

The molecular structure of **41** shows a piano stool type configuration of complex. The cobalt center is surrounded by three trimethylphosphine groups and an η^3 [C,N,C] coordination mode of an anionic N-benzylidenephenylimine ligand forming a π-allylic coordination to the metal like in half sandwich complexes. Regarding the midpoint [C,N,C] as a ligand position the resulting geometry of the cobalt center can be described as pseudotetrahedral. Three basal positions are

occupied by the trimethylphosphine donor atoms. The C116-C117 and C123-C124 bond length (1.493(13) Å) agree well with the average carbon carbon single bond distances in imino groups while distances N6-C116 = 1.420(11) Å and N6-C123 = 1.420(11) Å indicate a delocalized anionic ligand function.

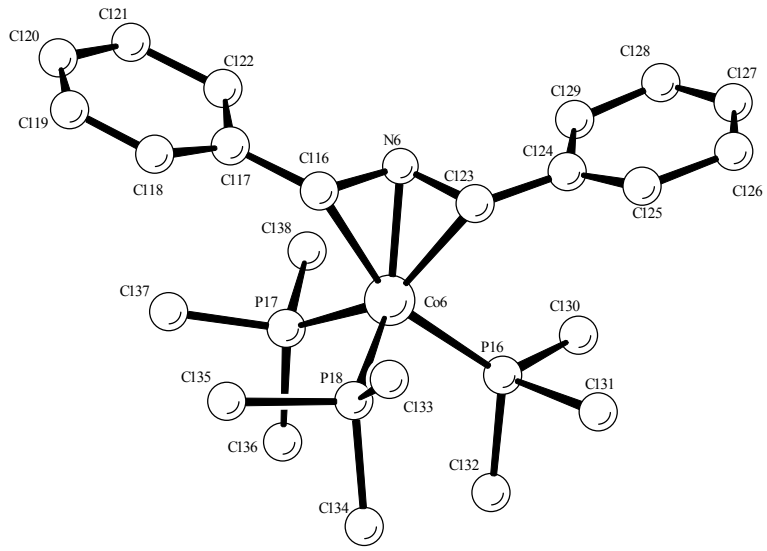

Figure 2.40 Molecular structure of **41**. Selected bond lengths (Å) and angles (°): Co6-N6 1.985(8), Co6-C123 2.099(9), Co6-C116 2.123(9), Co6-P16 2.222(4), Co6-P17 2.233(3), Co6-P18 2.231(3), N6-C116 1.420(11), N6-C123 1.420(11), C116-C117 1.493(13); C116-Co6-P16 158.9(3), N6-Co6-P18 125.3(3), C123-Co6-P17 146.9(3), N6-Co6-P16 119.1(3), N6-Co6-P17 108.8(2), P16-Co6-P17 94.87(16), P16-Co6-P18 100.5(2), P17-Co6-P18 103.26(16).

Discussion

The spectroscopic data of **40** indicate a coordination geometry similar with that of **36**. The source for the poor yield of **40** (11%) is explained by the concominant transformation to **41**.The Co-H function together with the methylene group of benzylideneimine initiate the reductive elimination of two Co-C bonds forming an η^3-coordinated cobalt I complex of C_s-symmetry. After C,C-coupling in the iron complex **30** here we have an example for reductive C,H elimination in a cobalt(III) intermediate to form complex **41**.

2.2.12 Iodomethane Reaction of 36

When iodomethane is added to the hydrido-cobalt(I) complex **36** at –70 °C, an evolution of gas is observed while warming up. The product **42** crystallizes from ether THF mixture at 4 °C. The claret crystals melt at 170 °C [Eq. 2.31].

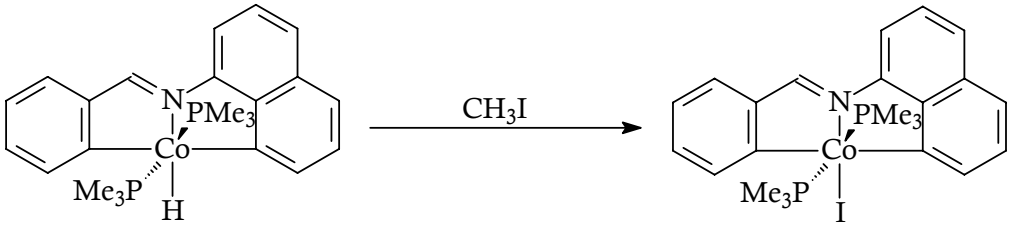

(2.31)

36 **42**

Spectroscopic Investigation of 42

In the IR spectrum the strong Fe-H absorption over 1860 cm^{-1} is absent and there is a bathochromic shift in all characteristic bands.

In ^{1}H NMR, the high region is empty and trimethylphosphine resonances are shifted to low field. The halides influence the chemical shifts of the PMe_3 protons and carbon nuclei. The *trans* trimethylphosphine groups resonate at 0.63 ppm as a pseudo triplet ($|^{2}J_{P,H} + {}^{4}J_{P,H}|$ = 7.7 Hz). The ten aromatic protons resonate between 6.94 ppm and 8.56 ppm. The imine proton experiences a low field shift to 8.86 ppm. In the ^{13}C NMR spectrum, the metalated carbon signals arise as triplets ($^{2}J_{P,C}$ = 23.5 Hz) at 174.9 ppm a and 194.9 ppm ($^{2}J_{P,C}$= 22.0 Hz) (Figure 2.41). The ^{31}P NMR spectrum confirms the octahedral coordination of the cobalt atom with a singlet resonance for two isochronic trimethylphosphine ligands.

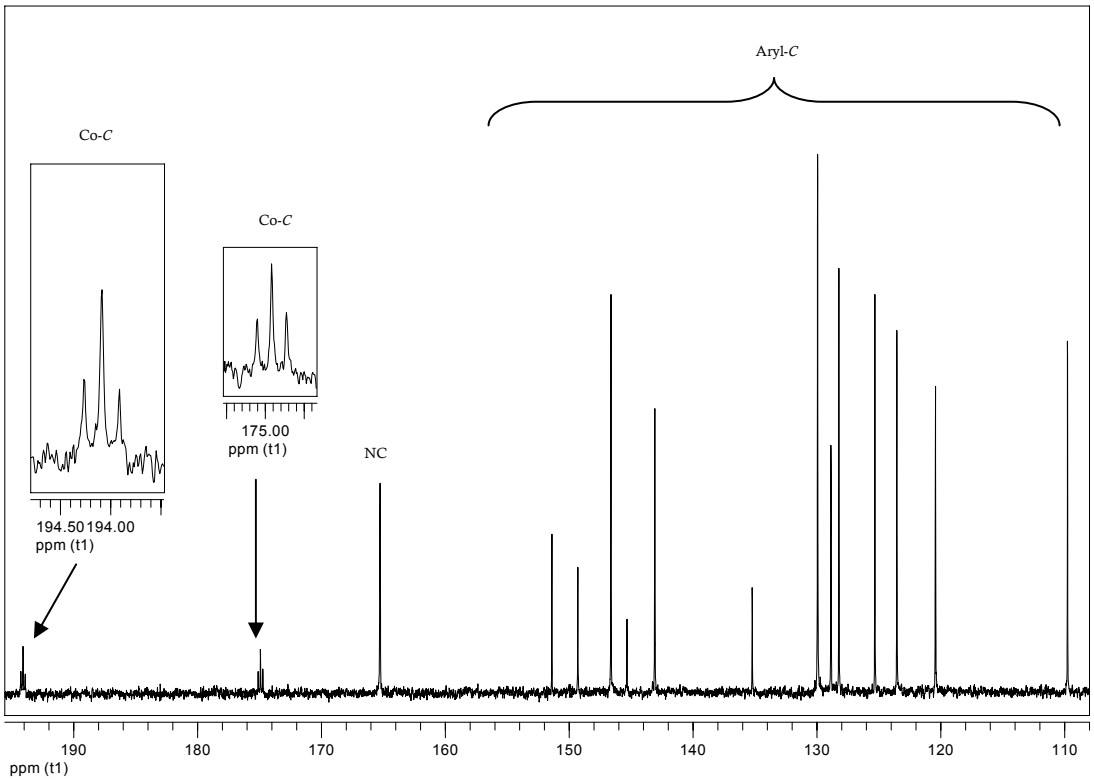

Figure 2.41 ^{13}C NMR spectra of **42** (125 MHz, [D_8]-THF, 300 K).

Molecular Structure of 42

The molecular structure of **42** is shown in Figure 2.42. The cobalt atom attains an octahedral coordination by two *trans* PMe_3 groups (P1-Co1-P2 = 178.00(5)°) a iodine donor (I1) *trans* to the nitrogen (N1) group (N1-Co1-I1 = 179.27(11)°), and the two metallated carbon atoms C7 and C16 *trans* to each other (C7-Co1-C16 = 166.08(17)°). Bond angles are close to 90°, with the smallest two (82.44(16)°) and 83.65(15)°) involving the two five-membered chelate rings. The sum of internal angles is 540° in each five-membered metallacycle.

The Co-P bond lengths (2.2174(12) and 2.2228(12) Å) fall within the range observed for other Co(III) complexes containing a pair of mutually *trans* PMe_3 groups.[258] The complex contains two different Co-C bonds with similar length (1.975(4) and 1.986(4) Å) which is consistent for those type of bond length reported in literature. The C1-I1 with 2.6159(6) Å is short compared to 2.63 – 2.72 Å for other Co(III) complexes, consistent with the less *trans* influence of the nitrogen atom. [259] The N1-C1 distance, 1.288(5) Å, is typical for a double bond, and N1-C8 is typical for a sp^3-hybridized single bond.

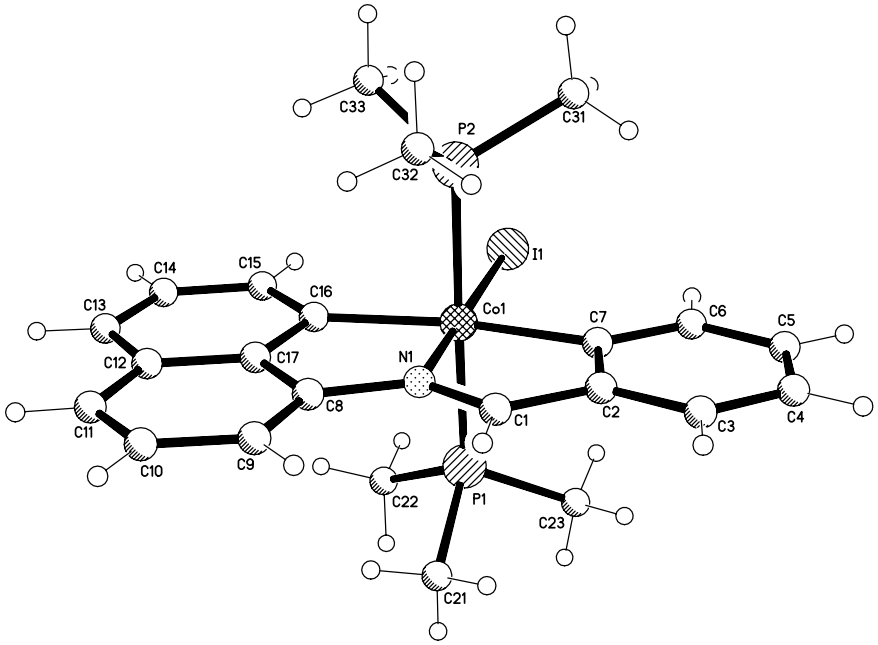

Figure 2.42 Molecular structure of **42**. Selected bond lengths (Å) and angles (°): Co1-I1 2.6159(6), Co1-N1 1.896(3), Co1-C7 1.975(4), Co1-C16 1.986(4), Co1-P1 2.2174(12), Co1-P2 2.2228(12), N1-C1 1.288(5), N1-C8 1.424(5); N1-Co1-C7 82.44(16), N1-Co1-C16 83.65(15), C7-Co1-C16 166.08(17), N1-Co1-I1 179.27(11), P1-Co1-P2 176.00(5), N1-Co1-P1 92.21(10), C7-Co1-P1 90.29(12), C16-Co1-P2 90.23(12).

2.2.13 Iodomethane Reaction of 38

Under the same reaction conditions as described for the oxidation of complex **15** and **16,** two equivalents iodomethane oxidize **39** affording compound **43** in 59 % yield [Eq.2.32].

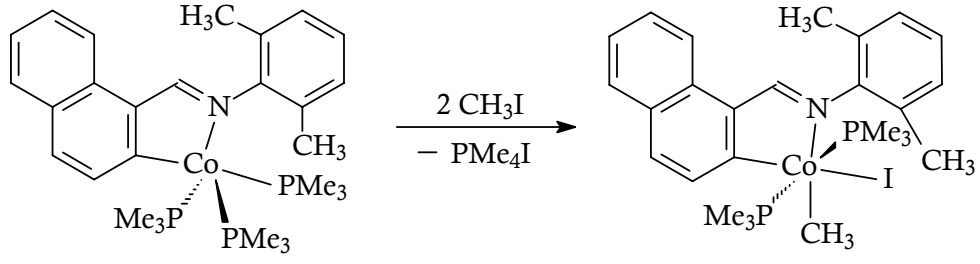

(2.32)

38 **43**

At 4 °C bunches of orange crystals precipitate from pentane which starts to decompose under nitrogen above 144 °C.

Spectroscopic Investigation of 43

In the ^{1}H NMR spectrum Co-CH_3 group resonates at 0.53 ppm as a triplet ($^{3}J_{PH}$ = 8.7 Hz) due to the coupling with two isochronic ^{31}P nuclei of trimethylphosphine. These two ligands in ^{1}H NMR display a pseudotriplet at 1.44 ppm with $|^{2}J_{P,H} + {}^{4}J_{P,H}| = 7.4$ Hz. In the ^{13}C NMR spectrum the Co-CH_3 appears as a singlet at -6.3 ppm. In the ^{13}C NMR spectrum the metalated carbon atom is shifted by 15 ppm downfield to 195.1 ppm in comparison to the parental compound **39**. No unusual shift from the two *ortho* methyl groups of the imine ligand can be detected. The resonances of trimethylphosphine and all aromatic and aliphatic carbon resonances arise in typical areas. The spectroscopic data suggest an octahedral coordination mode for the cobalt atom with two trimethylphosphine ligands in axial positions and perpendicular the aromatic backbone with the methyl group coordinated to the cobalt *trans* to nitrogen due to the strong *trans* influence.
A probable reaction pathway has been described before for complex **17** and **18**. For discussion see equation 2.9.

2.2.14 Carbon Monoxide Reaction of 38

In order to learn how the reactivity of the new cobalt complex **38** is affected by the presence of carbon monoxide, whether substitution, insertion or a demetallation steps take place, the reaction was conducted under ambient conditions as for other carbon monoxide reactions. In arylimine trimethylphosphine complexes a terminal coordination of CO is usually achieved through a smooth substitution reaction.

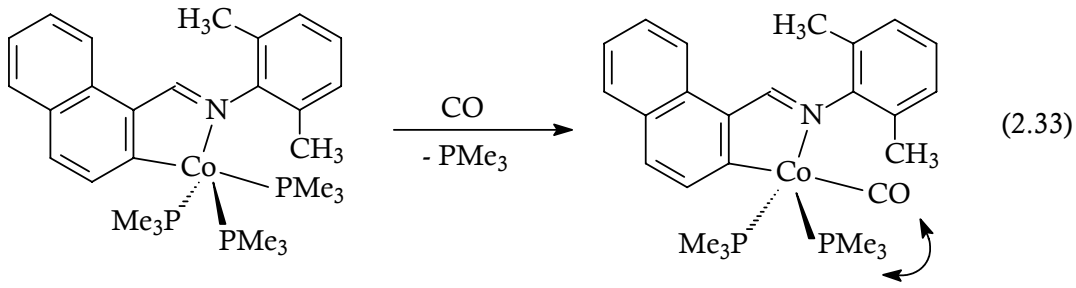

(2.33)

38 **44a**,**b**

Spectroscopic Investigation of 44

The IR spectrum contains one intensive band for a terminal carbonyl group at 1921 cm^{-1}. The ^{1}H NMR indicates the presence of two isomers in solution. The whole set of resonances is doubled. One set for an isomer with the carbonyl in axial position, indicated by a pseudo triplet at 1.16 ppm ($|^{2}J_{P,H} + {}^{4}J_{P,H}| = 7.4$ Hz). The second isomer is indicated in form of two doublets at 0.93 and 1.03 ppm with a $^{2}J_{P,H}$ coupling constant of 6.8 Hz and 7.4 Hz respectively. The calculated ratio between axial and equatorial carbonyl substitution from NMR spectrum is 1:1. Aromatic proton resonances appear with a typical shift between 6 – 9 ppm.

Molecular Structure of 44

Single crystals were obtained by keeping a pentane solution of **44** in at – 27 °C. Selected crystal data and data collection parameters are given at the index. Data were collected on a STOE IPDS diffractometer. X ray data reduction and structure solution and refinement were done using SHELXS-97 and SHELXL-97 programms.

The crystal was affixed to a glass fiber using silicone grease and transferred to the goniostat, where it was cooled to -123 °C using a gas flow cooling system of local design. Standard inert atmosphere techniques were used during the the handling and mounting process. The X ray structure could be solved in the triclinic crystal system with a space group *P-1*.

The structure confirms the presence of two trimethylphosphine ligands in the equatorial plane and shows that the incoming carbonyl ligand resides *trans* to the aryl ligand. In the third equatorial position is the nitrogen atom of the coordinated

imine backbone. The configuration is at variance with compound **19** where the carbonyl ligand replaces one of the equatorial PMe_3 groups.

A planar [C,N] metallacycle (sum of internal angles = 540°) spans the axial and equatorial positions wth a bite angle (N1-Co1-C1 = 81.55(9)°). The sum of the angles in the equatorial plane with 358.8° fits perfectly for a trigonal bipyramid.

The Co-P bond lengths (2.1842(8) and 2.1845(2) Å) fall within the range of for other Co(I) complexes containing aryl and carbonyl groups.

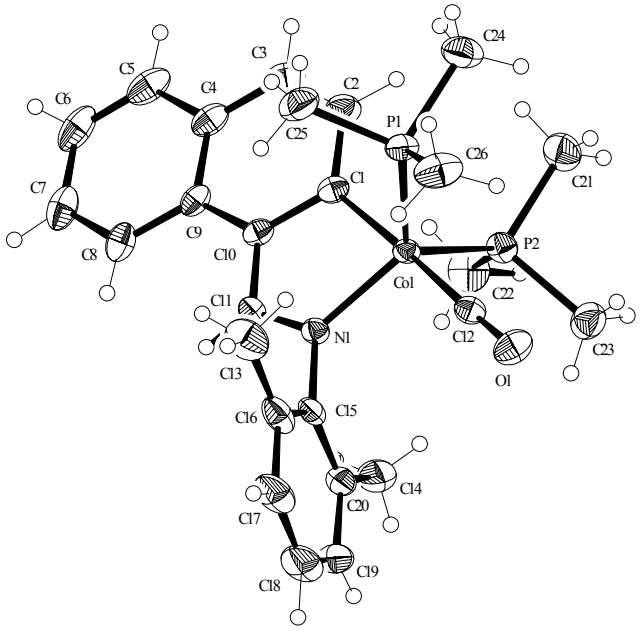

Figure 2.43 Molecular structure of **44**. Selected bond lengths (Å) and angles (°): Co1-C1 1.956(2), Co1-N1 1.951(2), Co1-P1 2.1842(8), Co1-P2 2.1845(2), N1-C11 1.312(2), Co1-C12 1.760(2), C12-O1 1.148(3); N1-Co1-C1 81.55(9), C12-Co1-C1 177.57(12), C1-Co1-P1 89.41(8), C1-Co1-P2 88.27(8), N1-Co1-P2 120.81(6), N1-Co1-P1 120.38(7), P1-Co1-P2 117.61(3).

Discussion

In order to learn how ligand properties are effected by strong π-acceptor ligands, carbonylation reaction under ambient conditions have been conducted with the result of a monosubstitution. In solid state IR only the isomer with an axial

carbonyl group exist. In the THF solution the ratio between axial and equatorial coordinated carbon monoxide in **44** is 1:1. In nonpolar solvents e.g. toluene, the ratio is changed and predominantly the isomer with axial carbonyl is formed with 95%.[258] Similar solvent depending isomer ratios have been reported with diphenylphosphanyl- phenylamino cobalt complexes. No sign of an insertion reactions or other transformations well known in derivatives of $Co_2(CO)_8$ could be detected.[259]

2.2.15 Reaction of $Ni(CH_3)_2(PMe_3)_3$ with N-Benzylidene-1-naphthylamine

Synthesis and Characterization

Diphenylimine reacts with $Ni(CH_3)_2(PMe_3)_3$ at -70 °C in THF according to [Eq. 2.34].

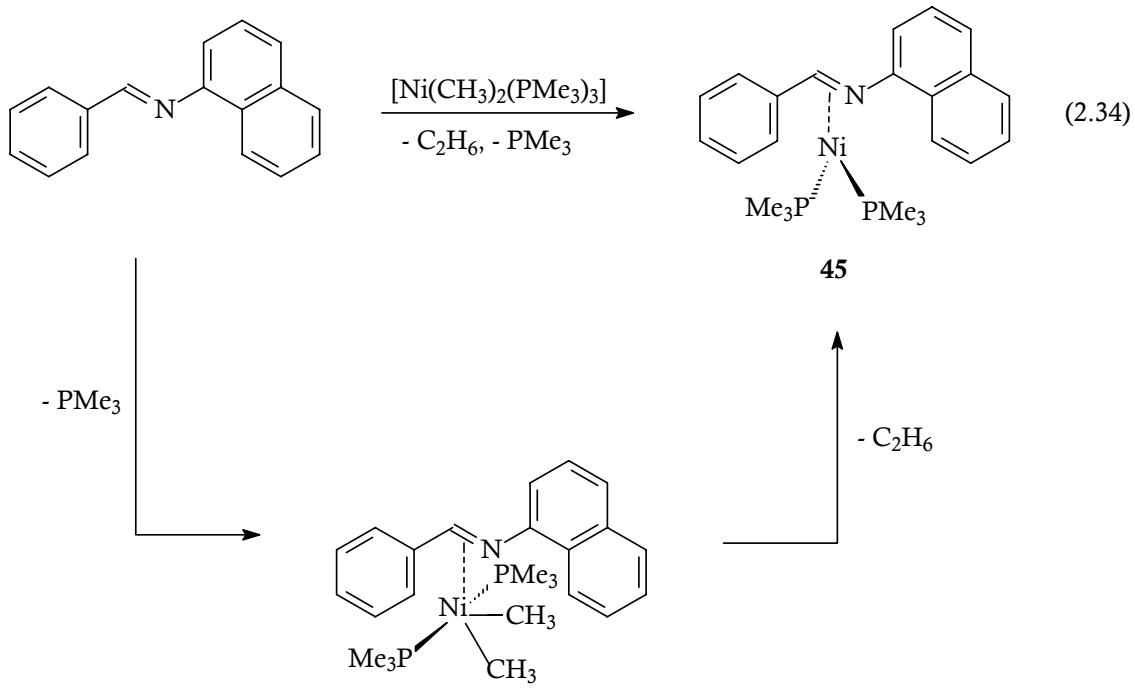

(2.34)

During warm up a color change from brown to orange red takes place. From pentane at -27 °C dark red rodes are obtained in 73% yield.

Spectroscopic Investigation of 45

In agreement with the postulated reaction pathway of complex **45** [Eq. 2.34] a band at 1567 cm^{-1} indicates a C=N coordination to the metal. The $NiCH_3$ group resonates at 0.81 ppm as a singlet. Typically for square planar nickel(II) complexes trimethylphosphine groups appears as singlets as ligand dissociation effects decoupling. The aromatic protons are found at 7.35 – 7.74 ppm. As a broad singlet the imine proton resonates at 10.12 ppm. In the ^{31}P NMR system phosphine ligands are found at -16.6 ppm representing an AB spin system (Figure 2.44).

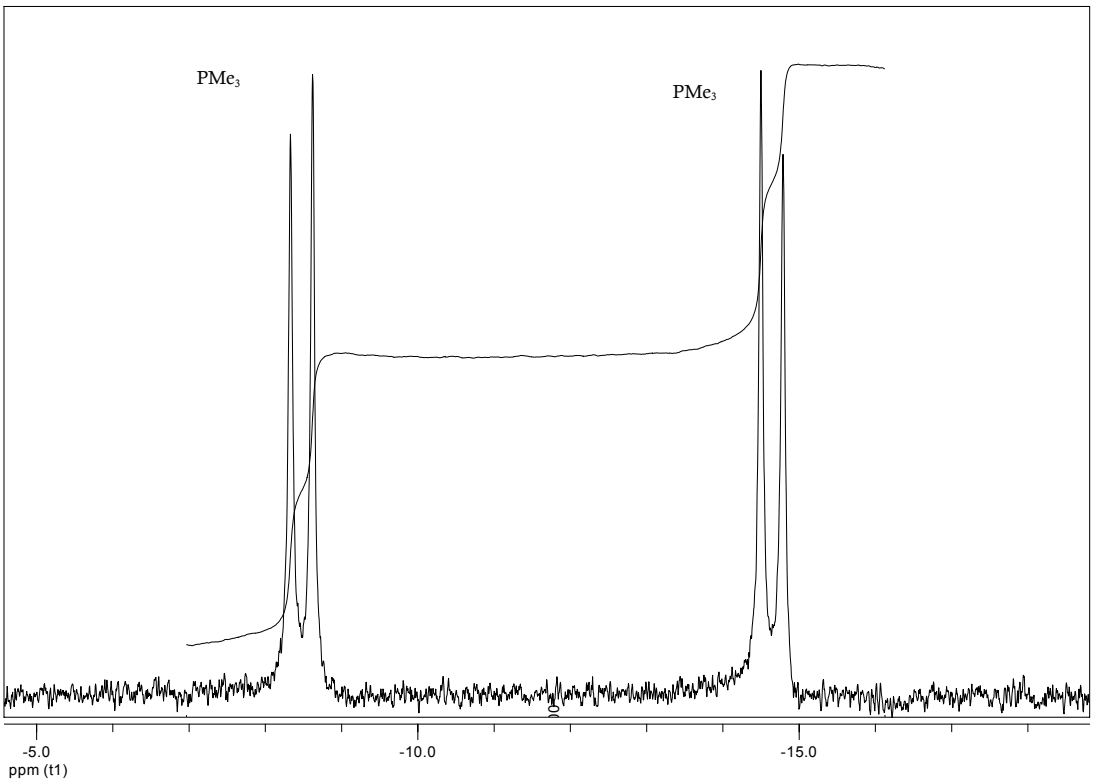

Figure 2.44 ^{31}P-NMR spectra of **45 .**

Discussion

Under similar reaction conditions diphenylimine with $NiCl(CH_3)(PMe_3)_2$ fails to react in a C-H activation step. As previously discussed in the nickel case the second methyl group has less basicity and no cyclometallation is expected to take place. The nitrogen donor atom just substitutes the chloro ligand leading to a square planar cationic nickel(II) species . This type of reaction pathways are well described in literature.[260]

3 EXPERIMENTAL PART

3.1 Working Techniques

All syntheses were carried out under vacuum by using a modified Schlenk technique so called Zweischenkelfritte.[261] This type of apparatus offers an opportunity of carrying out a complete synthesis in a closed system, in one run. Syntheses, transport and storages of chemicals were done under an atmosphere of purified argon (BTS - Catalyst[262]). Solvents (THF, diethyl ether, pentane) were dried according to known procedures and freshly distilled prior to use. All reagents (Aldrich, Acros, Fluka, Lancaster) were used as purchased without further purification.

3.2 Identification of Substances

3.2.1 Elemental Analyses

Air-sensitive samples were provided in capillaries sealed under vacuum and were analyzed by H. Kolbe Microanalytical Laboratory, Mülheim/Ruhr. C, H, N analyses identification of contents of air stable substances were performed in the microanalysis laboratory of Clemens-Schöpf-Institut for Organic Chemistry and Biochemistry in TU-Darmstadt using Perkin-Elmer CHN 240 A and CHN 240 B devices.

3.2.2 X-Ray Crystallography

Single crystals were sealed under argon in glass capillaries whereas air stable crystals were glued on a glass fibre. Crystallographic data were collected on STOE–IPDS (Eduard-Zintl Institute of TU-Darmstadt) and Bruker AXS SMART APEX CCD (University of Paderborn) diffractometer. Reflections were collected (ω-scans) by use of graphite-monochromated Mo-K_α radiation; a Lorentz polarization and

absorption corrections based on ψ-scans were applied. The structures were solved by direct and conventional Fourier methods. All non-hydrogen atoms were treated anisotropically, hydrogen atoms fixed in idealized positions were treated with a riding model.[174-175]

3.2.3 Infrared Spectrometry

IR spectra were obtained from as Nujol mulls between KBr plates using a Bruker FRA 106 spectrophotometer and were recorded in the range 4000 – 400 cm^{-1}.

3.2.4 Nuclear Magnetic Resonance Spectrometry

^{1}H, ^{13}C and ^{31}P NMR spectra were recorded on Bruker ARX 300 and Bruker DRX 500 spectrometers at the Organic Chemistry Institute of TU Darmstadt. ^{1}H and ^{13}C NMR chemical shifts were referenced to external TMS and ^{31}P chemical shifts were referenced to external H_3PO_4 85%. ^{13}C and ^{31}P resonances were obtained with broad-band proton decoupling.

3.2.5 Melting and Decomposition Point Measurements

The melting and decomposition points were measured on a Büchi 510 Melting point apparatus and are uncorrected. Air-sensitives substances were sealed in capillaries under 1 bar of Argon.

3.3 Preparation of Educts

3.3.1 Trimethylphosphine - [PMe_3]

Trimethylphoshine was synthesized in ether from methylmagnesiumchloride and triphenylphosphite according to a modified procedure given by Wolfsberger and Schmidbaur which allows a convenient synthesis in yields from 85 to 92%. [263]

3.3.2 Dichlorobis(trimethylphosphine)iron(II) - [$FeCl_2(PMe_3)_2$]

Anhydrous $FeCl_3$ was reduced to $FeCl_2$ in THF solution with a slightly excess of elemental iron (powder). Upon addition of two equivalents of trimethylphospine, the solution afforded a light gray powder of $FeCl_2(PMe_3)_2$ in 90% yield. [264]

3.3.3 Dimethyltetrakis(trimethylphosphine)iron(II) - [$Fe(CH_3)_2(PMe_3)_4$]

After adding two equivalents of trimethylphosphine to a THF solution of $FeCl_2(PMe_3)_2$, two mole equivalents of CH_3Li (in ether) were added at –70 °C. $Fe(CH_3)_2(PMe_3)_2$ was obtained from pentane as brown powder in 80% yield.[265]

3.3.4 Tetrakis(trimethylphosphine)iron(0) - [$Fe(PMe_3)_4$]

Reduction of $FeCl_2$ with magnesium turnings in THF in the presence of excess trimethylphospine afforded dark brown $Fe(PMe_3)_4$.[266]

3.3.5 Tetrakis(trimethylphosphine)cobalt(0) - [$Co(PMe_3)_4$]

$Co(PMe_3)_4$ was synthesized by reduction of anhydrous $CoCl_2$ with magnesium in THF containing four equivalents of trimethylphosphine as brown solid in 80-90% yield.[259]

3.3.6 Dichloro-tris(trimethylphosphine)cobalt(II) - [$CoCl_2(PMe_3)_3$]

$CoCl_2(PMe_3)_3$ was synthesized quantitatively by reacting in THF anhydrous $CoCl_2$ with three equivalents of trimethylphosphine and was obtained as dark violet crystals.[267]

3.3.7 Chloro-tris(trimethylphosphine)cobalt(I) - [$CoCl(PMe_3)_3$]

The comproportination reaction between $CoCl_2(PMe_3)_3$ and $Co(PMe_3)_4$ in diethylether gave shiny blue crystals of $CoCl(PMe_3)_3$ in 90% yield.[268]

3.3.8 Methyl-tetrakis(trimethylphosphine)cobalt(I) - [$CoCH_3(PMe_3)_4$]

Reaction of CH_3Li with $CoCl(PMe_3)_3$ in the presence of excess PMe_3 gave $CoCH_3(PMe_3)_4$ as reddish orange powder in 90-95% yield.[259]

3.3.9 *trans*-Dichloro-bis(trimethylphosphine)nickel(II) - [$NiCl_2(PMe_3)_2$]

After removing of water from a mixture of $NiCl_2 \times 6H_2O$ and two equivalents of trimethylphosphine in THF in vacuo, deep red crystals of $NiCl_2(PMe_3)_2$ were obtained in 96% yield.[269]

3.3.10 *trans*-Chloro(methyl)bis(trimethylphosphine)nickel(II) [$NiClCH_3(PMe_3)_2$]

Stoichiometric amounts of 1.6 M solution of CH_3Li in ether when added to a THF solution of $NiCl_2(PMe_3)_2$ at –80°C gave brown leafs of $NiClMeL_2$ in 97 % yield.[270]

3.3.11 *trans*-Dimethyl-tris(trimethylphosphine)nickel(II) [$Ni(CH_3)_2(PMe_3)_3$]

$Ni(CH_3)_2(PMe_3)_3$ was obtained as an orange solid from the reaction of 1.6 M CH_3Li with $NiCl_2(PMe_3)_2$ in THF containing excess of trimethylphosphine at –70°C in 96% yield.[271]

3.4 Ligand Synthesis

3.4.1 *tert*-Butylphenylketimine

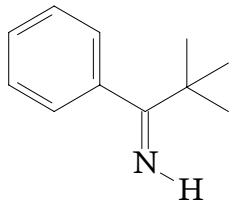

To a strirred THF solution of 5.2 g (50.4 mmol) of benzonitrile and 31.5 ml (50.4 mmol, 1.6 M in THF) of *tert.*-butylmagnesiumchloride, 250 mg (1.31 mmol) of copper(I)iodide at –78 °C were added. The reaction mixture turned dark brown immediately. Progress of the reaction was monitored by thin layer chromatography. After 48 h, the reaction was completed, and the mixture was then filtered off from magnesiumchloride followed by evaporation of the solvent in vacuo. The residue was distilled under reduced pressure to afford 4.2 g of an oily liquid (52%) boiling at 84 °C (at 0.6 torr).[272-273]

^{1}H NMR (300 MHz, [D_8]THF, 297 K, ppm):
δ = 1.22 (s, 9H, $C(CH_3)_3$); 7.18-7.24 (m, 2H, Ar–H); 7.32-7.36 (m, 3H, Ar–H); 9.43 (s_{br}, 1H, C=N–H).

^{13}C NMR (75 MHz, [D_8]THF, 297 K, ppm):
δ = 28.4 (s, $C(\underline{C}H_3)_3$); 39.8 (s, $\underline{C}(CH_3)_3$); 126.5 (s, CH); 127.7 (s, CH); 128.1 (s, CH); 142.9 (s, C); 180.4 (s, NC).

3.4.2 *N*-(1-naphthylmethylene)-aniline

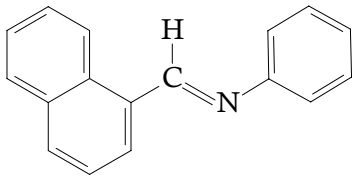

4.00 g (25.6 mmol) α-naphthylcarbaldehyde was combined with 2.38 g (25.6 mmol) of aniline in 50 ml toluene was refluxed for 6 hours. Toluene and the mixture was removed in vacuo, and the residue was recrystallized from ethanol to give 5.5 g of yellow powder (93%), m.p. 67 - 68 °C.[274-275]

^{1}H NMR (300 MHz, [D_8]THF, 297 K, ppm):
δ = 7.28 (tt, $^{3}J_{H,H}$ = 7.2 Hz, $^{4}J_{H,H}$ = 1.3 Hz, 1H, Ar–H); 7.35-7.38 (m, 2H, Ar–H); 7.43-7.49 (m, 2H, Ar–H); 7.59-7.71 (m, 3H, Ar–H); 8.03 (dd, $^{3}J_{H,H}$ = 8.3 Hz, $^{4}J_{H,H}$ =

1.4 Hz, 1H, Ar–H); 8.09 (d, $^{3}J_{H,H}$ = 8.2 Hz, 1H, Ar–H); 8.19 (dd, $^{3}J_{H,H}$ = 7.2 Hz, $^{4}J_{H,H}$ = 1.0 Hz, 1H, Ar–H); 9.20 (s, 1H, Ar–H); 9.33 (d, $^{4}J_{H,H}$ = 1.4 Hz, H–C=N).

^{13}C NMR (75 MHz, [D_8]THF, 297 K, ppm):
δ = 121.3 (s, CH); 125.1 (s, CH); 125.7 (s, CH); 126.2 (s, CH); 126.6 (s, CH); 127.7 (s, CH); 129.0 (s, CH); 129.5 (s, CH); 130.9 (s, CH); 131.7 (s, C); 131.9 (s, C); 132.2 (s, CH); 134.5 (s, C); 152.9 (s, C); 160.7 (s, H–C=N).

3.4.3 *N*-(1-naphthylmethylene)-2,6-dimethylaniline

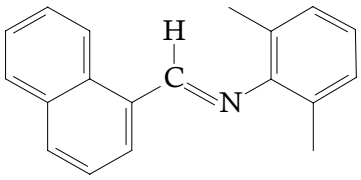

This ligand was prepared by refluxing a mixture of 7.40 g (47.3 mmol) of α-naphthylcarbaldehyde and of 5.74 g (47.3 mmol) of 2,6-dimethylaniline in 70 ml toluene for 6 hours. Toluene was removed in vacuo, and the residue was destilled to yield a yellow oil which slowly crystallized at 4 °C. 10.20 g of a yellow solid were collected in 83% yield, m.p. 71 - 72°C.

Elemental analysis: $C_{19}H_{17}N$, M_w : 259.35 g/mol

%	C	H	N
Calculated	87.99	6.61	5.40
Found	87.60	6.62	5.39

^{1}H NMR (300 MHz, [D_8]THF, 297 K, ppm):
δ = 2.17 (s, 6H, Ar–CH_3); 6.94 (t, $^{3}J_{H,H}$ = 7.7 Hz, 1H, Ar–H); 7.09 (d, $^{3}J_{H,H}$ = 7.5 Hz, 1H, Ar–H), 7.58-7.69 (m, 3H, Ar–H); 8.03 (dd, $^{3}J_{H,H}$ = 7.3 Hz, $^{4}J_{H,H}$ = 1.5 Hz, 1H, Ar–H); 8.10 (d, $^{3}J_{H,H}$ = 8.3 Hz, 1H, Ar–H); 8.14 (d, $^{3}J_{H,H}$ = 7.2 Hz, 1H, Ar–H); 8.91 (s, 1H, Ar–H); 9.29 (d, $^{4}J_{H,H}$ = 8.3 Hz, 1H, H–C=N).

^{13}C NMR (300 MHz, [D_8]THF, 297 K, ppm):

δ = 18.1 (s, Ar–CH_3); 117.2 (s, CH); 123.9 (s, CH); 125.2 (s, CH); 125.7 (s, CH); 126.7 (s, CH); 126.9 (s, C); 127.9 (s, C); 128.4 (s, CH); 129.1 (s, CH); 130.7 (s, CH); 131.8 (s, C); 132.3 (s, CH); 134.5 (s, C); 149.9 (s, C); 163.7 (s, H–C=N).

3.5 Synthesis of New Complex

3.5.1 Synthesis of Iron Complexes: Procedure A

$Fe(PMe_3)_4$ or $Fe(CH_3)_2(PMe_3)_4$ in pentane solutions were combined with stoichiometric amounts of ligands (imines or ketones) at –70 °C. The mixture was warmed to 20 °C and kept stirring for 16 h. The volatiles were then removed in vacuo and residue was extracted with pentane. Combined solutions were cooled to afford crystaline material.

3.5.2 Synthesis of Cobalt Complexes: Procedure B

$Co(PMe_3)_4$ or $CoCH_3(PMe_3)_4$ in THF were combined with stoichiometric amounts of ligands (imines or ketones) at –70 °C. The mixture was warmed to 20 °C and kept stirring for 16 h. The volatiles were then removed in vacuo. The residue was extracted with pentane and combined solutions were cooled to afford crystaline material.

3.5.3 Synthesis of Nickel Complexes: Procedure C

$NiClCH_3(PMe_3)_2$ and $Ni(CH_3)_2(PMe_3)_3$ in ether were combined with stoichiometric amounts of ligands (imines or ketones) at –70 °C. The mixture was warmed to 20 °C and kept stirring for 18h. The volatiles were then removed in vacuo. The residue was extracted with pentane and the combined solutions are cooled to afford crystaline material.

3.5.4 Iodomethane Reactions: Procedure D

Iodomethane was added to a sample of cyclometalated complex in pentane at –70 °C, and the mixture was allowed to warm to 20 °C. After 5h stirring, the mixture was filtered and the solution was kept at 4 °C to afford crystals.

3.5.5 Carbonmonoxide Reactions: Procedure E

A sample of cyclometalated complex was stirred under 1 bar of CO for 10 h. Upon filtration, the solution was cooled to 4 °C to afford crystals.

3.6 New Complexes

3.6.1 Hydrido[2-[(imino-κN)phenylmethyl]phenyl-κC]tris-(trimethylphosphine)iron(II) (1)

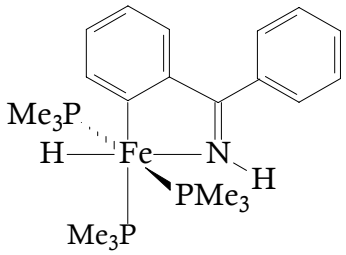

Procedure : A

1.44 g (3.99 mmol) of $Fe(PMe_3)_4$ in pentane were combined with 0.72 g (3.99 mmol) of diphenylketimine to afford 1.451 g of violet crystals (**1**) which crystallize in pentane at –27 °C.

Yield: 78 %

Melting point: 105 °C – 107 °C (decomposition)

Elemental analysis: $C_{22}H_{38}FeNP_3$, M_w: 465.32g/mol

%	C	H	N	P
Calculated	56.79	8.23	3.01	19.97
Found	57.06	7.58	2.96	20.09

IR (Nujol, 4000 – 400 cm^{-1}):

$\tilde{\nu}$ = 3281 w (ν H–N=C); 3068 vw, 3043 vw, 3020 w (ν H–C=C); 1730 vs (ν Fe–H); 1598 m, 1567 m (ν C=C); 1500 m (ν C=N); 1449 vw; 1427 m (δ_{as} PCH_3); 1392 s; 1293 m, 1273 s (δ_s PCH_3); 1229 w; 1191 vw; 1176 vw; 1143 m; 1099 vw; 1072 vw; 1028 w; 1010 vw; 994 w; 936 vs (ρ_1 PCH_3); 849 s (ρ_2 PCH_3); 834 vw; 812 m; 777 s, 758 w, 737 vw, 729 m (γ C–H_{arom}); 709 vw, 698 s (ν_{as} PC_3); 657 s (ν_s PC_3); 622 vw; 587 s; 512 m (ν Fe–C); 463 w, 433 m.

^{1}H NMR (500 MHz, [D_8]THF, 300 K, ppm):

δ = -16.4 (dt, $^{2}J_{P,H}$ = 22.8 Hz, $^{2}J_{P,H}$ = 81.3 Hz, 1H, Fe–H); 0.94 (s, 18H, PCH_3); 1.42 (d, $^{2}J_{P,H}$ = 4.7 Hz, 9H, PCH_3); 6.72 (t, $^{3}J_{H,H}$ = 7.0 Hz, 1H, Ar-H); 6.82 (t, $^{3}J_{H,H}$ = 7.1 Hz, 1H, Ar–H); 7.30 (t, $^{3}J_{H,H}$ = 7.1 Hz, 1H, Ar–H); 7.38 (t, $^{3}J_{H,H}$ = 7.2 Hz, 2H, Ar–H); 7.47 (t, $^{3}J_{H,H}$ = 7.8 Hz, 3H, Ar–H); 7.89 (d, $^{3}J_{H,H}$ = 6.4 Hz, 1H, Ar–H); 9.40 (s, 1H, N–H).

^{13}C NMR (125 MHz, [D_8]THF, 300 K, ppm):

δ = 22.5 (dt', $|^{1}J_{P,C} + {}^{3}J_{P,C}|$ = 12.1 Hz $^{3}J_{P,C}$ = 3.2 Hz, PCH_3); 22.3 (td, $^{1}J_{P,C}$ = 13.7 Hz, $^{3}J_{P,C}$ = 2.3 Hz, PCH_3); 118.6 (s, CH); 123.0 (d, $^{6}J_{P,C}$ = 1.7 Hz, CH); 125.9 (s, CH); 127.9 (s, CH); 128.1 (s, CH); 129.4 (s, CH); 142.1 (s, C); 146 (s, C); 152.3 (s, CH); 180.2 (d, $^{3}J_{P,C}$ = 10.3 Hz, C=N); 204.1 (m, Fe–C).

^{31}P NMR (202 MHz, [D_8]THF, 296 K, ppm):

δ = 18.2 (d, $^{2}J_{P,P}$ = 37.4 Hz, 2P, PCH_3), 22.5 (t, $^{2}J_{P,P}$ = 37.4 Hz, 1P, PCH_3).

3.6.2 Hydrido[2-[(imino-κN)phenylmethyl]-1,1-dimethylethyl-κC]tris (trimethylphosphine)iron(II) (2)

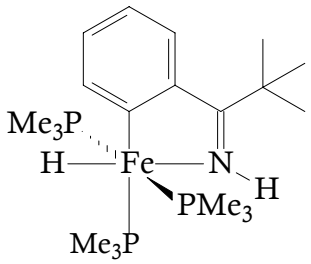

Procedure: A

1.27g (3.53 mmol) of $Fe(PMe_3)_4$ in pentane were combined with 0.57 g (3.53 mmol) of *tert*-butylphenylketimine to afford 0.753 g of reddish violet crystals (**2**) which crystallize at 4 °C.

Yield: 48%

Melting point: 118 °C– 120 °C (decomposition)

Elemental analysis: $C_{20}H_{42}FeNP_3$, M_w: 445.33g/mol

%	C	H	N	P
Calculated	53.94	9.51	3.15	20.87
Found	53.89	9.35	3.61	19.03

IR (Nujol, 4000 - 400 cm^{-1}):

$\tilde{\nu}$ = 3335 m (ν H–N=C); 3060 m, 3026 m (ν H–C=C); 1795 m_{br} (ν Fe–H); 1565 m (ν C=C); 1433 s (δ_{as} PCH_3); 1389 s; 1357 m; 1293 m, 1270 s (δ_s PCH_3); 1194 w; 1173 w; 1149 w; 999 vw; 940 vs (ρ_1 PCH_3); 852 m, 843 m (ρ_2 PCH_3); 813 w; 770 w, 730 s (γ C-H_{arom}); 698 m (ν_{as} PC_3); 656 s (ν_s PC_3); 618 vw; 506 vw; 409 s.

^{1}H NMR (500 MHz, [D_8]THF, 300 K, ppm):

δ = -17.5 (dt, $^2J_{P,H}$ = 21.8 Hz, $^2J_{P,H}$ = 80.0 Hz, 1H, Fe–H); 0.88 (s, 18H; PCH_3), 1.40 (d, $^2J_{P,H}$ = 4.5 Hz, 9H, PCH_3); 1.46 (s, 9H; $C(CH_3)_3$); 6.71 (dd, $^3J_{H,H}$ = 6.5 Hz, $^3J_{H,H}$ =

7.6 Hz, 2H, Ar–H); 7.74 (d, $^{3}J_{H,H}$ = 7.4 Hz, 1H, Ar–H); 7.85 (d, $^{3}J_{H,H}$ = 6.5 Hz, 1H; Ar–H); 9.13 (s, 1H, N–H).

^{13}C NMR (125 MHz, [D_8]THF, 300 K, ppm):
δ = 22.3 (tt, $^{3}J_{P,C}$ = 2.6 Hz, $^{1}J_{P,C}$ = 12.8 Hz, PCH_3); 23.3 (td, $^{1}J_{P,C}$ = 12.8 Hz, $^{3}J_{P,C}$ = 2.6 Hz, PCH_3); 29.8 (s, $C(\underline{C}H_3)_3$); 40.1 (s, $\underline{C}(CH_3)_3$); 117.6 (s, CH); 122.4 (s, CH); 126.5 (s, CH); 144.8 (s, C); 152.9 (s, CH); 186.1 (m; C=N), 200.1 (m; Fe–C).

^{31}P NMR (202 MHz, [D_8]THF, 300 K, ppm):
δ = 18.2 (d, $^{2}J_{P,P}$ = 36.5 Hz, 2P, PCH_3); 23.7 (t, $^{2}J_{P,P}$ = 36.5 Hz, 1P, PCH_3)

3.6.3 Hydrido[2-[(imino-κN)phenylmethyl]-2-methylphenyl-κC]tris-(trimethylphosphine)iron(II) (3)

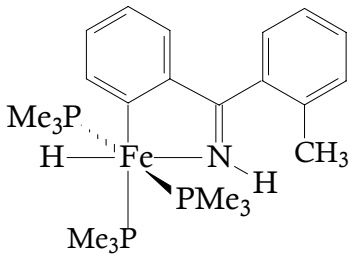

Procedure: A
0.94 g (2.41mmol) of $Fe(CH_3)_2(PMe_3)_4$ in pentane were combined with 0.44 g (2.41 mmol) of diphenylketimine to afford 0.74 g of violet crystals (**3**) which crystallize at –27 °C.

Yield: 64%

Melting point: 108 °C– 110 °C (decomposition)

Elemental analysis: $C_{23}H_{40}FeNP_3$, M_w: 479.35g/mol

%	C	H	N	P
Calculated	57.63	8.41	2.92	19.39
Found	56.01	8.43	2.92	18.99

IR (Nujol, 4000 – 400 cm^{-1}):

$\tilde{\nu}$ = 3279 vw (ν H–N=C); 3063 vw, 3021 vw (ν H–C=C); 1761 s (ν Fe–H); 1570 w (ν C=C), 1500 w (ν C=N); 1439 w, 1420 vw (δ_{as} PCH_3); 1396 m; 1293 m, 1268 m (δ_s PCH_3), 1277 vw; 1152 vw; 1111 vw; 1091 vw; 1042 vw; 993 vw; 955 w, 935 vs (ρ_1 PCH_3); 845 m (ρ_2 PCH_3); 802 vw; 764 m, 729 s (γ C–H_{arom}); 707 s, 681 w (ν_{as} PC_3); 660 m, 650 m (ν_s PC_3); 598 m, 505 w (ν Fe–C); 482 w.

^{1}H NMR (500 MHz, [D_8]THF, 300 K, ppm):

δ = -17.2 (dt, $^2J_{P,H}$ = 22.5 Hz, $^2J_{P,H}$ = 82.3Hz, 1H, Fe–H); 0.99 (s, 18H, PCH_3); 1.41 (d, $^2J_{P,H}$ = 3.3 Hz, 9H, PCH_3); 2.21 (s, 3H, Ar–CH_3); 6.65 (t, $^3J_{H,H}$ = 6.0 Hz, 1H, Ar–H); 6.79 (t, $^3J_{H,H}$ = 6.1 Hz, 1H, Ar–H); 7.02 (d, $^3J_{H,H}$ = 6.9 Hz, 1H, Ar–H); 7.10 (t, $^3J_{H,H}$ = 6.1 Hz, 1H, Ar–H); 7.16 (t, $^3J_{H,H}$ = 6.9 Hz, 1H, Ar–H); 7.23 (m, 2H, Ar–H); 7.89 (s, 1H, Ar–H); 9.25 (s, 1H, N–H).

^{13}C NMR (125 MHz, [D_8]THF, 300 K, ppm):

δ = 21.1 (s, Ar–CH_3); 23.2 (m, PCH_3); 118.2 (s, CH); 122.8 (s, CH); 126.4(d, $^3J_{P,C}$ = 8.1 Hz, CH), 128.5 (s, CH); 129.4 (s, CH); 131.2 (s; C); 136.6 (s, C); 142.6 (s, C); 147.3 (s, CH); 152.1 (s, CH); 181.2 (d, $^3J_{P,C}$ = 9.8 Hz, C=N); 203.1 (m, Fe–C).

^{31}P NMR (202 MHz, [D_8]THF, 296 K, ppm):

δ : 15.7 (m, 2P, PCH_3); 21.2 (t, $^2J_{P,P}$ = 38.3 Hz, 1P, PCH_3).

3.6.4 Methyl[2-[(methylimino-κN)methyl]phenyl-κC]tris-(trimethylphosphine) iron(II) (4)

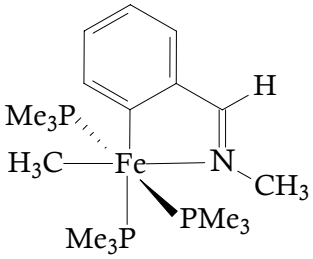

Procedure: A

1.0 g (2.56 mmol) of $Fe(CH_3)_2(PMe_3)_4$ were combined with 0.31 g (2.56 mmol) of *N*-methylbenzylidenimine in pentane to afford 0.753 g of violet crystals (**4**) which crystallize at 4°C.

Yield: 65%

Melting point: 115 °C – 117 °C (decomposition)

Elemental analysis: $C_{18}H_{38}FeNP_3$, M_w: 417.27g/mol

%	C	H	N	P
Calculated	51.81	9.18	3.36	22.27
Found	51.52	9.38	3.37	22.27

IR (Nujol, 4000 – 400 cm^{-1}):

$\tilde{\nu}$ = 3053 vw, 3034 vw (ν H–C=C); 1572 m (ν C=C); 1521 m (ν C=N); 1416 w (δ_{as} PCH_3); 1294 m, 1276 s (δ_s PCH_3); 1221 w; 1180 w (δ_s Fe-CH_3); 1118 w; 1020 w; 996 w ; 937 vs (ρ_1 PCH_3); 844 m (ρ_2 PCH_3); 746 w, 730 m (γ C–H_{arom}); 712 vw, 702 w (ν_{as} PC_3); 677 w, 658 w (ν_s PC_3); 646 vw.

^{1}H NMR (500 MHz, [D_8]THF, 298 K, ppm):

δ = -1.38 (s_{br}, 3H, Fe–CH_3); 0.71 (s_{br}, 18H, PCH_3); 1.49 (s_{br}, 9H, PCH_3); 3.65 (s, 3H, N–CH_3); 6.74 (s, 1H, Ar–H); 6.85 (s, 1H, Ar–H); 7.30 (s, 1H, Ar–H); 7.87 (s, 1H, Ar–H); 8.48 (s, 1H, N=C–H).

^{13}C NMR (125 MHz, [D_8]THF, 298 K, ppm):

δ = -16.6 (dt, $^2J_{P,C}$ = 25.6 Hz, $^2J_{P,C}$ = 8.2 Hz, Fe–CH_3); 16.9 (dt' $|^1J_{P,C}+ {}^3J_{PC}|$ = 9.3 Hz, $^3J_{PC}$ = 2.3Hz, PCH_3); 24.0 (d, $^1J_{P,C}$ = 12.5 Hz, PCH_3), 54.8 (d, $^3J_{P,C}$ = 3.6 Hz, N-CH_3); 119.1 (s, CH); 124.7 (s, CH); 126.0(s, CH); 143.5 (s, CH); 149.5 (s, C); 174.4 (d, $^3J_{P,C}$ = 5.5 Hz, C=N), 206.6 (dt, $^2J_{P,C}$ = 26.2 Hz, $^2J_{P,C}$ = 6.2 Hz, Fe –C).

^{31}P NMR (202 MHz, [D_8]-THF, 296 K, ppm):

δ = 7.6 (t, $^2J_{P,P}$ = 35.6 Hz, 1P, PCH_3), 16.7 (d, $^2J_{P,P}$ = 35.6 Hz, 2P, PCH_3).

3.6.5 Methyl[2-[[(1-methylethyl)imino]methyl]phenyl-κC]tris-(trimethylphosphine)iron(II) (5)

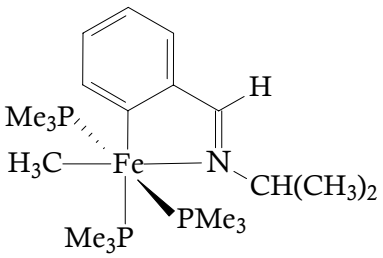

Procedure: A

1.06 g (2.72 mmol) of $Fe(CH_3)_2(PMe_3)_4$ in pentane were combined with 0.39 g (2.72 mmol) of *N*-(1-methylethyl)benzylidenimine to afford 0.84 g of violet crystals (**5**) which crystallize at –27 °C.

Yield: 69%

Melting point: 116 °C – 118 °C

Elemental analysis: $C_{20}H_{42}FeNP_3$, M_w: 445.33 g/mol

%	C	H	N	P
Calculated	53.94	9.51	3.15	20.87
Found	56.09	8.54	2.88	19.75

IR (Nujol, 4000 – 400 cm^{-1}):

$\tilde{\nu}$ = 3037 vw (ν H–C=C); 1571 m, 1561 m (ν C=C); 1519 m (ν C=N); 1415 s (δ_{as} PCH_3); 1360 w; 1292 s, 1272 s (δ_s PCH_3); 1222 m; 1162 m (δ_s Fe–CH_3); 1148 m; 1107 m; 1031 m; 941 vs (ρ_1 PCH_3); 868 w; 846 m (ρ_2 PCH_3); 748 s, 729 s (γ C–H_{arom}); 708 m, 695 s (ν_{as} PC_3); 658 s (ν_s PC_3); 636 w; 567 vw; 537 vw; 451 vw.

3.6.6 Methyl[2-[(phenylimino-κN)methyl]phenyl-κC]tris-(trimethylphosphine)iron(II) (6)

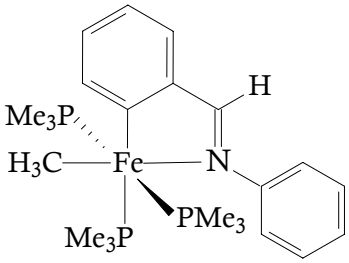

Procedure: A

1.40 g (3.58 mmol) of $Fe(CH_3)_2(PMe_3)_4$ in pentane were combined with 0.65 g (3.58 mmol) of *N*-phenylbenzylidenimine to give 1.48 g of violet crystals (**6**) which crystallize at 4 °C.

Yield: 73%

Melting point: 119 °C – 121 °C (decomposition)

Elemental analysis: $C_{23}H_{40}FeNP_3$, M_w: 479.35g/mol

%	C	H	N	P
Calculated	57.63	8.41	2.92	19.39
Found	57.80	8.10	2.95	19.32

IR (Nujol, 4000 – 400 cm^{-1}):

$\tilde{\nu}$ = 3038 vw (ν H–C=C); 1594 w, 1571 w (ν C=C); 1543 w (ν C=N); 1422 m, 1412 w (δ_{as} PCH_3); 1333 m; 1295 m, 1277 m (δ_s PCH_3); 1223 vw; 1193 w, 1170 w (δ_s Fe–CH_3); 1149 w; 1072 vw; 1026 vw; 993 vw; 942 vs (ρ_1 PCH_3); 886 w; 852 m (ρ_2 PCH_3); 765 s, 750 m (γ C–H_{arom}); 727 s, 701 s (ν_{as} PC_3); 659 w (ν_s PC_3); 636 vw; 572 w; 537 vw.

3.6.7 Iodo[2-[(imino-κN)phenylmethyl]phenyl-κC]tris-(trimethylphosphine)iron(II) (7)

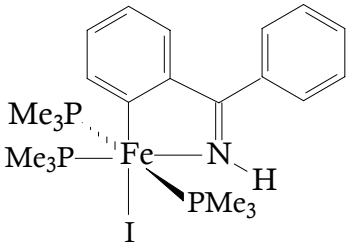

Procedure: D

610 mg (1.31 mmol) of **1** were combined with 186 mg (0.82 ml, 1.31 mmol) of CH_3I in pentane to afford 597 mg of reddish pink crystals (**7**) which crystallize at 4 °C.

Yield: 77%

Melting point: 143 °C – 145 °C

Elemental analysis: $C_{22}H_{37}FeINP_3$, M_w: 591.22g/mol

%	C	H	N	P
Calculated	44.69	6.31	2.37	15.72
Measured	44.68	6.67	2.31	15.64

IR (Nujol, 4000 – 400 cm^{-1}):

$\tilde{\nu}$ = 3287 w (ν H–N=C); 3055 w (ν H–C=C); 1597 vw , 1572 m, 1513 m (ν C=C); 1489 vw (ν C=N); 1407 m (δ_{as} PCH_3); 1298 m, 1271 m (δ_s PCH_3); 1236 w; 1213 w;1157 w; 1099 vw; 1077 vw; 995 w; 945 vs (ρ_1 PCH_3); 847 s (ρ_2 PCH_3); 783 s, 755 w, 727 s (γ C–H_{arom}); 700 vs (ν_{as} PC_3); 664 m (ν_s PC_3); 589 w; 513 w (ν Fe–C); 463 vw.

^{1}H NMR (500 MHz, [D_8]THF, 300 K, ppm):

δ = 1.09 (t', $|^2J_{P,H} + {}^4J_{P,H}|$ = 6.6 Hz, 18H, PCH_3); 1.66 (d, $^2J_{P,H}$ = 6.6 Hz, 9H, PCH_3); 6.67 (t, $^3J_{H,H}$ = 7.3 Hz, 1H, Ar-H); 6.79 (dt, $^3J_{H,H}$ = 8.1 Hz, $^4J_{H,H}$ = 1.5 Hz, 1H, Ar–H); 7.43 (dd, $^3J_{H,H}$ = 7.8 Hz, $^4J_{H,H}$ = 0.9 Hz, 1H, Ar–H); 7.47 (td, $^3J_{H,H}$ = 7.1 Hz, $^4J_{H,H}$ = 1.5 Hz, 1H, Ar–H); 7.49–7.53 (m, 2H, Ar–H); 7.57–7.59 (t, $^3J_{H,H}$ = 7.8 Hz, 3H, Ar–H); 7.61 (d, $^3J_{H,H}$ = 7.8 Hz, 1H, Ar–H); 9.49 (s_{br}, 1H, N–H).

^{13}C NMR (125 MHz, [D_8]THF, 300 K, ppm):

δ = 19.1 (t', $|^1J_{P,C} + {}^3J_{P,C}|$ = 22.3 Hz, PCH_3); 24.2 (d, $^1J_{P,C}$ = 18.8 Hz, PCH_3); 119.1 (s, CH); 127.1 (s, CH); 128.3 (s, CH); 129.7 (s, CH), 129.9 (s, CH); 149.4 (d, $^4J_{P,C}$ = 4.8 Hz, C); 181.9 (m, C=N), 208.1 (m, Fe–C).

^{31}P NMR (202 MHz, [D_8]THF, 296 K, ppm):

δ = 11.3 (d, $^2J_{P,P}$ = 57.0 Hz, 2P, PCH_3), 17.7 (t, $^2J_{P,P}$ = 57.0 Hz, 1P, PCH_3).

3.6.8 Iodo[2-[(imino-κN)phenylmethyl]-1,1-dimethylethyl-κC]tris-(trimethylphosphine)iron(II) (8)

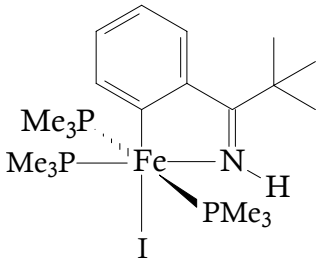

Procedure: D

774 mg (1.74 mmol) of **2** were combined with 247 mg (1.09 ml, 1.74 mmol) of CH_3I in pentane to afford 745 mg of reddish pink crystals (**8**) which crystallize at 4 °C.

Yield: 75%

Melting point: 160 °C – 162 °C (decomposition)

Elemental analysis: $C_{20}H_{41}FeINP_3$, M_w: 571.23g/mol

%	C	H	N	P
Calculated	42.05	7.23	2.45	16.27
Found	41.85	6.95	2.20	16.55

IR (Nujol, 4000 – 400 cm^{-1}):

$\tilde{\nu}$ = 3320 w (ν H–N=C); 3070 vw, 3042 vw, 3012 vw (ν H–C=C), 1565 m (ν H–C=C); 1565 m, 1556 w (ν C=C); 1525 vw (ν C=N); 1406 m (δ_{as} PCH_3); 1353 w; 1297 m, 1281 m (δ_s PCH_3); 1231 m; 1205 vw; 1176 vw; 1152 vw; 1107 w; 1016 w; 999 w; 941 vs (ρ_1 PCH_3); 868 vw; 851 m (ρ_2 PCH_3); 815 w; 776 w, 738 s (γ C-H_{arom}); 716 s, 692 w (ν_{as} PC_3); 660 m (ν_s PC_3); 648 vw; 507 vw.

^{1}H NMR Spectrum (500 MHz, [D_8]THF, 300 K, ppm) :

δ = 1.06 (s, 18H, PCH_3), 1.51 (s, 9H, $C(CH_3)_3$); 1.61 (d, $^2J_{P,H}$ = 5.9 Hz, PCH_3); 6.69 (m, 2H, Ar–H); 7.51 (d, $^4J_{P,H}$ = 7.4 Hz, 1H, Ar–H); 7.76 (d, $^3J_{H,H}$ = 6.7 Hz, 1H, Ar–H); 9.50 (s_{br}, 1H, N–H).

^{13}C NMR (125 MHz, [D_8]THF, 300 K, ppm):

δ = 18.9 (t', $|^1J_{P,C} + {}^3J_{P,C}|$ = 22.1 Hz, PCH_3); 24.3 (td, $^1J_{P,C}$ = 18.5 Hz, $^3J_{P,C}$ = 2.2 Hz, PCH_3); 29.3(s, C<u>C</u>H_3); 39.8 (s, <u>C</u>CH_3); 118.3 (s, CH); 126.2 (s, CH); 129.3 (s, CH); 146.1 (d, $^3J_{P,C}$ = 7.9 Hz, CH); 148.3 (d, $^4J_{P,C}$ = 4.6 Hz, C); 187.8 (t, $^3J_{P,C}$ = 8.6 Hz, C=N); 208.4 (m, Fe–C).

^{31}P NMR (202 MHz, [D_8]THF, 300 K, ppm):

δ = 13.1 (d, $^2J_{P,P}$ = 55.9 Hz, 2P, PCH_3); 19.9 (t, $^2J_{P,P}$ = 55.9 Hz, 1P, PCH_3).

3.6.9 Iodo[2-[(imino-κN)phenylmethyl]-2-methylphenyl-κC]tris-(trimethylphosphine)iron(II) (9)

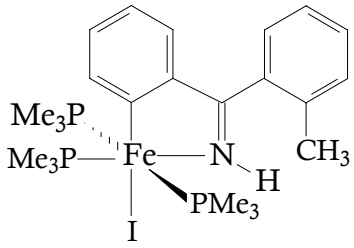

Procedure: D

598 mg (1.25 mmol) of **3** in pentane were combined with 177 mg (0.78 ml, 1.25 mmol) of CH_3I to afford 544 mg of reddish pink crystals (**9**) which crystallize at 4 °C.

Yield: 72%

Melting point: 146 °C – 148 °C

Elemental analysis: $C_{23}H_{39}FeINP_2$, M_w: 605.24 g/mol

%	C	H	N	P
Calculated	45.64	6.49	2.31	15.35
Found	45.17	5.38	1.80	16.28

IR (Nujol, 4000 – 400 cm^{-1}):

$\tilde{\nu}$ = 3289 vw (ν H–N=C); 3050 w, 3019 vw (ν H–C=C); 1570 m (ν C=C); 1514 w (ν C=N); 1408 m (δ_{as} PCH_3); 1297 w, 1280 w (δ_s PCH_3), 1231 vw; 1152 vw; 993 vw; 940 vs (ρ_1 PCH_3); 850 m (ρ_2 PCH_3); 782 w, 760 m (γ C–H_{arom}); 738 s, 719 m (ν_{as} PC_3); 658 m (ν_s PC_3); 596 w; 500 vw.

^{1}H NMR (500 MHz, [D_8]THF, 300 K, ppm) :

δ = 1.17 (t' $|^2J_{P,H} + {}^4J_{P,H}|$ = 6.4 Hz, 18H, PCH_3); 1.67 (d, $^2J_{P,H}$ = 6.4 Hz, 9H, PCH_3); 2.17 (s, 3H, Ar–CH_3); 6.61 (t, $^3J_{H,H}$ = 7.3 Hz, 1H, Ar–H); 6.75 (dt, $^3J_{H,H}$ = 8.1 Hz, $^4J_{H,H}$ = 1.4 Hz, 1H, Ar–H); 7.01 (d, $^3J_{H,H}$ = 8.1 Hz, 1H, Ar–H); 7.31 (t, $^3J_{H,H}$ = 7.8 Hz,

2H, Ar–H); 7.40 (dt, $^{3}J_{H,H}$ = 7.4 Hz, $^{4}J_{H,H}$ = 1.4 Hz, 1H, Ar–H); 7.42 (dd, $^{3}J_{H,H}$ = 6.5 Hz, $^{4}J_{H,H}$ = 1.2 Hz, 1H, Ar–H); 7.62 (d, $^{3}J_{H,H}$ = 7.8 Hz 1H, Ar–H); 9.42 (s, 1H, N–H).

^{13}C NMR (125 MHz, [D_8]THF, 300 K, ppm):
δ = 19.5 (t' $|^{1}J_{P,H} + {}^{3}J_{P,H}|$ = 22.5 Hz, PCH_3); 21.8 (s, Ar–CH_3); 24.1 (d, $^{1}J_{,C}$ = 18.8 Hz, PCH_3); 118.9 (s, CH); 126.7 (s, CH); 127.4(s, CH), 128.3 (s, C); 129.4 (s, CH); 130.1 (d; $^{3}J_{P,C}$ = 16.9 Hz, CH); 131.8 (s, C); 136.1 (s, C); 145.7 (d, $^{4}J_{P,C}$ = 7.1 Hz, CH); 182.9 (m, C=N); 228.4 (m, Fe–C).

^{31}P NMR (202 MHz, [D_8]THF, 296 K, ppm)
δ = 10.8 (d, $^{2}J_{P,P}$ = 57.5 Hz, 2P, PCH_3); 19.2 (t, $^{2}J_{P,P}$ = 57.5, 1P, PCH_3.

3.6.10 Iodo[2-[(methylimino-κN)methyl]phenyl- κC]tris-(trimethylphosphine)iron(II) (10)

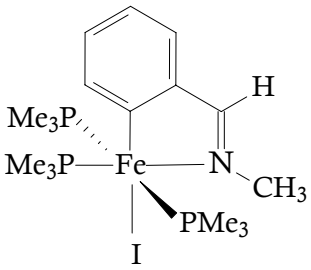

Procedure: D
623 mg (1.49 mmol) of **4** were combined with 211 mg (0.93 ml, 1.49 mmol) of CH_3I in pentane to afford 426 mg of rose crystals (**10**) which crystallize at 4 °C.

Yield: 54%

Melting point: 142 °C - 144 °C

Elemental analysis: $C_{17}H_{35}FeINP_3$, M_w: 529.14 g/mol

%	C	H	N	P
Calculated	38.59	6.67	2.65	17.56
Found	38.86	6.53	2.60	17.58

IR (Nujol, 4000 – 400 cm^{-1}):

$\tilde{\nu}$ = 3056 vw (ν H–C=C); 1591 s, 1572 s (ν C=C); 1529 m (ν C=N); 1421 s (δ_{as} PCH_3); 1296 s, 1280 s, 1273 s (δ_s PCH_3); 1236 w; 1219 w; 1156 w; 1124w; 1105 w; 1038 vw; 1008 w; 997 w; 939 vs (ρ_1 PCH_3); 856 m (ρ_2 PCH_3); 753 m, 746 m (γ C–H_{arom}); 727 s, 713 s (ν_{as} PC_3); 694 vw; 663 m (ν_s PC_3); 642 vw; 537 vw, 471 vw.

^{1}H NMR (500 MHz, [D_8]-THF, 298 K, ppm):

δ = 1.14 (s, 18H, PCH_3); 1.56 (s, 9H, PCH_3); 3.83 (s, 3H, N–CH_3); 6.70 (m, 2H, Ar–H); 7.27 (s, 1H, Ar–H); 7.54 (s, 1H, Ar–H); 8.43 (s, 1H, N=C–H).

^{13}C NMR (125 MHz, [D_8]-THF, 298 K, ppm):

δ = 18.9 (t' $|{}^1J_{P,C} + {}^3J_{P,C}|$ = 21.3 Hz, PCH_3); 24.5 (d, ${}^1J_{P,C}$ = 20.9 Hz, PCH_3); 55.3 (s, N-CH_3); 119.3 (s, CH); 126.7 (m, CH); 128.3 (s, CH); 146.3 (s, C); 162.4 (s, CH); 174.7 (s, C=N), 212.7 (s, Fe –C).

^{31}P NMR (202 MHz, [D_8]-THF, 296 K, ppm):

δ = 5.8 (d, ${}^2J_{P,P}$ = 54.3 Hz, 2P, PCH_3); 14.9 (t, ${}^2J_{P,P}$ = 54.3 Hz, 1P, PCH_3).

3.6.11 Iodo[2-[[(1-methylethyl)imino-κN]methyl]phenyl-κC]tris-(trimethylphosphine)iron(II) (11)

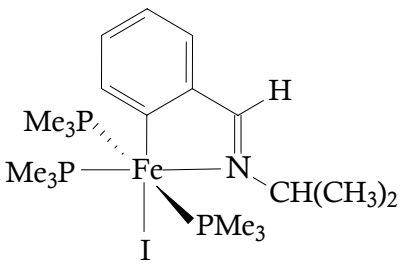

Procedure: D

1.02 g (2.29 mmol) of **5** were combined with 0.33 g (0.93 ml, 1.43 mmol) of CH_3I in pentane to afford 0.88 g of light violet crystals (**11**) which crystallize at 4 °C.

Yield: 69%

Melting point: 145 °C – 147 °C

Elemental analysis: $C_{19}H_{39}FINP_3$, M_w: 557.20 g/mol

%	C	H	N	P
Calculated	40.96	7.05	2.51	16.68
Found	40.94	7.15	2.46	16.47

IR (Nujol, 4000 – 400 cm^{-1}):

$\tilde{\nu}$ = 3088 w (ν H–C=C); 1594 m, 1572 m (ν C=C); 1533 w (ν C=N); 1423 m (δ_{as} PCH_3); 1313 w; 1298 s, 1273 m (δ_s PCH_3); 1236 w; 1221 w; 1163 w; 1121w; 1108 w; 1005 w; 944 vs (ρ_1 PCH_3); 870 w; 844 w (ρ_2 PCH_3); 746 m (γ C–H_{arom}); 728 s, 714 m (ν_{as} PC_3); 660 m (ν_s PC_3).

^{1}H NMR (500 MHz, [D_8]THF, 298 K, ppm):

δ = 0.84 (t', $|^2J_{P,H} + {}^4J_{P,H}|$ = 5.9 Hz, 18H, PCH_3); 1.69 (d, $^2J_{P,H}$ = 6.4 Hz, 6H, $CH(C\underline{H}_3)_2$); 1.50 (d, $^2J_{P,H}$ = 6.4 Hz, 9H, PCH_3); 5.38 (sep, $^2J_{H,H}$ = 6.2 Hz, 1H, $C\underline{H}(CH_3)_2$); 7.11 (m, 1H, Ar–H); 7.17 (m, 1H, Ar–H); 7.51 (m, 1H, Ar–H); 7.65 (m, 1H, Ar–H), 8.29 (s, 1H, N=C–H).

^{13}C NMR (125 MHz, [D_8]THF, 298 K, ppm):

δ = 12.3 (t' $|^1J_{P,C} + {}^3J_{P,C}|$ = 28.7 Hz, PCH_3); 15.8 (d, $^1J_{P,C}$ = 20.3 Hz, PCH_3); 19.2 (s, $CH(\underline{C}H_3)_2$); 49.5 (d, $^3J_{P,C}$ = 13.9 ppm, $\underline{C}H(CH_3)_2$); 129.1 (s, CH); 129.6 (d, $^4J_{P,C}$ = 4.4 Hz, CH); 130.1 (s, CH); 131.2 (s, CH); 158.9 (s, C); 160.4 (s, C=N); 199.7 (s, Fe –C).

^{31}P NMR (202 MHz, [D_8]THF, 296 K, ppm):

δ = 28.3 (d, $^2J_{P,P}$ = 28.3 Hz, 2P, PCH_3); 21.8 (t, $^2J_{P,P}$ = 28.3 Hz, 1P, PCH_3).

3.6.12 Methyl[2-[(methylimino-κN)methyl]phenyl-κC](carbonyl)bis-(trimethylphosphine)iron(II) (12)

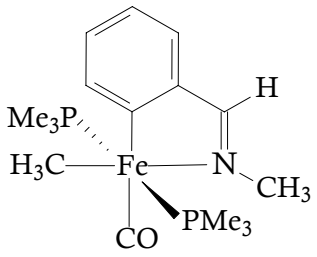

Procedure: E

A sample of **4** (770 mg, 1.84 mmol) of in pentane was stirred under 1 bar CO to provide 450 mg of reddish pink crystals (**12**) which crystallize at –27 °C.

Yield: 66%

Melting point: 134 °C – 136 °C

Elemental analysis: $C_{16}H_{29}FeNOP_2$, M_w: 369.21g/mol

%	C	H	N	P
Calculated	52.05	7.92	3.79	16.78
Found	52.30	7.91	3.10	17.32

IR (Nujol, 4000 – 400 cm^{-1}):

$\tilde{\nu}$ = 3068 vw, 3028 vw (ν H–C=C); 1869 vs (ν C≡O); 1595 m, 1573 w (ν C=C); 1531 w (ν C=N); 1420 m (δ_{as} PCH_3); 1298 w, 1281 m (δ_s PCH_3); 1240 w; 1218 w; 1153 w (δ Fe–CH_3); 1036 vw; 1008 vw; 946 vs (ρ_1 PCH_3); 854 m (ρ_2 PCH_3); 751 m (γ C–H_{arom}); 722 s (ν_{as} PC_3); 668 m (ν_s PC_3); 646 w; 620 w, 607 w.

^{1}H NMR (500 MHz, [D_8]THF, 298 K, ppm):

δ = - 0.67 (t, $^3J_{P,H}$ = 6.8 Hz, 3H, Fe–CH_3); 0.89 (s, 18H, PCH_3); 3.34 (s, 3H, N–CH_3); 6.72 (t, $^3J_{H,H}$ = 6.0 Hz 1H, Ar–H); 6.79 (t, $^3J_{H,H}$ = 6.0 Hz, 1H, Ar–H); 7.34 (d, $^3J_{H,H}$ = 6.0 Hz, 1H, Ar–H); 7.96 (d, $^3J_{P,H}$ = 5.4 Hz, 1H, Ar–H); 8.33 (s, 1H, N=C–H).

^{13}C NMR (125 MHz, [D_8]-THF, 298 K):

δ = -11.5 (t, $^{2}J_{P,C}$ = 18.4 Hz, Fe–CH_3); 15.0 (t' $|{}^{1}J_{P,C} + {}^{3}J_{PC}|$ = 23.0 Hz, PCH_3); 46.8 (s, N-CH_3); 120.0 (s, CH); 126.9 (s, CH); 128.1 (s, CH); 143.5 (s, CH); 148.9 (s, C); 174.3 (t, $^{3}J_{P,C}$ = 4.4 Hz, C=N), 211.6 (m, Fe –C); 224.2 (s, Fe –CO) ppm.

^{31}P NMR (202 MHz, [D_8]-THF, 296 K, ppm):

δ = 19.1 (s, PCH_3) ppm.

3.6.13 Methyl[2-[[(1-methylethyl)imino-κN]methyl]phenyl-κC(carbonyl)bis-(trimethylphosphine)iron(II) (13)

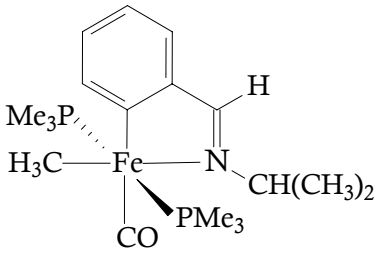

Procedure: E

A sample of **5** (650 mg, 1.46 mmol) of in pentane was stirred under 1 bar CO to provide 336 mg of reddish pink crystals (**13**) which crystallize at –27 °C.

Yield: 58%

Melting point: 131 °C – 133 °C

Elemental analysis: $C_{18}H_{33}FeNOP_2$, Mw: 397.26 g/mol

%	C	H	N	P
Calculated	54.42	8.37	3.53	15.59
Found	54.46	8.43	3.53	16.54

IR (Nujol, 4000 – 400 cm^{-1}):

$\tilde{\nu}$ = 3075 vw, 3040 w (ν H–C=C); 1879 vs (ν C≡O); 1591 m, 1573 w (ν C=C); 1532 w (ν C=N); 1420 m (δ_{as} PCH_3); 1299 w, 1279 m (δ_s PCH_3); 1239 vw; 1219 vw; 1151

vw (δ_s Fe–CH_3) ; 1126 vw; 1113 vw; 1032 vw; 1010 vw; 941 vs (ρ_1 PCH_3); 850 m (ρ_2 PCH_3); 754 m (γ C–H_{arom}); 721 s (ν_{as} PC_3); 667 (ν_s PC_3); 646 m; 629 w; 599 m.

^{1}H NMR (500 MHz, [D_8]THF, 298 K, ppm):
δ = - 0.59 (t, $^3J_{P,H}$ = 7.3 Hz, 3H, Fe–CH_3); 0.90 (s_{br}, 18H, PCH_3); 1.29 (d, $^3J_{H,H}$ = 6.5 Hz, 6H, CH(C$\underline{H}_3$)$_2$); 4.08 (sep, $^3J_{H,H}$ = 6.5 Hz, 1H, C$\underline{H}$(CH_3)$_2$); 6.75 (t, $^3J_{H,H}$ = 6.9 Hz 1H, Ar–H); 6.82 (t, $^3J_{H,H}$ = 6.9 Hz 1H, Ar–H); 7.40 (d, $^3J_{H,H}$ = 7.2 Hz, 1H, Ar–H); 7.91 (d, $^3J_{H,H}$ = 6.9 Hz, 1H, Ar–H); 8.49 (m, 1H, H–C=N).

^{13}C NMR (125 MHz, [D_8]THF, 298 K, ppm):
δ = -13.2 (t, $^2J_{P,C}$ = 17.2 Hz, Fe–CH_3); 13.2 (t', $|^1J_{P,C} + {}^3J_{PC}|$ = 11.2 Hz, PCH_3); 22.4 (s, CH(C$\underline{H}_3$)$_2$); 51.4 (s, C$\underline{H}$(CH_3)$_2$); 118.1 (s, CH); 124.9 (s, CH); 126.4 (s, CH); 141.4 (s, CH); 148.7 (s, C); 168.0 (t, $^3J_{P,C}$ = 3.6 Hz, CN); 207.3 (t, $^2J_{P,C}$ = 21.8 Hz, Fe–C); 222.6 (t, $^2J_{P,C}$ = 35.6 Hz , Fe–CO).

^{31}P NMR (202 MHz, [D_8]-THF, 296 K, ppm):
δ = 18.7 (s, 2P, PCH_3).

3.6.14 Methyl[2-[(phenylimino-κN)methyl]phenyl κC](carbonyl)bis-(trimethylphosphine)iron(II) (14)

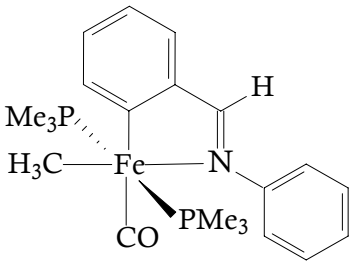

Procedure: E
A sample of **6** (490 mg, 1.02 mmol) in pentane was stirred under 1 bar CO to provide 347 mg of reddish pink crystals (**14**) which crystallize at –27 °C.

Yield: 73%

Melting point: 137 °C – 139 °C (decomposition)

Elemental analysis: $C_{24}H_{29}FeNOP_2$, M_w: 465.29g/mol

%	C	H	N	P
Calculated	58.48	7.25	3.25	14.36
Found	58.85	6.81	3.24	14.35

IR (Nujol, 4000 – 400 cm^{-1}):

$\tilde{\nu}$ = 3075 vw, 3063 w, 3012 vw (ν H–C=C); 1870 vs (ν Fe–C≡O); 1576 m (ν C=C), 1514 m (ν C=N); 1350 vw (δ_{as} PCH_3); 1302 w, 1280 m (δ_s PCH_3); 1230 vw; 1193 m (δ_s Fe–CH_3); 1107 m_{br}; 1008 vw; 944 vs (ρ_1 PCH_3); 852 m (ρ_2 PCH_3); 768 m, 748 m (γ C–H_{arom}); 722 s, 701 m (ν_{as} PC_3); 670 w (ν_s PC_3); 645 w; 628 w; 600 m; 566 w.

^{1}H NMR (500 MHz, [D_8]THF, 298 K, ppm):

δ = - 0.71 (t, $^3J_{P,H}$ = 8.1 Hz, 3H, Fe–CH_3); 0.93 (t' $|^2J_{P,H} + {}^4J_{P,H}|$ = 7.3 Hz, 18H, PCH_3); 6.83 (t, $^3J_{H,H}$ = 7.2 Hz 1H, Ar–H); 6.89 (t, $^3J_{H,H}$ = 7.2 Hz 1H, Ar–H); 7.02 (d, $^3J_{H,H}$ = 7.8 Hz, 2H, Ar–H); 7.19 (t, $^3J_{H,H}$ = 7.3 Hz, 1H, Ar–H); 7.33 (t, $^3J_{H,H}$ = 7.8 Hz, 2H, Ar–H); 7.57 (d, $^3J_{H,H}$ = 7.4 Hz, 1H, Ar–H); 8.08 (d, $^3J_{H,H}$ = 7.3 Hz, 1H, Ar–H); 8.49 (t, $^4J_{P,H}$ = 4.2 Hz, 1H, N=C–H).

^{13}C NMR (125 MHz, [D_8]-THF, 298 K, ppm):

δ = -7.1 (t, $^2J_{P,C}$ = 17.2 Hz, Fe–CH_3); 15.4 (t' $|^1J_{P,C} + {}^3J_{PC}|$ = 23.2 Hz, PCH_3); 120.7 (s, CH); 125.3 (s, CH); 129.2 (s, CH); 130.8 (s, CH); 144.1 (s, CH); 150.5 (s, C); 152.9 (s, C); 175.8 (t, $^3J_{P,C}$ = 4.5 Hz, C=N), 215.8 (m, Fe –C); 224.9 (t, $^2J_{P,C}$ = 35.6 Hz, Fe–CO).

^{31}P NMR (202 MHz, [D_8]-THF, 296 K, ppm):

δ = 18.3 (s, PCH_3).

3.6.15 [2-[(imino-κN)phenylmethyl]phenyl-κC]tris-(trimethylphosphine)cobalt (I) (15)

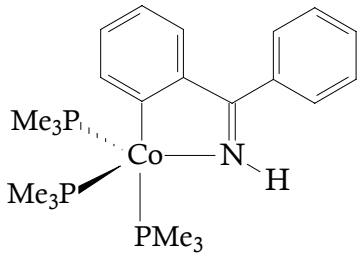

Procedure: B

1.27 g (3.36 mmol) of $CoMe(PMe_3)_4$ in THF were combined with 0.61 g (3.36 mmol) of diphenylketimine to afford 1.29 g green crystals (**15**) which crystallize from pentane at –27 °C.

Yield: 82%

Melting point: 106 °C – 108 °C (decomposition)

Elemental analysis: $C_{22}H_{37}CoNP_3$, M_w: 467.40g/mol

%	C	H	N	P
Calculated	56.53	7.98	3.00	19.88
Found	56.54	8.15	3.04	19.78

IR (Nujol, 4000 - 400 cm^{-1}):

$\tilde{\nu}$ = 3301 vw (ν H–N=C); 3063 w, 3041 w, 3022 w (ν H–C=C); 1590 s (ν C=C); 1494 s (ν C=N); 1417 s (δ_{as} PCH_3); 1285 s, 1275 w (δ_s PCH_3); 1174 w; 1072 vw; 1029 vw; 998 vw; 953 vs, 936 vs (ρ_1 PCH_3); 840 m (ρ_2 PCH_3); 766 s (γ C–H_{arom}); 749 vw; 736 vw; 719 s, 700 s (ν_{as} PC_3); 657 s (ν_s PC_3); 594 s (ν Co–C).

^{1}H NMR (500 MHz, [D_8]THF, 300 K, ppm):

δ = 1.23 (d, $^2J_{P,H}$ = 6.2 Hz, 27H, PCH_3); 6.69 (t, $^3J_{H,H}$ = 7.2 Hz,1H, Ar–H); 6.97 (t, $^3J_{H,H}$ = 7.2 Hz, 1H, Ar–H); 7.26 (m, 3H, Ar–H); 7.61 (m, 2H, Ar–H); 7.74 (d, $^3J_{H,H}$ = 7.5 Hz, 1H, Ar–H); 7.97 (s_{br}, 1H, N–H); 8.16 (d, $^3J_{H,H}$ = 8.0 Hz, 1H, Ar–H).

^{13}C NMR (125 MHz, [D_8]THF, 300 K, ppm):

δ = 22.5 (q', $^{1}J_{P,C}$ = 24.2 Hz, $^{1}J_{P,C}$ = 4.5 Hz, PCH_3); 118.8 (dd, $^{4}J_{P,C}$= 3.5 Hz, $^{3}J_{P,C}$= 5.7 Hz, CH); 119.8 (s, CH); 123.4 (s, CH); 125.2 (s, CH); 125.9 (t, $^{5}J_{P,C}$ = 2.4 Hz, CH); 129.8 (s, CH); 143.7 (s, C); 144.3 (d, $^{4}J_{P,C}$= 2.3 Hz, C); 146.8 (q, $^{3}J_{P,C}$ = 4.6 Hz, CH); 160.6 (q, $^{3}J_{P,C}$ = 8.0 Hz, C=N), 179.2 (s, Co–C).

^{31}P NMR (202 MHz, [D_8]THF, 300 K, ppm):

δ = - 0.26 (s_{br}, PCH_3).

3.6.16 [2-[(imino-κN)phenylmethyl]-1,1-dimethylethy κC]tris (trimethylphosphine)cobalt(I) (16)

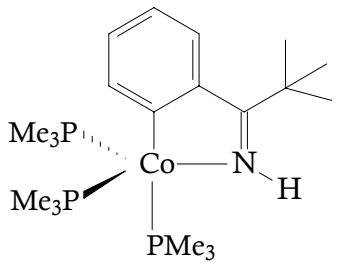

Procedure: B

1.34 g (3.54 mmol) of $CoMe(PMe_3)_4$ in THF were combined with 0.57 g (3.36 mmol) of *tert*-butylphenylketimine to afford 0.65 g of green of crystals (**16**) which crystallize from pentane at –27 °C.

Yield: 42 %

Melting point: 112 °C – 114 °C (decomposition)

Elemental analysis: $C_{20}H_{41}CoNP_3$, Mw: 447.41g/mol

%	C	H	N	P
Calculated	53.69	9.24	3.13	20.77
Found	53.65	9.04	3.08	21.06

IR (Nujol, 4000 – 400 cm^{-1}):

$\tilde{\nu}$ = 3358 m (ν H–N =C); 3065 m, 3020 vw (ν H–C=C); 1561 w (ν C=C); 1528 vw (ν C=N); 1423 m (δ_{as} PCH_3); 1358 w; 1293 w, 1283 vw, 1270 s (δ_s PCH_3); 1236 w; 1202 m; 1173 w; 1153 w; 1113 vw; 1038 w; 1019 w; 1004 w; 993 vw; 933 vs (ρ_1 PCH_3); 872 vw; 840 s (ρ_2 PCH_3); 816 m; 794 vw; 774 s, 758 w, 725 s (γ C–H_{arom}); 697s (ν_{as} PC_3), 655 vs (ν_s PC_3); 623 m; 566 w; 500 w (ν Co–C); 435 vw; 427 w; 405 vs.

^{1}H NMR (500 MHz, [D_8]THF, 300 K, ppm):

δ = 1.16 (d, $^2J_{P,H}$ = 5.8 Hz, 27H, PCH_3); 1.47 (s, 9H, $C(CH_3)_3$); 6.66 (t, $^3J_{H,H}$ = 7.0 Hz, 1H, Ar–H); 6.81 (t, $^3J_{H,H}$ = 7.0 Hz, 1H, Ar–H); 7.76 (d, $^3J_{H,H}$ = 8.0 Hz, 1H, Ar–H); 8.09 (d, $^3J_{H,H}$ = 7.5 Hz, 1H, Ar–H); 8.26 (s_{br}, 1H, N–H).

^{13}C NMR (125 MHz, [D_8]THF, 300 K, ppm):

δ = 20.4 (q', $^1J_{P,C}$ = 24.1 Hz, $^1J_{P,C}$ = 4.5 Hz, PCH_3); 27.1 (s, C<u>C</u>H_3); 37.6 (s, <u>C</u>CH_3); 115.8 (s, CH); 116.1 (m, CH); 122.6 (s, CH); 139.6 (s, C); 144.7 (dd, $^4J_{P,C}$ = 10.3 Hz, $^4J_{P,C}$ = 4.6 Hz, CH); 167.1 (m, C=N); 181.3 (m, Co–C).

^{31}P NMR (202 MHz, [D_8]THF, 300 K, ppm):

δ = - 4.5 (s_{br}, PCH_3).

3.6.17 Iodo(methyl)[2-[(imino-κN)phenylmethyl]phenyl-κC]bis (trimethylphosphine)cobalt(III) (17)

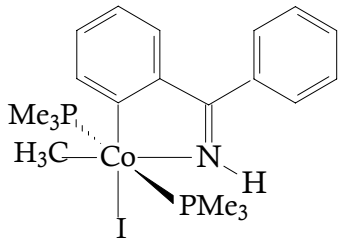

Procedure: D

640 mg (1.36 mmol) of 15 in pentane were combined with 388 mg (1.71 ml, 2.72 mmol) of CH_3I to afford 431mg of range crystals (**17**) which crystallize at 4 °C.

Yield: 59%

Melting point: 138 °C – 140 °C

Elemental analysis: $C_{22}H_{37}CoINP_2$, M_w: 533.26g/mol

%	C	H	N	P
Calculated	45.05	5.83	2.63	11.62
Found	44.96	5.86	2.57	11.70

IR (Nujol, 4000 - 400cm^{-1}):

$\tilde{\nu}$ = 3298 w (ν H–N=C); 3034 w (ν H–C=C); 1571 w, 1554 w (ν C=C); 1528 w (ν C=N); 1415 m (δ_{as} PCH_3); 1298 m, 1275 m (δ_s PCH_3); 1244 w; 1213 w; 1155 m (δ_s Co–CH_3); 1080 vw; 1014 vw; 944 vs (ρ_1 PCH_3); 854 s (ρ_2 PCH_3); 788 s; 728 vs (γ C–H_{arom}); 701s (ν_{as} PC_3); 670 m (ν_s PC_3); 654 m; 589 w.

^{1}H NMR (500 MHz, [D_8]THF, 300 K, ppm):

δ = 0.30 (t, $^3J_{P,H}$ = 9.7 Hz, 3H, Co–CH_3); 1.09 (t', $|^2J_{P,H} + {}^4J_{P,H}|$ = 7.41 Hz, 18H, PCH_3); 6.89 (t, $^3J_{H,H}$ = 7.4 Hz, 1H, Ar–H); 7.07 (t, $^3J_{H,H}$ = 7.8 Hz 3H, Ar–H); 7.29 (t, $^3J_{H,H}$ = 8.1Hz, 2H, Ar–H); 7.53 (m, 5H, Ar–H); 9.64 (s_{br}, 1H, N–H).

^{13}C NMR (125 MHz, [D_8]THF, 300 K, ppm):

δ = -7.5 (m, Co–CH_3); 15.2 (t', $|^1J_{P,C} + {}^3J_{P,C}|$ = 28.1 Hz, PCH_3); 121.9 (s, CH); 128.6 (s, CH); 125.3 (s, CH); 129.9 (s, CH); 130.9 (s, CH); 130.9 (s, CH); 136.1 (s, C); 138.6 (s, C); 135.1 (s, CH); 145.6 (s, C); 166.5 (m, C=N), 183.4 (m, Co–C).

^{31}P NMR (202 MHz, [D_8]THF, 300 K)

δ = 2.2 (s, PCH_3) ppm.

3.6.18 Iodo(methyl)[2-[(imino-κN)phenylmethyl]-1,1-dimethylethyl-κC]tris (trimethylphosphine)cobalt(III) (18)

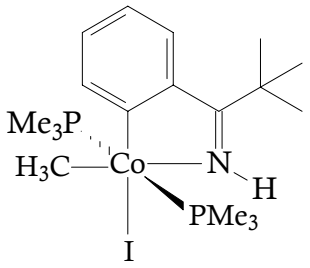

Procedure: D

510 mg (1.14 mmol) of **16** in pentane were combined with 324 mg (1.43 ml, 2.28 mmol) of CH_3I to afford 340 mg of orange crystals (**18**) which crystallize at 4 °C.

Yield: 58%

Melting point: 141 °C – 143 °C

Elemental analysis: $C_{18}H_{35}CoINP_2$, M_w: 513.27g/mol

	%C	%H	%N	%P
Calculated	42.12	6.87	2.73	12.07
Found	42.17	6.75	2.69	11.89

IR (Nujol, 4000 – 400 cm^{-1}):

$\tilde{\nu}$ = 3329 w (ν H–N=C); 3071 vw (ν H–C=C); 1568 m (ν C=C); 1537 vw (ν C=N); 1416 m (δ_{as} PCH_3); 1350 w; 1298 m, 1281 m (δ_s PCH_3); 1234 vw; 1191 w; 1157 m (δ_s Co–CH_3); 1113 vw; 1017 vw; 948 vs (ρ_1 PCH_3); 852 m (ρ_2 PCH_3); 817 vw; 799 vw; 781 vw; 739 m (γ C–H_{arom}); 718 vs (ν_{as} PC_3), 655 m (ν_s PC_3); 515 vw.

^{1}H NMR (500 MHz, [D_8]THF, 300 K, ppm):

δ = 0.54 (t, $^3J_{P,H}$ = 9.4 Hz, 3H, Co–CH_3); 1.45 (t', $|^2J_{P,H} + {}^4J_{P,H}|$ = 7.46 Hz, 18H, PCH_3); 1.48 (s, 9H, $C(CH_3)_3$); 6.89 (dt, $^4J_{H,H}$ = 0.9 Hz, $^3J_{H,H}$ = 6.9 Hz, 1H, Ar–H);

6.98 (dt, $^4J_{H,H}$ = 1.4 Hz, $^3J_{H,H}$ = 7.1 Hz, 1H, Ar–H); 7.19 (qd, $^4J_{H,H}$ = 1.3 Hz, $^3J_{H,H}$ = 7.8 Hz, 1H, Ar–H); 7.76 (dd, $^4J_{H,H}$ = 1.3 Hz, $^3J_{H,H}$ = 7.8 Hz, 1H, Ar–H); 9.60 (s_{br}, 1H, N–H).

^{13}C NMR (125 MHz, [D_8]THF, 300 K, ppm):
δ = -10.12 (m, Co–CH_3); 14.8 (t, $|^1J_{P,C} + {}^3J_{P,C}|$ = 26.8 Hz, PCH_3); 26.9 (s, C$\underline{C}H_3$); 37.6 (s, $\underline{C}CH_3$); 119.2 (s, CH); 126.3 (s, CH); 126.6 (s, CH); 137.2 (s, CH); 142.1 (s, C); 167.1 (m, C=N); 187.9 (s, C).

^{31}P NMR (202 MHz, [D_8]THF, 300 K):
δ = 3.6 (s_{br}, PCH_3) of ppm.

3.6.19 [2-[(imino-κN)phenylmethyl]phenyl-κC](carbonyl)bis (trimethylphosphine)cobalt(I) (19)

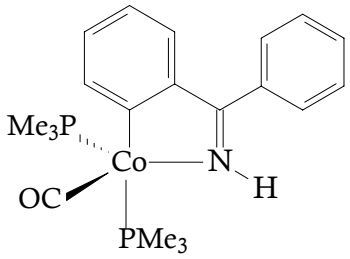

Procedure: E
A sample of **15** (850 mg, 1.82 mmol) in pentane was stirred under 1 bar CO to provide 351 mg of red crystals (**20**) which crystallize at –27 °C.

Yield: 46%

Melting point: 126 °C – 128 °C (decomposition)

Elemental analysis: $C_{22}H_{28}CoNOP_2$, M_w: 419.33g/mol

%	C	H	N	P
Calculated	57.29	6.73	3.34	14.77
Found	56.65	6.80	2.97	14.40

IR (Nujol, 4000 – 400 cm^{-1}):

$\tilde{\nu}$= 3314 vw (ν H–N=C); 3081 vw, 3048 vw, 3028 w (ν H–C=C); 1883 vs (ν C≡O); 1593 w, 1571 w (ν C=C); 1497 w (ν C=N); 1418 w (δ_{as} PCH_3); 1404 m; 1302 w, 1283 m, 1276 m (δ_s PCH_3); 1252 vw; 1238 vw; 1076 vw; 1025 vw; 950 vs (ρ_1 PCH_3); 912 w; 848 m (ρ_2 PCH_3); 800 w; 777 m; 753 w; 725 vs (γ C–H_{arom}); 702 s (ν_{as} PC_3); 666 s (ν_s PC_3); 598 s (ν Co–C); 551 w; 521 w; 504 w, 481 w; 439 m.

^{1}H NMR (500 MHz, [D_8]THF, 300 K, ppm):

δ = 1.33 (d, $^2J_{P,H}$ = 12.9 Hz, 9H, PCH_3); 1.57 (d, $^2J_{P,H}$ = 9.50 Hz, 9H, PCH_3); 6.92 (dt, $^3J_{H,H}$ = 7.1 Hz, $^4J_{H,H}$ = 1.2 Hz, 1H, Ar–H); 7.05 (tt, $^3J_{H,H}$ = 7.4 Hz, $^4J_{H,H}$ = 1.2 Hz 1H, Ar–H); 7.47 (m, 3H, Ar–H); 7.49 (dd, $^3J_{H,H}$ = 3.6 Hz, $^4J_{H,H}$ = 1.7 Hz, 1H, Ar–H); 7.54 (m, 2H, Ar–H); 8.04 (ddd, $^3J_{H,H}$ = 7.9 Hz, $^4J_{H,H}$ = 3.8 Hz, $^5J_{H,H}$ = 1.1 Hz, 1H, Ar–H); 9.69 (s_{br}, 1H, N-H).

^{13}C NMR (125 MHz, [D_8]THF, 300 K, ppm):

δ = 18.2 (s, PCH_3); 18.4 (s, PCH_3); 121.1 (s, CH); 126.8 (d, $^5J_{P,C}$ = 3.5 Hz, CH); 128.4 (s, CH); 129.4 (s, CH); 129.5 (s, C); 139.6 (s, CH); 141.8 (d, $^5J_{P,C}$ = 2.2 Hz, C); 144.7 (s, CH); 180.7 (s, C=N); 180.9 (s, Co–C); 215.1 (s, Co–CO).

^{31}P-NMR (202 MHz, [D_8]THF, 300 K, ppm):

δ : 14.9 (s, 1P, PCH_3); 31.9 (s, 1P, PCH_3).

3.6.20 [2-[(imino-κN)phenylmethyl]-1,1-dimethylethy-κC](carbonyl)bis (trimethylphosphine)cobalt(I) (20)

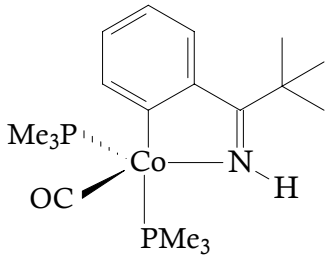

Procedure: E

A sample of **16** (910 mg, 2.04 mmol) in pentane were stirred under 1 bar CO to provide 632 mg of product mixture containing a few red crystals of **20** and orange crystals of **21**. They crystallize together at –27 °C and separation remained incomplete.

Yield: 67% (mixture of **20** and **21**)

Melting point of 20: 129 °C – 131 °C

Elemental analysis of 20: $C_{18}H_{32}CoNOP_2$, M_w= 399.34 g/mol.

%	C	H	N
Calculated	54.14	8.08	3.51
Found	54.73	8.01	3.53

IR (Nujol, 4000 - 400 cm^{-1}):

$\tilde{\nu}$ = 3362 vw (ν H–N=C); 3071 vw , 3037 vw (ν H–C=C); 1893 vs (ν C≡O); 1584 m (ν C=C); 1565 m (ν C=N); 1420 w (δ_{as} PCH_3); 1407 w; 1356 vw; 1304 vw, 1285 w, 1277 w (δ_s PCH_3); 1256 vw; 1197 vw; 1157 vw; 1115 vw; 1009 w; 941 vs (ρ_1 PCH_3); 851 w (ρ_2 PCH_3); 817 vw; 796 w; 766 w (γ C–H_{arom}); 731 vw, 713 s (ν_{as} PC_3); 674 m, 665 m (ν_s PC_3); 628 vw; 579 vw; 564 vw; 544 vw; 505 vw; 468 w.

3.6.21 2-[(imino-κN)phenylmethyl]-1,1-dimethylethy-κC]dicarbonyl (trimethylphosphine)cobalt(I) (21)

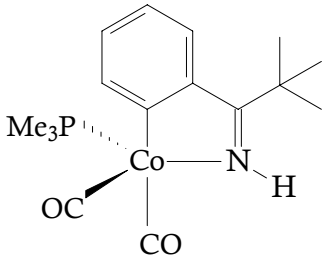

Melting point: 135 °C – 137 °C (decomposition)

Elemental analysis: $C_{16}H_{23}CNO_2P$, M_w = 351.27 g/mol.

%	C	H	P
Calculated	54.71	6.60	8.82
Found	50.23	5.76	8.15

IR (Nujol, 4000 - 400 cm^{-1}):

$\tilde{\nu}$ = 3347 w (ν H–N=C); 3069 vw (ν H–C=C); 1945 vs (ν C≡O); 1896 vs (ν CO); 1572 m (ν C=C); 1517 w (ν C=N); 1419 m (δ_{as} PCH_3); 1307 vw, 1288 m (δ_s PCH_3); 1258 w; 1244 vw; 1192 m; 1158 m; 1118 w; 1043 w; 1016 m; 950 vs (ρ_1 PCH_3); 850 w (ρ_2 PCH_3); 831 w; 817 vw; 777 m (γ C–H_{arom}); 738 vs (ν_{as} PC_3), 677 m (ν_s PC_3); 655 vw; 571 m; 540 s; 510 m; 489 m.

^{1}H NMR (500 MHz, [D_8]THF, 300 K, ppm):

δ = 1.49 (s, 9H, $C(CH_3)_3$); 1.53 (d, $^2J_{P,H}$ = 8.7 Hz, 9H, PCH_3); 6.93 (dt, $^4J_{H,H}$ = 1.4 Hz, $^3J_{H,H}$ = 7.9 Hz, 1H, Ar–H); 6.98 (tt, $^4J_{H,H}$ = 1.1 Hz, $^3J_{H,H}$ = 7.1 Hz, 1H, Ar–H); 7.93 (td, $^4J_{H,H}$ = 1.5 Hz, $^3J_{H,H}$ = 7.8 Hz, 1H, Ar–H); 7.98 (ddd, $^4J_{H,H}$ = 1.2 Hz, $^3J_{H,H}$ = 3.8 Hz, $^3J_{H,H}$ = 7.5 Hz, 1H, Ar–H); 9.10 (s_{br}, 1H, N–H).

^{13}C NMR (125 MHz, [D_8]THF, 300 K, ppm):

δ = 18.6 (d, $^1J_{P,C}$ = 25.3 Hz, PCH_3); 20.2 (s, C<u>C</u>H_3); 40.4 (s, <u>C</u>CH_3); 120.9 (s, CH); 126.6 (s, CH); 129.8 (d, $^3J_{P,C}$ = 2.4 Hz, CH); 142.9 (d, $^3J_{P,C}$ = 2.3 Hz, CH); 143.8 (s, C); 184.1 (m, C=N); 188.4 (d, $^2J_{P,C}$ = 8.3 Hz, Co-C), 204.4 (m, Co–CO), 228.2 (m, Co–CO).

^{31}P NMR (202 MHz, [D_8]THF, 300 K, ppm):

δ = 21.7 (s_{br}, PCH_3).

3.6.22 Dimethylbis(trimethylphosphine)bis[μ-(α-phenylbenzenemethaniminato)nickel(II)] (22)

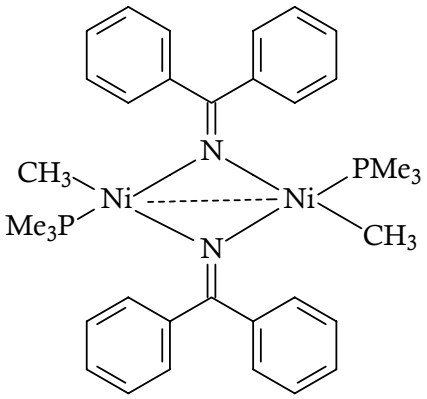

Procedure: C

1.05 g (3.31 mmol) of $Ni(CH_3)_2(PMe_3)_3$ in ether were combined with 0.60 g (3.31 mmol) of diphenylketimine to afford 1.48 g of red crystals of ***22*** which crystallize from pentane at 4 °C.

Yield: 68%

Melting point: 107°C – 109 °C (decomposition)

Elemental analysis: $C_{34}H_{44}N_2NiP_2$, M_w: 660.06 g/mol

%	C	H	N	P
Calculated	61.87	6.72	4.24	9.39
Found	62.40	6.76	4.20	9.46

IR (Nujol, 4000 - 400 cm^{-1}):

$\tilde{\nu}$ = 3097 vw, 3061 vw, 3018 vw (ν H–C=C); 2252 w (νC–H–Ni); 1612 vs, 1599 m (ν C=C); 1572 m (ν C=N); 1485 m; 1440 m, 1420 w (δ_{as} PCH_3); 1299 m, 1279 s (δ_s PCH_3); 1257 m; 1174 vw; 1153 w; 1138 m (δ Ni–CH_3); 1070 w; 1028 w; 969 m, 949 vs (ρ_1 PCH_3); 897 w; 848 m (ρ_2 PCH_3); 791 m, 770 m (γ C–H_{arom}); 729 vs, 700 vs (ν_{as} PC_3); 647 m (ν_s PC_3); 624 vw; 607 vw; 539 vw; 525 vw; 488 vw; 461 vw; 421 vw.

^{1}H NMR (500 MHz, [D_8]THF, 300 K, ppm):

δ = - 5.7 (s, 1H, Ni-H); -4.3 (s, 2H, Ni-H); -2.9 (s, 1H, Ni-H); -1.52 (dd, $^{3}J_{P,H}$ = 5.4 Hz, $^{3}J_{P,H}$ = 51.1 Hz, Ni–CH_3); -0.9 (d, $^{3}J_{P,H}$ = 8.9 Hz, 1H, Ni–CH_3); 0.77 (d, $^{2}J_{P,H}$ = 9.3 Hz, 9H, PCH_3); 0.89 (d, $^{2}J_{P,H}$ = 9H, PCH_3); 1.00 (d, $^{2}J_{P,H}$ = 9.1 Hz, 9H, PCH_3); 1.04 (d, $^{2}J_{P,H}$ = 8.2 Hz, 9H, PCH_3); 1.09 (d, $^{2}J_{P,H}$ = 5.8 Hz, 9H; PCH_3); 1.15 (s, 9H, PCH_3); 1.21 (d, $^{2}J_{P,H}$ = 8.3 Hz, 9H, PCH_3); 7.16–8.53 (m, 10H, Ar–H); 10.11 (s_{br}, 1H, N–H).

^{13}C NMR (125 MHz, [D_8]THF, 300 K, ppm):

δ = 13.7 (t, $^{1}J_{P,C}$ = 28.0 Hz, PCH_3); 14.5 (d, $^{1}J_{P,C}$= 26.2 Hz, PCH_3); 17.9–18.8 (m, PCH_3); 127.5 (s, C); 128. 0 (s, CH); 128.1 (s, CH); 128.6 (s, CH); 128.7 (s, CH); 128.9 (s, CH); 129.4 (s, CH); 129.5 (s, CH); 129.6 (s, CH); 130.2 (s, CH); 130.5 (s, CH); 131.2 (s, CH); 140.1 (s, C); 142.2 (s, C); 177.5 (s, C=N); 177.7 (s, C=N).

^{31}P NMR (202 MHz, [D_8]THF, 300 K, ppm):

δ = - 23.5 (s , PCH_3); -9.4 (s, PCH_3); -8.4 (s, PCH_3); -7.9 (s, PCH_3)

3.6.23 Methyl[(α-phenylbenzenemethanimine)κN]bis - (trimethylphosphan)nickel(II)chloride (23)

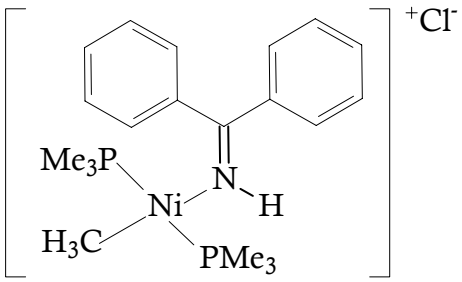

Procedure: C

730 mg (2.79 mmol) of $NiClCH_3(PMe_3)_2$ in ether were combined with 506 mg (2.79 mmol) of diphenylketimine to afford 889 mg of yellow crystals (**23**) which crystallize from pentane at 4 °C.

Yield: 72%

Melting point: 76 °C – 78 °C

Elemental analysis: $C_{20}H_{32}ClNNiP_2$, M_w: 442.57 g/mol

%	C	H	N	P
Calculated	54.28	7.29	3.16	14.00
Found	54.02	7.15	2.97	13.31

IR (Nujol, 4000 - 400 cm^{-1}):

$\tilde{\nu}$ = 3194 vw, 3159 vw, 3133 vw (ν H–C=C); 1596 m (ν C=C); 1567 m (ν C=N); 1420 m (δ_{as} PCH_3); 1300 m, 1283 s (δ_s PCH_3); 1236 s; 1167 m; 1155 s (δ Ni–CH_3); 1076 vw; 1031 vw; 998 vw; 945 vs (ρ_1 PCH_3); 850 m (ρ_2 PCH_3); 795 s, 772 m (γ C–H_{arom}); 726 s, 703 s (ν_{as} PC_3); 672 m (ν_s PC_3); 649 m; 620 vw; 594 m; 527 vw; 502 vw; 451 vw; 433 vw.

^{1}H NMR (500 MHz, [D_8]THF, 300 K, ppm):

δ = 0.81 (s, 3H, Ni–CH_3); 1.23 (s, 18H, PCH_3); 7.35–7.43 (m, 8H, Ar– H); 7.74 (s_{br}, 2H, Ar–H); 10.12 (s_{br}, 1H, N–H).

^{13}C NMR (125 MHz, [D_8]THF, 300 K, ppm):

δ = -16.5 (s, Ni–CH_3); 13.1 (s, PCH_3); 128.7 (d, $^5J_{P,C}$ = 38.9 Hz, CH); 129.5 (s, CH); 130.4 (d, $^6J_{P,C}$ = 34.9 Hz, CH); 131.2 (s, CH); 140.1 (s, C); 177.6 (s, CN).

^{31}P NMR (202 MHz, [D_8]THF, 300 K, ppm):

δ = - 16.6 (s, PCH_3).

3.6.24 [2-(Benzoyl-κO)phenyl-κC]tris(trimethylphosphine)cobalt(I) (24)

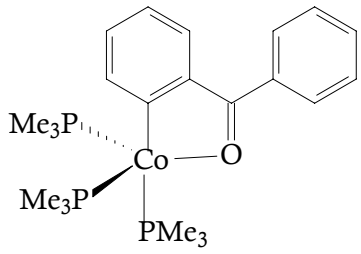

Procedure: C

920 mg (2.43 mmol) of $CoCH_3(PMe_3)_4$ in THF were combined with 443 mg (2.43 mmol) of benzophenone to afford 924 mg of brown crystals of **24** which crystallize at 4 °C.

Yield: 81%

Melting point: 111 °C – 113 °C (decomposition)

Elemental analysis: $C_{22}H_{36}CoOP_3$, M_w: 468.83g/mol.

%	C	H	P
Calculated	56.42	7.75	19.84
Found	56.95	7.53	20.68

IR (Nujol, 4000 – 400 cm^{-1}):

$\tilde{\nu}$ = 3057 w (ν H–C=C); 1582 m (ν C=C); 1484 m (ν C=O); 1422 w ($\delta_{as}PCH_3$); 1352 m; 1295 w, 1273 m ($\delta_s PCH_3$); 1156 w; 1075 vw; 1022 vw; 999 vw; 954 s, 935 vs (ρ_1 PCH_3); 842 m ($\rho_2 PCH_3$); 771 m, 753 vw (γ C–H_{arom}); 718 s, 701 m ($\nu_{as} PC_3$); 661 vs ($\nu_s PC_3$); 633 w; 587 vw.

^{1}H NMR (500 MHz, [D_8]THF, 300 K, ppm):

δ = 1.30 (d, $^2J_{P,H}$ = 6.5 Hz, 27H, PCH_3); 6.61 (dt, $^4J_{H,H}$ = 0.8 Hz, $^3J_{H,H}$ = 7.8 Hz, 1H, Ar–H); 7.12 (t, $^3J_{H,H}$ = 7.8 Hz, 2H, Ar–H); 7.33 (tt, $^4J_{H,H}$ = 1.2 Hz, $^3J_{H,H}$ = 8.0 Hz, 1H, Ar–H); 7.46 (dt, $^4J_{H,H}$ = 0.9 Hz, $^3J_{H,H}$ = 7.4 Hz, 1H, Ar–H); 8.11 (d, $^3J_{H,H}$ = 8.1

Hz, 2H, Ar–H); 8.19 (d_{br}, $^{3}J_{H,H}$ = 8.1 Hz, 1H, Ar–H); 8.22 (d, $^{3}J_{H,H}$ = 8.2 Hz, 1H, Ar–H).

^{13}C NMR (125 MHz, [D_8]THF, 300 K, ppm):
δ = 21.3 (m, PCH_3); 118.3 (q, $^{4}J_{P,C}$ = 4.6 Hz, CH); 121.9 (s, CH); 122.6 (s, CH); 123.7 (d, $^{5}J_{P,C}$= 2.4 Hz, CH); 124.2 (dd, $^{4}J_{P,C}$ = 3.4 Hz, $^{4}J_{P,C}$ = 2.2 Hz, CH); 130.4 (s, CH); 145.2 (q, $^{4}J_{P,C}$ = 4.6 Hz, C); 146.2 (s, C); 147.8 (q, $^{5}J_{P,C}$ = 2.2 Hz, CH); 170.8 (q, $^{3}J_{P,C}$ = 11.8 Hz; C=O), 173.9 (m, Co–C).

^{31}P NMR (202 MHz, [D_8]THF, 300 K, ppm):
δ = 5.1 (s_{br}, PCH_3).

3.6.25 [2-(Benzoyl-κO)benzyl-κC]tris(trimethylphosphine)cobalt(I) (25)

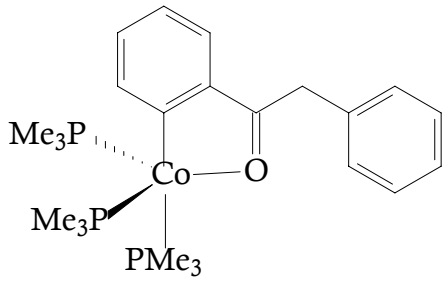

Procedure: C
1.15 g (3.04 mmol) of $CoCH_3(PMe_3)_4$ in THF were combined with 0.60 g (3.04 mmol) of benzylphenylketone to afford 0.97 g of brown crystals (**24**) which crystallize from pentane at -27 °C.

Yield: 66%

Melting point: 107 °C – 109 °C (decomposition)

Elemental analysis: $C_{23}H_{38}CoOP_3$, M_w: 482.41g/mol

%	C	H	P
Calculated	57.27	7.94	19.26
Found	56.49	7.39	19.53

IR (Nujol, 4000 – 400 cm^{-1}):

$\tilde{\nu}$ = 3048 m, 3023 m (ν H–C=C); 1580 s, 1570 s, 1547 s (ν C=C); 1483 m (ν C=O); 1446 s; 1421 s ($\delta_{as}PCH_3$); 1296 m, 1278 m ($\delta_s PCH_3$); 1236 w; 1206 w; 1169 s; 1084 s; 1069 s; 1027 w; 995 w; 959 s, 937 vs ($\rho_1 PCH_3$); 874 m ($\rho_2 PCH_3$); 843 vw; 797 m; 770 s; 748 (γ C–H_{arom}); 712 s, 698 vs ($\nu_{as} PC_3$); 657 vs ($\nu_s PC_3$); 619 vw; 594 vw; 577 w, 519 m; 502 m.

^{1}H NMR (500 MHz, [D_8]THF, 300 K, ppm):

δ = 1.05 (s_{br}, 27H, PCH_3); 4.20 (s, 2H, CH_2); 7.25–7.55 (m, 6H, Ar–H); 8.03 (m, 1H, Ar–H); 8.95 (m, 1H, Ar–H); 9.19 (m, 1H, Ar–H).

^{13}C NMR (125 MHz, [D_8]THF, 300 K, ppm):

δ = 20.9 (m, PCH_3); 46.1 (s, CH_2); 127.5 (s, CH); 129.4 (s, CH); 129.6 (d, $^3J_{P,C}$= 8.2 Hz, CH); 130.6 (s, CH); 133.8 (s, CH); 136.5 (s, CH); 138.2 (s, C); 151.2 (m, C); 158.4 (s, CH); 166.1 (s, Co–C=O); 183.7 (m, Co–C).

^{31}P NMR (202 MHz, [D_8]THF, 300 K, ppm):

δ = 1.5 (s_{br}, 3P, PCH_3).

3.6.26 Iodo(methyl)[2-(Benzoyl-κO)phenyl-κC]tris-(trimethylphosphine)cobalt(III) (26)

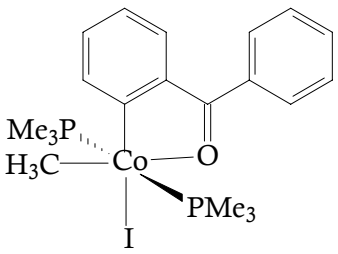

Procedure: D

540 mg (1.15 mmol) of **24** in pentane were combined with 327 mg (1.44 ml, 2.30 mmol) of CH_3I to afford 431 mg of dark orange crystals (**26**) which crystallize at 4 °C.

Yield: 67 %

Melting point: 133 °C – 135 °C

Elemental analysis: $C_{20}H_{30}CoIOP_2$, M_w: 534.24g/mol.

%	C	H	P
Calculated	44.96	5.66	11.60
Found	44.77	5.80	11.66

IR (Nujol, 4000 - 400cm^{-1}):

$\tilde{\nu}$ = 3058 vw, 3034 vw (ν H–C=C); 1587 w, 1569 m (ν C=C); 1547 m (ν C=O); 1524 vw; 1510 vw; 1418 w (δ_{as} PCH_3); 1345 vw; 1327 m; 1298 vw, 1270 m (δ_s PCH_3); 1243 vw; 1158 w (δs Co–CH_3); 1118 w; 1073 vw; 1016 vw; 958 vw; 947 vs (ρ_1 PCH_3); 852 m (ρ_2 PCH_3); 812 w; 773 w; 742 m, 720 m (γ C–H_{arom}); 706 m (ν_{as} PC_3); 664 m (ν_s PC_3); 643 m.

^{1}H NMR (500 MHz, [D_8]THF, 300 K, ppm):

δ = 0.21 (t, $^3J_{P,H}$ = 9.4 Hz, 3H, Co–CH_3); 1.11 (t', $|^2J_{P,H} + {}^4J_{P,H}|$ = 7.8 Hz, 18H, PCH_3); 6.97 (tt, $^3J_{H,H}$ = 7.8 Hz, $^4J_{H,H}$ = 0.9 Hz, 1H, Ar–H); 7.21 (dt, $^3J_{H,H}$ = 7.0 Hz, $^4J_{H,H}$ = 1.5 Hz, 1H, Ar–H); 7.39 (td, $^3J_{H,H}$ = 7.3 Hz, $^4J_{H,H}$ = 3 Hz, 1H, Ar–H); 7.53 (tt, $^3J_{H,H}$ = 7.8 Hz, $^4J_{H,H}$ = 1.5 Hz, 2H, Ar–H); 7.59 (tt, $^3J_{H,H}$ = 7.3 Hz, $^4J_{H,H}$ = 1.3 Hz, 1H, Ar–H); 7.75 – 7.82 (m, 3H, Ar–H).

^{13}C NMR (125 MHz, [D_8]THF, 300 K, ppm):

δ = -10.1 (m, Co–CH_3); 14.6 (t', $|^1J_{P,C} + {}^3J_{P,C}|$ = 27.6 Hz, PCH_3); 122.2 (s, CH); 129.7 (s, CH); 130.2 (s, CH); 131.6 (t, $^4J_{P,C}$= 2.2 Hz, CH); 132.9 (s, CH); 133.5 (d

$^4J_{P,C}$ = 2.5 Hz, CH); 138.1 (s, C); 139.1 (s, C); 144.0 (s, CH); 171.8 (m, C=O); 188.6 (m, Co–C).

^{31}P NMR (202 MHz, [D_8]THF, 300 K, ppm):
δ = 2.03 (s_{br}, PCH_3).

3.6.27 (η^2(κC-κO)-Benzophenone)bis(trimethylphosphine)nickel(0) (27)

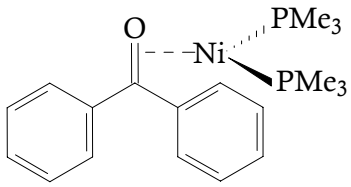

Procedure: C
1.64 g (5.17 mmol) of $Ni(CH_3)_2(PMe_3)_3$ in ether were combined with 0.94 g (5.17 mmol) of benzophenone to afford 0.85 g of red crystals of **27** which crystallize from pentane at 4 °C.

Yield: 42%

Melting point: 78 °C – 80 °C

Elemental analysis: $C_{13}H_{28}NiOP_2$, M_w: 393.07g/mol.

%	C	H	P
Calculated	58.06	7.18	15.76
Found	57.70	7.20	15.74

IR (Nujol, 4000 – 400 cm^{-1}):
$\tilde{\nu}$ = 3075 vw, 3051 w, 3021 w (ν H–C=C); 1666 w; 1591 s, 1572 m (ν C=C); 1485 s (ν C=O); 1422 m (δ_{as} PCH_3); 1320 w; 1298 w, 1280 s (δ_s PCH_3); 1252 m; 1174 w; 1122 vw; 1074 m; 1028 m; 942 vs (ρ_1 PCH_3); 900 w; 861 w; 841 m (ρ_2 PCH_3); 774

m, 761 m (γ C–H_{arom}); 722 vs, 699 vs (ν_{as} PC_3); 669 m, 645 s (ν_s PC_3); 622 vs; 522 vw; 479 vw.

^{1}H NMR (500 MHz, [D_8]THF, 300 K, ppm):
δ = 0.86 (d, $^3J_{P,H}$ = 5.6 Hz, 9H, PCH_3); 1.31 (d, $^3J_{P,H}$ = 6.2 Hz, 9H, PCH_3); 7.03 (t, $^3J_{H,H}$ = 7.2 Hz, 2H, Ar–H); 7.07 (t, $^4J_{H,H}$ = 1.4 Hz, 1H, Ar–H); 7.09 (m, 2H, Ar–H); 7.10 (t, $^4J_{H,H}$ = 1.6 Hz, 1H, Ar–H); 7.70 (m, 4H, Ar–H).

^{13}C NMR (125 MHz, [D_8]THF, 300 K, ppm):
δ = 14.7 (d, $^1J_{P,C}$ = 18.2 Hz, PCH_3); 15.2 (d, $^1J_{P,C}$ = 23.3 Hz, PCH_3); 122.5 (s, CH); 125.4 (s, CH); 126.1 (s, CH); 127.1 (s, CH); 128.7 (s, CH); 131.1 (s, C); 147.1 (s, C=O).

^{31}P NMR (202 MHz, [D_8]THF, 300 K, ppm):
δ = -11.9 (d, $^2J_{P,P}$ = 62.7 Hz, 1P, PCH_3); -14.5 (d, $^2J_{P,P}$ = 62.7 Hz, 1P, PCH_3).

3.6.28 [2-(3,4,5,6-Tetrafluoro-benzoyl-κO)phenyl-κC]tris-(trimethylphosphine)cobalt(I) (28)

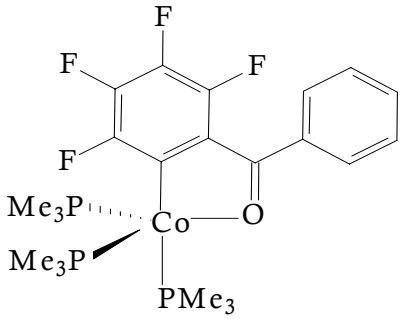

Procedure: B
1.20 g (3.17 mmol) of $CoCH_3(PMe_3)_4$ in THF were combined with 0.86 g (3.17 mmol) of 2,3,4,5,6-pentafluorobenzophenone to afford 1.08 g of brown crystals (**28**) which crystallize from pentane at -27 °C.

Yield: 63%

Melting point: 152 °C – 154 °C (decomposition)

Elemental analysis: $C_{22}H_{32}CoF_4OP_3$, M_w: 540.34 g/mol

%	C	H	P
Calculated	48.90	5.97	17.20
Found	48.58	5.70	16.88

IR (Nujol, 4000 – 400 cm^{-1}):

$\tilde{\nu}$ = 3077 vw (ν H–C=C); 1617 m (ν C=C); 1590 m (ν C=C); 1490 m (ν C=O); 1420 w (δ_{as} PCH_3); 1339 s (ν F–C=C) of ; 1298 w, 1277 s (δ_s PCH_3); 1102 vw; 1068 vw; 1037 w; 1025; 996 vw; 979 m; 939 vs (ρ_1 PCH_3); 830 m (ρ_2 PCH_3); 771 m, 760 m (γ C–H_{arom}); 715 m, 701 m (ν_{as} PC_3); 665 m (ν_s PC_3); 562 w.

^{1}H NMR (500 MHz, [D_8]THF, 300 K, ppm):

δ = 1.32 (d, $^2J_{P,H}$ = 6.1 Hz, 27H, PCH_3); 7.09 (t, $^3J_{H,H}$ = 7.2 Hz, 2H, Ar–H); 7.48 (t, $^3J_{H,H}$ = 7.0 Hz, 1H, Ar–H); 7.81 (t, $^3J_{H,H}$ = 6.5 Hz, 2H, Ar–H).

^{13}C NMR (125 MHz, [D_8]THF, 300 K, ppm):

δ = 20.5 (d, $^1J_{P,C}$ = 20.5 Hz, PCH_3); 124.0 (s, CH); 124.3 (s, CH); 128.5 (m, CF); 128.8 (m, CF); 129.1 (s, CH); 129.4 (m, CF); 134.5 (m, CF); 141.5 (m, C); 147.4 (s, C); 167.9 (s, C=O); 168.7 (m, Co–C).

^{31}P NMR (202 MHz, [D_8]THF, 300 K, ppm):

δ = 3.6 (s_{br} , PCH_3).

3.6.29 [2-[(8-naphthyl-κC)imino-κN)methyl]phenyl-κC]tris-(trimethylphosphine)iron(II) (29)

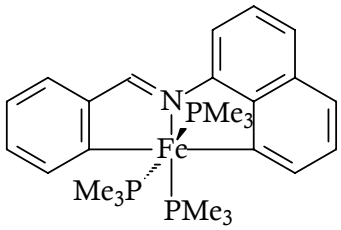

Procedure: A

950 mg (2.43 mmol) of $Fe(CH_3)_2(PMe_3)_4$ in pentane were combined with 563 mg (2.43 mmol) of N-benzylidene-1-naphthylamine to afford 899 mg of green crystals (**29**) which crystallize at 4 °C.

Yield: 72%

Melting point: 120 °C – 122 °C (decomposition)

Elemental analysis: $C_{26}H_{38}FeNP_3$, M_w: 513.36g/mol.

%	C	H	N	P
Calculated	60.83	7.46	2.73	18.10
Found	60.38	6.68	2.73	18.79

IR (Nujol, 4000 - 400 cm^{-1}):

$\tilde{\nu}$ = 3061 vw, 3040 vw, 3031 vw (ν H–C=C); 1597 w, 1573 w (ν C=C); 1537 s, 1509 s (ν C=N); 1423 vw ($\delta_{as}PCH_3$); 1404 w; 1354 vw; 1298 m, 1275 m ($\delta_s PCH_3$); 1242 vw; 1211 w; 1153 w; 1104 vw; 1078 vw; 1023 vw; 941 vs ($\rho_1 PCH_3$); 903 vw; 849 m ($\rho_2 PCH_3$); 812 m; 766 s, 747 m (γ C–H_{arom}); 719 s ($\nu_{as} PC_3$); 687 w; 666 w ($\nu_s PC_3$); 602 vw, 524 vw (ν Fe–C); 456 vw.

^{1}H NMR (500 MHz, [D_8]THF, 300 K, ppm):

δ = 0.51 (t', $|^{2}J_{P,H} + {}^{4}J_{P,H}|$ = 5.4 Hz, 18H, PCH_3); 1.64 (d, $^{2}J_{P,H}$ = 5.9 Hz, 9H, PCH_3); 6.85 (t, $^{3}J_{H,H}$ = 7.0 Hz, 1H, Ar–H); 6.93 (t, $^{3}J_{H,H}$ = 7.6 Hz, 1H, Ar–H); 6.95 (t, $^{3}J_{H,H}$ = 7.4 Hz, 1H, Ar–H); 7.06 (d, $^{3}J_{H,H}$ = 7.8 Hz, 1H, Ar–H); 7.15 (t, $^{3}J_{H,H}$ = 7.7 Hz, 1H, Ar–H); 7.44 (d, $^{3}J_{H,H}$ = 7.9 Hz, 1H, Ar–H); 7.65 (d, $^{3}J_{H,H}$ = 7.4 Hz, 1H, Ar–H); 7.71 (d, $^{3}J_{H,H}$ = 7.4 Hz, 1H, Ar–H); 7.89 (d, $^{3}J_{H,H}$ = 6.4 Hz, 1H, Ar–H); 8.22 (d, $^{3}J_{H,H}$ = 7.4 Hz, 1H, Ar–H); 9.36 (s, 1H, H–C=N).

^{13}C NMR (125 MHz, [D_8]THF, 300 K, ppm):

δ = 17.1 (t', $|^{1}J_{P,C} + {}^{3}J_{P,C}|$ = 20.6 Hz, PCH_3); 23.9 (td, $^{1}J_{P,C}$ = 16.1 Hz, $^{3}J_{P,C}$ = 2.2 Hz, PCH_3); 106.9 (s, CH); 117.5 (d, $^{4}J_{P,C}$ = 2.2 Hz, CH); 120.4 (s, CH); 124.9 (s, CH); 125.9 (t, $^{4}J_{P,C}$ = 2.9 Hz, CH); 126.0 (s, CH); 126.9 (s, CH); 130.6 (s, CH); 135.5 (d, $^{4}J_{P,C}$ = 2.6 Hz, C); 141.4 (s, CH); 146.2 (d, $^{4}J_{P,C}$ = 2.4 Hz, CH); 148.3 (m, C); 151.6 (s, C); 154.7 (d, $^{3}J_{P,C}$ = 5.9 Hz, C); 161.6 (t, $^{4}J_{P,C}$ = 3.5 Hz, C=N); 194.3 (dt, $^{2}J_{P,C}$ = 24.0 Hz, $^{2}J_{P,C}$ = 11.0 Hz, Fe–C); 212.1 (dq, $^{2}J_{P,C}$ = 19.5 Hz, $^{2}J_{P,C}$ = 5.7 Hz, Fe–C).

^{31}P NMR (202 MHz, [D_8]THF, 300 K, ppm):

δ = 16.8 (dd, $^{2}J_{P,P}$ = 59.9 Hz, $^{2}J_{P,P}$ = 63.2 Hz 2P, PCH_3); 22.9 (t, $^{2}J_{P,P}$ = 59.9Hz, $^{2}J_{P,P}$ = 63.2 Hz 1P, PCH_3) of ppm.

3.6.30 (η^4-κN,κC,κC,κC)-[N-(1-(2-methyl-naphthyl)methylene)-aniline]tris-(trimethylphosphine)iron(0) (30)

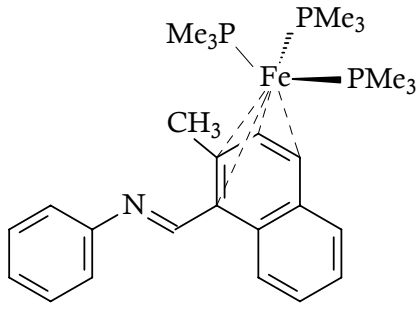

Procedure: A

560 mg (1.43 mmol) of $Fe(CH_3)_2(PMe_3)_4$ in pentane were combined with 332 mg (1.43 mmol) of N-(1-naphthylmethylene)aniline to afford 463 mg of brown crystals (**30**) which crystallize at 4 °C.

Yield: 81%

Melting point: 104 °C – 106 °C (decomposition)

Elemental analysis: $C_{27}H_{42}FeNP_3$, M_w: 529.41g/mol

%	C	H	N	P
Calculated	61.26	8.00	2.65	17.55
Found	62.11	6.45	2.78	16.89

IR (Nujol, 4000 - 400 cm^{-1}):

$\tilde{\nu}$ = 3049 vw, 3030 vw (ν H–C=C); 1603 m (ν H–C=N); 1567 vs (ν C=C); 1483 s; 1451 s (δ_{as} PCH_3); 1352 m; 1296 m, 1277 m (δ_s PCH_3); 1257 w; 1236 vw; 1215 vw; 1195 vw; 1166 w; 1148 w; 1132 vw; 1092 vw; 1074 vw; 1034 vw; 1023 w; 993 vw; 952 s, 937 vs (ρ_1 PCH_3); 849 w; 850 m (ρ_2 PCH_3); 766 m, 743 s (γ C–H_{arom}); 705 s, 694 s (ν_{as} PC_3); 658 s (ν_s PC_3); 619 m; 585 vw; 552 vw; 543 vw; 519 vw; 508 vw; 447 m.

3.6.31 [2-[((2-Benzyl-κC)imino-κN)methyl]phenyl-κC]tris-(trimethylphosphine)iron(II) (31)

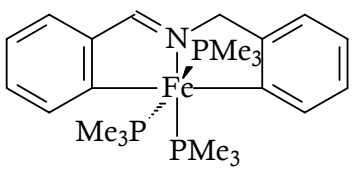

Procedure: A

1.33 g (3.41 mmol) of $Fe(CH_3)_2(PMe_3)_4$ in pentane were combined with 0.67 g (3.41 mmol) of N-benzylbenzylideneimine to afford 1.28 g of redish brown crystals (**31**) which crystallize at 4 °C.

Yield: 79 %

Melting point: 107 °C – 109 °C (decomposition)

Elemental analysis: $C_{23}H_{38}FeNP_3$, M_w: 477.33g/mol.

%	C	H	N	P
Calculated	57.87	8.02	2.93	19.47
Found	57.84	7.82	2.97	19.46

IR (Nujol, 4000 – 400 cm^{-1}):

$\tilde{\nu}$ = 3091 vw, 3072 vw, 3061 vw, 3046 w, 3027 w (ν H–C=C); 1586 w, 1568 m (ν C=C); 1527 w (ν C=N); 1437 m (δ_{as} PCH_3);1415 w; 1296 m, 1277 m (δ_s PCH_3); 1237 vw; 1204 vw; 1151 vw; 1107 vw; 1053 vw; 999 w; 987 w; 941 vs (ρ_1 PCH_3); 853 m (ρ_2 PCH_3); 806 w; 754 w, 741 m (γ C–H_{arom}); 723 s, 714 m, 692 w (ν_{as} PC_3); 687 w; 660 w (ν_s PC_3); 635 w; 536 vw; 497 vw; 461 w; 436 vw; 412 m.

^{1}H NMR (500 MHz, [D_8]THF, 300 K, ppm):

δ = 0.70 (s, 18H, PCH_3); 1.58 (d, $^2J_{P,H}$ = 4.3 Hz, 9H, PCH_3); 5.04 (s, 2H, N–CH_2); 6.85 (t, $^3J_{H,H}$ = 7.0 Hz, 1H, Ar–H); 6.93 (t, $^3J_{H,H}$ = 7.6 Hz, 1H, Ar–H); 6.61–6.83 (m, 5H, Ar–H); 7.34 (d, $^3J_{H,H}$ = 6.8 Hz, 1H, Ar–H); 7.61 (m, 1H, Ar–H); 8.00 (d, $^3J_{H,H}$ = 7.4 Hz, 1H, Ar–H); 8.52 (s, 1H, H–C=N).

^{13}C NMR (125 MHz, [D_8]THF, 300 K, ppm):

δ = 17.83 (dt', $|^1J_{P,C} + {}^3J_{P,C}|$ = 19.4 Hz, $^3J_{P,C}$ = 1.95 Hz, PCH_3); 24.1 (td, $^1J_{P,C}$ = 14.9 Hz, $^3J_{P,C}$ = 2.1 Hz, PCH_3); 66.6 (s, CH_2); 118.4 (s, CH); 119.6 (s, CH); 120.5 (t, $^5J_{P,C}$

= 2.0 Hz, CH); 124.3 (t, $^{5}J_{P,C}$ = 2.2 Hz, CH); 126.4 (s, CH); 127.2 (s, CH); 144.5 (s, CH); 146.4 (s, CH); 152.9 (m, C); 155.3 (d, $^{4}J_{P,C}$ = 5.1 Hz, C); 170.5 (t, $^{4}J_{P,C}$ = 4.5 Hz, H–C=N); 184.8 (m, Fe–C); 204.8 (q, $^{2}J_{P,C}$ = 9.2 Hz, Fe–C).

^{31}P NMR (202 MHz, [D_8]THF, 300 K, ppm):
δ = 16.1 (dd, $^{2}J_{P,P}$ = 60.0 Hz, $^{2}J_{P,P}$ = 63.0 Hz 2P, PCH_3); 20.5 (dd, $^{2}J_{P,P}$ = 60.0 Hz, $^{2}J_{P,P}$ = 63.0 Hz, 1P, PCH_3).

3.6.32 Iodo[2-[(2-Benzyl-κC)imino-κN)methyl]phenyl-κC]bis-(trimethylphosphine)iron(III) (32)

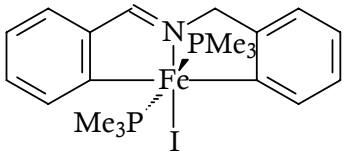

Procedure: D
605 mg (1.27 mmol) of **31** in pentane were combined with 359 mg (1.58 ml, 2.54 mmol) of CH_3I to afford 355 mg of green crystals (**32**) which crystallize at 4 °C.

Yield: 53%

Melting point: 144 °C – 148 °C (decomposition)

Elemental analysis: $C_{20}H_{29}FeINP_2$, M_w: 528.16 g/mol.

%	C	H	N	P
Calculated	45.48	5.53	2.65	11.73
Found	45.21	5.65	2.57	11.67

IR (Nujol, 4000 – 400 cm^{-1}):
$\tilde{\nu}$ = 3044 vw, 3018 vw (ν H–C=C); 1585 m, 1574 m (ν C=C); 1530 w (ν C=N); 1419 w (δ_{as} PCH_3); 1318 vw; 1295 w, 1277 m (δ_s PCH_3); 1242 vw; 1212 vw; 1154 vw;

1109 vw; 1053 vw; 1016 vw; 945 vs (ρ_1 PCH_3); 851 w (ρ_2 PCH_3); 750 m (γ C–H_{arom}); 729 s (ν_{as} PC_3); 687 w; 669 m (ν_s PC_3); 640 vw; 499 vw.

^{1}H NMR (500 MHz, [D_8]THF, 300 K, ppm):
δ = 0.93 (t', $|^2J_{P,C} + {}^4J_{P,C}|$ = 14.3 Hz, 18H, PCH_3); 4.81 (m, 2H, N–CH_2); 12.94 (m, 4H, Ar–H); 13.43 (m, 4H, Ar–H); 18.2 (m, 1H, H–C=N).

^{13}C NMR (125 MHz, [D_8]THF, 300 K, ppm):
δ = 11.9 (s, PCH_3); 32.7 (s, N–CH_2); 102.2 (s, CH); 118.7 (s, CH); 123.3 (s, CH); 148.7 (s, CH); 168.7 (s, C); 173.7 (s, H–C=N); 189.8 (s, Fe–C).

^{31}P NMR (202 MHz, [D_8]THF, 300 K, ppm):
δ = 2.5 (s_{br}, 2P, PCH_3).

3.6.33 [2-[((8-naphthyl-κC)imino-κN)methyl]phenyl-κC](carbonyl)bis-(trimethylphosphine)iron(II) (33)

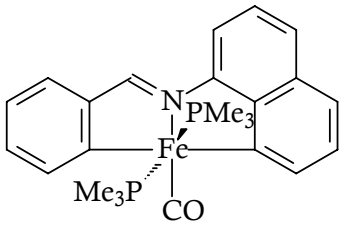

Procedure: E
A sample of **29** (580 mg, 1.13 mmol) in pentane was stirred under 1 bar CO to provide 321 mg of green crystals (**33**) which crystallize at –27 °C.

Yield: 61%

Melting point: 184 °C – 186 °C

Elemental analysis: $C_{24}H_{29}FeNOP_2$, M_w: 465.29g/mol.

%	C	H	N	P
Calculated	61.95	6.28	3.01	13.31
Found	61.68	6.43	2.95	13.18

IR (Nujol, 4000 – 400 cm^{-1}):

$\tilde{\nu}$ = 3028 vw (ν H–C=C), 1883 vs (ν Co–C≡O), 1842 vw (ν Co–C_{13}≡O), 1599 vw, 1579 w, 1542 m (ν C=C), 1519 s (ν C=N), 1413 m (δ_{as} PCH_3),1336 w; 1301 w, 1284 m (δ_s PCH_3); 1248 vw; 1233 vw; 1212 m; 1153 w; 1110 vw; 1078 vw; 1004 vw; 938 s (ρ_1 PCH_3); 856 w (ρ_2 PCH_3); 814 m; 773 m, 753 m (γ C–H_{arom}); 731 m (ν_{as} PC_3); 667 w (ν_s PC_3); 650 w; 627 vw; 615 vw; 600 w; 586 vw; 454 vw.

^{1}H NMR (500 MHz, [D_8]THF, 300 K, ppm):

δ = 0.63 (t', $|^2J_{P,H} + {}^4J_{P,H}|$ = 7.9 Hz, 18H, PCH_3); 6.89 – 6.95 (m, 2H, Ar–H); 7.07 (t, $^3J_{H,H}$ = 6.8 Hz, 1H, Ar–H); 7.16 (d, $^3J_{H,H}$ = 7.7 Hz, 1H, Ar–H); 7.24 (t, $^3J_{H,H}$ = 7.9 Hz, 1H, Ar–H); 7.51 (d, $^3J_{H,H}$ = 7.9 Hz, 1H, Ar–H); 7.68 (d, $^3J_{H,H}$ = 7.4 Hz, 2H, Ar–H); 7.77 (d, $^3J_{H,H}$ = 6.4 Hz, 1H, Ar–H); 8.13 (d, $^3J_{H,H}$ = 6.9 Hz, 1H, Ar–H); 9.28 (t, $^3J_{P,H}$ = 4.9 Hz, 1H, H–C=N).

^{13}C NMR (125 MHz, [D_8]THF, 300 K, ppm):

δ = 11.8 (t', $|^1J_{P,C} + {}^3J_{P,C}|$ = 26.2 Hz, PCH_3); 105.0 (s, CH); 115.5 (s, CH); 118.4 (s, CH); 122.1 (s, CH); 124.1 (s, CH); 124.2 (s, CH); 124.4 (s, CH); 127.2 (s, CH); 132.2 (s, C); 135.9 (s, CH); 140.8 (s, CH); 143.1 (s, C); 147.2 (s, C); 148.6 (s, C); 157.4 (s, H–C=N); 186.7 (t, $^2J_{P,C}$ = 22.5 Hz, Fe–C); 209.1 (t, $^2J_{P,C}$ = 33.2 Hz, Fe–C), 218.7 (t, $^2J_{P,C}$ = 32.5 Hz, Fe–CO).

^{31}P NMR (202 MHz, [D_8]THF, 300 K, ppm):

δ = 19.2 (s, 2P, PCH_3).

3.5.34 [2-[(2-Benzyl-κC)imino-κN)methyl]phenyl-κC](carbonyl)bis-(trimethylphosphine)iron(II) (34)

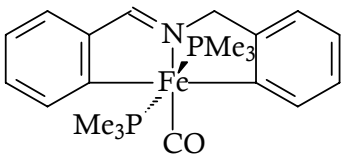

Procedure: E

A sample of **31** (740 mg, 1.55 mmol) in pentane was stirred under 1 bar CO to provide 507 mg of a product mixture containing large dark crystals of (**34**) and violet crystals of (**35**). They crystallize at –27 °C, and **34** were manually separated for characterization.

Yield : 67%

Melting point: 116 °C – 118 °C

Elemental analysis: $C_{21}H_{29}FeNOP_2$+$C_{11}H_{27}FeO_2P_3$, Mw: 769.36g/mol

%	C	H	N	P
Calculated	49.96	7.34	1.82	20.13
Found	49.78	7.27	1.77	19.40

IR (Nujol, 4000 – 400 cm^{-1}):

$\tilde{\nu}$ = 3068 vw, 3029 w (ν H–C=C); 1883 vs, 1862 vs (ν Fe–C≡O); 1593 w, 1571 w (ν C=C); 1531 w (ν C=N); 1432 m, 1420 m (δ_{as} PCH_3); 1311 vw, 1300 w, 1282 m (δ_s PCH_3); 1245 vw; 1206 vw; 1189 vw; 1150 vw; 1125 w; 1110 m; 1052 vw; 1019 vw; 1004 w; 944 vs (ρ_1 PCH_3); 881 vw; 855 m (ρ_2 PCH_3); 810 vw; 733 vs (γ C–H_{arom}); 670 m (ν_{as} PC_3); 647 w (ν_s PC_3); 631 w; 622 w; 597 w; 536 vw; 498 vw; 455 vw.

^{1}H NMR (500 MHz, [D_8]THF, 300 K, ppm):

δ = 0.76 (t', $|^{2}J_{P,H} + {}^{4}J_{P,H}|$ = 7.8 Hz, 18H, PCH_3); 5.15 (s_{br}, 2H, N–CH_2); 6.69 (qt, $^{3}J_{H,H}$ = 7.3 Hz, $^{4}J_{H,H}$ = 1.4 Hz, 1H, Ar–H); 6.76 (dt, $^{3}J_{H,H}$ = 7.3 Hz, $^{4}J_{H,H}$ = 1.4 Hz, 1H, Ar–H); 6.79–6.82 (m, 2H, Ar–H); 6.88 (dt, $^{3}J_{H,H}$ = 7.3 Hz, $^{4}J_{H,H}$ = 1.1 Hz, 1H, Ar–H); 7.42 (d, $^{3}J_{H,H}$ = 7.1 Hz, 1H, Ar–H); 7.62 (qd, $^{3}J_{H,H}$ = 6.9 Hz, $^{4}J_{H,H}$ = 1.7 Hz, 1H, Ar–H); 7.94 (d, $^{3}J_{H,H}$ = 6.8 Hz, 1H, Ar–H); 8.52 (tt, $^{4}J_{P,H}$ = 5.5 Hz, $^{4}J_{H,H}$ = 1.9 Hz, 1H, H–C=N).

^{13}C NMR (125 MHz, [D_8]THF, 300 K, ppm):

δ = 15.6 (t', $|^{1}J_{P,C} + {}^{3}J_{P,C}|$ = 25.6 Hz, PCH_3); 65.1 (s, CH_2); 119.8 (s, CH); 120.9 (s, CH); 121.3 (s, C); 125.5 (s, CH); 127.5 (s, CH); 128.1 (s, CH); 143.8 (s, CH); 144.0 (s, CH); 150.6 (s, C); 169.5 (s, H–C=N); 183.4 (m, Fe–C); 196.4 (m, Fe–C); 220.8 (m, Fe–CO).

^{31}P NMR (202 MHz, [D_8]THF, 300 K, ppm):

δ = 16.1 (s, 2P, PCH_3).

3.6.35 [2-[((2-Benzyl-κC)imino-κN)methyl]phenyl-κC](dicarbonyl)bis-(trimethylphosphine)iron(II) (35)

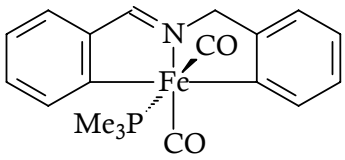

Melting point: 128 °C – 130 °C

IR (Nujol, 4000 – 400 cm^{-1}):

$\tilde{\nu}$ = 3044 w (ν H–C=C); 1992 vs (ν Fe–C≡O); 1922 vs (ν Fe–C≡O); 1607 m, 1575 m (ν C=C); 1540 w (ν C=N); 1430 m (δ_{as} PCH_3); 1317 w; 1304 w, 1285 m (δ_s PCH_3); 1250 vw; 1210 w; 1153 vw; 1111 vw; 1052 vw; 1033 vw; 1010 w; 986 vw; 955 vs (ρ_1 PCH_3); 854 m (ρ_2 PCH_3); 753 m, 733 vs (γ C–H_{arom}); 672 m (ν_{as} PC_3); 648 s (ν_s PC_3); 623 vw; 610 s; 598 s; 529 vw; 4981 vw; 439 m.

^{1}H NMR (500 MHz, [D_8]THF, 300 K, ppm):

δ = 0.78 (d, $^{2}J_{P,H}$ = 9.5 Hz, 9H, PCH_3); 5.18 (m, 2H, N–CH_2); 6.81- 6.96 (m, 3H, Ar–H); 6.96 (tt, $^{3}J_{H,H}$ = 7.3 Hz, $^{4}J_{H,H}$ = 0.9 Hz, 1H, Ar–H); 7.06 (dt, $^{3}J_{H,H}$ = 7.2 Hz, $^{4}J_{H,H}$ = 1.4 Hz, 1H, Ar–H); 7.52 (d, $^{3}J_{H,H}$ = 7.0 Hz, 1H, Ar–H); 7.59 (td, $^{3}J_{H,H}$ = 6.9 Hz, $^{4}J_{H,H}$ = 1.9 Hz, 2H, Ar–H); 7.89 (d, $^{3}J_{H,H}$ = 7.4 Hz, 1H, Ar–H); 8.56 (td, $^{4}J_{P,H}$ = 5.9 Hz, $^{4}J_{H,H}$ = 1.9 Hz, 1H, H–C=N).

^{13}C NMR (125 MHz, [D_8]THF, 300 K, ppm):

δ = 14.1 (d, $^{1}J_{P,C}$ = 28.5 Hz, PCH_3); 64.9 (s, CH_2); 118.9 (s, CH); 121.2 (d, $^{5}J_{P,C}$ = 2.9 Hz, CH); 121.8 (s, CH); 123.4 (s, CH); 126.6 (d, $^{5}J_{P,C}$ = 3.1 Hz, CH); 129.0 (s, CH); 129.5 (s, CH); 143.1 (s, CH); 143.3 (s, CH); 155.8 (s, C); 173.2 (m, C); 192.8 (s, Fe–C); 204.6 (s, Fe–C); 219.1 (m, Fe–CO); 233.5 (m, Fe–CO).

^{31}P NMR (202 MHz, [D_8]THF, 300 K, ppm):

δ = 22.3 (s, 1P, PCH_3).

3.6.36 Hydrido[2-[((8-naphthyl-κC)imino-κN)methyl]phenyl-κC]bis-(trimethylphosphine)cobalt(III) (36)

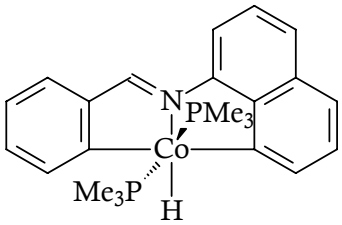

Procedure: B

950 mg (2.51 mmol) of $CoCH_3(PMe_3)_4$ in THF were combined with 581 mg (2.51 mmol) of N-benzylidene-1-naphthylamine to afford 743 mg of red crystals (**36**) which crystallize at -27 °C.

Yield: 67%

Melting point: 101 °C – 103 °C

Elemental analysis: $C_{23}H_{30}CoNP_2$, M_w: 441.38g/mol

%	C	H	N	P
Calculated	62.59	6.85	3.17	14.04
Found	62.75	6.46	3.17	14.16

IR (Nujol, 4000 – 400 cm^{-1}):

$\tilde{\nu}$ = 3035 vw (ν H–C=C); 1860 s (ν Co–H); 1629 vw, 1603 w, 1573 m (ν C=C); 1544 s, 1521 m (ν C=N); 1487 vw; 1433 w, 1417 m (δ_{as} PCH_3); 1333 w; 1298 m, 1279 m (δ_s PCH_3); 1245 s; 1230 w; 1207 s; 1165 w; 1149 w; 1105 m; 1078 w; 1016 vw; 1003 vw; 943 vs (ρ_1 PCH_3); 909 vw; 857 s, 848 vw (ρ_2 PCH_3); 815 s; 797 vw; 776 s, 753 s (γ C–H_{arom}); 728 vs (ν_{as} PC_3); 690 vw; 672 s(ν_s PC_3); 601 m; 561 m; 530 w (ν Co–C); 516 vw; 494 vw; 454 w.

^{1}H NMR (500 MHz, [D_8]THF, 300 K, ppm):

δ = -19.05 (t, $^2J_{P,H}$ = 71.7 Hz, 1H, Co–H); 0.72 (t', $|^2J_{P,H} + {}^4J_{P,H}|$ = 7.4 Hz, 18H, PCH_3); 6.93 (t, $^3J_{H,H}$ = 7.1 Hz, 1H, Ar–H); 6.97 (dt, $^3J_{H,H}$ = 7.0, $^4J_{H,H}$ = 1.0 Hz, 1H, Ar–H); 7.07 (t, $^3J_{H,H}$ = 7.0 Hz, 1H, Ar–H); 7.18 (d, $^3J_{H,H}$ = 8.0 Hz, 1H, Ar–H); 7.24 (t, $^3J_{H,H}$ = 7.7 Hz, 1H, Ar–H); 7.44 (m, 1H, Ar–H); 7.50 (d, $^3J_{H,H}$ = 8.0 Hz, 1H, Ar–H); 7.63 (d, $^3J_{H,H}$ = 7.0 Hz, 1H, Ar–H); 7.70 (d, $^3J_{H,H}$ = 7.4 Hz, 1H, Ar–H); 7.78 (d, $^3J_{H,H}$ = 6.8 Hz, 1H, Ar–H); 9.28 (s, 1H, H–C=N).

^{13}C NMR (125 MHz, [D_8]THF, 300 K, ppm):

δ = 17.5 (t', $|^1J_{P,C} + {}^3J_{P,C}|$ = 29.7 Hz, PCH_3); 108.5 (s, CH); 119.1 (s, CH); 121.7 (s, CH); 125.2 (s, CH); 127.2 (m, CH); 127.4 (s, CH); 127.5 (s, CH); 128.9 (s, CH); 134.9 (s, C); 141.5 (s, CH); 146.3 (s, CH); 146.6 (s, C); 150.3 (s, C); 151.8 (s, C); 158.8 (m, C=N); 181.1 (m, Co–C); 197.9 (m, Co–C).

^{31}P NMR (202 MHz, [D_8]THF, 300 K, ppm):

δ = 9.5 (s, PCH_3).

3.6.37 (η^2(κC-κN)-*N*-Benzylidene-1-naphthylamine)tris-(trimehylphosphine)cobalt(0) (37)

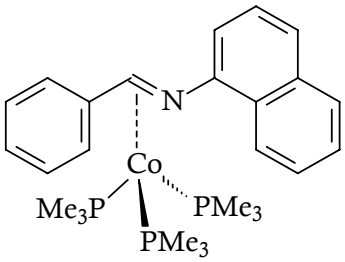

Procedure: B

1.08 g (2.97 mmol) of $Co(PMe_3)_4$ in THF were combined with 0.69 g (2.97 mmol) of N-benzylidene-1-naphthylamine to afford 0.85 g of brown crystals (**37**) which crystallize at -27 °C.

Yield: 55%

Melting point: 94 °C - 96 °C

Elemental analysis: $C_{26}H_{40}CoNP_3$, M_w: 518.46 g/mol

%	C	H	N	P
Calculated	60.23	7.78	2.70	17.92
Found	58.93	7.62	2.48	17.25

IR (Nujol, 4000 – 400 cm^{-1}):

$\tilde{\nu}$ = 3055 vw (ν H–C=C); 1591 m, 1560 s (ν C=C); 1502 w (ν C=N); 1399 s (δ_{as} PCH_3); 1304 m, 1274 m (δ_s PCH_3); 1242 m; 1213 w; 1163 s; 1088 vw; 1066 vw; 1029 vw; 1013 vw; 955 vs, 934 vs (ρ_1 PCH_3); 869 w; 845 w (ρ_2 PCH_3); 792 m, 771 m, 752 m (γ C–H_{arom}); 731 vw; 701 m (ν_{as} PC_3); 660 w (ν_s PC_3); 629 vw; 584 w; 540 w.

^{1}H NMR (500 MHz, [D_8]THF, 300 K, ppm):

δ = 1.07 (d, $^{2}J_{P,H}$ = 6.1 Hz, 27H, PCH_3); 7.11 (d, $^{3}J_{H,H}$ = 7.3 Hz,1H, Ar–H); 7.43–7.51 (m, 5H, Ar–H); 7.71 (d, $^{3}J_{H,H}$ = 8.2 Hz, 1H, Ar–H); 7.84 (d, $^{3}J_{H,H}$ = 8.2 Hz, 1H, Ar–H); 8.05 (m, 2H, Ar–H); 8.35 (d, $^{3}J_{H,H}$ = 7.9 Hz, 1H, Ar–H); 8.62 (s, 1H, Ar–H); 9.67 (s_{br}, 1H, H–C=N).

^{13}C NMR (125 MHz, [D_8]THF, 300 K, ppm):

δ = 15.6 (d, $^{1}J_{P,C}$ = 12.5 Hz, PCH_3); 63.8 (s, C=N); 108.5 (s, CH); 113.5 (s, CH); 125.1 (s, CH); 126.5 (s, CH); 126.8 (s, CH); 127.1 (s, CH); 127.3 (s, CH); 128.6 (s, CH); 129.8 (s, CH); 130.1 (s, CH); 130.4 (s, C); 132.4 (s, CH); 135.4 (s, C); 138.2 (s, C); 150.6 (s, C); 161.4 (s, CH).

^{31}P NMR (202 MHz, [D_8]THF, 300 K, ppm):

δ = 25.9 (s , 3P, PCH_3).

3.6.38 [2-[(phenylimino-κN)methyl]naphthyl-κC]tris-(trimethylphosphine)cobalt(I) (38)

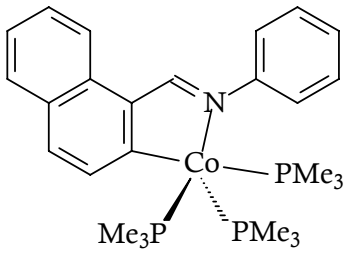

Procedure: B

875 mg (2.31 mmol) of $CoCH_3(PMe_3)_4$ in THF were combined with 535 mg (2.31 mmol) of N-(1-naphthylmethylene)aniline to afford 981 mg of dark green crystals of (**38**) which crystallize at -27 °C.

Yield: 82%

Melting point: 109 °C – 111 °C (decomposition)

Elemental analysis: $C_{26}H_{39}CoNP_3$, Mw: 517.46 g/mol.

%	C	H	N	P
Calculated	60.35	7.60	2.71	17.96
Found	60.12	7.86	2.71	17.95

IR (Nujol, 4000 – 400 cm^{-1}):

$\tilde{\nu}$ = 3048 w (ν H–C=C); 1587 m (ν C=C); 1340 w (δ_{as} PCH_3); 1294 m, 1277 m (δ_s PCH_3); 1191 w; 1167 m; 936 vs (ρ_1 PCH_3); 810 w (ρ_2 PCH_3); 767 w (γ C–H_{arom}); 741 m, 700 m (ν_{as} PC_3); 654 m (ν_s PC_3).

^{1}H NMR (500 MHz, [D_8]THF, 300 K, ppm):

δ = 1.06 (s, 27H, PCH_3); 7.07 (t, $^3J_{H,H}$ = 7.3 Hz, 1H, Ar–H); 7.15 - 7.28 (m, 6H, Ar–H); 7.46 (d, $^3J_{H,H}$ = 8.5 Hz, 1H, Ar–H); 7.64 (d, $^3J_{H,H}$ = 8.3 Hz, 1H, Ar–H); 7.97 (d, $^3J_{H,H}$ = 8.3 Hz, 1H, Ar–H); 8.39 (d, $^3J_{H,H}$ = 8.5 Hz, 1H, Ar–H); 9.51 (s_{br}, 1H, H–C=N).

^{13}C NMR (125 MHz, [D_8]THF, 300 K, ppm):

δ = 22.3 (m, PCH_3); 112.2 (s, CH); 121.8 (s, CH); 122.1 (s, CH); 123.7 (s, CH); 124.1 (s, CH); 126.6 (s, CH); 127.5 (s, CH); 131.3 (s, CH); 141.1 (s, C); 142.6 (s, C); 145.8 (s, C); 153.3 (s, C); 158.6 (s, C=N); 179.2 (m, Co–C).

^{31}P NMR (202 MHz, [D_8]THF, 300 K, ppm):

δ = -16.3 (m, 2P, PCH_3); - 3.8 (m, 1P, PCH_3).

3.6.39 [2-[(2,6-dimethylphenylimino-κN)methyl]naphthyl-κC]tris (trimethylphosphine cobalt(I) (39)

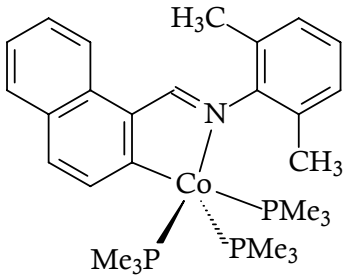

Procedure: B

1.45 g (3.83 mmol) of $CoCH_3(PMe_3)_4$ in THF were combined with 0.88 g (3.83 mmol) of N-(1-naphthylmethylene)aniline to afford 1.25 g of dark green crystals (**38**) which crystallize at -27 °C.

Yield: 60%

Melting point: 112 °C – 114 °C

Elemental analysis: $C_{28}H_{43}CoNP_3$, M_w:545.51 g/mol

%	C	H	N	P
Calculated	61.76	7.77	2.57	17.07
Found	60.61	8.35	2.64	17.35

IR (Nujol, 4000 – 400 cm^{-1}):

$\tilde{\nu}$ = 3047 w (ν H–C=C); 1637 vw; 1606 vw, 1590 vw (ν C=C); 1531 vw (ν C=N); 1423 m (δ_{as} PCH_3); 1327 m; 1318 m; 1296 m, 1275 s (δ_s PCH_3); 1253 vw; 1187 m; 1143 vw; 1092 vw; 1042 vw; 956 s, 940 vs (ρ_1 PCH_3); 875 w; 845 w (ρ_2 PCH_3); 818 w; 804 s, 760 s (γ C–H_{arom}); 734 m; 697 m (ν_{as} PC_3); 664 m (ν_s PC_3); 624 vw; 599 vw; 571 vw; 542 vw; 503 vw; 460 w; 436 w; 417 w.

^{1}H NMR (500 MHz, [D_8]THF, 300 K, ppm):

δ = 1.01 (s_{br}, 9H, PCH_3); 1.07 (s, 18H, PCH_3); 2.14 (s, 6H, Ar–CH_3); 7.02 - 7.08 (m, 4H, Ar–H); 7.18 (t, $^3J_{H,H}$ = 7.4 Hz, 1H, Ar–H); 7.48 (d, $^3J_{H,H}$ = 8.2 Hz, 1H, Ar–H); 7.64 (d, $^3J_{H,H}$ = 7.9 Hz, 1H, Ar–H); 7.94 (d, $^3J_{H,H}$ = 8.2 Hz, 1H, Ar–H); 8.53 (d, $^3J_{H,H}$ = 8.6 Hz, 1H, Ar–H); 9.34 (s, 1H, H–C=N).

^{13}C NMR (125 MHz, [D_8]THF, 300 K, ppm):

δ = 19.1 (s, Ar–CH_3); 23.3 (dt, $^3J_{P,C}$ = 2.2 Hz, $^1J_{P,C}$ = 10.6 Hz, PCH_3); 118.9 (dd, $^5J_{P,C}$ = 3.4 Hz, $^4J_{P,C}$ = 5.6 Hz, CH); 122.8 (s, CH); 123.4 (s, CH); 124.9 (d, $^5J_{P,C}$ = 4.5 Hz, CH); 128.6 (s, CH); 128.8 (s, CH); 131.8 (s, C); 132.5 (s, C); 133.6 (s, C); 138.9

(s, C); 142.8 (s, C); 144.4 (m, CH); 153.3 (m, CH); 160.4 (d, $^{4}J_{P,C}$ = 3.4 Hz, C=N); 181.2 (m, Co–C).

^{31}P NMR (202 MHz, [D_8]THF, 300 K, ppm):
δ = -14.9 (s_{br}, 2P, PCH_3); - 4.5 (s_{br}, 1P, PCH_3).

3.6.40 Hydrido[2-[(2-Benzyl-κC)imino-κN)methyl]phenyl-κC]tris-(trimethylphosphine)cobalt(III) (40)

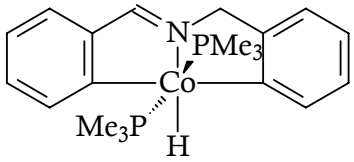

Procedure: B
840 mg (2.22 mmol) of $CoCH_3(PMe_3)_4$ in THF were combined with 434 mg (2.22 mmol) of *N*-benzylbenzylideneimine to afford 99 mg of orange crystals **40** which crystallize from pentane at 4 °C.

Yield: 11%

Melting point: 116 °C – 118 °C

Elemental analysis: $C_{20}H_{30}CoNP_2$, M_w: 405.35g/mol

%	C	H	N	P
Calculated	59.26	7.46	3.46	15.28
Found	59.11	7.71	3.84	16.79

IR (Nujol, 4000 – 400 cm^{-1}):
$\tilde{\nu}$ = 3096 vw, 3069 vw (ν H–C=C); 1879 m (ν Co–H); 1588 w, 1573 s (ν C=C); 1531 w (ν C=N); 1427 m, 1416 m (δ_{as} PCH_3); 1309 w, 1298 w (δ_s PCH_3); 1274 s; 1254 vw; 1204 w; 1149 vw; 1109 w; 1056 w; 1020 vw; 1005 w; 936 vs (ρ_1 PCH_3);

855 s, 841 s (ρ_2 PCH_3); 811 vw; 756 s (γ C–H_{arom}); 726 vs (ν_{as} PC_3); 670 m (ν_s PC_3); 619 vw; 535 vw; 477 vw; 458 vw.

^{1}H NMR (500 MHz, [D_8]THF, 300 K, ppm):
δ = - 18.73 (t, $^2J_{P,H}$ = 72.4 Hz, 1H, Co–H); 0.80 (s, 27H, PCH_3); 5.08 (s, 2H, CH_2); 6.69 (m, 1H, Ar–H); 6.72 (t, $^3J_{H,H}$ = 6.8 Hz, 1H, Ar–H); 6.80 (d, $^3J_{H,H}$ = 6.8 Hz, 1H, Ar–H); 6.85 (t', $^3J_{H,H}$ = 6.9 Hz, 1H, Ar-H); 6.91 (t, $^3J_{H,H}$ = 6.8 Hz, 1H, Ar–H); 7.29 (d, $^4J_{P,H}$ = 5.3 Hz, 1H, Ar–H); 7.39 (d, $^3J_{H,H}$ = 7.1 Hz, 1H, Ar–H); 7.63 (d; $^3J_{H,H}$ = 6.5 Hz, 1H, Ar–H); 8.56 (s, 1H, H–C=N).

^{13}C NMR (125 MHz, [D_8]THF, 300 K, ppm):
δ = 17.7 (t', $|^1J_{P,C} + {}^3J_{P,C}|$ = 29.6 Hz, PCH_3); 64.4 (s, CH_2); 119.6 (t, $^5J_{P,C}$ = 2.3 Hz, CH); 120.8 (s, CH); 121.4 (t, $^5J_{P,C}$ = 2.2 Hz, CH); 124.9 (t, $^5J_{P,C}$ = 3.4 Hz, CH); 126.6 (s, CH); 126.9 (s, CH); 145.9 (s, CH); 146 (d, $^5J_{P,C}$ = 2.0 Hz, CH); 151.3 (m, C); 152.1 (s, C); 166.8 (t, $^3J_{P,C}$ = 3.61 Hz, C=N); 176.7 (m, Co–C); 194.6 (m, Co–C).

^{31}P NMR (202 MHz, [D_8]THF, 300 K, ppm):
δ = 9.98 s, PCH_3.

3.6.41 (η^3-κC,κN,κC)[[[(Phenylmethyl)imino]methyl]phenyl]tris-(trimethylphosphine)cobalt(I) (41)

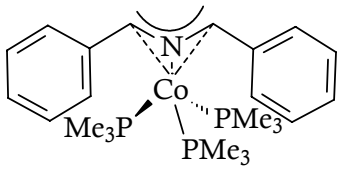

Procedure: B
840 mg (2.22 mmol) of $CoCH_3(PMe_3)_4$ in THF were combined with 434 mg (2.22 mmol) of N-benzylbenzylideneimine to afford 568 mg of brown crystals (**41**) which crystallize at 4 °C.

Yield: 58%

Melting point: 115 °C - 117 °C (decomposition)

Elemental analysis: $C_{23}H_{30}CoNP_2$, M_w: 441.38g/mol

%	C	H	N	P
Calculated	57.26	8.36	2.09	19.26
Found	57.59	7.97	2.82	19.27

IR (Nujol, 4000 – 400 cm^{-1}):

$\tilde{\nu}$ = 3073 vw, 3055 w, 3018 m (ν H–C=C); 1591 vs (ν C=C); 1486 s (ν C=N); 1425 s (δ_{as} PCH_3); 1294 m, 1275 m (δ_s PCH_3); 1245 w; 1220 w; 1153 w; 1140 w; 1063 m; 1024 w; 996 vw; 953 vs, 936 vs (ρ_1 PCH_3); 847 m (ρ_2 PCH_3); 756 vs γ(C–H_{arom}); 699 vs (ν_{as} PC_3); 657 vs (ν_s PC_3); 636 w; 627 vw; 611 vw; 575 m; 527 m; 505 vw; 419 vw.

^{1}H NMR (500 MHz, [D_8]THF, 300 K, ppm):

δ = 1.06 (s, 27H, PCH_3); 2.21 ($s_{br,}$ 1H, NCH); 7.03 (m, 6H, Ar–H); 7.66 (m, 4H, Ar–H).

^{13}C NMR (125 MHz, [D_8]THF, 300 K, ppm):

δ = 22.8 (m, PCH_3); 64.1 (s, N–CH); 124.0 (s, CH); 128.6 (s, CH); 128.8 (s, CH); 150.1 (s, C).

^{31}P NMR (202 MHz, [D_8]THF, 300 K, ppm):

δ = - 5.3 (s, PCH_3).

3.6.42 Iodo[2-[((8-naphthyl-κC)imino-κN)methyl]phenyl-κC]bis-(trimethylphosphine)cobalt(III) (42)

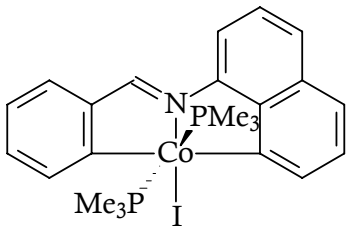

Procedure: D

485 mg (1.10 mmol) of **36** in pentane were combined with 156 mg (0.69 ml, 1.10 mmol) of CH_3I to afford 268 mg of claret crystals (**42**) which crystallize in ether THF mixture at 4 °C.

Yield: 43%

Melting point: 170 °C – 172 °C

Elemental analysis: $C_{23}H_{29}CoINP_2$, Mw: 567.27g/mol.

%	C	H	N	P
Calculated	48.70	5.15	2.47	10.92
Found	48.90	4.81	2.48	10.88

IR (Nujol, 4000 – 400 cm^{-1}):

$\tilde{\nu}$ = 3024 vw (ν H–C=C); 1578 m, 1547 m (ν C=C); 1524 m (ν C=N); 1416 w (δ_{as} PCH_3); 1338 w; 1298 w, 1280 m (δ_s PCH_3); 1217 m; 1109 w; 945 vs (ρ_1 PCH_3); 857 w (ρ_2 PCH_3); 816 s; 772 m; 757 s (γ C–H_{arom}); 728 s (ν_{as} PC_3); 673 w (ν_s PC_3); 563 vw; 523 vw (ν Co–C); 452 vw.

^{1}H NMR (500 MHz, [D_8]THF, 300 K, ppm):

δ = 0.63 (t', $|^2J_{P,H} + {}^4J_{P,H}|$ = 7.7 Hz, 18H, PCH_3); 6.94 (t, $^3J_{H,H}$ = 7.2 Hz, 1H, Ar–H); 7.02 (t, $^3J_{H,H}$ = 7.2 Hz, 1H, Ar–H); 7.08 (t, $^3J_{H,H}$ = 7.7 Hz, 1H, Ar–H); 7.12 (t, $^3J_{H,H}$ = 7.7 Hz, 1H, Ar–H); 7.19 (d, $^3J_{H,H}$ = 7.9 Hz, 1H, Ar–H); 7.43 (d, $^3J_{H,H}$ = 7.9 Hz, 1H,

Ar–H); 7.50 (d, $^{3}J_{H,H}$ = 7.4 Hz, 1H, Ar–H); 7.57 (d, $^{3}J_{H,H}$ = 7.4 Hz, 1H, Ar–H); 8.24 (d, $^{3}J_{H,H}$ = 6.4 Hz, 1H, Ar–H); 8.56 (d, $^{3}J_{H,H}$ = 7.3 Hz, 1H, Ar–H); 8.86 (t, $^{3}J_{P,H}$ = 4.2 Hz 1H, H–C=N).

^{13}C NMR (125 MHz, [D_8]THF, 300 K, ppm):
δ = 15.3 (t', $|^{1}J_{P,C} + {}^{3}J_{P,C}|$ = 31.1 Hz, PCH_3); 109.8 (s, CH); 120.4 (s, CH); 123.8 (s, CH); 125.3 (s, CH); 128.2 (m, CH); 128.9 (s, CH); 129.9 (s, CH); 128.9 (s, CH); 135.2 (s, C); 143.1 (s, CH); 145.3 (s, CH); 146.6 (s, CH); 149.3 (s, C); 151.4 (s, C); 157.4 (m, CH); 165.3 (s, H–C=N); 174.9 (t, $^{2}J_{P,C}$ = 23.5 Hz, Co–C); 194.9 (t, $^{2}J_{P,C}$= 22.0 Hz, Co–C).

^{31}P NMR (202 MHz, [D_8]THF, 300 K, ppm):
δ = 2.3 (s, PCH_3).

3.6.43 [2-[(2,6-dimethylphenylimino-κN)methyl]naphthyl-κC]tris (trimethylphosphine)cobalt(III) (43)

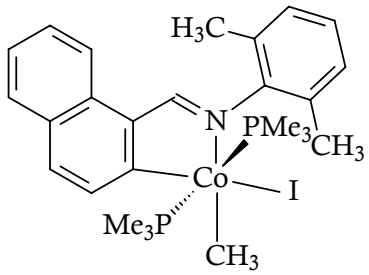

Procedure: D

440 mg (0.81 mmol) of **39** in pentane were combined with mg (1.01 ml, 1.62 mmol) of CH_3I to afford 291 mg of orange crystals (**42**) which crystallize at –27 °C.

Yield: 59%

Melting point: 144 °C - 146 °C

Elemental analysis: $C_{26}H_{37}CoINP_2$, M_w: 611.37 g/mol

%	C	H	N
Calculated	51.08	6.10	2.29
Found	51.11	6.07	2.28

IR (Nujol, 4000 - 400cm^{-1}):

$\tilde{\nu}$ = 3085 w, 3057 w, 3025 w (ν H–C=C); 1594 w, 1578 w (ν C=C); 1497 w (ν C=N); 1412 m (δ_{as} PCH_3); 1337 m; 1297 m, 1282 m (δ_s PCH_3); 1218 w; 1200 w; 1158 w (δ Co–CH_3); 1104 w; 1076 m; 1026 m; 993 m; 948 vs (ρ_1 PCH_3); 862 w (ρ_2 PCH_3); 795 m, 753 s (γ C–H); 729 vs; 700 vs, 688 vs (ν_{as} PC_3); 665 m (ν_s PC_3); 620 vw; 594 vw; 567 m(Co–C); 513 vw; 481 w.

^{1}H NMR (500 MHz, [D_8]THF, 300 K, ppm):

δ = 0.53 (t, $^3J_{P,H}$ = 8.7 Hz, 3H, Co–CH_3); 1.44 (t' $|^2J_{P,H} + {}^4J_{P,H}|$ = 6.7 Hz,18H, PCH_3); 2.49 (s, 6H, Ar–CH_3); 7.16 (m, 1H, Ar–H); 7.24 - 7.27 (m, 4H, Ar–H); 7.44 (t, $^3J_{H,H}$ = 7.8 Hz 2H, Ar–H); 7.58 (t, $^3J_{H,H}$ = 7.2Hz, 1H, Ar–H); 8.01 (s, 1H, Ar–H); 8.05 (s, 1H, N–H).

^{13}C NMR (125 MHz, [D_8]THF, 300 K, ppm):

δ = -6.3 (s, Co–CH_3); 14.2 (t', $|^1J_{P,C} + {}^3J_{P,C}|$ = 18.1 Hz, PCH_3); 125.3 (s, CH); 126.7 (s, CH); 127.0 (s, C); 127.1 (s, C); 127.4 (s, CH); 127.5 (s, CH); 127.6(s, CH);128.1 (s, C); 128.4 (s, CH); 131.6 (s, CH); 134.4 (s, C); 136.1 (s, C); 157.8 (s, C=N), 195.1 (s, Co–C).

^{31}P NMR (202 MHz, [D_8]THF, 300 K, ppm):

δ = 0.7 (s, PCH_3) ppm.

3.6.44 [2-[(2,6-dimethylphenylimino-κN)methyl]naphthyl-κC](carbonyl)bis (trimethylphosphine)cobalt(I) (44a-44b)

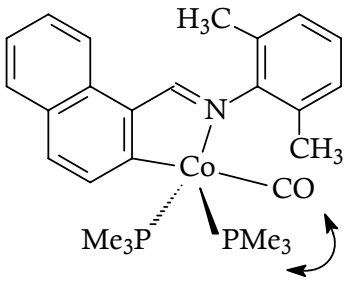

Procedure: E

A sample of **39** (500 mg, 0.92mmol) in pentane was stirred under 1 bar CO to provide 214 mg of blue crystals (**44**) which crystallize at 4 °C.

Yield: 51%

Melting point: 132 °C - 134 °C

Elemental analysis: $C_{26}H_{34}CoNOP_2$, Mw:497.44 g/mol.

%	C	H	N	P
Calculated	62.78	6.89	2.82	12.45
Found	62.88	6.83	2.78	12.34

IR-Data (Nujol, 4000 – 400 cm^{-1}):

$\tilde{\nu}$ = 3040 vw, 3015 vw (ν H–C=C); 1921 vs (ν Co–C≡O); 1637 vw; 1566 w, 1536 vw (ν C=C); 1485 m (ν C=N); 1422 vw (δ_{as} PCH_3); 1298 vw, 1277 m (δ_s PCH_3); 1203 vw; 1185 m; 1156 vw; 1094 vw; 1043 vw; 938 vs (ρ_1 PCH_3); 903 vw; 878 vw; 846 w (ρ_2 PCH_3); 805 m, 768 s (γ C–H_{arom}); 716 m (ν_{as} PC_3); 668 m (ν_s PC_3); 601 vw; 576 w; 536 w; 515 w; 459 w.

≈ Isomer 44a (CO in axial position) ≈

^{1}H NMR of 44a (500 MHz, [D_8]THF, 300 K, ppm):
δ = 1.16 (t', $|^{2}J_{P,H} + {}^{4}J_{P,H}|$ = 7.4 Hz,18H, PCH_3); 2.16 (s, 6H, Ar–CH_3); 6.98 (d, $^{3}J_{H,H}$ = 7.2 Hz, 1H, Ar–H); 7.06 (d, $^{3}J_{H,H}$ = 7.5 Hz, 1H, Ar–H); 7.06 (d, $^{3}J_{H,H}$ = 7.5 Hz, 1H, Ar–H); 7.10 (s_{br}, 1H, Ar–H); 7.17 (q, $^{3}J_{H,H}$ = 7.3 Hz, 1H, Ar–H); 7.26 (t, $^{3}J_{H,H}$ = 8.0 Hz, 1H, Ar–H); 7.45 (d, $^{3}J_{H,H}$ = 8.4 Hz, 1H, Ar–H); 7.71 (d, $^{3}J_{H,H}$ = 8.0 Hz, 1H, Ar–H); 8.12 (d, $^{3}J_{H,H}$ = 8.2 Hz, 1H, Ar–H); 8.24 (d, $^{3}J_{H,H}$ = 8.4 Hz, 1H, Ar–H); 9.20 (t, $^{4}J_{P,H}$ = 1.6 Hz, 1H, H–C=N).

^{13}C NMR of 44a (125 MHz, [D_8]THF, 300 K, ppm):
δ = 20.1 (s, Ar–CH_3); 20.8 (t', $|^{1}J_{P,C} + {}^{3}J_{P,C}|$ = 24.5 Hz, PCH_3); 112.6 (s, CH); 123.4 (s, CH); 123.7 (s, C); 124.9 (s, C); 125.7 (s, CH); 127.6 (s, C); 128.8 (s, CH); 129.3 (s, CH); 131.2 (s, C); 133.5 (s, CH); 140.9 (s, CH); 145.9 (s, C); 161.1 (t, $^{4}J_{P,C}$ = 4.7 Hz, C=N); 182.7 (m, Co–C); 205.1 (s, Co–CO).

^{31}P NMR of 44a (202 MHz, [D_8]THF, 300 K, ppm):
δ = -6.5 (m, PCH_3).

≈ Isomer 44b (CO in equatorial position) ≈

^{1}H NMR of 44b (500 MHz, [D_8]THF, 300 K, ppm):
δ = 0.93 (d, $^{2}J_{P,H}$ = 6.8 Hz, 9H, PCH_3); 1.03 (d, $^{2}J_{P,H}$ = 7.4 Hz, 9H, PCH_3); 2.06 (s, 3H, Ar–CH_3); 2.44 (s, 3H, Ar–CH_3); 6.97 (d, $^{3}J_{H,H}$ = 7.8 Hz, 1H, Ar–H); 7.05 (d, $^{3}J_{H,H}$ = 7.3 Hz, 1H, Ar–H); 7.09 (s_{br}, 1H, Ar–H); 7.20 (q, $^{3}J_{H,H}$ = 7.7 Hz, 1H, Ar–H); 7.28 (t, $^{3}J_{H,H}$ = 7.1 Hz, 1H, Ar–H); 7.46 (d, $^{3}J_{H,H}$ = 8.4 Hz, 1H, Ar–H); 7.73 (d, $^{3}J_{H,H}$ = 7.5 Hz, 1H, Ar–H); 8.11 (d, $^{3}J_{H,H}$ = 7.5 Hz, 1H, Ar–H); 8.28 (dd, $^{3}J_{H,H}$ = 8.4 Hz, $^{4}J_{H,H}$ = 3.0 Hz 1H, Ar–H); 9.13 (d, $^{4}J_{P,H}$ = 4.9 Hz, 1H, H–C=N).

^{13}C NMR of 44b (125 MHz, [D_8]THF, 300 K, ppm):
δ = 18.6 (dd, $^{1}J_{P,C}$ = 20.8 Hz, $^{3}J_{P,C}$ = 2.0 Hz, PCH_3); 18.9 (dd, $^{1}J_{P,C}$ = 20.9 Hz, $^{3}J_{P,C}$ = 5.4 Hz, PCH_3); 20.3 (s, Ar–CH_3); 20.4 20.3 (s, Ar–CH_3); 113.8 (s, CH); 122.8 (s,

CH); 123.9 (s, CH); 124.2 (s, C); 125.9 (s, CH); 126.8 (s, C); 128.2 (s, C); 128.4 (s, C); 128.7 (s, CH); 129.2 (s, CH); 130.9 (s, C); 132.8 (s, CH); 139.4 (s, CH); 143.7 (s, C); 157.6 (m, C=N); 178.6 (m, Co–C); 217.5 (s, Co–CO).

^{31}P NMR of 47b (202 MHz, [D_8]THF, 300 K, ppm):
δ = -13.6 (m, PCH_3); 0.7 (m, PCH_3).

3.6.45 (η^2(κC-κN)-*N*-Benzylidene-1-naphthylamine)tris-(trimehylphosphine)nickel(0) (45)

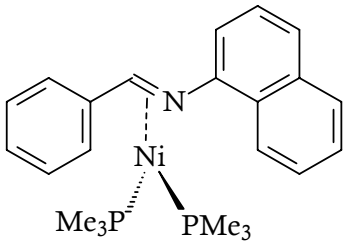

Procedure: C

700 mg (2.21 mmol) of $Ni(CH_3)_2(PMe_3)_3$ in ether were combined with 510 mg (2.21 mmol) of N-benzylidene-1-naphthylamine to afford 713 mg of red crystals (**29**) which crystallize from pentane at 4 °C.

Yield: 73 %

Melting point: 101 °C– 103 °C

Elemental analysis: $C_{23}H_{31}NNiP_2$, M_w: 442.14 g/mol

%	C	H	N	P
Calculated	62.48	7.07	3.17	14.01
Found	62.89	7.66	3.10	13.68

IR (Nujol, 4000 – 400 cm^{-1}):

$\tilde{\nu}$ = 3065 w, 3032 w, 3016 w (ν H–C=C); 1593 m (ν C=C); 1560 s (ν C=N); 1458 m (ν C=C); 1432 m (δ_{as} PCH_3); 1300 m, 1281 m (δ_s PCH_3); 1264 m; 1237 m; 1211 w; 1160 w; 1080 w; 1065 w; 1030 w; 1011 w; 940 vs (ρ_1 PCH_3); 839 m (ρ_2 PCH_3); 795 s (γ C–H_{arom}); 724 s, 694 s (ν_{as} PC_3); 668 m (ν_s PC_3); 633 m; 582 m; 531 s; 459 vw; 433 vw.

^{1}H NMR (500 MHz, [D_8]THF, 300 K, ppm):

δ = 0.84 (s, 9H, PCH_3); 1.03 (s, 9H, PCH_3); 6.96 (t, $^3J_{H,H}$ = 6.9 Hz, 1H, Ar–H); 7.09 (t, $^3J_{H,H}$ = 7.4 Hz, 2H, Ar–H); 7.17 (t, $^3J_{H,H}$ = 7.7 Hz, 1H, Ar–H); 7.24 (d, $^3J_{H,H}$ = 7.3 Hz, 1H, Ar–H); 7.27–7.31 (m, 2H, Ar–H), 7.46 (m, 1H, Ar–H); 7.51 (s, 1H, Ar–H), 7.57 (d, $^3J_{H,H}$ = 7.4 Hz, 1H, Ar–H); 7.64 (d, $^3J_{H,H}$ = 8.2 Hz, 1H, Ar–H); 8.99 (d, $^3J_{P,H}$ = 5.6 Hz, 1H, H–C=N).

^{13}C NMR (125 MHz, [D_8]THF, 300 K, ppm):

δ = 17.8 (d, $^1J_{P,C}$ = 20.4 Hz, PCH_3); 113.5 (s, CH); 115.7 (s, CH); 120.3 (s, CH); 123.6 (s, CH); 123.7 (s, CH); 124.5 (s, CH); 124.9 (s, CH); 126.2 (s, CH); 126.8 (s, CH); 127.2 (s, CH); 128.1 (s, CH); 129.1 (s, CH); 132.4 (s, C); 132.6 (s, C); 148.6 (s, C); 154.5 (s, C); 161.4 (s, C=N).

^{31}P NMR (202 MHz, [D_8]THF, 300 K, ppm):

δ = -12.6 (d, $^2J_{P,P}$ = 58.8 Hz, 1P, PCH_3); -18.8 (d, $^2J_{P,P}$ = 58.8 Hz, 1P, PCH_3).

4 CONCLUSION

Since the decisive breakthrough by *Murai* et al., who achieved a highly efficient ruthenium-catalyzed addition of aromatic C-H bonds to unsaturated substrates this reaction is recognized as a new category of chemistry. The compounds which were synthesized and presented in this thesis serve as stable models of reactive intermediates, proposed in catalytic transformations with the ruthenium counterparts. It is also of general interest to study the reactivity of trimethylphosphine stabilized iron, cobalt and nickel compounds toward aromatic imines and ketones.

Other than some cyclomanganated products, there are no examples of cyclometalated products of 3d row transition metals with imines. In this section, a review of reactions in the activation and functionalization of C-H bonds by solution-phase transition metal-based systems are presented, with an emphasis on the activation of aromatic C-H bonds.

Phenyl ketimines react smoothly under mild contions with low–valent iron (0) and methyl-cobalt(I) adducts to form five-membered metallacycles (Scheme 4.1). Stable cobalt(I) complexes are formed through reductive elimination of methane, and hydrido-iron(II) compounds arise from formal insertion of iron into the aromatic C-H bond. While cobalt(I) compounds prefer trigonal bipyramidal coordination geometry, iron(II) compounds prefer octahedral coordination geometry. Products are usually diamagnetic substances, all crystallize from pentane and have moderate air sensitivity (stable up to 20 minutes in air). Therefore they could be fully characterized by spectroscopy and crystallography.

Scheme 4.1

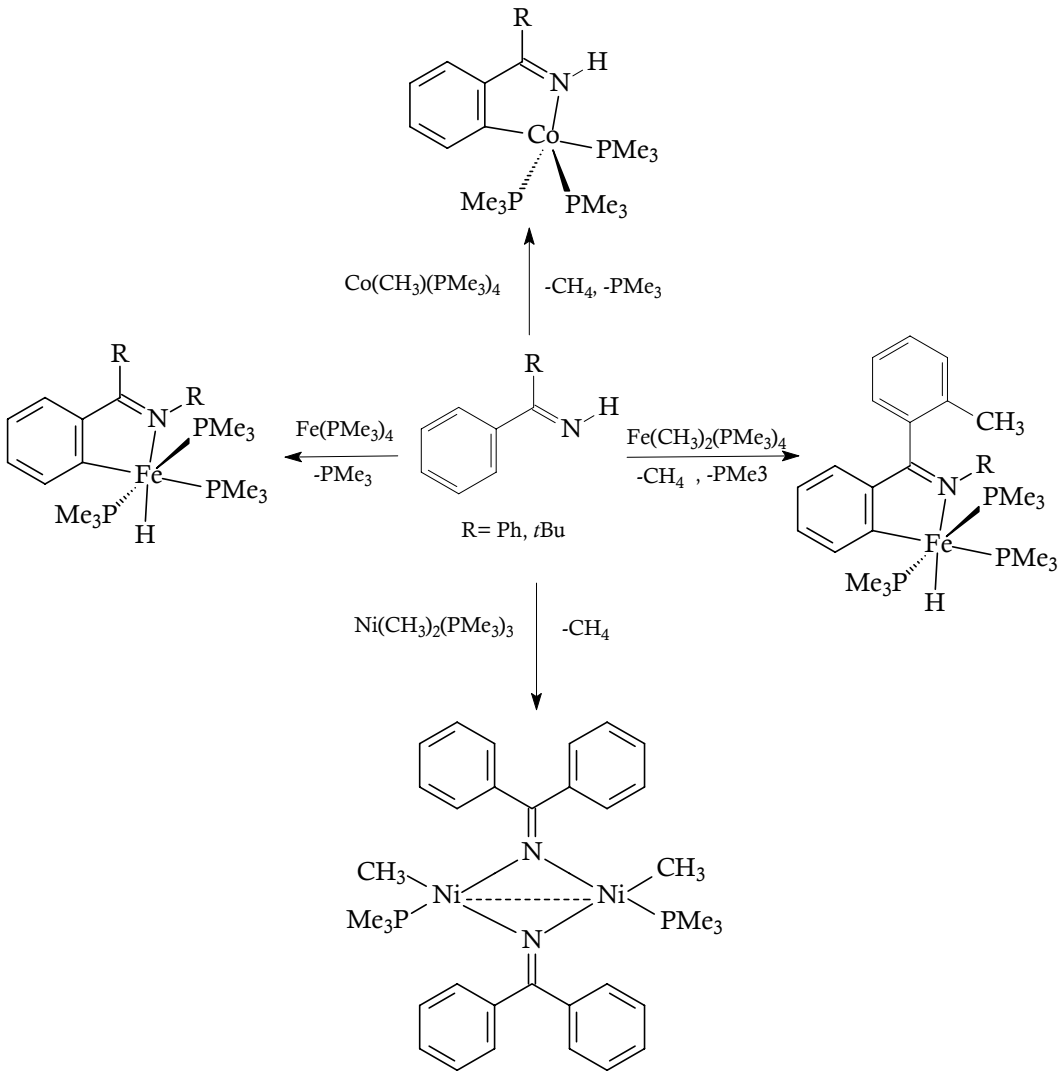

The reaction of diphenylketimine with $Fe(CH_3)_2(PMe_3)_4$ generates a hydrido-iron(II) complex via C,C-coupling between an sp^2 carbon of the aromatic backbone and the sp^3 carbon of CH_3 group.

Benzylic imines react with $Fe(CH_3)_2(PMe_3)_4$ by elimination of methane to afford hexacoordinate methyl-iron(II) complexes (Table 4.1).

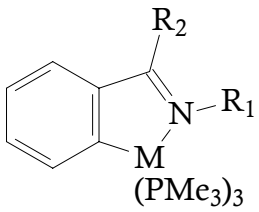

M	R_1	R_2	Compound
FeH	H	C_6H_5	**1**
FeH	H	$C(CH_3)_3$	**2**
$FeCH_3$	CH_3	H	**4**
$FeCH_3$	$CH(CH_3)_2$	H	**5**
$FeCH_3$	C_6H_5	H	**6**
Co	H	C_6H_5	**15**
Co	H	$C(CH_3)_3$	**16**

Table 4.1 Metalacyclic iron and cobalt compounds.

These are the first examples of *ortho*-metalated iron and cobalt complexes with imine anchoring groups which are fully characterized.

Iodomethane reactions of hydrido- and methyl-iron compounds form iodo-iron(II) complexes. The oxidation state and the geometry does not change in the resulting complexes. The proposed intermediate in these reactions is an Fe(IV) compound. Oxidative addition reactions of cyclometalated cobalt(I) compounds form octahedral, low-spin cobalt(III) complexes.

Carbon monoxide smoothly substitutes one of the trimethylphosphine ligand in cobalt(I) and methyl-iron (II) compounds. No insertion into metal-carbon or nitrogen-metal bonds are indicated. Carbon monoxide does not react with hydrido-iron (II) compounds.

With dimethylnickel(II), instead of *ortho*-metalation, an imine bridged dinickel complex forms by deprotonating the imine proton which was not observed with iron(0) and cobalt(I).

These findings demonstrate that the N-donor function in the course of cyclometalation reactions is first coordinated, followed by activation and regiospecific cleavage of the suitable ligand C-H bond. The M-H function thus formed either remains in the final product, as observed after reaction at the iron (0) center, or is eliminated as methane with an adjacent M-CH_3 unit as in all other cyclometalation reactions described here.

An imine function is the nitrogen analogue of a carbonyl group. Following the isolecetronic principle, $CoCH_3(PMe_3)_4$ with ketones affords cyclometalated, diamagnetic cobalt(I) compounds through methane elimination under same reaction conditions. Even though C-F bonds are about 30 kcal/mol stronger than C-H bonds, partially fluorinated 2,3,4,5,6-pentafluorobenzophenone reacts with $CoCH_3(PMe_3)_4$ via C-F activation by elimination of fluoromethane (Eq. 4.1).

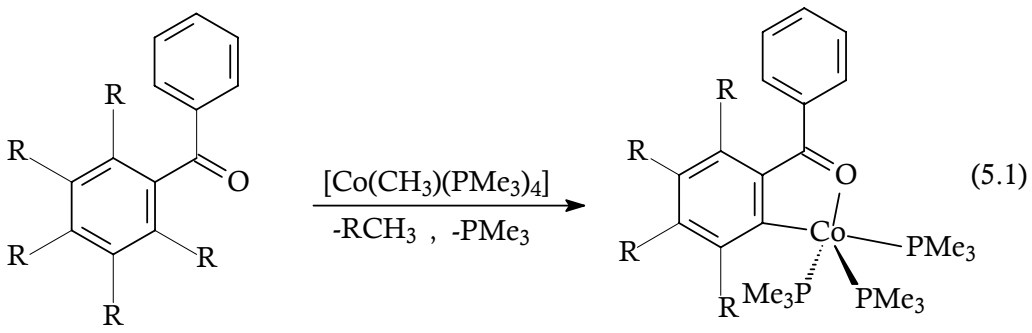

(5.1)

R= H, **24**

R= H, **28**

These cyclometalated cobalt compounds with ketones and partially activated ketones are the first examples in literature. They have an interesting potential as catalyst precursors in *Murai* type reactions and C-F activation.

In cyclometalation reactions of iron and cobalt, the metals retain their low oxidation states in the products and since the effects of donor ligands are similar before and after reaction, except for the chelate effect, it should be possible to perform a second C-H activation. Subsequent elimination accompanied by C,C coupling would facilitate a catayltic reaction mode. Using complexes of low-valent iron and cobalt with imines which have proper positions for second C-H activation, bicyclometalation reactions have been performed for the first time at one central atom.

Table 4.2 shows the summary of bicyclometalated compounds of iron and cobalt. Upon combining a dimethyliron compound with certain diarylated imines, a reaction sequence is observed consisting of double metalation at the same metal complex center leading to a metallabicycle. $Fe(CH_3)_2(PMe_3)_4$ affords bicyclometalated iron(II) compounds with *N*-(1-naphthylmethylene)-aniline and *N*-Benzylbenzylideneimine. $Co(CH_3)(PMe_3)_4$ forms hydrido-cobalt(III) complexes.

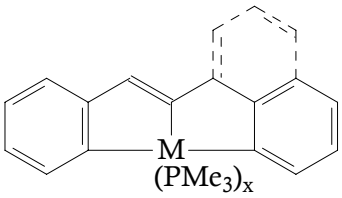

M	x	Compound
Fe	3	**29**
Fe	3	**31**
CoH	2	**36**
CoH	2	**40**

Table 4.2 Bicyclometalated iron and cobalt compounds.

When the isostructural imine ligand, *N*-(1-naphthylmethylene)-aniline is used instead of N-benzylidene-1-naphthylamine, bicyclometalation does not take place and a η^4-iron(0) complex is formed (**A**). At variance with the **29**, the reaction starts

with the β C-H activation. The β-position of the naphthyl part contains a methyl group throughout a former *ortho*-metalation step with $Fe(CH_3)_2(PMe_3)_4$ followed by a reductive elimination with a C,C-coupling and a release of a $Fe(PMe_3)_3$ fragment that coordinates in a η^4-fashion to the α-part of the N-naphthylidenphenylimine ligand. The reaction pathway makes it clear that the switched coordination mode of the N=C part in the imine ligand does not react with the phenyl part of the imine ligand which might lead to a more stable bicylometalated product. The only possibility would be the second C H activation from the phenyl ring forming a less favorable four membered metallacyle.

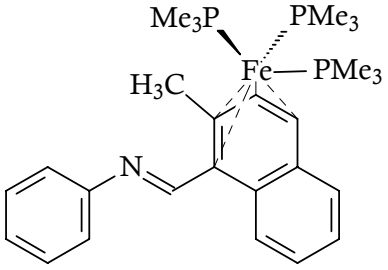

A

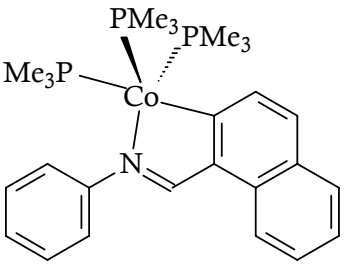

B

Reaction of $Co(CH_3)(PMe_3)_4$ with *N*-(1-naphthylmethylene)-aniline gives a similar result (**B**) with a dimethyliron complex. Again no bicyclometalation is observed which is due to the sterical demand in the second C-H activation step forming a four memberd metalacycle. The spectroscopic data and the deduced coordination geometry are very similar with the *ortho*metalated complexes **15** and **16**.

Proximity of a C-H bond to the metal and a perpendicular orientation are believed to be necessary and prequisite for a cyclometalation to occur. It has been already shown that with *N*-phenylbenzylideneimine the small bite angle does not support a second step of metalation (**6**). The reaction of $Co(CH_3)(PMe_3)_4$ with *N*-(1-naphthylmetylene)-2,6-dimethylaniline stops at the ortho-metalation in the naphthyl part forming a five memberd metalacycle and no further C-H activation

step of the methyl groups in the aromatic backbone occurs (**C**). This shows that the bicyclometalation reactions only occur when the two C-H bonds are aromatic.

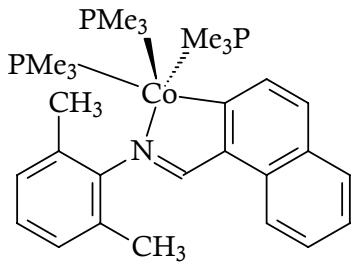

C

In the carbon monoxide reactions of bicyclometalated iron(II) compounds, monosubstitution is observed for **29** and disubstitution is observed for **31**. Bicyclometalated Co(III) compounds do not react with CO. Iodomethane does not add to compound **29** but forms an iodo-iron (III) compound

This thesis introduces some novel imine chelating systems of iron and cobalt. Their model character for the homogenous catalysis make them very interesting and attractive.

Their regioselective *ortho*-metalations make a particular attention on them for the synthesis of organic compounds.

Meridional bicyclometalation reactions are a novel way of forming dianionic [CNC] – ligands. Demetalation steps in bicyclometalation reactions give the possibility to synthesize organic compounds which are not accessible by classical methods.

5 ZUSAMMENFASSUNG

Seit dem entscheidenden Durchbruch von Murai et al., die eine hocheffiziente Ruthenium-katalysierte Addition aromatischer C–H-Bindungen an ungesättigte Substrate entwickelt haben, wird diese Methode einer neuen Kategorie organisch-chemischer Synthesen zugerechnet. Alle neuen Verbindungen, die in der vorliegenden Dissertation präsentiert werden, lassen sich als stabile Modelle reaktiver Zwischenstufen ansehen, die in katalytischen Umwandlungen mit analog zusammengesetzten Rutheniumkomplexen vorgeschlagen werden. Darüber hinaus ist es von allgemeinem Interesse, die Reaktivität Trimethylphosphin-gestützter Eisen-, Cobalt- und Nickel-Verbindungen gegenüber aromatischen Iminen und Ketonen zu untersuchen.

Abgesehen von einigen cyclomanganierten Produkten gibt es von Metallen der 3d Übergangsreihe keinerlei Beispiele für Cyclometallierungen mit Iminen. In diesem Abschnitt wird ein Überblick von Reaktionen mit Aktivierung und Funktionalisierung von C-H-Bindungen durch Übergangsmetall-Verbindungen in Lösung gegeben unter besonderer Berücksichtigung der Aktivierung aromatischer C–H-Bindungen.

Phenylketimine reagieren unter milden Bedingungen glatt mit niedervalenten Komplexen von Eisen(0) und Cobalt(I) unter Ausbildung fünfgliedriger Metallacyclen (Schema 5.1). Stabile Cobalt(I)-Komplexe bilden sich durch reduktive Eliminierung von Methan, während Hydridoeisen(II)-Komplexe durch formale Insertion des Eisens in eine aromatische C–H-Bindung generiert werden. Während Cobalt(I)-Verbindungen eine trigonal bipyramidale Koordinations-geometrie bevorzugen, werden Eisen(II)-Verbindungen meistens in oktaedrischer Koordination gefunden. In der Regel sind die Produkte diamagnetische Substanzen, sie kristallisieren aus Pentan-Lösung und sind nur

mäßig luftempfindlich, so daß sie auch ohne Inertgassschutz bis zu etwa 20 Minuten unzersetzt gehandhabt werden können. Diese Eigenschaften erleichtern ihre vollständige analytische und kristallographische Charakterisierung.

Schema 5.1

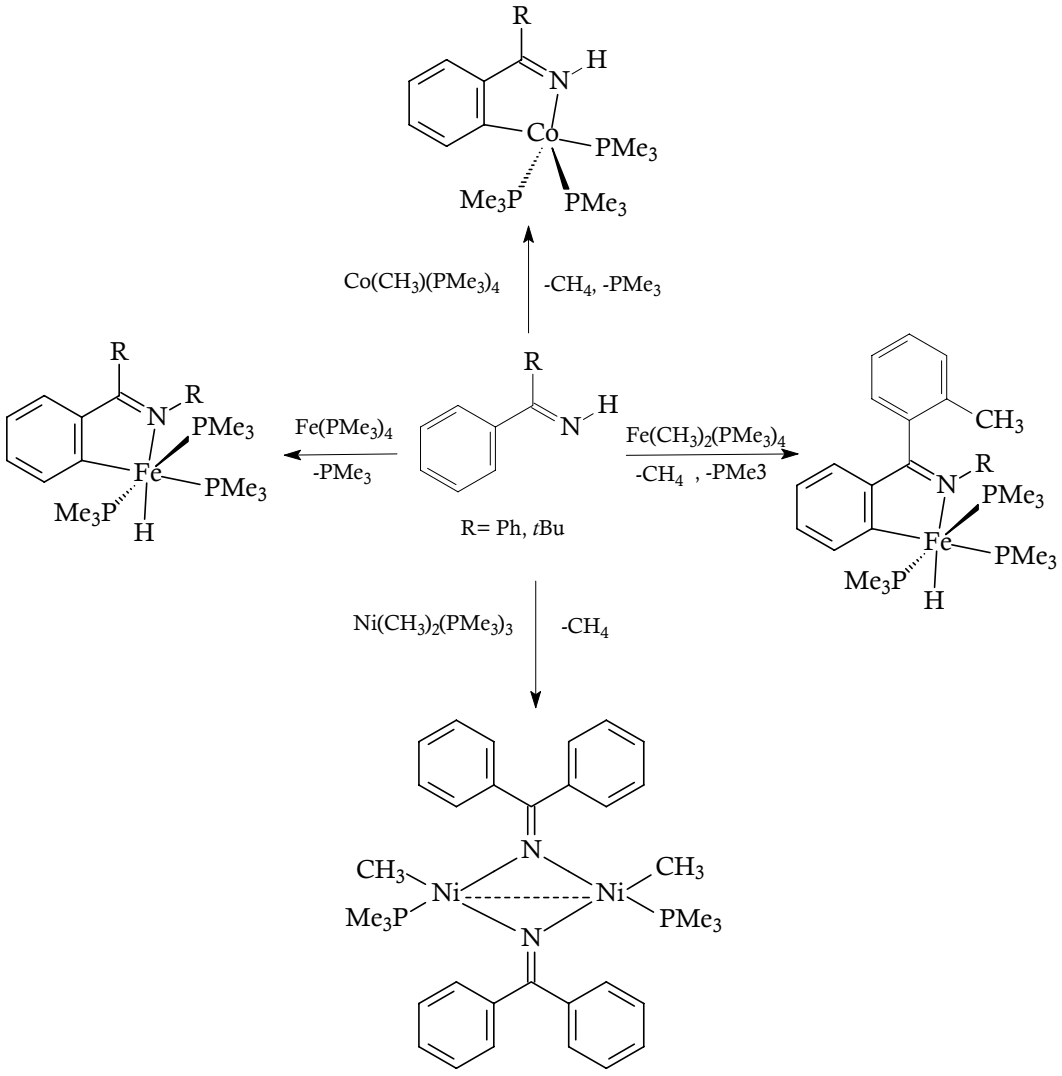

Die Reaktion von Diphenylketimin mit $Fe(CH_3)_2(PMe_3)_4$ liefert einen Hydridoeisen(II)-Komplex via C,C-Kupplung zwischen einem (sp^2)C-Atom des aromatischen Gerüsts und dem (sp^3)C-Atom einer Methylgruppe.

Benzylimine reagieren mit $Fe(CH_3)_2(PMe_3)_4$ unter Eliminierung von Methan zu hexakoordinierten Methyleisen(II)-Komplexen (Tabelle 5.1).

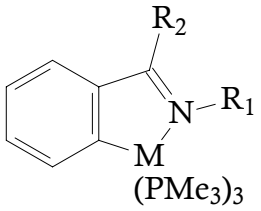

M	R_1	R_2	Compound
FeH	H	C_6H_5	**1**
FeH	H	$C(CH_3)_3$	**2**
$FeCH_3$	CH_3	H	**4**
$FeCH_3$	$CH(CH_3)_2$	H	**5**
$FeCH_3$	C_6H_5	H	**6**
Co	H	C_6H_5	**15**
Co	H	$C(CH_3)_3$	**16**

Tabelle 5.1 Metallacyclische Eisen- und Cobalt-Verbindungen.

Diese Verbindungen sind die ersten Beispiele für *ortho*-metallierte Einsen- und Cobalt-Komplexe mit Imin-Ankergruppen, die umfassend charakterisiert werden konnten.

Reaktionen von Hydrido- und Methyleisen-Verbindungen mit Iodmethan ergeben Iodoeisen(II)-Komplexe. Oxidationszahl und Koordinationsgeometrie in den erhaltenen Komplexen sind unverändert. Vermutet wird in diesen Reaktionen eine Eisen(IV)-Zwischenstufe. Oxidative Additionen an cyclometallierten Cobalt(I)-Verbindungen liefern oktaedrische low-spin Cobalt(III)-Komplexe.

Mit Dimethylnickel wird anstelle einer *ortho*-Metallierung ein Imin-verbrückter Dinickel-Komplex gebildet unter Deprotonierung des Imin-Protons, was weder mit Eisen(0) noch mit Cobalt(I) beobachtet wird.

Diese Befunde zeigen, dass im Verlauf der Cyclometallierungsreaktion zunächst die N-Donorfunktion koordiniert wird, woran sich die Aktivierung und regiospezifische Spaltung einer geeigneten C–H-Bindung im Liganden anschließt. Die so gebildete M–H-Funktion bleibt entweder im Endprodukt erhalten, was nach Reaktion am Eisen(0)-Zentrum gefunden wird, oder sie wird mit einer benachbarten M–CH_3-Einheit als Methan eliminiert wie in den übrigen hier beschriebenen Cyclometallierungsreaktionen.

Eine Imin-Funktion ist das N-Analogon einer Carbonylgruppe. Auf der Basis dieser isoelektronischen Verwandtschaft reagiert unter gleichen Bedingungen $CoCH_3(PMe_3)_4$ mit Ketonen unter Eliminierung von Methan zu cyclometallierten, diamagnetischen Cobalt(I)-Verbindungen. Obwohl C–F-Bindungen um etwa 30 kJ/mol stärker sind als C–H-Bindungen, reagiert hälftig fluoriertes 2,3,4,5,6-Pentafluorbenzophenon mit $CoCH_3(PMe_3)_4$ unter C–F-Aktivierung und Eliminierung von Fluormethan (Gl. 5.1).

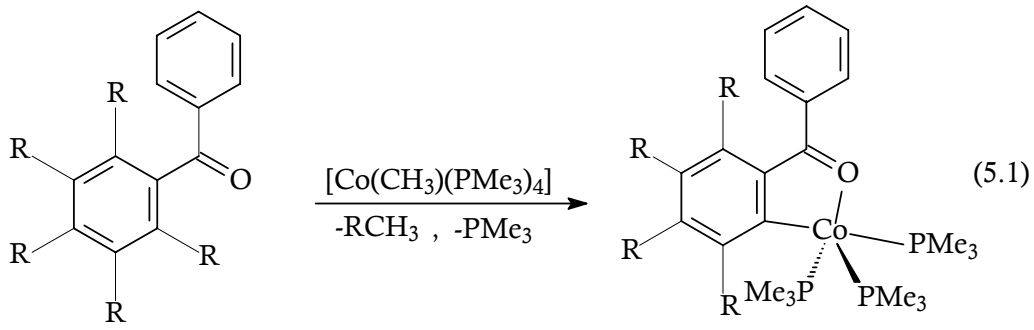

(5.1)

R= H, **24**
R= H, **28**

Cyclometallierte Verbindungen des Cobalts mit Ketonen und partiell aktivierten Ketonen werden hier erstmals beschrieben. Sie besitzen ein interessantes Potential

als Katalysator-Vorstufen in Reaktionen vom Murai-Typ sowie in der C–F-Aktivierung.

In Cyclometallierungsreaktionen des Eisens und Cobalts behalten die Metalle in den Produkten ihre niedrigen Oxidationsstufen, und da auch die Einflüsse der Donorliganden vor und nach der Reaktion, abgesehen vom Chelateffekt, sehr ähnlich sind, müsste sich eine zweite C–H-Aktivierung anschließen lassen. Nachfolgende Eliminierung unter C,C-Kupplung würde eine katalytische Reaktionsweise begünstigen. Mit Komplexen des niedervalenten Eisens und Cobalts von solchen Iminen, die eine passende Konformation für eine zweite C–H-Aktivierung bereit halten, konnte erstmals eine Bicyclometallierungsreaktion an ein und demselben Metallzentrum durchgeführt werden.

Tabelle 5.2 gibt eine Zusammenstellung bicyclometallierter Eisen- und Cobalt-Verbindungen. Vereinigt man Dimethyleisen mit bestimmten diarylierten Iminen, wird eine Reaktionssequenz beobachtet, die in einer doppelten Metallierung am gleichen Metallkomplexzentrum besteht und einen Metallabicyclus generiert. Während $Fe(CH_3)_2(PMe_3)_4$ mit N-(1-naphthylmethylen)anilin und N-Benzyl-benzylidenimin bicyclometallierte Eisen(II)-Verbindungen liefert, bildet $CoCH_3(PMe_3)_4$ entsprechende Hydridocobalt(III)-Komplexe.

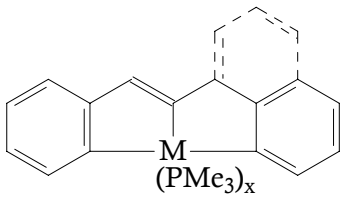

M	x	Compound
Fe	3	**29**
Fe	3	**31**
CoH	2	**36**
CoH	2	**40**

Tabelle 5.2 Bicyclometallierte Eisen- und Cobalt-Verbindungen.

Verwendet man den isostrukturellen Liganden *N*-(1-naphthylmethylen)anilin anstelle von N-Benzyliden-1-naphthylamin, dann bleibt eine Bicyclometallierung aus und ein η^4-Dien-eisen(0)-Komplex wird erhalten. Im Unterschied zu **29** beginnt die Reaktion mit einer β- C–H-Aktivierung. Durch einen vorgeschalteten *ortho*-Metallierunggschritt mit $Fe(CH_3)_2(PMe_3)_4$ und reduktive Eliminierung unter C,C-Kupplung erhält die β-Position des Naphthylteils eine Methylgruppe, wodurch ein $Fe(PMe_3)_3$-Fragment verfügbar wird, das mit einer η^4-Koordination vom α-Teil des *N*-naphthylidenphenylamin-Liganden gebunden wird (**A**). Eine solche Reaktionsweise macht deutlich, dass eine vertauschte Koordinationsweise im N=C-Teil des Imins eine Reaktion an der Phenylgruppe unterbindet, die zu einem stabileren cyclometallierten Produkt führen könnte. Die einzige Möglichkeit wäre eine zweite C–H-Aktivierung im Phenylring mit Ausbildung eines weniger günstigen viergliedrigen Metallacyclus.

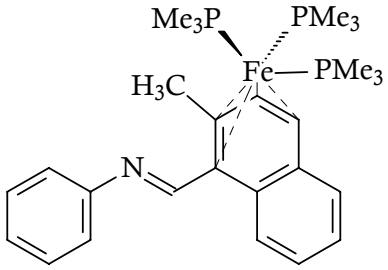

A

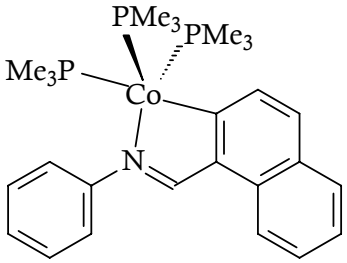

B

Die Reaktion von $CoCH_3(PMe_3)_4$ mit *N*-(1-naphthylmethylen)anilin liefert ein ähnliches Ergebnis (**B**) wie mit dem Dimethyleisen-Komplex. Wiederum bleibt eine Bicyclometallierung aus, was auf den Raumbedarf im zweiten C–H-Aktivierungsschritt zurückgeführt wird, der zum Metallavierring führen würde. Die spektroskopischen Daten und die daraus abgeleitete Koordinationsgeometrie ergeben ein ganz ähnliches Bild wie bei den *ortho*-metallierten Komplexen **15** und **16**.

Die Nähe-Konformation einer C–H-Bindung zum Metall, das darüber senkrecht positioniert ist, sind notwendige Voraussetzungen für das Eintreten einer

Cyclometallierung. Oben war schon aufgezeigt worden, dass mit *N*-phenylbenzylidenimin der enge Beißwinkel den zweiten Metallierungsschritt in **6** unterbindet. Die Reaktion von $CoCH_3(PMe_3)_4$ mit *N*-(1-naphthylmethylen)-2,6-dimethylanilin bleibt nach der *ortho*-Metallierung im Naphthylteil auf der Stufe mit fünfgliedrigem Metallacyclus stehen, und keine weitere Metallierung einer Methylgruppe am aromatischen Gerüst schließt sich an. Damit zeigt sich, dass hier die Reaktion nur mit aromatischen C–H-Bindungen erfolgt.

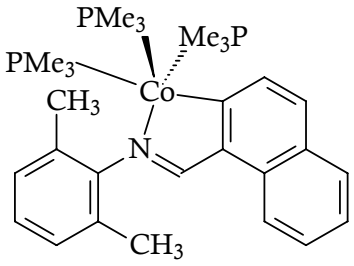

C

In der Normaldruck-Carbonylierung bicyclometallierter Eisen(II)-Verbindungen wird am Metallzentrum von **29** Monosubstitution und bei **31** Disubstitution beobachtet, während bicyclometallierte Co(III)-Verbindungen mit CO nicht reagieren. Iodmethan wird an Verbindung **29** nicht oxidativ addiert sondern bildet eine Iodoeisen(III)-Verbindung.

In dieser Arbeit werden neuartige, chelatisierende Iminliganden am Eisen und Cobalt eingeführt. Ihr Modellcharakter für die homogene Katalyse macht sie interessant und attraktiv. Die regioselektive *ortho*-Metallierung erweckt besondere Aufmerksamkeit im Hinblick auf organische Synthesen.
Die meridionale Bicyclometallierung stellt eine neue Bildungsweise dianionischer [CNC]-Liganden dar. Demetallierungsschritte in Bicylometallierungsreaktionen eröffnen die Möglichkeit einer Synthese organischer Substanzen, die mit klassischen Methoden nicht zugänglich sind.

6 REFERENCES

[1] M. Schlosser, *Organometallics in Synthesis,* Wiley, New York, **1994**.

[2] S. G. Davies, *Organotransition Metal Chemistry: Applications to Organic Synthesis*, Pergamon Press, Oxford, **1982**.

[3] P. J.Harrington, *Transition Metals in Total Synthesis*, Wiley, New York, **1990**.

[4] S. J. Lippard, J. Berg *Principles of Bioinorganic Chemistry,* University Science Books, Mill Valley, California, **1994**.

[5] F. A. Cotton, W. M. Bochmann, C. A. Murillo, *Advanced Inorganic Chemistry*, 6th edition, Wiley, New York, 1998.

[6] K. Bowman-James, R. B. King, *Encyclopedia of Inorganic Chemistry*, Wiley, New York, **1994**.

[7] B. Cornils, W. A. Hermann, *Applied Homoenous Catalysis with Organometallic Compounds: A Comprehensive Handbook*, VCH, New York, **1996**.

[8] K. I. Goldberg, A. S. Goldman, *Activation and Functionalization of C-H Bonds,* ACS Symposium Series 885, **2004**, -43.

[9] A. Sen, *Acc. Chem. Res.* **1998**, *31*, 550-557.

[10] Y. Guari, S. Sabo-Etiennne, B. Chaudret, *Eur. J. Inorg. Chem*. **1999**, 1047-1055.

[11] W. D. Jones, *Science* **2000**, *287*, 1942-1943.

[12] R. H. Crabtree, *J. Chem. Soc. Dalton Trans.* **2001**, *17*, 2437-2450.

[13] J. A. Labinger, J. E.Bercaw, *Nature*, **2002**, *417*, 507-514.

[14] V. Ritling, C. Sirlin, M. Pfeffer, *Chem. Rev.* **2002**, *102*, 1731-1769.

[15] J. Chatt, J. M. Davidson, *J. Chem.Soc.* **1965**, 843-855.

[16] G. J. Kubas, R.R. Ryan, B. I. Swanson, P. J. Vergamini, H. J. Wasserman, *J. Am. Chem. Soc.* **1984**, *106*, 451-452.

[17] G. J. Kubas, *Acc. Chem. Res.* **1988**, *21*, 120-128.

[18] W. D. Jones, *Acc. Chem. Res.* **2003**, *36*, 140-146.

[19] S. S. Stahl, J. A. Labinger, J. E. Bercaw, *J. Am. Chem. Soc.* **1996**, *118*, 596-5976.

[20] S. S. Stahl, J. A. Labinger, J. E. Bercaw, *Angew. Chem. Int. Edn.* **1998**, *37*, 2180-2192.

[21] A. E. Shilov, A. A. Shteinman, *Coord. Chem. Rev.* **1977**, *24*, 97-143.

[22] R. A. Periana, O. Mironov, D. Taubde, G. Bhalla, J. C. Jones, *Science* **2003**, *301*, 814-818.

[23] M. D. K. Boele, G. P. F. van Strijdonck, A: H. M. de Vries, P. C. J. Kamer, J. G. de Vries, P. W. N. M. van Leeuwen, *J. Am. Chem. Soc*. **2002**, *124*, 1586-1587.

[24] A. H. Janowicz, R. G. Bergman, *J. Am. Chem. Soc.* **1982**, *104*, 352-354.

[25] P. Foley, G. M. Whitesides, *J.Am. Chem. Soc.* **1979**,*101*, 2732-2733.

[26] M. A. Bennett, D. L. Milner, *Chem. Commun.***1967**, 581-582

[27] C. J. Moulton, B. L. Shaw, *J. Chem. Soc. Dalton. Trans.* **1976**, 1020-1024.

[28] M. E. van der Boom, D. Milstein, *Chem. Rev*. **2003**, *103*, 1759-1792.

[29] J. T. Singleton, *Tetrahedron* **2003**, *59*, 1837-1857.

[30] R. L. Bennett, M. I. Bruce, I. Matsuda, R. J. Nicholson, *J. Organomet. Chem.*, **1974,** *67***,** C72-C74.

[31] R. L. Bennett, M. I. Bruce F. G. A. Stone, *J. Organomet. Chem.*, **1975**, *94*, 65-74.

[32] R. L. Bennett, B. L. Goodall , I. Matsuda, *Aust. J. Chem*. **1975**, *28*, 1259-1264.

[33] R. L. Bennett, M. I. Bruce, B. L. Goodall, F. G. A. Stone, *Aust. J. Chem*. **1974**, *27*, 2132-2133.

[34] M. I. Bruce, M. J. Liddell, M. R. Snow, E. R. T. Tienkink, *Aust. J. Chem*. **1988**, *41*, 1407-1415.

[35] M. I. Bruce, B. L. Goodall, F. G. A. Stone, *J. Chem. Soc. Dalton. Trans*. **1978**, 687-694.

[36] R. M. Ceder, J. Sales, X. Solans, M. Font-Altaba, *J. Chem. Soc. Dalton Trans.* **1986**, 1351-1358.

[37] G. C. Martin, J. M. Boncella, E. J. Wucherer, *Organometallics* **1991**, *10*, 2804-2811.

[38] H. Werner, T. Daniel, W. Knaup, O. Nürnberg, *J. Organomet. Chem*. **1993**, *462*, 309-318.

[39] K. Hiraki, Y. Kinoshita, H. Ushiroda, S. Koyama, H. Kawano, *Chem. Lett.* **1997**, 1243-1244.

[40] K. R. Floewer, R. G. Pitchard, J. E. Warren, *Eur. J. Inorg. Chem*. **2003**, 1929-1938.

[41] S. Murai, F. Kakiuchi, S. Sekine, Y. Tanaka, A. Kamatani, M. Sonoda, N. Chatani, *Nature* **1993**, *366*, 529-561.

[42] K. Hiraki, M. Koizumi, S. Kira, H. Kawano, *Chem. Lett.* **1998**, 47-48.

[43] L.-Y. Huang, U. R. Aulwurm, F. W. Heinemann, F. Knoch, H. Kisch *Chem. Eur. J.* **1998**, *4*, 1642-1641.

[44] H. Werner, N. Mahr, J. Wolf, A. Fries, M. Laubender, E. Bleuel, R. Garde, P. Lahuerta, *Organometallics* **2003**, *22*, 3566-3576.

[45] C. Krug, J. F. Hartwig, *J. Am. Chem. Soc*. 2004, *126*, 2694-2695.

[46] P. Marcazzan, B. O. Patrick, B. R. James, *Organometallics* **2005**, *24,* 1445-1451.

[47] A. D. Ryabov, *Synthesis,* **1985**, 233-252.

[48] J. Albert, J. Granell, J. Sales, X. Solans, M. Font-Albata, *Organometallics* **1986**, *5*, 2567-2568.

[49] M. A. Esteruelas, E. G. Puebla, A. M. López, E. Oñate, J. I. Tolosa, *Organometallics* **2000**, *19*, 275-284.

[50] M. A. Esteruelas, A. Lledós, M. Oliván, E. Oñate, M. A. Tajada, G. Ujaque, *Organometallics* **2003**, *22*, 3753-3765.

[51] M. Crespo, X. Solans, M. Fonta-Bardia, *J. Organomet. Chem*. **1994**, *483,* 187-192.

[52] M. Crespo, X. Solans, M. Fonta-Bardia, *J. Organomet. Chem*. **1996**, *518*, 105-113.

[53] M. Crespo, X. Solans, M. Fonta-Bardia, *Polyhedron* **1998**,*17*, 1651-1657.

[54] C. Anderson, M. Crespo, X. Solans, M. Fonta-Bardia, *J. Organomet. Chem.* **2000**, *601*, 22-23.

[55] C. Anderson, M. Crespo, X. Solans, M. Fonta-Bardia, *J. Organomet. Chem.* **2000**, *604*, 178-185.

[56] C. Anderson, M. Crespo, F. D. Rochon, *J. Organomet. Chem.* **2001**, *631*, 164-174.

[57] M. Crespo, X. Solans, M. Fonta-Bardia, *Polyhedron* **2002**,*21*, 105-113.

[58] R. A. Sánchez-Delgado, M. Rosales, *Coord. Chem. Rev*. **2000**, *196*, 249-280.

[59] D. Seebach, *Angew. Chem. Int. Ed.* **1990**, *29*, 1320-1367.

[60] F. Kakiuchi, S. Murai, *Acc. Chem. Res*. **2002**, *35*, 826-834.

[61] S. Murai, F. Kakiuchi, S. Sekine, Y. Tanaka, A. Kamatani, M.Sonoda, N. Chatani, *Pure Appl. Chem.* **1994**, *66*, 1527-1534.

[62] M. Sonoda, F. Kakiuchi, N. Chatani, S. Murai, *J. Organomet. Chem*. **1995**, *504*, 151-152.

[63] F. Kakiuchi, Y. Tanaka, T. Sato, N . Chatani, S. Murai, *Chem. Lett*. **1995**, 679-680.

[64] F. Kakiuchi, Y. Yamamoto, N . Chatani, S. Murai, *Chem. Lett*. **1995**, 681-682.

[65] M. Sonoda, F. Kakiuchi, A. Kamatani, N. Chatani, S. Murai, *Chem. Lett*. **1996**, 109-110.

[66] N. Fuji, F. Kakiuchi, N . Chatani, S. Murai, *Chem. Lett*. **1996**, 939-640.

[67] S. Murai, N. Chatani, F. Kakiuchi, *Pure Appl. Chem.* **1997**, *69*, 589-594.

[68] N. Fuji, F. Kakiuchi, A. Yamada, N . Chatani, S. Murai, *Chem. Lett*. **1997**, 425-426.

[69] T. Sato, F. Kakiuchi, S. Murai, *Chem. Lett*. **1998**, 893-894.

[70] F. Kakiuchi, T. Sato, T. Tsujimoto, M. Yamauchi, N. Chatani S. Murai, *Chem. Lett*. **1998**, 1053-1054.

[71] F. Kakiuchi, T. Sato, M. Yamauchi, N. Chatani S. Murai, *Chem. Lett*. **1999**, 19-20.

[72] F. Kakiuchi, M. Sonoda, T. Tsujimoto, N. Chatani, S. Murai, *Chem. Lett.* **1999**, 1083-1084.

[73] F. Kakiuchi, P. Le Gendre, A. Yamada, H. Ohtaki, S. Murai, *Tetrahedron: Asymmetry*, **2001**, *11*, 2647-2651.

[74] F. Kakiuchi, T. Sato, N. Chatani, S. Murai, *Chem. Lett.* **2001**, 386-387.

[75] F. Kakiuchi, T. Tsujimoto, M. Sonoda, N. Chatani, S. Murai, *Synlett*, **2001**, 948.

[76] T. Tsujimoto, H. Ohtaki, M. Sonoda, N. Chatani, S. Murai, *Chem. Lett.* **2001**, 918-919.

[77] F. Kakiuchi, T. Uetsuhara, Y. Tanaka, N. Chatani, S. Murai, *J. Mol. Catal. A: Chem.* **2002**, *182-183*, 511-514.

[78] F. Kakiuchi, M. Matsumoto, M. Sonoda, T. Fukuyama, N. Chatani, S. Murai, *Chem. Lett*. **2000**, 750-751.

[79] F. Kakiuchi, K. Igi, M. Matsumoto, N. Chatani, S. Murai, *Chem. Lett*. **2001**, 750-751.

[80] F. Kakiuchi, K. Igi, M. Matsumoto, T. Hayamizu, N. Chatani,S . Murai, *Chem. Lett*. **2002**, 396-397.

[81] T. Matsubara, N. Koga, D. G. Musaev, K.Morokuma, *Organometallics* **2000**, *19*, 2318-2329.

[82] F. Kakiuchi, M. Yamauchi, N. Chatani, S. Murai, *Chem. Lett*. **1996**, 111-112.

[83] N. Chatani, Y. Ishii, Y. Ie, F. Kakiuchi, S. Murai, *J. Org. Chem*. **1998**, *63*, 5129-5136.

[84] C.-H. Jun, J.-B. Hong, Y.–H. Kim, K.–Y. Kim,K.-Y. Chung, *Angew. Chem. Int. Ed.* **2000**, *39*, 3440-3442.

[85] N. Miyaura, A. Suzuki, *Chem. Rev*. **1995**, *95*, 2457-2483.

[86] A. Suzuki, *J. Organomet. Chem.* **1999**, *576*, 147-168.

[87] H. Weissman, D. Milstein, *Chem. Commun*. **1999**, 1901-1902.

[88] R. B. Bedford, C. S. J. Cazin, M. B. Hursthouse, M. E. Light, k. J. Pike, S. Wimperia, *J. Organomet. Chem.* **2001**, *633*, 173-181.

[89] R. B. Bedford, C. S. J. Cazin, *Chem. Commun*. **2001**, 1540-1541.

[90] R. B. Bedford, C. S. J. Cazin, S. J. Coles, T. Gebrich, M. B. Hursthouse, V. J. M., Scordia, *Dalton Trans.* **2003**, 3350-3356.

[91] R. B. Bedford, C. S. J. Cazin, *Organometllaics* **2003**, *22*, 987-999.

[92] B. L. Small, M. Brookhart, A. M. A. Bennett, *J. Am. Chem. Soc*. **1998**, *120*, 4090-4050.

[93] S. A. Svejda, M. Brookhart, *Organometallics* **1999**, *18*, 65-74.

[94] D. P. Gates, S. A. Svejda, E. Oñate, C. M. Killian, L. K. Johnson, P. S. White, M. Brookhart, *Macromolecules* **2000**, *33*, 2320-2334.

[95] G. J. P. Britovsek, V. C. Gibson, B. S. Kimbedrely, P. J. Maddox, S. J. McTavish, G. A. Solan, A. J. P. White, D. J. Williams, *Chem. Commun*. **1998**, 849-850.

[96] B. L. Small, M. Brookhart, *J. Am. Chem. Soc*. **1998**, *120*, 7143-7144.

[97] L. K. Johnson, C. M. Killian, M. Brookhart, *J. Am. Chem. Soc*. **1995**, *117*, 6414-6415.

[98] C. M. Killian, D. J. Tempel, L. K. Johnson, M. Brookhart, *J. Am. Chem. Soc*. **1996**, *118*, 11664.

[99] S. Mecking, L. K. Johnson, L. Wang, M. Brookhart, *J. Am. Chem. Soc.* **1998**, *120*, 888.

[100] L. K. Johnson, S. Mecking, M. Brookhart, *J. Am. Chem. Soc*. **1996**, *118*, 267-268.

[101] G. J. P. Britovsek, V. C. Gibson, O. D. Hoarau, S. K. Spitzmesser, A. J. P. White, D. J. Williams, *Inorg. Chem*. **2003**, *42*, 3454-3465.

[102] G. J. P. Britovsek, M. Bruce, V. C. Gibson, B. S. Kimberely, P. J. Maddox, S. Mastroianni, S. J. McTavish, D: J: Williams, *J. Am. Chem. Soc*. **1999**, *121*, 8728-8740.

[103] G. J. P. Britovsek, V. C. Gibson, S. K. Spitzmesser, K. P. Tellmann, A. J. P. White, D. J. Williams, *J. Chem. Soc. Dalton. Trans*. **2002**, 1159-1171.

[104] G. J. P. Britovsek, V. C. Gibson, D. F. Wass, *Angew. Chem. Int. Ed*. **1999**, *38*, 428-447.

[105] R. H. Crabtree, *The Organometallic Chemistry of the Transition Metals,* 3rd Ed, John Wiley & Sons, New York, **2001**.

[106] H.-F. Klein, *Angew. Chem. Int. Ed. Engl.* **1980**, *19*, 362-375.

[107] C. A. Tolman, *Inorg. Chem*. **1972**, *11*, 3128-3129.

[108] A. C. Cope, R. W. Siekman, *J. Am. Chem. Soc*. **1965**, *87*, 3272-3273.

[109] A. C. Cope, E. C. Friedrich, *J. Am. Chem. Soc*. **1968**, *90*, 909-913.

[110] I. Omae, *Chem. Rev*. **1979**, *79*, 287-321.

[111] M. I. Bruce, *Angew. Chem*. **1977**, *89*, 75-89.

[112] A. D. Ryabov, *Chem. Rev.* **1990**, *90*, 403-424.

[113] K. R. Flower, V. J. Howard, R. G. Pritchard, J. E. Warren, *Organometallics* **2002**, *21*, 1184 -1189.

[114] J. Dupont, M. Pfeffer, J. Spencer, *Eur. J. Inorg. Chem*. **2001**, 1917-1927.

[115] A. W. Kleij, R. J. M. K. Gebbink, H. Kooijman, M. Lutz, A. L. Spek, G. Van Koten, *Organometallics* **2001**, *20*, 634-647.

[116] A. Sundermann, O. Uzman, J. M. L. Martin, *Chem. Eur. J.* **2001**, *7*, 1703-1711.

[117] V. V. Grushin, N. Herron, D. D. LeCloux, W. J. Marshall, V. A. Petrov, Y. Wang, *Chem. Commun.***2001**, 1494-1495.

[118] B. B. Eran, D. Singer, K. Praefcke, *Eur. J. Inorg. Chem*. **2001**, 111-116.

[119] P. A. Bonnardel, R. V. Parish, R. G. Pritchard, *J. Chem. Soc. Dalton Trans.* **1996**, 3185-3193.

[120] M. B. Dinger, W. J. Henderson, *J. Organomet. Chem*. **1998**, *560*, 233-241

[121] M. I. Bruce, M. Z. Iqbal, F. G. A. Stone, *J. Chem. Soc. A*. 1970, 3204-

[122] M. I. Bruce, *Chem. Commun*. **1971**, 1595-1596.

[123] R. H. Crabtree, H. Felkin, T. Fillebeen-Khan, C. Pascard, J. M. Quirk, *J. Organomet. Chem.* **1980**, *187*, C32-C36.

[124] G. M. Whitesides, *J. Am. Chem. Soc*. **1981**, *103*, 948-949.

[125] M. I. Bruce, *J. Organomet. Chem*. **1971**, *31*, 275-281.

[126] S. Trofimenko, *Inorg. Chem.* **1973**, *12*, 1215 -1221.

[127] H.- F. Klein, S. Camadanli, R. Beck, D. Leukel, U. Flörke, *Angew. Chem. Int. Ed.* **2005**, *44*, 975-977.

[128] J. N. Coalter, W. E. Streib, K. G. Caulton, *Inorg. Chem.* **2000**, *39*, 3749-3756.

[129] M. A. Esteruelas, F.J. Lahoz, A. M. Lopez, E. Oñate, L.A. Oro, *Organometallics* **1995**, *14*, 2496-2500.

[130] G. Barea, M. A. Esteruelas, A. Lledós, A. M. Lopez, E. Oñate, J. I. Tolosa, *Organometallics* **1998**, 4065-4076.

[131] A.G. Orpen, L. Brammer, F.H. Allen, O. Kennard, D.G. Watson, R.Taylor, *J. Chem. Soc. Dalton. Trans*. **1989**, S1-S83.

[132] H.-W. Frühauf, G. Wolmershäuser, *Chem. Ber.* **1982**, *115*, 1070-1082.

[133] R. Bau, H. S. H. Yuan, M. V. Baker, L. Field, *Inorg. Chim. Acta* **1986**, *114*, L27-L28.

[134] M. V. Baker, L. Field, *Appl. Organomet. Chem.* **1990**, *4(5)*, 543-549.

[135] H.- W. Frühauf, R. Siebenlist, K. Vrieze, *Organometallics* **2002**, *21*, 5628-5641.

[136] A. Dedieu, *Transition Metal Hydrides*, VCH, New York, **1992**.

[137] C. Masters, *Homogenous Catalysis,* Chapman, Hall, London, **1981**.

[138] G. W. Parshall, *Homogenous Catalysis*, Wiley-Interscience, New York, **1980**.

[139] R. B. Jordan, *Reaction Mechanisms of Inorganic and Organometallic Systems,* Oxford University Press, Oxford, **1991**.

[140] J. L. Kersten, A. L. Rheingold, K. H. Theopold, C. P. Casey, *Angew. Chem.* **1992**, *31*, 1341-1343.

[141] M. Barrow, N.L. Cromhout, D. Cunningham, A. R. Manning, P. McArdle, *J. Organomet. Chem.* **2000**, *612*, 61-68.

[142] M. Barrow, N.L. Cromhout, A. R. Manning, J. F. Gallagher, *J. Chem. Soc.Chem. Dalton Trans.* **2001**, 1352-1358.

[143] M. V. Baker, L. D. Field, *Organometallics* **1986**, *5*, 821-823.

[144] M. V. Baker, L. D. Field, *J. Am. Chem. Soc.* **1986**, *108*, 7433-7434.

[145] M. V. Baker, L. D. Field, *J. Am. Chem. Soc.* **1987**, *109*, 2825-2826.

[146] L. D. Field, A. V. George, B. A. Messerle, *Chem. Commun.* **1991**, 1339-1341.

[147] M. D. Fryzuk, W. E. Piers, *Organometallics* **1990**, *9*, 986-998.

[148] G. C. Martin, J. M. Boncella, *Organometallics* **1989**, *8*, 2968-2970.

[149] O. Lopez, M. Crespo, M. Font-Bardia, X. Solans, *Organometallics* **1997**, *16*, 1233-1240.

[150] D. A. Knight, M. A. Dewey, G. A. Stark, B. K. Bennett, A. M. Arif, J. A. Gladysz, *Organometallics* **1993**, *12*, 4523-4534.

[151] J. W. Faller, Y. Ma, C. J. Smart, M. J. DiVerdi, *J. Organomet. Chem.* **1991**, *420*, 237-252.

[152] Y. Makioka, Y. Taniguchi, Y. Fujiwara, K. Takaki, Z. Hou, Y. Wakatsuki, *Organometallics* **1996**, *15*, 5476-5478.

[153] R. J. Cross, M. F. Davidson, M. Rocamora, *J. Chem. Soc. Dalton Trans.* **1988**, 1147-1152.

[154] H. B. Burgi, J. D. Dunitz, *Helv. Chim. Acta* **1970**, *53*, 1747-1764.

[155] A. J. Carty, G. N. Mott, N. J. Taylor, *J. Organomet. Chem.* **1979**, *182*, C69-C73.

[156] R. C. Kerber, *Comprehensive Organometallic Chemistry II*, Pergamon, Vol 7, **1995.**

[157] G. O. Spessard, G. L. Miessler, *Organometallic Chemistry*, Prentice Hall, NJ, **1996**.

[158] G. W. Parshall, J. Mrowca, *Advan. Chem Ser.*. **1971**, *76*, 219-247.

[159] K. Fagnon, M. Lautens, *Angew. Chem. Int. Ed.* **2002**, *41*, 26-47.

[160] A.R. Manning, D. Cunningham, J. F. Gallagher, *Inorg. Chim. Acta* **2002**, *37*, 98-107.

[161] T. R. Cundari, P. L. Holland, *Organometallics* **2004**, *23*, 5226-5239.

[162] H.-W.Frühauf, N. Feiken, P. Schreuder, R. Siebenlist, K. Vrieze *Organometallics* **1996**, *15*, 2148-2169.

[163] P. J. Chirik, E. Lobkovsky, A. K. Schmisseur, S. C. Bart, E. J. Hawrelak, *Organometallics* **2004**, *23*, 237-246.

[164] B. L. Small, M. Brookhart, *Macromolecules* **1999**, *32*, 2120-2130.

[165] G. J. P. Britovsek, S. Mastroianni, G. A. Solan, S. P. D. Baugh, C. Redshaw, V. C. Gibson, A. J. P. White, D. J. Williams, M. R. J. Elsegood, *Chem. Eur. J.* **2000**, *6*, 2221-2231.

[166] G. J. P. Britovsek, V. C. Gibson, S. Mastroianni, D. C. H. Oakes, C. Redshaw, G. A. Solan, A. J. P. White, D. J. Williams, *Eur. J. Inorg. Chem.* **2001**, 431-437.

[167] G. Bellachioma, G. Cardaci, A. Macchioni, G. Reichenbach, E. Foresti, P. Sabatino, *J. Organomet. Chem.* **1997**, *531*, 227-235.

[168] A. G. Orpen , L. Brammer, F. H. Allen, O. Kennard, D. G. Watson, R. Taylor, *Structure Correlation* , Vol.2, VCH, Weinheim, **1994**.

[169] R. M. Cravero, M. Gonzalez-Sierra, A. C. Oliveri, *J. Chem. Soc. Perkin Trans. II* **1993**, 1067-1071.

[170] Z. Chen, H. W. Schmalle, T. Fox, H. Berke *Dalton Trans*. **2005**, 580-587.

[171] F.P. Liang, H. W. Schmalle, T. Fox, H. Berke, *Organometallics* **2000**, *19*, 1950-1962.

[172] J. Höck, H. Jacobsen, H. W. Schmalle, G. R. J. Artus, T. Fox, J. I. Amor, F. Bäth, H. Berke *Organometallics* **2001**, *20*, 1533-1544.

[173] M. R. Meneghetti, M. Grellier, M. Pfeffer, J. Dupont, J. Fischer, *Organometallics* **1999**, *18*, 5560-5570.

[174] G. M. Sheldrick, C. Krüger, R. Goddard, *Acta. Crytallogr. Sect. A* **1990**, *46*, 467-473.

[175] G. M. Sheldrick, C. Krüger, R. Goddard, *SHELXS –97 and SHELXL-97*, Universität Göttingen **1997.**

[176] H.–F. Klein, R. Beck, U. Flörke, H.–J. Haupt, *Eur. J. Inorg. Chem*. **2003**, 240-248.

[177] H.–F. Klein, S. Schneider, M. He, U. Flörke, H.-J. Haupt, *Eur. J. Inorg. Chem*. **2000**, 2295-2301.

[178] H.–F. Klein, M. Helwig, U. Koch, U. Flörke, H.-J. Haupt, *Z. Naturforsch.* **1993**, *48b*, 778-784.

[179] G. W. Parshall, *Acc. Chem. Res.* **1977**, *3*, 139-144.

[180] B. L. Shaw, *J. Chem. Soc. Dalton Trans.* **1976**, 1020-1024.

[181] M. Kilner, *Adv. Organomet. Chem*. **1972**, *10*, 115-198.

[182] M. I. Bruce, B. L. Goodall, *The Chemistry of Hydrazo-, Azo-, and Azoxy-Groups*, Vol1, John Wiley&Sons, New York, **1975**.

[183] G. S. Ashby M. I. Bruce, I. B. Tomkins, R. C. Wallis, *Austr. J. Chem*. **1979**, *32*, 1003-1016.

[184] H.-F. Klein, U. Lemke, M. Lemke, A. Brand, *Organometallics* **1998**, *17*, 4196-4201.

[185] H.-F. Klein, R. Beck, U. Flörke, H.-J. Haupt, *Eur. J. Inorg. Chem* **2002,** 3305-3312.

[186] H.-F. Klein, A. Brand, G. Cordier, *Z. Naturforsch*. **1998**, *53b*, 307-314.

[187] H.-F. Klein, R. Beck, U. Flörke, H.-J. Haupt *Eur. J. Inorg. Chem* **2003,** 853-862.

[188] R. Beck, *Dissertation*, Technische Universität Darmstadt, **2001**.

[189] H.-F. Klein, R. Beck, *unpublished results*.

[190] R. M. Ceder, J. Granell, G. Muller, M. Font-Bardia, X. Solans, *Organometallics*, **1995**, *14*, 5544-5551.

[191] R. M. Ceder, J. Granell, G. Muller, *J. Chem. Soc. Dalton Trans.* **1998**, 1047-1051.

[192] L. Brammer , *J. Chem. Soc. Dalton Trans.* **2003**, 3145-3157.

[193] M. A. Esteruelas, F. J. Lahoz, M. Olivan, E. Onate, L. A. Oro, *Organometallics* **1994**, *13*, 3315-3323.

[194] W. J. Youngs, J. D. Kinder, J. D. Bradshaw, C. A. Tessier, *Organometallics* **1993**, *12*, 2406-2407.

[195] H.-F. Klein, A. Schmidt, U. Floerke, H.-J. Haupt, *Angew. Chem. Int. Ed.* **1998**, *37*, 2385-2387.

[196] H. Werner, M. Müller, P. Steinert *Z. Anorg. Allg. Chem.* **2003**, *629*, 1337-1346.

[197] E. Kogut, A. Zeller, T. H. Warren, T. Strassner, *J. Am. Chem. Soc.* **2004**, *126,* 11984-11994

[198] H. R. Keable, M. Kilner, E. E. Robertson, *J. Chem. Soc. Dalton Trans.* **1974**, 639-644.

[199] T. Carofiglio, S. Stella, C. Floriani, A. Chiesi-Villa, C. Guastini, *J. Chem. Soc. Dalton Trans.* **1989**, 1957-1962.

[200] H.-F. Klein, H. H. Karsch, *Chem. Ber*. **1974**, *107*, 537-546.

[201] H.-F. Klein, H. H. Karsch, *Chem. Ber*. **1972**, *105*, 2628-2636.

[202] A. Yamamoto, *Organotransition Metal Chemistry*, Wiley, New York, **1990**.

[203] T. P. Fehlner, *Adv. Organomet. Chem.* **1990**, *30*, 189-242.

[204] L. Main, B. K. Nicholson, *Adv. Met. Org. Chem.* **1994**, *3*, 1-50.

[205] L. H. P. Gommans, L. Main, B. K. Nicholson, *J. Chem. Soc. Chem. Commun.* **1987**, 761-762.

[206] R. C. Cambie, M. R. Metzler, P.S. Rutledge, P. D. Woodgate, *J. Organomet. Chem.* **1992**, *429*, 41-59.

[207] R. C. Cambie, P.S. Rutledge, D. R. Welch, P. D. Woodgate, *J. Organomet. Chem.* **1994**, *467*, 237-244.

[208] M. L. H. Green, J. Haggitt, C. P. Mehnert, *J. Chem. Soc. Chem. Commun.* **1995**, 1853-1854.

[209] Spectral Database for Organic Compounds, *http://www.aist.go.jp/RIODB/SDBS/menu-e.html*, AIST, Japan.

[210] H.-F. Klein, E. Auer, A. Dal, U. Lemke, M. Lemke, T. Jung, C. Röhr, U. Röhr, U. Flörke, H.-J. Haupt, *Inorg. Chim. Acta* **1999**, *287*, 167-172.

[211] H.-F. Klein, A. Bickelhaupt, T. Jung, G. Cordier, *Organometallics*, **1994**, *13*, 2557-2559.

[212] H.-F. Klein, A. Bickelhaupt, B. Hammerschmidt, U. Flörke, H.–J. Haupt, *Organometallics* **1994**, *13*, 2944-2950.

[213] T. Matsubara, N. Koga, d. G. Musaev, K. Morokuma, *J. Am. Chem. Soc.* **1998**, *120*, 12692-12693.

[214] M. J. S. Dewar, *Bull. Soc. Chim. Fr*. **1951**, *18*, C71-C79.

[215] J. Chatt, L. A. Duncanson, *J. Chem. Soc.* **1973**, *12*, 2939-2947.

[216] R. Countryman, B.R. Penfold, *J. Cryst. Mol. Struct.* **1972**, *2*, 281-290.

[217] T. T. Tsou, J. C. Huffman, J. K. Kochi, *Inorg. Chem*. **1979**, *18*, 231-2317.

[218] J. H. Clark, B. Wails, T. W. Bastock, *Aromatic Fluorination,* CRC Press, Boca Raton, **1996**.

[219] C. F. Rodriguez, D. K. Bohme, A. C. Hopkinson, *J. Phys. Chem*. **1996**, *100*, 2942-2949.

[220] S. Papasavva, K. H. Illinger, J. E. Kenny, *J. Phys. Chem*. **1996**, *100*, 10100-10110.

[221] P. J. Crutzen, *Angew. Chem. Int. Ed.* **1996**, *35*, 1758-1777.

[222] M. Molina, *Angew. Chem. Int. Ed.* **1996**, *35*, 1778-1785.

[223] F. S. Rowland, *Angew. Chem. Int. Ed.* **1997**, *35*, 1787-1798.

[224] J. Burdeniuc, B. Jedlicka, R. H. Crabtree, *Chem. Ber*. **1997**, *130*, 145-154.

[225] M. Aizenberg, D. Milstein, *Science* **1994**, *265*, 359-361.

[226] M. Aizenberg, D. Milstein, *J. Am. Chem. Soc.* **1994**, *265*, 359-361.

[227] A. D. Selmeczy, W. D. Jones, M. G. Partridge, N. R. Perutz, *Organometallics*, **1994**, *13*, 522-532.

[228] R. Bosque, E. Clot, S. Fantacci, F. Maseras, O. Eisenstein, R. N. Perutz, K. B. Renkema, K. G. Caulton, *J. Am. Chem. Soc.* **1998**, *120*, 12634-12640.

[229] M. K. Whittlesey, R. N. Perutz, M. H. Moore, *J. Chem. Soc. Chem. Commun*. **1996**, 787-788.

[230] P. Barrio, R. Castarlenas, M. A. Esteruelas, A. Lledós, F. Maseras, E. Oate, J. Tomàs, *Organometallics* **2001**, *20*, 442-452.

[231] T. G. Richmond, C. E. Osterberg, M. A. Arif, *J. Am. Chem. Soc. 1987, 109,* 8091-8092.

[232] B. L. Lucht, M. J. Poss, M. A. King, T. G. Richmond, *J. Chem. Soc. Chem. Commun.* **1991**, 400-401.

[233] J. L. Kilinger, M. A. King, M. A. Arif, T. G. Richmond *Organometallics*, **1993**, 12, 3382-3384.

[234] M. Crespo, M.Martinez, J. Sales, *J. Chem. Soc. Chem. Commun.***1992**, 822-823.

[235] C. M. Anderson, M. Crespo, G. Fergusin, A. J. Lough, R. J. Puddephatt, *Organometallics* **1992**, 11, 1177-1181.

[236] M. Crespo, M. Martinez, E. de Pablo, *J. Chem. Soc. Dalton. Trans*. **1997**, 1231-1235.

[237] M. D. Su, S.-Y. Chu, *J. Am. Chem. Soc.* **1997**, *119*, 10178-10185.

[238] H.–F. Klein, S. Camadanli, R. Beck, U. Flörke, *Chem. Commun*. **2005**, 381-382.

[239] M. Crespo, M. Font-Bardia, S. Perez, X. Solans, *J. Organomet. Chem.* **2002**, *642*, 171-178.

[240] M. Pfeffer, N. S. Beydoun, A. de Cian, J. Fischer, *J. Organomet. Chem.* **1993**, *453*, 139-146.

[241] S. Mao, *Dissertation*, Technische Universität Darmstadt, **1999**.

[242] A. Polo, C. Claver, S. Castillon, A. Ruiz, J. C. Bayon, J. Real, C.Mealli, D. Masi, *Organometallics* **1992**, *11*, 3525-3533.

[243] J. Albert, J. Granell, J. Sales, M. Font-Bardia, X. Solans, *Organometallics*, **1995**, *14*, 1393-1404.

[244] M. Crespo, x. Solans, M. Font-Bardia, *J. Organomet. Chem*. **1994**, *483*, 187-192

[245] J. Albert, R. Bosque, J. Granell, R. Tavera, *Polyhedron* **2001**, *20*, 3225-3229.

[246] J. Albert, M. Cadena, A. Gonzalez, J. Granell, M. Font-Bardia, X. Solans, *J. Organomet. Chem*. **2002**, *663*, 277-283.

[247] J. Albert, M. Cadena, A. Gonzalez, J. Granell, M. Font-Bardia, X. Solans, *J. Organomet. Chem*. **2004**, *689*, 4889-4896.

[248] M. Crespo*, Polyhedron* **1996**, *15*, 1981-1988

[249] M. Crespo, M. Martinez, E. de Pablo, *J. Chem. Soc. Dalton Trans.* **1997***,* 1231-1235.

[250] C. Venturi, G. Bellachioma, G. Cardaci, A. Macchioni *Inorg. Chim. Acta* **2004**, *357*, 3172-3720.

[251] L.-C. Song, G.-L. Lu, Q.-M. Hu, H.-T. Fan, J. Chen, J. Sun, X.-Y. Huang, *J. Organomet. Chem.* **2001**, *627*, 255-262.

[252] H. König, *Dissertation*, Technische Universität Darmstadt, **1991**.

[253] D. J. Mindiola, G. L. Hillhouse, *J. Am. Chem. Soc.* **2001**, *123*, 4623-4624.

[254] A. E. Shilov, G. B. Shul´pin, *Chem. Rev*. **1997**, *97*, 2879-2932.

[255] L. Castelhano, D. J. Griller, *J. Am. Chem. Soc.* **1982**, *104*, 3655-3659.

[256] W. D. Jones, F. J. Feher, *Acc. Chem. Res*. **1989**, *22*, 91-100.

[257] J. Halpern, *Inorg. Chim. Acta*. **1985**, *100*, 41.

[258] H.-F. Klein, X. Li, H. Sun, R. Beck, U. Floerke, H.-J. Haupt, *Inorg. Chim. Acta*, **2000**, *298*, 63-69.

[259] H.-F. Klein, H. H. Karsch, *Chem. Ber.* **1975**, *108*, 944-955.

[260] F. Bernardi, A. Bottoni, M. Nicastro, I. Rossi, *Organometallics* **2000**, *19*, 2170-2178.

[261] W. Strohmeier, *Chem. Ber*. **1955**, *88*, 1212 - 1223.

[262] M. Schulze, *Angew. Chem.* **1958**, *70*, 697 - 699.

[263] W. Wolfsberger, H. Schmidbaur, *Syn. React. Inorg. Metal-Org. Chem.* **1974**, *4*, 149 - 156.

[264] H. H. Karsch, *Chem. Ber.* **1977**, 110, 2222-2235.

[265] H. H. Karsch, *Chem. Ber.* **1977**, 110, 2699-2711.

[266] H.-F. Klein, H. H. Karsch, H. Schmidbaur, *Chem. Ber.* **1977**, *110*, 2200-2212

[267] H.-F. Klein, H. H. Karsch, *Chem. Ber.* **1976**, *109*, 1453-1464.

[268] H.-F. Klein, H. H. Karsch, *Inorg. Chem.* **1975**, 473-477.

[269] K. A. Jensen, O. Dahl, *Acta Chem. Scand*. **1968**, 3, 1044-1045.

[270] H.-F. Klein, H. H. Karsch, *Chem. Ber.* **1973**, 106, 1433-1452.

[271] H.-F. Klein, H. H. Karsch, *Chem. Ber.* **1972**, 105, 2628-2636.

[272] F. J. Weibert, S. S. Hall, *J.Org. Chem*. **1987**, 52, 3901-3904.

[273] H. G. Richey, *J.Org. Chem*. **1983**, 48, 4349-4357.

[274] W. Imhof, *Organometallics* **1999**, 18, 4845-4855

[275] L. Cronenberger, *Bullet. de la Soc. de Chim. Bio.* **1964**, 46(5-6), 703-15.

6 DANK

Mein besonderer Dank gilt Prof. Dr. H.-F. Klein

für die mir gewährte Freiheit, die stete Bereitschaft zu wissenschaftlichen Diskussion und die Förderung bei der Anfertigung dieser Arbeit.

Ferner danke ich:

Herrn Prof. Dr. W.-D. Fessner für seine Tätigkeit als Mitberichterstatter.

den Sekretärinen Frau T. Solms de Bercher und Frau K. Heinze.

insbesondere Dr. R. Beck für die anregende Arbeitsatmosphäre im gemeinsamen Labor und viele fruchtbare Diskussionen und meinen Kollegen Dipl.-Ing. M. Frey, Dr. A. Ländner und H. Benour für ihre freundliche Kooperation und ihre Geduld.

für die Durchführung und Lösung der Röntgenstrukturanalyse aller vorgestellten Verbindungen, Herrn Dr. U. Flörke von der Universität/GH Paderborn, sowie Herrn Dr. R. Beck vom Eduard-Zintl-Institut für Anorganische und Physikalische Chemie der Technischen Universität Darmstadt.

für die Elementaranalysen luftstabiler Substanzen Frau R. Lewerenz.

für die Aufnahme der NMR-Spektren Herrn Dr. R. Meusinger, Herrn Dipl.-Ing. K. O. Runzheimer und Frau K. Jungk vom Institut für Organische Chemie der TU Darmstadt, sowie für die aufwendigen Tieftemperaturmessungen bei Frau J. Wendlig.

Frau E. Pfeifer und Herrn Dr. K. J. Wannowius für ihre Gastfreundschaft und für die herzliche Aufnahme in Darmstadt und Spachbrücken .

den Mitarbeitern der Chemikalienausgabe Frau A. Przewosnik und F. Toran, sowie Herrn G. Wittmann für die Glasbläserarbeiten.

allen ehemaligen Mitarbeitern der Arbeitsgruppe Anorganische Chemie I, Herrn Dr. U. Möller, Dr. A. Dal, Dr. O. Hetche und Frau W. Litzius für das gute Betriebsklima und die sehr gute Zusammenarbeit.

8 SUPPLEMENTARY DATA

1. Crystallographic data of complex **1**
2. Crystallographic data of complex **2**
3. Crystallographic data of complex **3**
4. Crystallographic data of complex **4**
5. Crystallographic data of complex **6**
6. Crystallographic data of complex **7**
7. Crystallographic data of complex **8**
8. Crystallographic data of complex **10**
9. Crystallographic data of complex **14**
10. Crystallographic data of complex **15**
11. Crystallographic data of complex **16**
12. Crystallographic data of complex **17**
13. Crystallographic data of complex **19**
14. Crystallographic data of complex **22**
15. Crystallographic data of complex **24**
16. Crystallographic data of complex **28**
17. Crystallographic data of complex **29**
18. Crystallographic data of complex **30**
19. Crystallographic data of complex **31**
20. Crystallographic data of complex **32**
21. Crystallographic data of complex **33**
22. Crystallographic data of complex **37**
23. Crystallographic data of complex **39**
24. Crystallographic data of complex **41**
25. Crystallographic data of complex **42**
26. Crystallographic data of complex **44**

8.1 Crystal data and structure refinement for 1

Empirical formula	C22 H38 Fe N P3	
Formula weight	465.29	
Temperature	293(2) K	
Wavelength	0.71073 Å	
Crystal system	triclinic	
Space group	P-1	
Unit cell dimensions	a = 9.2765(12) Å	α = 65.433(9)°.
	b = 11.4028(13) Å	β = 78.456(10)°.
	c = 13.4638(16) Å	γ = 74.800(10)°.
Volume	1243.2(3) $Å^3$	
Z	2	
Density (calculated)	1.243 Mg/m^3	
Absorption coefficient	0.807 mm^{-1}	
F(000)	496	
Crystal size	0.15 x 0.2 x 0.5 mm^3	
Theta range for data collection	1.67 to 26.92°.	
Index ranges	-11<=h<=11, -14<=k<=14, -17<=l<=17	
Reflections collected	18486	
Independent reflections	5253 [R(int) = 0.0990]	
Completeness to theta = 26.92°	97.7 %	
Refinement method	Full-matrix least-squares on F^2	
Data / restraints / parameters	5253 / 0 / 396	
Goodness-of-fit on F^2	1.109	
Final R indices [I>2sigma(I)]	R1 = 0.0294, wR2 = 0.0778	
R indices (all data)	R1 = 0.0317, wR2 = 0.0791	
Largest diff. peak and hole	0.461 and -0.517 $e.Å^{-3}$	

8.2 Crystal data and structure refinement for 2

Empirical formula	C20 H42 Fe N P3	
Formula weight	445.31	
Temperature	298(2) K	
Wavelength	0.71073 Å	
Crystal system	Orthorhombic	
Space group	Pnma	
Unit cell dimensions	a = 9.6581(7) Å	α= 90°.

	b = 13.5905(10) Å	β= 90°.
	c = 18.7569(14) Å	γ = 90°.
Volume	2462.0(3) $Å^3$	
Z	4	
Density (calculated)	1.201 Mg/m^3	
Absorption coefficient	0.812 mm^{-1}	
F(000)	960	
Crystal size	0.40 x 0.20 x 0.18 mm^3	
Theta range for data collection	1.85 to 28.20°.	
Index ranges	-11<=h<=12, -18<=k<=18, -24<=l<=24	
Reflections collected	29358	
Independent reflections	3145 [R(int) = 0.0486]	
Completeness to theta = 28.20°	99.8 %	
Absorption correction	Semi-empirical from equivalents	
Max. and min. transmission	0.948 and 0.744	
Refinement method	Full-matrix least-squares on F^2	
Data / restraints / parameters	3145 / 0 / 143	
Goodness-of-fit on F^2	0.997	
Final R indices [I>2sigma(I)]	R1 = 0.0378, wR2 = 0.1010	
R indices (all data)	R1 = 0.0483, wR2 = 0.1098	
Largest diff. peak and hole	0.493 and -0.299 $e.Å^{-3}$	

8.3 Crystal data and structure refinement for 3

Empirical formula	C23 H40 Fe N P3	
Formula weight	479.32	
Temperature	298(2) K	
Wavelength	0.71073 Å	
Crystal system	Triclinic	
Space group	P-1	
Unit cell dimensions	a = 9.2537(4) Å	α = 94.603(1)°.
	b = 9.3794(4) Å	β = 90.404(1)°.
	c = 14.8576(6) Å	γ = 93.928(1)°.
Volume	1282.27(9) $Å^3$	
Z	2	
Density (calculated)	1.241 Mg/m^3	
Absorption coefficient	0.784 mm^{-1}	
F(000)	512	

Crystal size	0.45 x 0.30 x 0.20 mm^3
Theta range for data collection	2.18 to 28.24°.
Index ranges	-12<=h<=12, -12<=k<=12, -19<=l<=18
Reflections collected	16331
Independent reflections	6316 [R(int) = 0.0194]
Completeness to theta = 28.24°	99.6 %
Absorption correction	Semi-empirical from equivalents
Max. and min. transmission	0.992 and 0.805
Refinement method	Full-matrix least-squares on F^2
Data / restraints / parameters	6316 / 0 / 263
Goodness-of-fit on F^2	1.067
Final R indices [I>2sigma(I)]	R1 = 0.0365, wR2 = 0.1005
R indices (all data)	R1 = 0.0438, wR2 = 0.1048
Largest diff. peak and hole	0.683 and -0.214 $e.Å^{-3}$

8.4 Crystal data and structure refinement for 4

Empirical formula	C18 H38 Fe N P3	
Formula weight	417.25	
Temperature	150(2) K	
Wavelength	0.71073 Å	
Crystal system	triclinic	
Space group	P-1	
Unit cell dimensions	a = 8.6470(14) Å	α=103.140(16)°.
	b = 14.882(4) Å	β= 95.330(13)°.
	c = 17.814(3) Å	γ = 90.060(17)°.
Volume	2222.1(7) $Å^3$	
Z	4	
Density (calculated)	1.247 Mg/m^3	
Absorption coefficient	0.895 mm^{-1}	
F(000)	896	
Crystal size	0.25 x 0.2 x 0.1 mm^3	
Theta range for data collection	1.62 to 26.86°.	
Index ranges	-10<=h<=10, -18<=k<=18, -22<=l<=22	
Reflections collected	26214	
Independent reflections	9308 [R(int) = 0.0727]	
Completeness to theta = 26.86°	97.7 %	
Refinement method	Full-matrix least-squares on F^2	

Data / restraints / parameters	9308 / 0 / 778
Goodness-of-fit on F^2	1.053
Final R indices [I>2sigma(I)]	R1 = 0.0526, wR2 = 0.1186
R indices (all data)	R1 = 0.0744, wR2 = 0.1274
Largest diff. peak and hole	1.753 and -0.440 e.Å^{-3}

8.5 Crystal data and structure refinement for 6

Empirical formula	C23 H40 Fe N P3	
Formula weight	479.32	
Temperature	150(2) K	
Wavelength	0.71073 Å	
Crystal system	monoclinic	
Space group	P 21/n	
Unit cell dimensions	a = 8.6450(6) Å	α= 90°.
	b = 17.2303(9) Å	β= 102.068(6)°.
	c = 17.5171(12) Å	γ = 90°.
Volume	2551.6(3) Å^3	
Z	4	
Density (calculated)	1.248 Mg/m^3	
Absorption coefficient	0.788 mm^{-1}	
F(000)	1024	
Crystal size	0.3 x 0.2 x 0.3 mm^3	
Theta range for data collection	1.68 to 26.85°.	
Index ranges	-10<=h<=10, -21<=k<=21, -22<=l<=22	
Reflections collected	35729	
Independent reflections	5410 [R(int) = 0.0562]	
Completeness to theta = 26.85°	98.7 %	
Refinement method	Full-matrix least-squares on F^2	
Data / restraints / parameters	5410 / 0 / 253	
Goodness-of-fit on F^2	1.043	
Final R indices [I>2sigma(I)]	R1 = 0.0290, wR2 = 0.0752	
R indices (all data)	R1 = 0.0322, wR2 = 0.0769	
Largest diff. peak and hole	0.416 and -0.427 e.Å^{-3}	

8.6 Crystal data and structure refinement for 7

Empirical formula	C22 H37 Fe I N P3	
Formula weight	591.19	
Temperature	293(2) K	
Wavelength	0.71073 Å	
Crystal system	Orthorhombic	
Space group	P2(1)2(1)2(1)	
Unit cell dimensions	a = 10.4504(9) Å	α= 90°.
	b = 13.7867(12) Å	β= 90°.
	c = 18.3930(15) Å	γ = 90°.
Volume	2650.0(4) $Å^3$	
Z	4	
Density (calculated)	1.482 Mg/m^3	
Absorption coefficient	1.924 mm^{-1}	
F(000)	1200	
Crystal size	0.45 x 0.40 x 0.35 mm^3	
Theta range for data collection	1.85 to 28.34°.	
Index ranges	-13<=h<=13, -18<=k<=18, -23<=l<=24	
Reflections collected	27374	
Independent reflections	6596 [R(int) = 0.0426]	
Completeness to theta = 28.34°	99.9 %	
Absorption correction	Semi-empirical from equivalents	
Max. and min. transmission	0.993 and 0.621	
Refinement method	Full-matrix least-squares on F^2	
Data / restraints / parameters	6596 / 0 / 262	
Goodness-of-fit on F^2	0.965	
Final R indices [I>2sigma(I)]	R1 = 0.0347, wR2 = 0.0739	
R indices (all data)	R1 = 0.0416, wR2 = 0.0768	
Largest diff. peak and hole	0.971 and -0.412 $e.Å^{-3}$	

8.7 Crystal data and structure refinement for 8

Empirical formula	C20 H41 Fe I N P3
Formula weight	571.20
Temperature	293(2) K
Wavelength	0.71073 Å
Crystal system	monoclinic

Space group	P21/n	
Unit cell dimensions	a = 9.6624(11) Å	α= 90°.
	b = 20.4062(15) Å	β= 90°.
	c = 40.835(3) Å	γ = 90°.
Volume	8051.6(12) $Å^3$	
Z	12	
Density (calculated)	1.414 Mg/m^3	
Absorption coefficient	1.897 mm^{-1}	
F(000)	3504	
Crystal size	0.20 x 0.25 x 0.5 mm^3	
Theta range for data collection	1.00 to 19.50°.	
Index ranges	-9<=h<=9, -19<=k<=18, -38<=l<=38	
Reflections collected	30533	
Independent reflections	6669 [R(int) = 0.0967]	
Completeness to theta = 19.50°	95.5 %	
Refinement method	Full-matrix least-squares on F^2	
Data / restraints / parameters	6669 / 0 / 453	
Goodness-of-fit on F^2	1.248	
Final R indices [I>2sigma(I)]	R1 = 0.1638, wR2 = 0.3741	
R indices (all data)	R1 = 0.1710, wR2 = 0.3767	
Largest diff. peak and hole	1.991 and -2.286 $e.Å^{-3}$	

8.8 Crystal data and structure refinement for 10

Empirical formula	C17 H35 Fe I N P3	
Formula weight	529.12	
Temperature	150(2) K	
Wavelength	0.71073 Å	
Crystal system	orthorhombic	
Space group	P 21 21 21	
Unit cell dimensions	a = 8.9609(14) Å	α= 90°.
	b = 14.722(2) Å	β= 90°.
	c = 33.98(5) Å	γ = 90°.
Volume	4483(7) $Å^3$	
Z	8	
Density (calculated)	1.568 Mg/m^3	
Absorption coefficient	2.264 mm^{-1}	
F(000)	2144	

Crystal size	0.3 x 0.5 x 0.25 mm^3
Theta range for data collection	1.51 to 27.02°.
Index ranges	-11<=h<=11, -18<=k<=18, -43<=l<=43
Reflections collected	29481
Independent reflections	8867 [R(int) = 0.0873]
Completeness to theta = 27.02°	91.7 %
Refinement method	Full-matrix least-squares on F^2
Data / restraints / parameters	8867 / 0 / 463
Goodness-of-fit on F^2	1.018
Final R indices [I>2sigma(I)]	R1 = 0.0378, wR2 = 0.0981
R indices (all data)	R1 = 0.0426, wR2 = 0.1001
Absolute structure parameter	-0.010(16)
Largest diff. peak and hole	0.675 and -0.911 e.$Å^{-3}$

8.9 Crystal data and structure refinement for 14

Empirical formula	C21 H31 Fe N O P2	
Formula weight	431.26	
Temperature	150(2) K	
Wavelength	0.71073 Å	
Crystal system	monoclinic	
Space group	P 21/c	
Unit cell dimensions	a = 13.037(2) Å	α= 90°.
	b = 10.774(3) Å	β= 111.64(13)°.
	c = 16.757(3) Å	γ = 90°.
Volume	2187.7(7) $Å^3$	
Z	4	
Density (calculated)	1.309 Mg/m^3	
Absorption coefficient	0.845 mm^{-1}	
F(000)	912	
Crystal size	0.5 x 0.1 x 0.3 mm^3	
Theta range for data collection	1.68 to 27.08°.	
Index ranges	-16<=h<=16, -13<=k<=13, -21<=l<=20	
Reflections collected	26860	
Independent reflections	4650 [R(int) = 0.0922]	
Completeness to theta = 27.08°	96.5 %	
Refinement method	Full-matrix least-squares on F^2	
Data / restraints / parameters	4650 / 0 / 323	

Goodness-of-fit on F^2	1.090
Final R indices [I>2sigma(I)]	R1 = 0.0491, wR2 = 0.1423
R indices (all data)	R1 = 0.0526, wR2 = 0.1495
Largest diff. peak and hole	1.274 and -0.620 e.Å^{-3}

8.10 Crystal data and structure refinement for 15

Empirical formula	C_{22} H_{37} Co N P_3	
Formula weight	467.37 g/mol	
Temperature	293(2) K	
Wavelength	0.71073 Å	
Crystal system	Orthorhombic	
Space group	P n a 2_1	
Unit cell dimensions	a = 16.815(4) Å	α= 90°
	b = 9.473(3) Å	β= 90°
	c = 15.676(5) Å	γ = 90°
Volume	2497.0(13) Å^3	
Z	4	
Density (calculated)	1.243 g/cm^3	
Absorption coefficient	0.887 mm^{-1}	
F(000)	992	
Crystal size	0.20 x 0.25 x 0.35 mm^3	
Theta range for data collection	2.42 to 24.99°	
Index ranges	-1<=h<=19, -1<=k<=11, -1<=l<=18	
Reflections collected	2974	
Independent reflections	2464 [R(int) = 0.0925]	
Completeness to theta = 24.99°	99.9 %	
Absorption correction	None	
Refinement method	Full-matrix least-squares on F^2	
Data / restraints / parameters	2464 / 1 / 244	
Goodness-of-fit on F^2	1.026	
Final R indices [I>2sigma(I)]	R1 = 0.0460, wR2 = 0.1073	
R indices (all data)	R1 = 0.0673, wR2 = 0.1172	
Largest diff. peak and hole	0.593 and -0.373 e · Å^{-3}	

8.11 Crystal data and structure refinement for 16

Empirical formula	C20 H41 Co N P3	
Formula weight	447.38	
Temperature	150(2) K	
Wavelength	0.71073 Å	
Crystal system	monoclinic	
Space group	P 21/c	
Unit cell dimensions	a = 9.0104(14) Å	α= 90°.
	b = 29.169(5) Å	β= 111.95(12)°.
	c = 9.8726(14) Å	γ = 90°.
Volume	2406.5(6) $Å^3$	
Z	4	
Density (calculated)	1.235 Mg/m^3	
Absorption coefficient	0.917 mm^{-1}	
F(000)	960	
Crystal size	0.2 x 0.15 x 0.15 mm^3	
Theta range for data collection	1.40 to 27.42°.	
Index ranges	-11<=h<=11, -37<=k<=36, -11<=l<=12	
Reflections collected	26943	
Independent reflections	5304 [R(int) = 0.3247]	
Completeness to theta = 27.42°	96.6 %	
Refinement method	Full-matrix least-squares on F^2	
Data / restraints / parameters	5304 / 0 / 390	
Goodness-of-fit on F^2	1.368	
Final R indices [I>2sigma(I)]	R1 = 0.1933, wR2 = 0.1995	
R indices (all data)	R1 = 0.2010, wR2 = 0.2108	
Largest diff. peak and hole	0.591 and -0.741 $e.Å^{-3}$	

8.12 Crystal data and structure refinement for 17

Empirical formula	C20 H31 Co I N P2
Formula weight	533.23
Temperature	293(2) K
Wavelength	0.71073 Å
Crystal system	triclinic
Space group	*P*-1

Unit cell dimensions	a = 10.1933(9) Å	α= 104.980(7)°.
	b = 14.2724(13) Å	β= 106.146(7)°.
	c = 16.8829(15) Å	γ = 91.095(7)°.
Volume	2268.1(4) $Å^3$	
Z	4	
Density (calculated)	1.562 Mg/m^3	
Absorption coefficient	2.262 mm^{-1}	
F(000)	1072	
Crystal size	0.5 x 0.4 x 0.25 mm^3	
Theta range for data collection	1.69 to 29.60°.	
Index ranges	-14<=h<=14, -19<=k<=19, -23<=l<=23	
Reflections collected	45100	
Independent reflections	12602 [R(int) = 0.0761]	
Completeness to theta = 29.60°	98.6 %	
Refinement method	Full-matrix least-squares on F^2	
Data / restraints / parameters	12602 / 0 / 451	
Goodness-of-fit on F^2	0.910	
Final R indices [I>2sigma(I)]	R1 = 0.0494, wR2 = 0.1330	
R indices (all data)	R1 = 0.0566, wR2 = 0.1393	
Largest diff. peak and hole	4.941 and -3.668 $e.Å^{-3}$	

8.13 Crystal data and structure refinement for 19

Empirical formula	C20 H28 Co N O P2	
Formula weight	419.30	
Temperature	293(2) K	
Wavelength	0.71073 Å	
Crystal system	orthorhombic	
Space group	*P*bca	
Unit cell dimensions	a = 18.5460(6) Å	α= 90°.
	b = 12.2713(4) Å	β= 90°.
	c = 18.7768(7) Å	γ = 90°.
Volume	4273.3(3) $Å^3$	
Z	8	
Density (calculated)	1.303 Mg/m^3	
Absorption coefficient	0.960 mm^{-1}	
F(000)	1760	
Crystal size	0.3 x 0.25 x 0.25 mm^3	

Theta range for data collection	2.17 to 27.01°.
Index ranges	-23<=h<=23, -15<=k<=15, -23<=l<=23
Reflections collected	62889
Independent reflections	4647 [R(int) = 0.0704]
Refinement method	Full-matrix least-squares on F^2
Data / restraints / parameters	4647 / 0 / 226
Goodness-of-fit on F^2	1.052
Final R indices [I>2sigma(I)]	R1 = 0.0284, wR2 = 0.0774
R indices (all data)	R1 = 0.0335, wR2 = 0.0792
Largest diff. peak and hole	0.291 and -0.476 e.Å^{-3}

8.14 Crystal data and structure refinement for 22

Empirical formula	C34 H44 N2 Ni2 P2	
Formula weight	660.07	
Temperature	150(2) K	
Wavelength	0.71073 Å	
Crystal system	triclinic	
Space group	P-1	
Unit cell dimensions	a = 9.0873(12) Å	α= 83.87(2)°.
	b = 12.4309(15) Å	β= 74.00(2)°.
	c = 16.4964(13) Å	γ = 68.59(2)°.
Volume	1667.6(3) Å^3	
Z	2	
Density (calculated)	1.315 Mg/m^3	
Absorption coefficient	1.249 mm^{-1}	
F(000)	696	
Crystal size	0.3 x 0.3 x 0.45 mm^3	
Theta range for data collection	1.76 to 27.03°.	
Index ranges	-11<=h<=11, -15<=k<=15, -21<=l<=20	
Reflections collected	25328	
Independent reflections	7215 [R(int) = 0.0462]	
Completeness to theta = 27.03°	98.8 %	
Refinement method	Full-matrix least-squares on F^2	
Data / restraints / parameters	7215 / 0 / 537	
Goodness-of-fit on F^2	0.960	
Final R indices [I>2sigma(I)]	R1 = 0.0282, wR2 = 0.0569	
R indices (all data)	R1 = 0.0453, wR2 = 0.0608	
Largest diff. peak and hole	0.332 and -0.433 e.Å^{-3}	

8.15 Crystal data and structure refinement for 24

Empirical formula	C22 H36 Co O P3	
Formula weight	468.35	
Temperature	298(2) K	
Wavelength	0.71073 Å	
Crystal system	Orthorhombic	
Space group	Pna2(1)	
Unit cell dimensions	a = 16.4913(9) Å	α= 90°.
	b = 9.5041(5) Å	β= 90°.
	c = 15.8471(9) Å	γ = 90°.
Volume	2483.8(2) $Å^3$	
Z	4	
Density (calculated)	1.252 Mg/m^3	
Absorption coefficient	0.893 mm^{-1}	
F(000)	992	
Crystal size	0.50 x 0.45 x 0.40 mm^3	
Theta range for data collection	2.47 to 28.30°.	
Index ranges	-21<=h<=21, -12<=k<=12, -19<=l<=21	
Reflections collected	23133	
Independent reflections	5960 [R(int) = 0.0234]	
Completeness to theta = 28.30°	99.8 %	
Absorption correction	Semi-empirical from equivalents	
Max. and min. transmission	0.983 and 0.699	
Refinement method	Full-matrix least-squares on F^2	
Data / restraints / parameters	5960 / 1 / 254	
Goodness-of-fit on F^2	1.051	
Final R indices [I>2sigma(I)]	R1 = 0.0295, wR2 = 0.0705	
R indices (all data)	R1 = 0.0339, wR2 = 0.0727	
Largest diff. peak and hole	0.256 and -0.266 $e.Å^{-3}$	

8.16 Crystal data and structure refinement for 28

Empirical formula	C22 H32 Co F4 O P3
Formula weight	540.32
Temperature	150(2) K
Wavelength	0.71073 Å
Crystal system	triclinic

Space group	P-1	
Unit cell dimensions	a = 12.7954(16) Å	α= 90.220(11)°.
	b = 13.2517(16) Å	β= 89.935(12)°.
	c = 14.830(2) Å	γ = 95.992(10)°.
Volume	2.5008(6) nm^3	
Z	4	
Density (calculated)	1.435 Mg/m^3	
Absorption coefficient	0.920 mm^{-1}	
F(000)	1120	
Crystal size	0.2 x 0.3 x 0.28 mm^3	
Theta range for data collection	1.55 to 26.86°.	
Index ranges	-16<=h<=16, -16<=k<=16, -18<=l<=18	
Reflections collected	35118	
Independent reflections	10617 [R(int) = 0.1728]	
Completeness to theta = 26.86°	98.5 %	
Refinement method	Full-matrix least-squares on F^2	
Data / restraints / parameters	10617 / 0 / 559	
Goodness-of-fit on F^2	0.973	
Final R indices [I>2sigma(I)]	R1 = 0.0604, wR2 = 0.1135	
R indices (all data)	R1 = 0.1142, wR2 = 0.1280	
Largest diff. peak and hole	0.542 and -0.582 e.$Å^{-3}$	

8.17 Crystal data and structure refinement for 29

Empirical formula	C26 H38 Fe N P3	
Formula weight	513.33	
Temperature	298(2) K	
Wavelength	0.71073 Å	
Crystal system	Triclinic	
Space group	P-1	
Unit cell dimensions	a = 9.6040(4) Å	α= 76.523(1)°.
	b = 10.3792(5) Å	β= 81.368(1)°.
	c = 14.1341(6) Å	γ = 75.938(1)°.
Volume	1322.52(10) $Å^3$	
Z	2	
Density (calculated)	1.289 Mg/m^3	
Absorption coefficient	0.766 mm^{-1}	
F(000)	544	

Crystal size	0.30 x 0.28 x 0.25 mm^3
Theta range for data collection	1.49 to 28.29°.
Index ranges	-12<=h<=12, -13<=k<=13, -18<=l<=17
Reflections collected	13779
Independent reflections	6537 [R(int) = 0.0169]
Completeness to theta = 28.29°	99.5 %
Absorption correction	Semi-empirical from equivalents
Max. and min. transmission	0.991 and 0.717
Refinement method	Full-matrix least-squares on F^2
Data / restraints / parameters	6537 / 0 / 289
Goodness-of-fit on F^2	1.034
Final R indices [I>2sigma(I)]	R1 = 0.0317, wR2 = 0.0839
R indices (all data)	R1 = 0.0384, wR2 = 0.0879
Largest diff. peak and hole	0.370 and -0.242 e.$Å^{-3}$

8.18 Crystal data and structure refinement for 30

Empirical formula	C27 H42 Fe N P3	
Formula weight	529.38	
Temperature	298(2) K	
Wavelength	0.71073 Å	
Crystal system	Orthorhombic	
Space group	P2(1)2(1)2(1)	
Unit cell dimensions	a = 9.5617(7) Å	α= 90°.
	b = 15.7600(12) Å	β= 90°.
	c = 18.7820(14) Å	γ = 90°.
Volume	2830.3(4) $Å^3$	
Z	4	
Density (calculated)	1.242 Mg/m^3	
Absorption coefficient	0.717 mm^{-1}	
F(000)	1128	
Crystal size	0.45 x 0.40 x 0.35 mm^3	
Theta range for data collection	1.69 to 28.29°.	
Index ranges	-12<=h<=12, -20<=k<=20, -25<=l<=23	
Reflections collected	35612	
Independent reflections	7011 [R(int) = 0.0667]	
Completeness to theta = 28.29°	99.9 %	
Absorption correction	Semi-empirical from equivalents	

Max. and min. transmission	0.955 and 0.717
Refinement method	Full-matrix least-squares on F^2
Data / restraints / parameters	7011 / 2 / 310
Goodness-of-fit on F^2	0.974
Final R indices [I>2sigma(I)]	R1 = 0.0415, wR2 = 0.0868
R indices (all data)	R1 = 0.0681, wR2 = 0.0950
Absolute structure parameter	0.347(16)
Largest diff. peak and hole	0.566 and -0.198 e.Å^{-3}

8.19 Crystal data and structure refinement for 31

Empirical formula	C23 H38 Fe N P3	
Formula weight	477.30	
Temperature	298(2) K	
Wavelength	0.71073 Å	
Crystal system	Orthorhombic	
Space group	Pbca	
Unit cell dimensions	a = 16.5705(7) Å	α= 90°.
	b = 16.9427(6) Å	β= 90°.
	c = 17.8219(7) Å	γ = 90°.
Volume	5003.5(3) Å^3	
Z	8	
Density (calculated)	1.267 Mg/m^3	
Absorption coefficient	0.804 mm^{-1}	
F(000)	2032	
Crystal size	0.50 x 0.40 x 0.18 mm^3	
Theta range for data collection	2.06 to 28.24°.	
Index ranges	-22<=h<=22, -22<=k<=22, -23<=l<=23	
Reflections collected	60720	
Independent reflections	6194 [R(int) = 0.0521]	
Completeness to theta = 28.24°	100.0 %	
Absorption correction	Semi-empirical from equivalents	
Max. and min. transmission	0.952 and 0.799	
Refinement method	Full-matrix least-squares on F^2	
Data / restraints / parameters	6194 / 0 / 262	
Goodness-of-fit on F^2	0.992	
Final R indices [I>2sigma(I)]	R1 = 0.0334, wR2 = 0.0762	
R indices (all data)	R1 = 0.0523, wR2 = 0.0811	
Largest diff. peak and hole	0.331 and -0.224 e.Å^{-3}	

8.20 Crystal data and structure refinement for 32

Empirical formula	C20 H29 Fe I N P2	
Formula weight	528.13	
Temperature	298(2) K	
Wavelength	0.71073 Å	
Crystal system	Monoclinic	
Space group	P2(1)/c	
Unit cell dimensions	a = 8.813(2) Å	α= 90°.
	b = 13.947(3) Å	β= 91.057(5)°.
	c = 21.002(5) Å	γ = 90°.
Volume	2581.1(11) $Å^3$	
Z	4	
Density (calculated)	1.359 Mg/m^3	
Absorption coefficient	1.907 mm^{-1}	
F(000)	1060	
Crystal size	0.45 x 0.20 x 0.18 mm^3	
Theta range for data collection	1.75 to 28.24°.	
Index ranges	-11<=h<=11, -18<=k<=18, -27<=l<=24	
Reflections collected	21471	
Independent reflections	6368 [R(int) = 0.0694]	
Completeness to theta = 28.24°	99.9 %	
Absorption correction	Semi-empirical from equivalents	
Max. and min. transmission	0.933 and 0.505	
Refinement method	Full-matrix least-squares on F^2	
Data / restraints / parameters	6368 / 0 / 232	
Goodness-of-fit on F^2	0.922	
Final R indices [I>2sigma(I)]	R1 = 0.0463, wR2 = 0.0977	
R indices (all data)	R1 = 0.2074, wR2 = 0.1179	
Largest diff. peak and hole	0.676 and -0.324 $e.Å^{-3}$	

8.21 Crystal data and structure refinement for 33

Empirical formula	C24 H29 Fe N O P2
Formula weight	465.27
Temperature	298(2) K
Wavelength	0.71073 Å
Crystal system	Monoclinic

Space group	P2(1)/n	
Unit cell dimensions	a = 11.9318(5) Å	α= 90°.
	b = 13.0301(6) Å	β= 98.485(1)°.
	c = 15.1028(7) Å	γ = 90°.
Volume	2322.37(18) $Å^3$	
Z	4	
Density (calculated)	1.331 Mg/m^3	
Absorption coefficient	0.802 mm^{-1}	
F(000)	976	
Crystal size	0.40 x 0.20 x 0.16 mm^3	
Theta range for data collection	2.04 to 28.24°.	
Index ranges	-15<=h<=15, -16<=k<=17, -20<=l<=20	
Reflections collected	24771	
Independent reflections	5740 [R(int) = 0.0578]	
Completeness to theta = 28.24°	100.0 %	
Absorption correction	Semi-empirical from equivalents	
Max. and min. transmission	0.948 and 0.725	
Refinement method	Full-matrix least-squares on F^2	
Data / restraints / parameters	5740 / 0 / 268	
Goodness-of-fit on F^2	0.878	
Final R indices [I>2sigma(I)]	R1 = 0.0368, wR2 = 0.0818	
R indices (all data)	R1 = 0.0616, wR2 = 0.0877	
Largest diff. peak and hole	0.451 and -0.201 $e.Å^{-3}$	

8.22 Crystal data and structure refinement for 37

Empirical formula	C26 H40 Co N P3	
Formula weight	518.43	
Temperature	293(2) K	
Wavelength	0.71073 Å	
Crystal system	monoclinic	
Space group	P21/n	
Unit cell dimensions	a = 9.500(3) Å	α= 90°.
	b = 20.203(10) Å	β= 95.55°.
	c = 14.512(9) Å	γ = 90°.
Volume	2772(2) $Å^3$	
Z	4	
Density (calculated)	1.242 Mg/m^3	

Absorption coefficient	0.806 mm^{-1}
F(000)	1100
Crystal size	0.3 x 0.25 x 0.20 mm^3
Theta range for data collection	1.73 to 21.21°.
Index ranges	-9<=h<=9, -20<=k<=20, -14<=l<=14
Reflections collected	21601
Independent reflections	3048 [R(int) = 0.0941]
Completeness to theta = 21.21°	99.3 %
Refinement method	Full-matrix least-squares on F^2
Data / restraints / parameters	3048 / 0 / 440
Goodness-of-fit on F^2	1.048
Final R indices [I>2sigma(I)]	R1 = 0.0238, wR2 = 0.0649
R indices (all data)	R1 = 0.0265, wR2 = 0.0663
Largest diff. peak and hole	0.282 and -0.233 $e.Å^{-3}$

8.23 Crystal data and structure refinement for 39

Empirical formula	C28 H43 Co N P3	
Formula weight	545.47	
Temperature	298(2) K	
Wavelength	0.71073 Å	
Crystal system	Orthorhombic	
Space group	Pbca	
Unit cell dimensions	a = 9.2326(3) Å	α= 90°.
	b = 18.5977(7) Å	β= 90°.
	c = 34.0872(12) Å	γ = 90°.
Volume	5852.9(4) $Å^3$	
Z	8	
Density (calculated)	1.238 Mg/m^3	
Absorption coefficient	0.767 mm^{-1}	
F(000)	2320	
Crystal size	0.40 x 0.38 x 0.35 mm^3	
Theta range for data collection	2.19 to 28.20°.	
Index ranges	-11<=h<=12, -24<=k<=24, -45<=l<=44	
Reflections collected	58842	
Independent reflections	7206 [R(int) = 0.0503]	
Completeness to theta = 28.20°	100.0 %	
Absorption correction	Semi-empirical from equivalents	

Max. and min. transmission	0.980 and 0.806
Refinement method	Full-matrix least-squares on F^2
Data / restraints / parameters	7206 / 15 / 340
Goodness-of-fit on F^2	0.984
Final R indices [I>2sigma(I)]	R1 = 0.0370, wR2 = 0.0807
R indices (all data)	R1 = 0.0633, wR2 = 0.0865
Largest diff. peak and hole	0.463 and -0.155 e.Å^{-3}

8.24 Crystal data and structure refinement for 41

Empirical formula	C23 H39 Co N P3	
Formula weight	481.39	
Temperature	293(2) K	
Wavelength	0.71073 Å	
Crystal system	triclinic	
Space group	P-1	
Unit cell dimensions	a = 15.4413(13) Å	α= 90.20(2)°.
	b = 19.1241(10) Å	β= 89.93(2)°.
	c = 26.8570(12) Å	γ = 90.18(2)°.
Volume	7.9308(9) nm^3	
Z	12	
Density (calculated)	1.210 Mg/m^3	
Absorption coefficient	0.840 mm^{-1}	
F(000)	3072	
Crystal size	0.17 x 0.20 x 0.42 mm^3	
Theta range for data collection	1.52 to 29.55°.	
Index ranges	-18<=h<=21, -26<=k<=26, -37<=l<=36	
Reflections collected	123946	
Independent reflections	43020 [R(int) = 0.1416]	
Completeness to theta = 29.55°	96.9 %	
Refinement method	Full-matrix least-squares on F^2	
Data / restraints / parameters	43020 / 0 / 1483	
Goodness-of-fit on F^2	1.718	
Final R indices [I>2sigma(I)]	R1 = 0.1606, wR2 = 0.3607	
R indices (all data)	R1 = 0.2532, wR2 = 0.3902	
Largest diff. peak and hole	2.968 and -2.839 e.Å^{-3}	

8.25 Crystal data and structure refinement for 42

Empirical formula	C23 H29 Co I N P2	
Formula weight	567.24	
Temperature	298(2) K	
Wavelength	0.71073 Å	
Crystal system	Trigonal	
Space group	P-3	
Unit cell dimensions	a = 22.4083(5) Å	α= 90°.
	b = 22.4083(5) Å	β= 90°.
	c = 8.7961(3) Å	γ = 120°.
Volume	3825.06(18) $Å^3$	
Z	6	
Density (calculated)	1.478 Mg/m^3	
Absorption coefficient	2.018 mm^{-1}	
F(000)	1704	
Crystal size	0.42 x 0.20 x 0.10 mm^3	
Theta range for data collection	1.05 to 28.24°.	
Index ranges	-29<=h<=28, -29<=k<=29, -11<=l<=11	
Reflections collected	41941	
Independent reflections	6306 [R(int) = 0.0496]	
Completeness to theta = 28.24°	100.0 %	
Absorption correction	Semi-empirical from equivalents	
Max. and min. transmission	0.948 and 0.794	
Refinement method	Full-matrix least-squares on F^2	
Data / restraints / parameters	6306 / 0 / 259	
Goodness-of-fit on F^2	0.999	
Final R indices [I>2sigma(I)]	R1 = 0.0358, wR2 = 0.1028	
R indices (all data)	R1 = 0.0643, wR2 = 0.1168	
Largest diff. peak and hole	0.953 and -0.247 $e.Å^{-3}$	

8.26 Crystal data and structure refinement for 44

Empirical formula	C26 H34 Co N O P2
Formula weight	497.41
Temperature	150(2) K
Wavelength	0.71073 Å

Crystal system	P-1	
Space group	triclinic	
Unit cell dimensions	a = 8.4246(14) Å	α= 83.308(13)°.
	b = 9.0101(14) Å	β= 86.268(13)°.
	c = 17.464(3) Å	γ = 76.216(13)°.
Volume	1.2777(4) nm^3	
Z	2	
Density (calculated)	1.293 Mg/m^3	
Absorption coefficient	0.814 mm^{-1}	
F(000)	524	
Crystal size	0.2 x 0.2 x 0.17 mm^3	
Theta range for data collection	2.34 to 26.99°.	
Index ranges	-10<=h<=10, -11<=k<=11, -22<=l<=22	
Reflections collected	17133	
Independent reflections	5385 [R(int) = 0.0560]	
Completeness to theta = 26.99°	96.6 %	
Refinement method	Full-matrix least-squares on F^2	
Data / restraints / parameters	5385 / 0 / 416	
Goodness-of-fit on F^2	0.958	
Final R indices [I>2sigma(I)]	R1 = 0.0389, wR2 = 0.0804	
R indices (all data)	R1 = 0.0649, wR2 = 0.0861	
Largest diff. peak and hole	1.093 and -0.403 $e.Å^{-3}$	

CURRICULUM VITAE

Name	Şebnem Camadanlı
Date of Birth	February/02/1972
Place of Birth	İnegöl, Turkey
Nationality	Turkish
Marital Status	Single

1977 - 1982	Primary school (İshakpasa İlkokulu)
1982 - 1988	High School (İnegöl Lisesi)
1989 - 1994	Middle East Technical University Bachelor of Science Degree in Chemistry Graduation Project: Potential Energy Surface Mapping of 2-Hydroxymethylacetoacetate
July 1993 - September1993	ROCHE-Istanbul Trainee
1994 – 1997	Middle East Technical University Master of Science Degree in Inorganic Chemisrty “Axial Ligand Substituion Reaction Kinetics of Hydrogenphosphato Bridged Binuclear Platinum (III) Complexes„
1998 - 2000	Middle East Technical University Research Assistant and Teaching Assistant in “Inorganic Chemistry Laboratory„ “Instrumental Analysis Laboratory„“ and “Chemistry Olympics Turkish Team„

Şebnem Camadanli

Schafnussbaumweg 9
64297 Eberstadt

Eberstadt, den 03. Juni 2005

Erklärung

Ich erkläre hiermit, noch keinen Promotionsversuch unternommen zu haben.

Şebnem Camadanli

Schafnussbaumweg 9
64297 Eberstadt

Eberstadt, den 03. Juni 2005

Eidesstattliche Erklärung

Ich erkläre hiermit an Eides Statt, dass ich meine Dissertation selbständig und nur mit den angegebenen Hilfsmitteln angefertigt habe.